Master Degree in Automotive Engineering

ACOUSTIC AND VIBRATIONAL COMFORT IN PASSENGER VEHICLES

Supervisors

prof. Enrico Galvagno

prof. Alessandro Vigliani

prof. Mauro Velardocchia

Candidate

Marco Nesci

2018

Content

List of Tables

List of Figures

1   Introduction

In the last decades, the matter concerning both the acoustic and vibrational comfort perceived by the occupants of the various road vehicles, generally enclosed in the NVH designation, has become more and more important; indeed, problems that were considered in the past as negligible issues and represented a waste of resources, nowadays constitute a serious key element for responding in the best way to the Voice of Customers, satisfying their needs not only in terms of objective parameters, but also from the subjective feeling point of view.

Among literature sources, several studies approached the NVH issue, often following different paths and particular aspects, whereas a large number of regulations have been developed by the international entities and accepted by the science and engineering community.

 This project aims at studying experimentally the acoustic and vibrational comfort in passenger cars, by observing, measuring, analysing and processing the relevant parameters derived from real vehicles on the field, in such a way to obtain the corresponding vibrational and psychoacoustic objective indexes, which are commonly related to subjective feelings and judgments. In its first part, the project contains an overview on the current state of the art as far as acoustic and vibrational comfort is concerned, accompanied by the main methodologies exploited in modern industrial field to apply the regulation prescriptions to the experimental analysis of the topic, together with graphs and examples of several common practices exploited by different scientific entities.

The procedure then focuses on the implementation of a methodology suitable to provide a realistic and appreciable interrelationship between these two sides of the study, combining the objective indexes with the subjective parameters to get a unique and comprehensive comfort assessment criteria.

 In the second part, the work depart from the theoretical side to the practical one, explaining and applying the previous concepts on a real example of automotive study, performed with two vehicles and personally driven by the Co-Relator Enrico Galvagno and the Candidate, choosing selected paths and driving manoeuvres to replicate daily usage conditions to collect first hand data on real roads, for studying and comparing the different parameters concerning NVH field, thanks to the acquisition and post processing tools provided by Siemens in its LMS Test.Lab software and using LMS and PCB Piezoelectronics instruments.

In the end, the different results will be illustrated together with the relative considerations, on the basis of the previously explained concepts, concluding with final perspectives on future developments.

2   Vibrational comfort overview

The study of the interaction between vibrational phenomena and the human response to such stimuli is a complex discipline, involving many fields of the modern science; in this regard, several studies have been focusing on this topic along the years and among the most important contributions, the work of N. J. Mansfield [1] represented a real milestone in collecting a deep knowledge to understand the world of human response to vibration. In Figure 2.1, the science branches related to this topic are collected and linked to the three main disciplinary subjects.
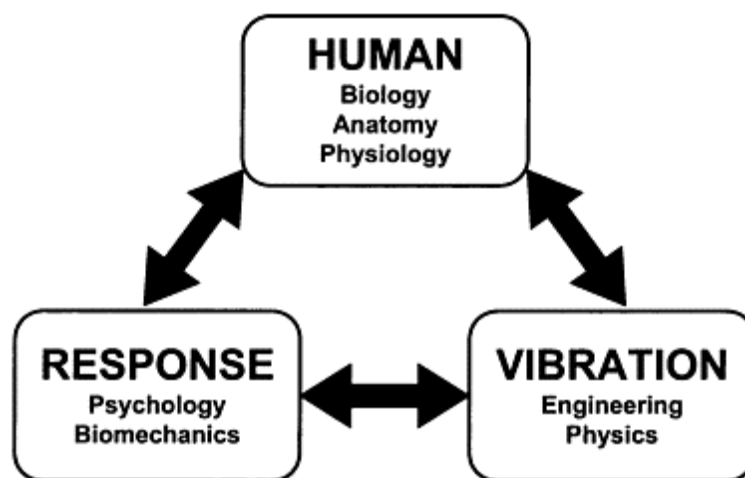
Figure 2.1: Component parts and topic areas for the discipline of "human response to vibration." (From [1])

 A comfortable ride is essential for a vehicle to obtain passenger satisfaction; indeed, since ride comfort is a very important problem in vehicle design as well as in vehicle judgment, there have been lots of studies attempted to identify factors contributing to the ride quality. Concerning a passenger vehicle, seating comfort is associated with various factors such as dynamic, postural, visual, sonic and thermal comfort.

Among these typologies of contribution, one of the principal components of a vehicle environment which can affect overall passenger's comfort is vibrational excitation.

According to Mansfield [1], vibration can be defined as a mechanical movement oscillating about a fixed point. Thus, it is a sort of mechanical wave, capable to transfer energy but not matter. Regarding the nature of vibration phenomenon, a mechanical structure is needed by the wave to travel in the surrounding space, such structure might be part of a machine, a vehicle, a tool, even a human body; however, if a mechanical coupling is lost, then the vibration propagation is impeded.

As a matter of fact, vibration transmission to passengers has a large influence on comfort, performance, and health. Concerning the several consequences caused by vibrational exposure, passenger's ability to carry out tasks, such as eating, reading and writing is one of the most relevant ones.

Besides, under more severe conditions, vibration will have psychological and physiological effects other than motion sickness, such as headaches and even chronic health effects.

2.1 Classification of vibration

Human response to vibration is a multidisciplinary topic involving biology, psychology, biomechanics, and engineering.

Although these topics are sometimes considered in isolation, understanding the interactions between them is the key to gain a proper comprehension of the topic area; Indeed, having defined vibration as a mechanical oscillation about a fixed reference point, it is important to acknowledge that, in practice, people are exposed to complex waveforms, although these can be represented by their component parts defined as a summation of sine waves.

Generally, human vibration is usually classified as either hand-transmitted vibration, whole-body vibration, or motion sickness, and these sub-disciplines are often considered separately from one another.

Motion sickness is only concerned with frequencies below 1 Hz, whole-body vibration is mainly related to frequencies from about 1 to 100 Hz, whereas hand-transmitted vibration involves frequencies from about 8 to 1000 Hz; the different fields of these vibration typologies are enhanced in Figure 2.2.

Commonly, vibrational phenomena occur on several axes simultaneously.

About whole-body vibration, these are the x-axis, y-axis, and z-axis (fore-and-aft, lateral, vertical, respectively) and rotation about these axes (roll, pitch, and yaw).

Often, rotational vibration is neglected in vibration analysis.

Concerning hand-transmitted vibration the x-axis passes through the palm, the y-axis across the palm, and the z-axis parallel with the back of the hand in the direction of the fingers.
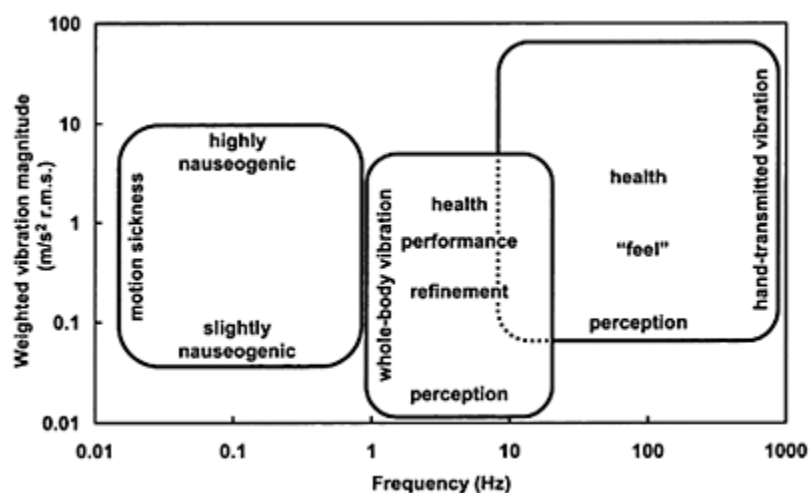
Figure 2.2: Typical frequency ranges and magnitudes of interest for the study of motion sickness, whole-body vibration, and hand-transmitted vibration.

2.1.1 The concept of whole body vibration

Human exposure to vibration can be broadly classified as whole-body and localized vibration. Whole-body vibration, (WBV), is defined as a motion transmitted to the human body as a whole through supporting surfaces, as opposed to vibration directed more locally, such as hand-arm vibration.

As stated in the Mansfield's volume [1], that constitutes a treasure-trove of information concerning the whole field focusing on the interaction between human body and vibrational phenomena, general whole-body vibration occurs when a human is supported by a surface that is shaking and the vibration affects body parts remote from the site of exposure. Generally, people are most sensitive to whole-body vibration within the frequency range of 1 to 20 Hz, although many measurements include higher frequencies.

On the other hand, since the whole-body vibration excitation can affect the comfort, performance and health of individuals, particular attention has been paid to the issues concerning the health and comfort of motor vehicles' drivers.

Considering the automotive field of study, vibration is usually transmitted through the vehicle to the seat and footrest, which are the surfaces that support the driver.

The vibration is then transmitted through the body of the driver to the head, which will move. This transmission path includes the seat, the surface of the driver in contact with the vehicle, including the driver's nervous system, the skeleton together with the spine, which represents a possible location of injuries, and ultimately the skull, characterized by its own dynamic responses to the transmitted vibration.

Actually, since comfort and health relate in many ways, the method for estimating the health effects in automotive field is the same as for evaluating comfort.

A proper description of the evaluation methods of the vibrational exposure and the ride comfort in vehicles has been provided by the article of Se Jin Park [2].

Among the standards exploited to evaluate human responses to whole-body vibration, the most common are the international ISO 2631 [3] and the British BS 6841 [4] regulations. Actually, despite BS 6841 being established as a British standard, it has been widely adopted also outside Britain. On the other hand, ISO 2631–1 have been more and more utilized within Britain since its publication, despite the concurrently accepted British standard, thus highlighting the matter of harmonization between more than one accepted existent method. Specifically, the former legislation concentrates on methodologies to assess in quantitative terms WBV with respect to human health and comfort, also referring to the probability to actually perceive the vibration and the motion sickness relationship.

In particular :

- ISO 2631-1 regards human exposure to whole-body vibration due to mechanical vibration and shock;

- ISO 2631-2 concerns human exposure to whole-body vibration and shock in buildings with respect to the comfort and annoyance of the occupants.

The frequency range considered by this regulation is:

- 0.5Hz to 80Hz for health, comfort and perception;

- 0.1Hz to 0.5Hz for motion sickness.

According to the ISO, vibration measurements in automotive field should be performed on the three translational axes of the seat pan reference system, however, vibration severity is assessed by considering only the axis where vibration excitation is the highest.

On the other hand, the BS 6841 regulation, which was designed to consolidate methods that were already being used in the industry but were only specified in a draft revision of ISO 2631, collects methods for quantifying vibration and repeated shocks in relation to human health, interference with activities, discomfort, the probability of vibration perception and the incidence of motion sickness.

This standard, which focuses on a frequency range comprised between 0.5Hz to 80Hz too, recommends to estimate vibration severity by performing the measurement on four axes on the seat, three translational at the seat cushion and an additional one for longitudinal translation of the seat backrest, then combining them in a unique evaluation assessment. Indeed, when dealing with WBV understanding in a vehicle, it is important to have in mind both the methodology of measuring vibrations and the associate vibration phenomena terminology.

2.1.2 The concept of hand arm vibration

Hand-transmitted or hand-arm vibration occurs whenever an individual holds a vibrating tool, such a jack-hammer or a simple steering wheel.

In origin, hand-transmitted vibration was mainly an industrial phenomenon; indeed, miners, shipbuilders, and chainsaw operators have been traditionally associated with vibration-induced health problems, although it is now accepted that many more sectors are affected, including passenger cars and commercial vehicles drivers. Today, improvements in understanding the health risks and the increased availability of low-vibration emission tools can help to gradually reduce that the incidence of hand-transmitted vibration injuries.

Nevertheless, with the trend towards globalization it is likely that populations with vibration problems will become more relevant in the developing world due to the currently less sophisticated health and safety cultures in these nations.

Most of the interest with hand-transmitted vibration is due to the disorders that are often observed in populations who use vibrating tools. Such disorders can be broadly divided into vascular and nonvascular categories [5].

In addition, nonvascular disorders can be further subdivided into bone and joint, neurological, muscular and other disorders. Collectively, both types of symptoms are referred to as hand-arm vibration syndrome or HAVS.

2.1.2 The concept of motion sickness and its causes

Motion sickness can occur when a person is exposed to real or apparent low-frequency motion, always below 1 Hz. Considering all the situations related to this phenomenon, all the environments in which it occur are characterized by the common presence of a real or apparent motion, as is described in Table 2.1.

Table 2.1: Typical examples of environments where motion sickness might occur.
(Table from [1], modified)

Sickness Associated with Mode of Transport
Cars
Large sea vessels (e.g., ferries, navy ships)
Small sea vessels (e.g., yachts, small boats)
Coaches (buses/horse-drawn)
Aircraft
Space travel
Trains
Camel or Elephant rides (but not horses)
Sickness Associated with a Moving Visual Scene
Virtual reality
Film/video editing
Microfiche readers
Microfilm readers
Simulators (fixed base)
Computer games
Cinema
Other Situations Where Motion Sickness Might Occur
Coriolis stimulation (e.g., merry-go-rounds)
Barbecue-spit rotation
Sea swimming
Wearing distorting spectacles
Fairground rides
Simulators (moving base)
Coriolis stimulation (e.g., merry-go-rounds)

Even if the term *sickness* implies a problem of a medical nature, motion sickness represents a normal and natural response to some particular forms of movement. Fortunately, motion sickness in itself is not directly fatal, however, its related effects might lead to a requirement for treatment.

A typical problem that is frequently associated with motion sickness consists in a state of apathy and/or impaired performance, which could result in an increased probability of misjudgement. Conversely, being almost all modes of transport more or less associated with motion sickness, since they have become more affordable and available to the general public, the incidence of travel sickness has increased in the recent years.

Concerning this issue, two major elements can be distinguished: the physiological response to the motion, i.e., the response to the undulation and visual instability; the psychological response, i.e., the ability to reduce the symptoms through distraction.

An individual exposed to a nauseogenic stimulus, defined as a stimulus that induces motion sickness, might experience a variety of symptoms caused by a combination of physiological and psychological responses [1].

Furthermore, it is important to take into account that, these symptoms could occur in a real or virtual environment. Actually, although almost everybody can be made to

feel sick if a stimulus is generated at the most critical frequency, individuals might be able to habituate themselves or take other preventative measures to minimize their adverse responses.

To understand and deal with motion sickness related issues, finding and studying its causes has been a fundamental focus point for the experts, whose efforts have been spent along many years in the pursue of a satisfactory and valuable explanation.

Motion sickness had been attributed to a variety of theories before the theory of sensory conflict was accepted.

The currently accepted thinking, also known as "sensory rearrangement" theory, combines physiological and psychological components. Deep studies regarding this topic have been conducted by several experts, while a detailed overview of the several related aspects is found in Mansfield work [1].

Considering normal motion conditions, the human brain simultaneously receives a battery of motion-sensing signals from the four somatic, visual, vestibular and control systems. As an example, while bending a corner in a car, the visual system will perceive objects moving to the left or right, the semi-circular canals of the vestibular system will sense the rotational movement, the otoliths in the saccule and utricle will respond to the centrifugal forces, moreover, the somatic system will feel the changes in pressure across the body and the driver will know that the process of cornering is happening because the steering wheel had been previously turned.

This provides a consistent cognitive model of the motion environment through which all systems are providing coherent information to the brain (Figure 2.3a).

In some situations, however, the motion-sensing signals being integrated by the brain are inconsistent with each other, as in the case of a passenger in a car reading a newspaper while the driver steers the vehicle around a corner.

In this case, since the passenger is not controlling the steering wheel or concentrating on the route, the turn probably will not be anticipated, and the visual system will not see the moving visual scene but only the words on the page, which move with the car and therefore appear to be stationary. Nevertheless, the semi-circular canals will sense the rotational movement, the otoliths will respond to the centrifugal forces and the somatic system will feel the changes in pressure across the body. This provides a cognitive model of the motion environment that is internally inconsistent (Figure 2.3b). The visual system is in conflict with the other senses, and the lack of control input fails to reinforce the correct cognitive model.
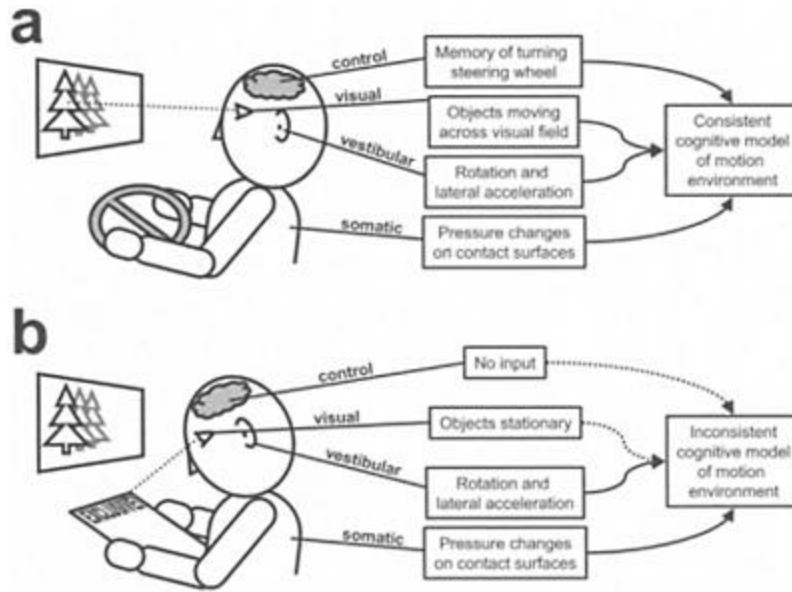
Figure 2.3: Illustrative model of the multiple pathways through which a motion environment is perceived: (a) for a driver of a car and (b) for a passenger in the same car reading a newspaper. (From Human Response to Vibration [1])

On the basis of the previous considerations, the central concept for a theory on the cause of motion sickness is that if there is a conflict between the expected and the actually experienced sensory signals, the consequent sense of imbalance can result in sickness. This is known as the *sensory conflict* or *sensory rearrangement theory* (Figure 2.4). In other words, if the experienced combination of signals matches the expected combination there is no change in physiological state and homeostasis is maintained. Instead, if the perceived combination of signals does not match the expected combination, then sensory rearrangement is detected and the symptoms of motion sickness might appear. On the other hand, in case a novel combination of signals is experienced, i.e., a combination which is not found in the memory of expected combinations of sensory inputs, then the memory is updated.
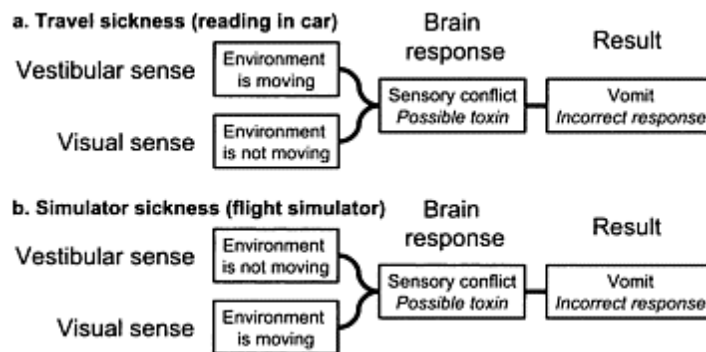
Figure 2.4: Examples of sensory conflict between the visual and vestibular senses, the brain responses, and ultimate results for (a) most forms of travel sickness (e.g., reading in a car), and (b) most forms of simulator sickness (e.g., fixed-base flight simulator for non-habituated individuals. For both types of sickness the brain response and result are incorrect. (From [1])

2.2 Method for measurement

 The evaluation of the effects related to vibrations involves measuring the vibrational solicitations in terms of accelerations; specifically, according to the standard regulations, the vibration measurement should be performed at the interface between the human body and a determined vibrating platform. In the following, the essential setup for measuring the WBV at the feet, hip and back is briefly described.
 A comprehensive model describing the measuring scheme for vibrational analysis regarding vehicle passengers has been proposed by Griffin in 1990 [5], based on a 12-axis system widely adopted also in the automotive industry and by BS 6841, as represented in Figure 2.5 and figure 2.6.
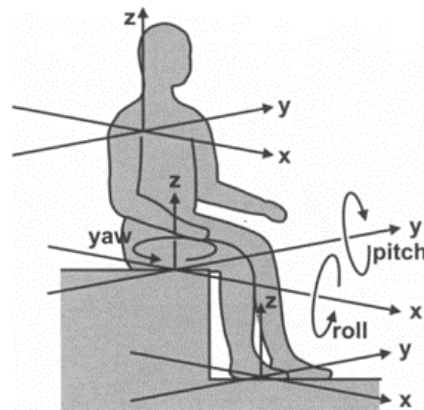
Figure 2.5a: Vibration axes for whole-body vibration centred at the feet, seat, and back.
(Adapted from [4])
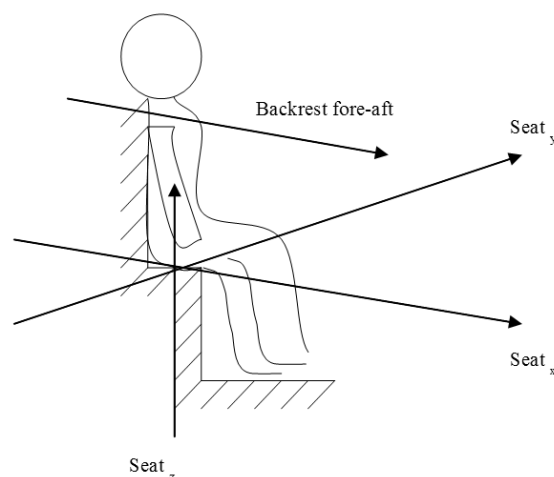
Figure 2.5b: Schematic of four-axis vibration of a driver as considered by BS 6841.

This system considers three translations (X_f, Y_f, Z_f) at the feet, three translations at the hip (X_s, Y_s, Z_s), other than three rotations at the hip (rX_s, rY_s, rZ_s), together with three translations (X_b, Y_b, Z_b) at the back.

On the other hand, being contributions of the three rotations at the hip and the y translation at the back negligible in relation with the ride comfort value severity, a common vibration measuring system consists in 8-axes estimation, omitting the four components.

In Figure 2.6 an example of measurement scheme for the evaluation of whole body vibration are depicted.
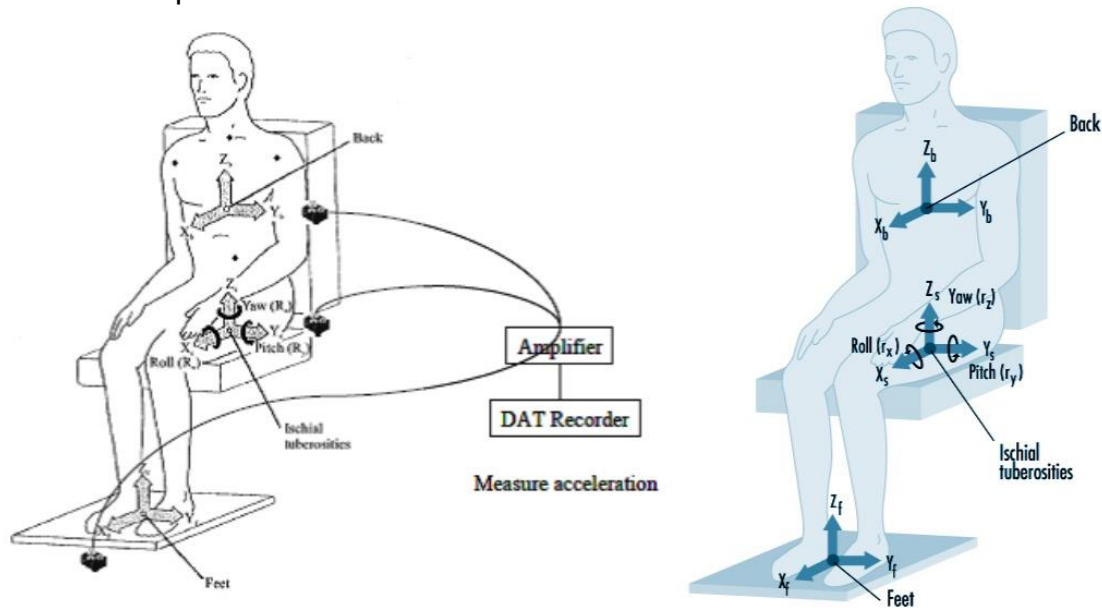
Figure 2.6: Schematic configuration for the measurement of whole-body vibration.
(Park et al., [6]).

As far as hand-transmitted vibration is concerned, there is a single coordinate system that is based on the head of the third metacarpal, i.e., the middle knuckle.

The x-axis is through the palm, the y-axis is across the palm towards the thumb, and the z-axis extends towards the fingers parallel with the back of the hand (Figure 2.7).
Defining the coordinate system at the third metacarpal ensures that there is no confusion regarding axes for palm or power grips or any orientation of the hand. Besides, although being probable that rotational vibration will affect the hand, no standardized terminology exists other than rotation about the x, y, or z-axes.
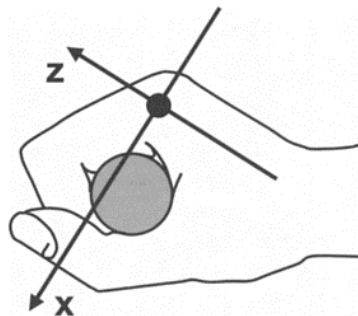
Figure 2.7: Vibration axes for hand-transmitted vibration.
Adapted from [7])

2.3 Analysis procedure

2.3.1 Frequency weighting

Depending on the frequency content of the excitation, vibration affects health, perception, comfort and motion sickness to a different extent.

About this issue, various experimental test methods have been developed; in particular, concerning the automotive field, the focus has been on the estimation of the seat vibrational comfort. Thus, to derive comfort ratings, several frequency weighting filters have been established in the regulations ISO 2631 and BS 6841.

As is listed in these two standards, the different vibration axes and frequency make the human response to vibration subject to change; specifically, these weighting factors have been obtained from the study conducted by Griffin [5].

On the other hand, while determining the equivalent comfort contours curves during the rating tests, the most severe challenge faced by the engineers has been the correct assessment of the subjects' responses, especially for what concerns the obtainment of the inverse of such equivalent comfort curves, which form the 'frequency weighting functions.

As a relevant remark, it is important to observe that, for different axes of vibrations, different frequency weightings are necessary; despite this consideration, some frequency weightings are generally adopted for more than one axis, by making the product between them and different axis multiplying factors, with the purpose of minimizing the number of weightings for axes.

In Table 2.1 and Figure 2.8, referred to [4], the several weighting functions and the related axis multiplying factors exploited for the 8-axis system are described.

Table 2.1: Weighting functions and axis multiplying factors.
(BS 6841, 1987)

Position	Weighting function (w_i)	Axis multiplying factors (m_i)
X_f	w_b	0.25
Y_f	w_b	0.25
Z_f	w_b	0.40
X_s	w_d	1.00
Y_s	w_d	1.00
Z_s	w_d	1.00
X_b	w_c	0.80
Z_b	w_d	0.40
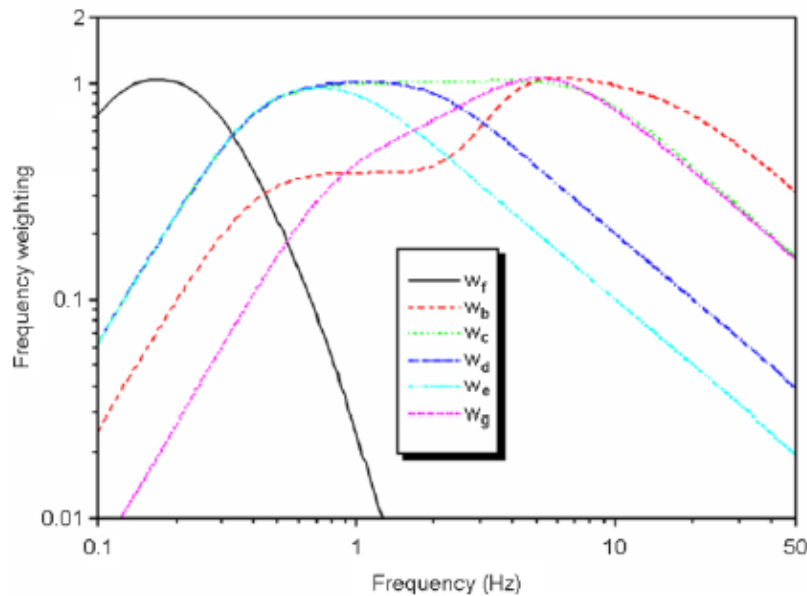
Figure 2.8: British standard frequency weighting functions.
(From [4])

Considering hand-transmitted vibration, a single frequency weighting is adopted, named W_h, regardless of its direction.
The weighting, defined in standards [8] and [9], is designed to simulate the response of the hand-arm system to vibration and can be applied when assessing the risk of injury from vibration or when an indication of the sensation magnitude is required (Figure 2.9).
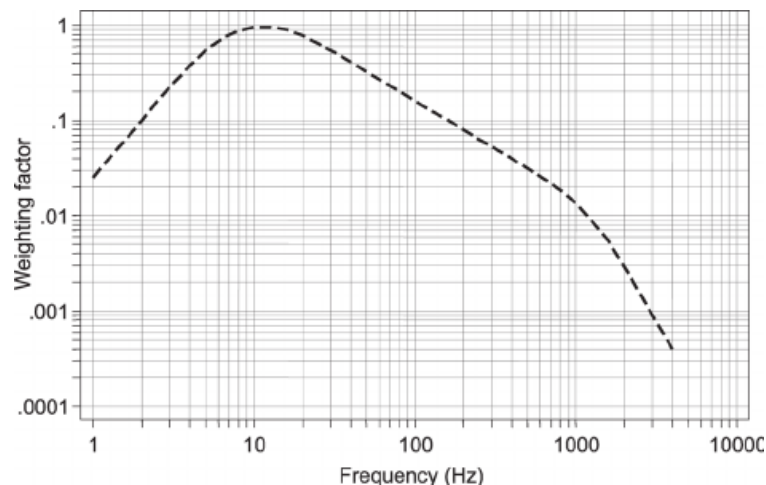
Figure 2.9: Frequency weighting curve W_h for hand-transmitted vibration according to ISO 5349-1

Between 8 and 16 Hz the idealized weighting is "flat", i.e., the human response to vibration is similar at any frequency within this range.
Between 16 and 1000 Hz, the idealized weighting has a roll-off rate of 6 dB/octave, i.e., as the frequency increases, the human response to vibration decreases.

Below 8 Hz and above 1000 Hz, ISO 5349-1 legislation [9] states that "the frequency dependence is not agreed," and therefore vibration outside this frequency range should not be included in analyses based on standardized techniques.

In practice, frequency weightings are usually implemented using digital or analogue signal-processing techniques. A "realizable" W_h weighting consisting of a series of curves defined by the characteristics of a filter has also been defined.

A complete assessment of the various weighting function for vibration in buildings and in motor vehicles has been provided in the ISO 2631-1 standard [3], resumed in Figure 2.10, Figure 2.11, Table 2.2 and Table 2.3.

In particular, as it's possible to observe by looking at the W_k weighting function curve, the most critical range for vertical WBV excitation frequency is comprised between 4 – 8 Hz; this interval is usually avoided through a proper design planning and building by OEM. Besides, the range in between 1 – 4 Hz represents a sensitive zone too for what concerns human response to vertical vibrational excitation, thus requiring proper countermeasures and clever design.

Conversely, considering the W_f weighting function curve relative to motion sickness sensitivity, the most critical range for vertical WBV involving a standing, seated or recumbent person is characterized by the frequency boundaries of around 0.05 Hz and 0.5 Hz, in perfect accordance with the main interval o study for these phenomena. As a further remark, it is worth of notice that all these critical interval are related to the frequency ranges in which the filtering action is almost null, therefore, as put in evidence by the graph below, the attenuation is minimal.

Similar consideration can be applied also to the function curves exploited for the additional weightings.
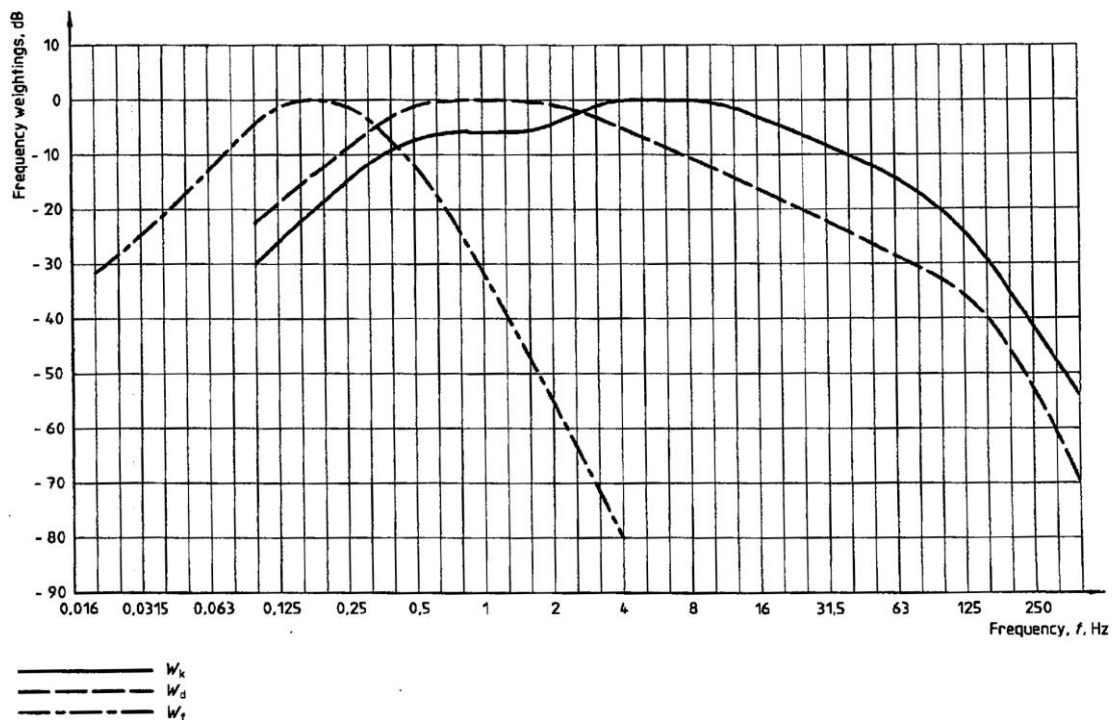
Figure 2.10: Frequency weighting curves for principal weightings.
(From [3])
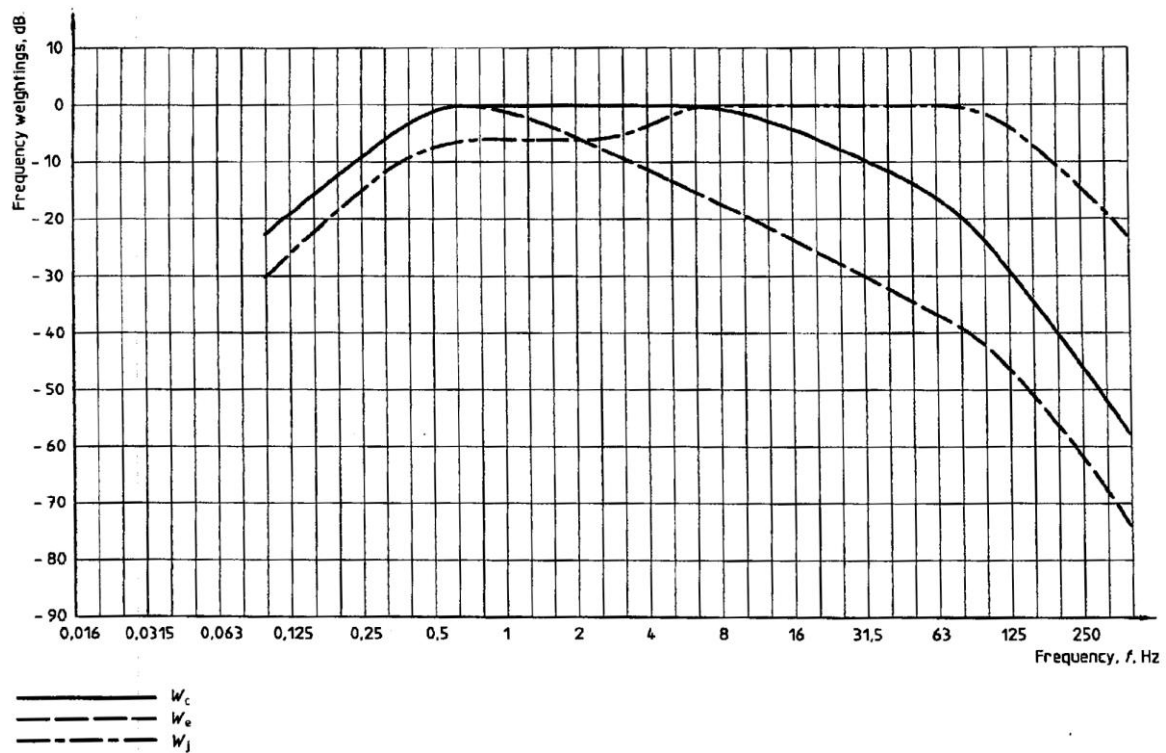
Figure 2.11: Frequency weighting curves for additional weightings.(From [3])

Table 2.2: Vibration weighting classes as defined in ISO 8041:2005.

WEIGHT CLASS	DESCRIPTION
W_b	Weighting for the vertical whole body vibration (seated, standing or recumbent person, z direction): ISO 2631-4
W_c	Weighting for the horizontal whole body vibration (seat back, x direction): ISO 2631-1
W_d	Weighting for the horizontal whole body vibration (seated/standing/recumbent person, x/ y directions): ISO 2631-1
W_e	Weighting for the rotational whole body vibration (seat all direction): ISO 2631-1
W_f	Weighting for the vertical whole body vibration (seated/standing person, z direction, motion sickness): ISO 2631-1
W_h	Weighting for hand arm vibration (all directions): ISO 5349-1
W_k	Weighting for the vertical whole body vibration (seated/standing/recumbent person, z direction): ISO 2631-1
W_j	Weighting for the vertical whole body vibration (recumbent person, x direction): ISO 2631-1
W_m	Weighting for the whole body vibration in building (all directions): ISO 2631-2

Table 2.3: Summary of the Most Common Frequency Weightings Used for Analysis of Human Vibration Signals.

Frequency Weighting	Application Area	Frequency Range	Direction
W$_b$	Whole-body	0.5 - 80 Hz	z-seat
W$_c$	Whole-body	0.5 - 80 Hz	x-backrest
W$_d$	Whole-body	0.5 - 80 Hz	x-seat, y-seat
W$_e$	Whole-body	0.5 - 80 Hz	Rotational-seat
W$_f$	Motion Sickness	0.1 - 0.5 Hz	z–vertical
W$_h$	Hand-transmitted	8 – 1000 Hz	x-y-z-hand
W$_k$	Whole-body	0.5 - 80 Hz	z-seat

2.3.2 Root mean square acceleration

According to the [3], the vibration evaluation should always include measurements of the weighted root mean square (R.M.S) acceleration. The R.M.S. method is a statistical measure of the magnitude of a changing quantity. In detail, it is particularly suitable for calculating mean of acceleration values, that can be both positive and negative signals, as this methodology weights every value as positive.

Concerning its unit measure, the weighted R.M.S acceleration is expressed as:

•   m/s^2 for translational vibrations

•   rad/s^2 for rotational vibrations

Moreover, bearing in mind that [3] evaluates the vibration transmitted to the body through the supporting surfaces, the ride comfort considering the regulation prescription is assessed exploiting the frequency weighted r.m.s. acceleration as defined by the expression below:

$$r.m.s\left(\frac{m}{s^2}\right) = [\frac{1}{T}\int_0^T a^2(t)dt]^{\frac{1}{2}} \tag{2.1}$$

Where:

•   a (t) is the frequency-weighted acceleration time history

•   T is the duration of the measurement in seconds.

2.3.3 Running root mean square acceleration

The running r.m.s evaluation method takes into consideration occasional shocks and transient vibration by adopting a properly short integration time constant τ.
The excitation magnitude is defined as a Maximum Transient Vibration Value (MTVV), representing the maximum in time of a$_w$(t$_0$), which is expressed as follows:

$$a_w(t_0) = \left[\frac{1}{\tau}\int_{t_0-\tau}^{t_0}[a_w(t)^2]\,dt\right]^{\frac{1}{2}} \tag{2.2}$$

On the other hand, the maximum transient vibration value (MTVV) is defined as:

$$MTVV = max[a_w(t_0)]$$
(2.3)

Where:

- $a_w(t)$ is the instantaneous frequency-weighted acceleration

- τ is the integration time for running averages

- t is the time (integration variable)

- t_0 is the time of observation (instantaneous time)

2.3.4 Vibration dose value VDV

According to BS 6841, the VDV index is considered more useful for the vibration entity assessment in all the cases in which the motion of a vehicle includes shocks or impulsive velocity changes. Several studies focused on this issue, in particular those performed by Griffin and Paddan [10]. More in detail, the so-called vibration dose value index provides a measure concerning the amount of the total exposure to vibration, considering in specific manner the related magnitude, frequency and exposure duration. Taking into account the obtained results, VDV computation furnishes information regarding the total exposure to vibration over the measurement period, instead of just focusing on the average; therefore, it is considered more suitable in case the vibration signal is not statistically stationary.

Such index generally represents a cumulative measurement of the vibration level received over an 8-hour or 16-hour period. According to the standards, the final VDV value is computed by the fourth root of the integral with respect to the time of the fourth power of the previously weighted acceleration.

Furthermore, it is worth of notice that the main difference with respect to the usual root mean square method, that constitutes also the main advantage and usefulness of this parameter, lies in the use of the fourth-power, making the VDV more sensitive to peaks in the acceleration waveform. This is enhanced in the expression below:

$$VDV \left(\frac{m}{s^{1.75}} \right) = [\int_0^T a^4 (t)dt]^{\frac{1}{4}}$$
(2.4a)

Where:
- VDV is the vibration dose value in m/s$^{1.75}$
- $a(t)$ is the frequency-weighted acceleration time history
- T is the period of time over which vibration occurs

Moreover, it is possible to estimate the vibration dose value using an alternative formulae, adopting the Estimated Vibration Dose Value : eVDV.

$$eVDV = k * a(r.m.s) * t^{0.25}$$
(2.4b)

Where:

- k is nominally 1.4 for crest factors below 6
- $a(r.m.s)$ is the weighted root mean square acceleration (m/s^2)
- t is the total cumulative time (seconds) of the vibration events (s)

Nevertheless, it is worth to notice that for crest factors above 6, the eVDV equation may be inaccurate, and this estimate should not be used.

In particular, crest factor is the ratio of the instantaneous peak amplitude of a waveform to its root mean square RMS value, this parameter indicates the extreme peaks of a waveform and is expressed as follows:

$$Crest\ Factor(peak-to-RMS\ ratio) = \frac{(peak\ value)}{(RMS\ value)} \qquad (2.4c)$$

2.4. Ride quality

Concerning vibration parameters more related to the automotive field, relevant importance has the ride quality issue, that is clearly a matter influenced by subjective feelings and sensations; in fact, for every individual, comfort degree is possible to be perceived differently even with a fixed vibration level, constant for everyone.

Thus, to quantify the ride value is not an easy task; however, many researches and studies have been conducted along the years by experts, aiming to accomplish a ride value quantification method as correct as possible. Approaching this matter, the ride values can be evaluated taking into account the presence of three different components, as defined by Parsons and Griffin [11] among the others:

- The component ride value
- The overall ride value
- The seat effective amplitude transmissibility

2.4.1 The component ride value

According to Griffin [5], this parameter represents the effective vibration magnitude at a single contact point between the human and the seat, considering a single axis after it has been weighted for frequency and axis multiplying factor, taking into account the relationship to the human sensitivity.

This value is computed multiplying power spectral density by weighting function for each axis and integrating it, then its square root is multiplied by the specific axis multiplying factor, so that the relative contributions of each axis can be assessed.

$$Component\ ride\ value_i = m_i \times [\int P_{ii}(f)w_i(f)^2 df]^{\frac{1}{2}} \qquad (2.5)$$

Where:
- m_i is the axis multiplying factor
- P_{ii} (f) is the power spectral density of each axis
- w_i is the weighting function of the each axis

2.4.2 The overall ride value

Differently from the previous one, this parameter represents the effective vibration magnitude occurring in one or more axes and input positions after it has been weighted for frequency, axis and input position, taking into account the relationship to the human sensitivity. The overall ride value can be assimilated to the 2-norm of the component ride value. In addition, this parameter is able to provide the total vibration amount, thus making it useful for comparing vehicles with different suspensions and seat interfaces. Moreover, it is possible to observe that a higher degree of overall ride value generally implies a higher degree of vibrational discomfort.

$$Overall\ Ride\ Value = \left[\sum_{i=1}^{N}(Component\ ride\ value_i)^2\right]^{\frac{1}{2}} \qquad (2.6)$$

2.4.3 Ride comfort and seat effective amplitude transmissibility (SEAT)

SEAT contribution represents the ratio of the vibration experienced on the top of the seat and the vibration that a subject would withstand when sitting directly on the vibrating floor. SEAT parameters have been largely exploited to determine the vibration isolation efficiency of a seat, as SEAT values are perfectly adequate to assess the vibrational attenuation of a seat with respect to excitations from the floor. According to [5] and [12], SEAT value is expressed as the weighted vibration ratio between Z_f of the floor and Z_s of the hip.

$$SEAT = \left[\frac{\int P_{ss}(f)|w_b(f)|^2 df}{\int P_{ff}(f)|w_b(f)|^2 df}\right]^{\frac{1}{2}} \qquad (2.7)$$

Where:

- P_{ss} (f) and P_{ff} (f) are the seat and the floor acceleration power spectra
- W_b, which is the weighting for vibration on the seat, constant in both the numerator and denominator, taken from the British Standard BS 6841.

It is worth of notice that, even though during the past year SEAT value has been utilized also as a predictor for dynamic seat comfort, it is designed and mainly exploited for evaluating seat damping characteristic.
In other words, SEAT value equal or greater than 1 implies an increased contribution in vibration discomfort performed by the seat, whereas SEAT value lower than 1 indicates a positive contribution in reducing the vibration level by the seat, capable of assuring a proper isolation.
The SEAT value is a measure of how well the transmissibility of a seat is adequate for the spectrum of input vibration, considering the sensitivity of the seat occupant to different frequencies.
According to standard [4], SEAT values less than 100% indicate isolation or attenuation of vibration. Thus, this parameter allows for the comparison of seat performance on a variety of road surfaces.

Furthermore, as defined by [5], SEAT parameter, which is strictly related to seat isolation performance, can be computed from the frequency-weighted r.m.s acceleration on the seat surface and seat base, $a_{seat,w}$ and $a_{base,w}$, respectively.

$$SEAT_{r.m.s}(\%) = \frac{a_{seat,w}}{a_{base,w}} \times 100\% \qquad (2.8)$$

However, it must be always taken into account that current standards, [4] and [3], recommend to the determine SEAT value using the VDV on the seat surface and seat base, VDV_{seat} and VDV_{base}, in case the input motion contains shocks.

$$SEAT_{VDV}(\%) = \frac{VDV_{seat}}{VDV_{base}} \times 100\% \qquad (2.9)$$

2.5 Standards procedures and comparison in automotive analysis field

2.5.1 BS 6841 guidelines

According to the British standard, vibration measurements on compliant seats should be performed by exploiting an accelerometer mounted in a device such as an SAE pad placed on the seat surface. In addition, methods for assessing vibration measured at the seat back and at the feet are also included in the regulation.

As first remark, it is recommended to weigh acceleration signals frequency considering W_b for seat vertical, W_c for backrest fore-and-aft and W_d for horizontal vibration at the seat; conversely, concerning the hand control and vision assessments, the frequency weighting W_g is generally preferred to W_b, while as far as motion sickness is concerned, W_f weighting should be used.

Moreover , when evaluating the vibration effects on health, the condition to calculate the r.m.s of frequency-weighted acceleration signals is bounded by the signals magnitude; in case it is constant and the stationary signals have a crest factor of less than 6, the r.m.s acceleration should be used; then, the estimated vibration dose value (eVDV) should be calculated. Conversely, if signals are not stationary, or if the crest factors are equal or greater than 6, then the vibration dose value (VDV) should be calculated, while the axes should be combined using a 4th power method. Considering VDV intensity levels, a threshold of a VDV of 15 m/s$^{1.75}$ is defined by the standard as a general indicator in case of severe discomforts, although it do not represent a safe or unsafe border, indeed:*"…there is currently no consensus of opinion on the precise relation between vibration dose values and the risk of injury…it is reasonable to assume that increased exposure to vibration will be accompanied by increased risk of injury."* [4] The flowchart of the procedure described and the relationship between acceleration RMS and exposure time with a VDV value of 15 is resumed in Figure 2.12 and Figure 2.13.
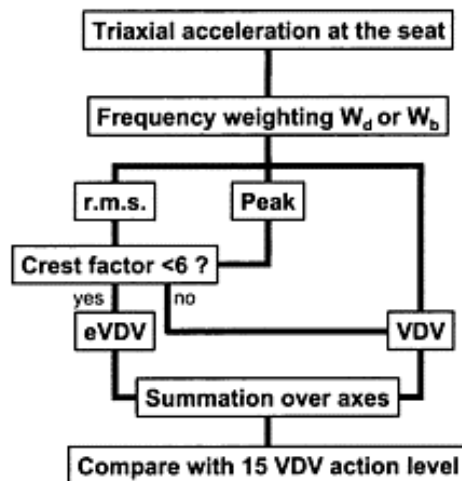
Figure 2.12: Method of evaluation and assessment according to health criteria in BS 6841 (1987). (Adapted from Griffin [13])
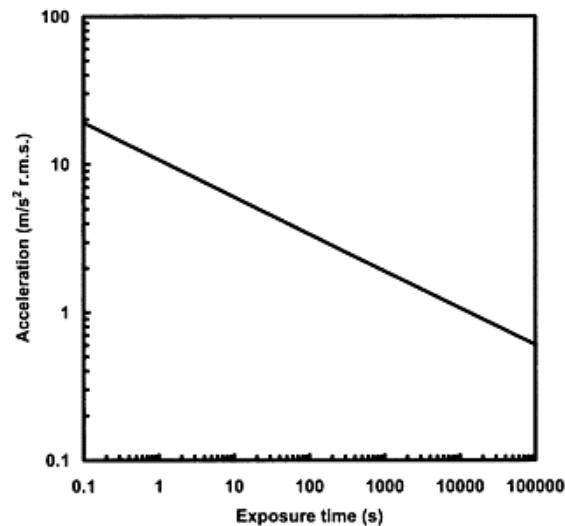
Figure 2.13: Root-mean-square acceleration (r.m.s.) corresponding to a vibration dose value (VDV) of 15 m/s$^{1.75}$ for exposure durations from 0.1 to 100'000 s. A doubling of r.m.s. acceleration magnitude results in a reduction of exposure time by a factor of 16 for the same VDV.

To a wider extent BS 6841 provides a really helpful guidance on vibration discomfort and perception, which, other than assessments performed by exploiting just tri-axial translational acceleration measurements on the seat surface, also includes rotational vibration and vibration at the feet and backrest together with methods on the assessment of low-frequency vibration related to the incidence of motion sickness are comprised in the regulation too.

As far as the analysis procedure is concerned, the different frequency weightings and multiplying factors adopted by the British standard are collected in Table 2.4.

Table 2.4: Frequency weightings and multiplying factors as specified in British Standard 6841 [4] for seated person

Location	Axis	Weighting	Multiplying factor
Seat	x	W_d	1.0
	y	W_d	1.0
	z	W_b	1.0
Backrest	x	W_c	0.8
Floor	z	W_b	0.4

Regarding motion sickness analysis, it is recommended to weigh vertical vibration exposures using W_f , which has a peak of 0.2 Hz (Figure 2.14), before to assess them using the motion sickness dose value ($MSDV_z$). The motion sickness dose value is defined in British Standard 6841 as:

$$MSDV = \sqrt{a_w^2 t} \qquad (2.10)$$

Where:
- *aw* is the r.m.s. of the frequency-weighted acceleration
- *t* is the duration of the motion exposure

For a mixed population, the percentage of unadapted persons who are likely to vomit can be estimated using:

$$Vomiting\ incidence\% = MSDV_z \qquad (2.11)$$
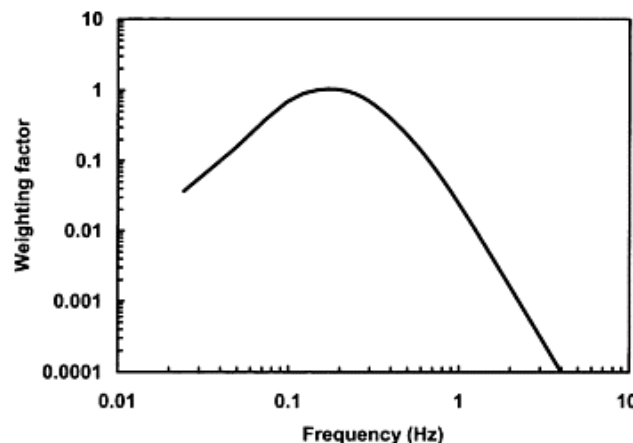
Figure 2.14: Wf frequency-weighting curve for prediction of sea-sickness incidence on passenger ferries as used by BS 6841 (1987).

2.5.2 ISO 2631 guidelines

According to the prescriptions listed in the regulation, vibration measurement has to be performed at the interface between the human body and the vibration source, hence, taking into account a compliant seat measurements on a seat should be made beneath the ischial tuberosities utilizing an accelerometer mount as an SAE pad. Moreover, approaches for vibration measurements at the seat back and at the feet are contained in the standard too.

Acceleration signals should normally be frequency weighted using W_k for seat vertical, W_c for backrest fore-and-aft, and W_d for horizontal vibration at the seat, while, concerning motion sickness, W_f is the preferred parameter choice. Furthermore, as stated in ISO 2631-1 [3], when evaluating the effects of vibrations on health, the frequency-weighted r.m.s. for each axis of translational motion on the supporting surface is to be computed only if the crest factor is less than 9. Considering the assessments, they are generally executed independently in each direction, a scaling factor of 1.4 being multiplied by the horizontal vibration, whereas the overall analysis is usually carried out according to the worst axis of frequency-weighted r.m.s. acceleration, including multiplying factors; conversely, if two axes have comparable magnitudes, then these can be combined using the vector sum method. As a further remark, two alternative methods of assessment are proposed in case crest factors equal or exceed 9: the maximum transient vibration value (MTVV) and the VDV. The MTVV, as introduced before, is defined as the highest value of the running r.m.s. for the measurement period, where the running r.m.s. is a measure of the acceleration magnitude in the previous second.

Nevertheless r.m.s. should be reported even though VDV or MTVV are used. Regarding safety thresholds, ISO prescription comprises two "health guidance caution zones" HGCZ to assist with interpreting the worst axis of the frequency-weighted r.m.s. acceleration (Figure 2.15).
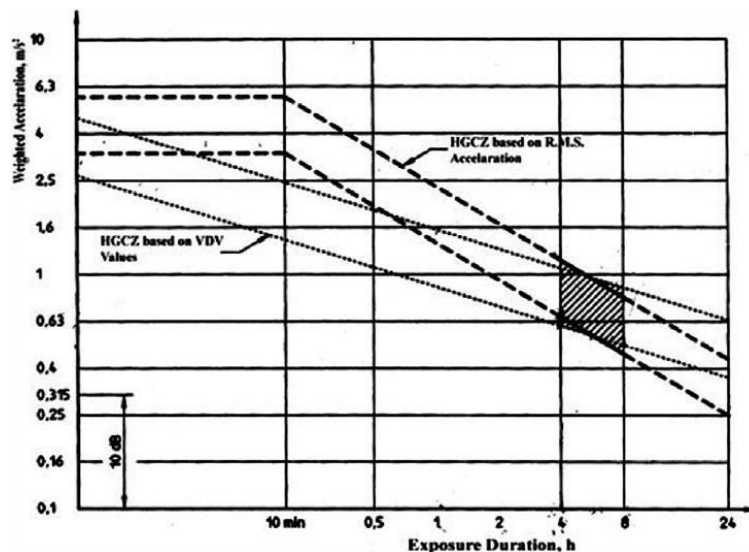
Figure 2.15: The two "health guidance caution zones" given in ISO 2631 (1997) .

Such two indicated zones are derived from r.m.s. and VDV approaches; indeed, standard states that: *"For exposures below the zone, health effects have not been clearly documented and/or objectively observed; in the zone, caution with respect to potential health risks is indicated and above the zone health risks are likely."*

The zones are almost coincident for durations of about 4 to 8 h, whereas using the zones for shorter durations is not recommended.

A doubling of r.m.s. acceleration magnitude results in a reduction of exposure time by a factor of 16 for one of the methods and a reduction of exposure time by a factor of 4 for the other.

In addition, for assessments according to VDV, the health guidance caution zone has upper and lower bounds at 8.5 and 17 $m/s^{1.75}$, respectively, while there is no equivalent zone for MTVV.

The key procedure constituting the focus of the standard id the method of using frequency-weighted r.m.s., this being the primary method that most users apply, whereas VDV is sometimes used for signals with high crest factors.

Figure 2.16 shows a simplified flowchart suitable for most assessments.
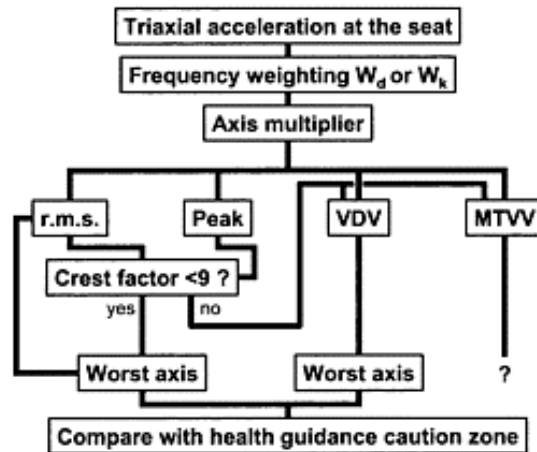
Figure 2.16: Simplified method of evaluation and assessment of whole-body vibration according to health criteria defined in ISO 2631 (1997).

Concerning vibrational comfort and perception analysis according to ISO 2631, the frequency-weighted r.m.s. acceleration is determined for the three translational axes on the seat. In addition, such standard lists several methods taking into account rotational vibration too. In addition, the same frequency weightings are used for health assessments. When it is not possible to perform vibration measurement at the backrest, then multiplying factors of 1.4 for the horizontal axes and 1 for the vertical axis should be used for health; though, talking about perception, on all translational vibration axes multiplying factors of 1 are preferred.

On the other hand, if the crest factor equals or exceeds 9, then VDV or MTVV should be exploited. Afterwards, vibration from all axes should be combined.

It is worth to notice that the standard contains also guidance with respect to predicting the incidence of motion sickness, such methods are pretty identical to those found in BS 6841 , however, International Standard ISO 2631 usually suggests indication that are often controversial, with several clauses that have to be interpreted and judged by analyst, thus bringing to misleading conclusions [14].

Table 2.5: Frequency weightings and multiplying factors for health aspects of whole-body vibration as specified in International Standard 2361-1 [3] for seated persons

Location	Axis	Weighting	Multiplying factor
Seat	x	W_d	1.4
	y	W_d	1.4
	z	W_k	1.0
Backrest	x	W_c	0.8

2.5.3 Comparison of BS 6841 (1987) and ISO 2631 (1997)

Comparing the two standards analyzed, British Standard BS 6841 and International Standard ISO 2631 are similar in most parts.

Actually, for motion sickness assessments the standards are practically identical and broadly similar in the field of perception and comfort evaluation, even alike considering the procedures of acquiring data and measurement locations.

In other words, by interpreting ISO 2631, it is allowed to carry out with a similar approach to BS 6841 most vibration analyses.

Nevertheless, these two legislations are different on five key concepts, summarize in Table 2.4, which include:

- the different vertical frequency weightings;
- the multiplication factors for horizontal vibration in ISO 2631;
- the use of VDV or r.m.s. as the criteria for assessment of health;
- whether assessment should be made using combined axes or the worst axis only;
- the value for the crest factor at which r.m.s. becomes unreliable.

Table 2.6: Key Differences between British Standard BS 6841 and International Standard ISO 2631-1

BS 6841	ISO 2631–1
Uses W_b frequency weighting for vertical vibration	Uses W_k frequency weighting for vertical vibration
No multiplication factors required for measurement of seat surface vibration	Horizontal vibration is scaled by a factor of 1.4 for measurements of seat surface vibration
Use of 15 VDV as criteria for health risk	Use of two "health guidance caution zones" HGCZ as criteria for health risk
Use of combined axes for assessments	Use of "worst axis" for assessments, with option to use combined axes
Crest factor of 6 used as threshold for unreliability of r.m.s. methods	Crest factor of 9 used as threshold for unreliability of r.m.s. methods

3 Acoustical comfort

As far as the acoustic comfort in a vehicle is concerned, an essential parameter to be considered is the perceived noise. Such noise can be produced by a wide range of sources, including engine, driveline, tire contact patch and road surface, braking system, wind and atmospheric phenomena, heating ventilation air conditioning system and alternator system, together with other engine accessories.
NVH phenomena can be classified mainly in two categories according to [15]:

- "structure-borne" noise, consisting in either vibration or noise, is propagated through solid structures via a variety of paths, and then diffused acoustically into the cabin; isolation countermeasures can be adopted to attenuate it.
- "air-borne" noise represents the progressive movement of mass particles transmitted in the form of sound waves at the speed of sound, thus it's generated acoustically and propagated by air paths; absorption and acoustic isolating properties of barrier materials are usually exploited to reduce it.

Noise and vibration play an important role in what is called the overall harmony of the vehicle, such term describes the relationship between form on one extreme of the spectrum and function at the other extreme; hence, it is associated to the well-known statement of "form follows function" [16].
In Figure 3.1 are listed the different characteristics affected by noise and vibration components in the regard of the overall vehicle harmony.
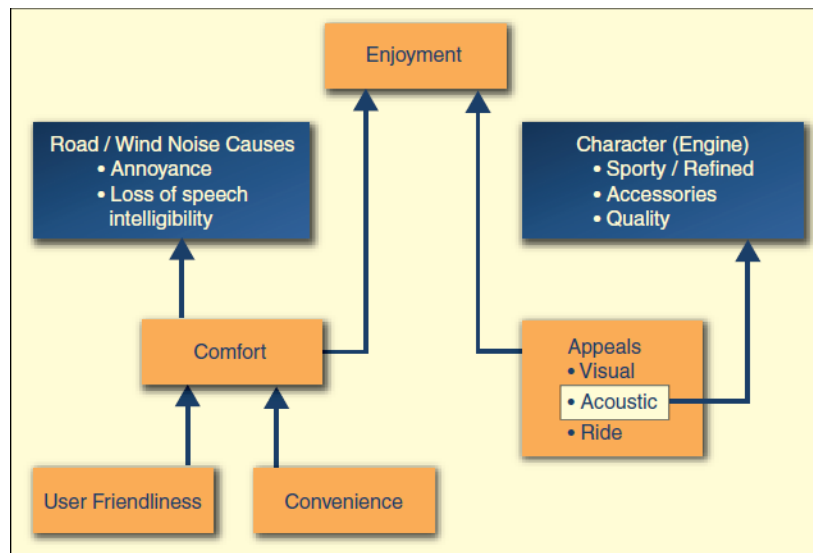
Figure 3.3.1: Impact of NVH on overall vehicle harmony.
(From [16])

As a matter of fact, today's vehicles have to perform all the functions that drivers and passengers expect while providing a comfortable and enjoyable environment.

In this regard, it's job of the experts to fill the gap between form and function and establish a target balance between these two elements for each vehicle class and type.

Talking about noise, vibration, harshness disturbs, NVH elements such as gear whine, boom, tire and wind noise strictly affect comfort, while others, such as engine noise in acceleration, ride and handling, have a more direct impact on overall appeal.

In modern world, due to the ever growing importance of the comfort related issues, NVH design is often tightly integrated with vehicle development since its early stages, when the NVH attributes are frequently designed to express a very strong brand identity, with many examples existing in the automotive field, where several car makers spend time and resources for developing a determined feature conveying their uniqueness, thus distinguishing them form the competitors.

This is pretty common for sports car manufacturers, which take great care of their engines sound to communicate to the customers a carefully selected feeling and emotion, so to enclose in an acoustic sensation a large part of a brand identity.

Figure 3.2 summarize the sound portfolio of a sports car manufacturer, showing the two main noise attributes at 100 km/h (engine noise and wind/road noise), plotted against each other, whereas the two diagonal lines represent the thresholds for a sporty characteristic (to the right) and a comfortable characteristic (to the left).
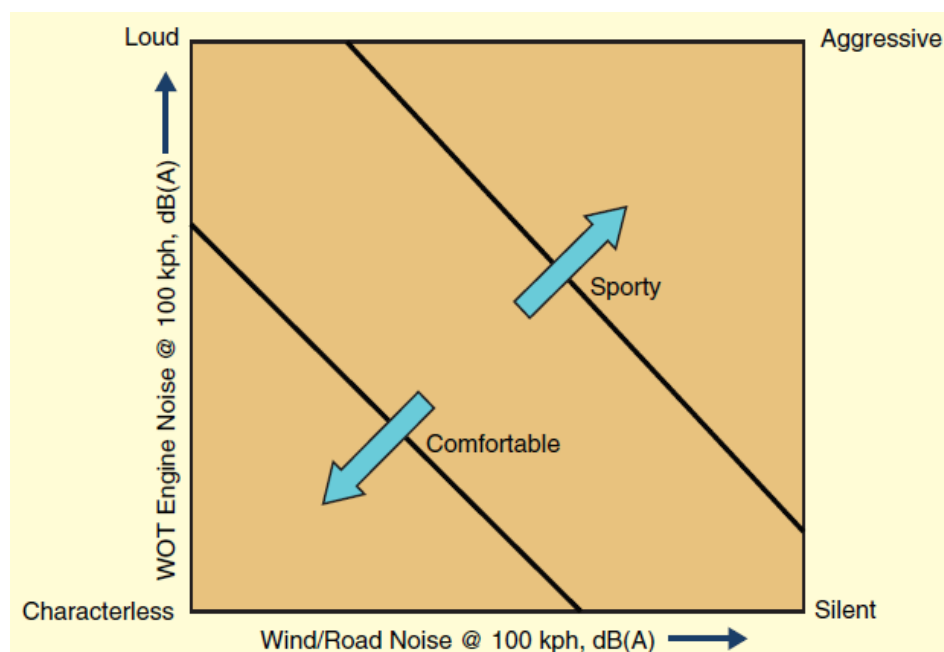
Figure 3.3.2: Example of brand sound design.
(Adapted from [17])

The sound/vibration quality concerns related to detectability issues are generally easier to investigate, because they are one dimensional in the sound quality space.

On the other hand, the acoustic image of the vehicle is multidimensional; indeed, multiple components that are time and frequency dependent interact and combine to create an overall vehicle sound. The never-ending effort in achieving the desired level of acoustic image of a vehicle respecting the requirements imposed by the regulations and the qualitative standards established by the OEM have led to a

growing attention on the sound quality analysis in automotive field. The concept of acoustic image and detectability related to sound quality are expressed relatively to the brand identity concept, especially during brand sound design.

The detectability definition refers to the components that should not be detected in normal driving conditions, as transmission, gears, A/C compressor, alternator, fuel pump, tyres, power steering and so on; conversely, acoustic image is related to the components expected to produce audible noise, still having to match the customer expectations; these may involve character, mainly affected by the engine, quality, subject to accessories, comfort, defined in large part by road and wind noise [16].

Being the topic quite many-sided and complex, considering it applies not only to automotive but also to general acoustics, in order to express sound and noise characteristics several physical magnitudes have been developed along the years together with many indexes purposely implemented to characterize a specific side of an acoustic phenomenon. A detailed explanation of the basis of sound, acoustics and psychoacoustics is provided in the works of D. Drioli and N. Orio [18]

3.1 Sound intensity and audibility thresholds

In pure physical terms, the sound is represented by the air pressure variation, measured in Pascal (Pa); indeed, the volume perception of a sound, the so called loudness, is directly related to the magnitude of the pressure variations; this is equivalent to say that a direct proportionality links the two entities.

Nowadays, it is common practice to refer preferably to the effective pressure p_{rms} rather than to the pressure variation peaks, this magnitude refers to the quadratic average of the pressure variations.

$$p_{rms} = \frac{1}{t2-t1}\sqrt{\int_{t1}^{t2} p(t)^2 dt} \qquad (3.1)$$

Where the integration is performed:
- On a period for periodic sounds
- On an ideally defined interval for aperiodic sounds

As far as the audibility range is concerned, the minimum perceived effective pressure is equal to 20 µPa, while the pain threshold is located around the 20 Pa.

Another entity that has been defined is the acoustic intensity (*I*), corresponding to the average power transmitted for surface unit in the wave propagation direction.

About this entity, it has been demonstrated the following expression, valid for both plane and spherical waves:

$$I = \frac{p_{rms}^2}{\rho c} \qquad (3.2)$$

Where:

- ρ is the transmission medium density
- P_{eff} is the effective pressure
- c is the sound velocity in the medium

The acoustic intensity range is considerably wide, in fact, it assumes value from 10^{-12} W/m^2 to 1 W/m^2.

Concerning the sound measurement scale, due to the quite extended range within which the pressure, power and acoustic intensity values are distributed, a logarithmic scale is generally preferred. Therefore, it is defined as Pressure Level (*PL*) the logarithm of the ratio of the measured pressure on a reference pressure p_{ref}:

$$PL = 20 * log_{10} \frac{p}{p_{ref}} \qquad (3.3)$$

The *PL* entity is a-dimensional, however, the general unit measure exploited to express it is the decibel (dB). A guide of the ratios between certain dB levels is reported in Table 3.1.

Table 3.1: Decibel levels scale with respective ratios.

dB	-20	0	6.02	10	20	40	60
ratio	1/10	1/1	2/1	$\sqrt{10}$	10/1	100/1	1000/1

It is noticeable that 0 dB corresponds to the minimum audibility threshold, while 120 dB level constitutes the pain threshold.

Regarding the reference pressure level, it is commonly accepted to adopt as a standard reference the minimum audible effective pressure $p0$ = 20 µPa.

This way, the Sound Pressure Level (*SPL*) entity is established:

$$SPL = 20 * log_{10} \frac{p}{p_0} = 20 * log_{10} \frac{p}{0.00002} \rightarrow SPL = 20 * log_{10}p + 94 \qquad (3.4)$$

SPL values can be converted in acoustic pressure levels by means of the inverse formula below:

$$\boldsymbol{p = p_0 * 10^{L_p/20}} \qquad (3.5)$$

Analogously, the sound-power level (L_W) can be expressed in dB too:

$$\boldsymbol{L_W = 10 * log_{10} \frac{P}{P_{ref}}} \qquad (3.6)$$

Where:
- *P* is the sound-power in Watt
- P_{ref} is a reference power, conventionally equal to 10^{-12} W.

The stimulus of the sound pressure level needs to be interpreted as a hearing sensation and one approach consists of multiplying the frequency spectrum of the

acoustic pressure signal with a weighting function before calculating the RMS level. In this regard, several weighting functions have been defined, of which the A-B-C and D weightings are the most widely used. Such functions are based on experimentally determined equal loudness contours which express the loudness sensation of single tones as a function of sound pressure level and frequency.

About this matters, ISO established two specific standards: ISO1996/1-1982 and ISO1999:1990 to provide a definition for the equivalent A- weighted sound pressure level in decibels identified as $L_{Aeq,T}$, such function gives the value of the A-weighted sound pressure level of a continuous, steady sound that, within a specified time interval T, has the same mean square sound pressure as the sound under consideration whose level varies with time. This leads to the expression:

$$LAeq, T = 10log \left[\frac{1}{t_1 - t_2} \int_{t_1}^{t_2} \frac{p_A^2(t)}{p_0^2} dt \right] \qquad (3.6a)$$

Where:

- $L_{Aeq,T}$ is the equivalent continuous A-weighted sound pressure level, in decibels, determined over a time interval T starting at t_1 and ending at t_2
- p_0 is the reference sound pressure (20 µPa);
- p_A is the instantaneous A-weighted sound pressure of the sound signal.

In practice with sampled data the equivalent sound pressure level is computed by a summation of the sampled values of the pressure level, in dB over the number of samples required. On the other hand, the intensity level (*IL*) is computed with the expression listed below:

$$IL = 10 * log_{10} \frac{I}{I_{ref}} \qquad (3.7)$$

Where:

- I_{ref} is a reference power, conventionally equal to $I_0 = 10^{-12}$ W/m^2.
- the factor 10 utilized instead of the factor 20 is due to the proportionality between the intensity and the square of the pressures

As an ulterior remark, in case two incoherent sounds are analyzed, respectively with intensity levels IL_1 and IL_2, the resulting level is given by the sum of the powers:

$$IL_{tot} = 10 * log_{10} \frac{P_1 + P_2}{P_0} = 10 * log_{10}(10^{IL_1/10} + 10^{IL_2/10}) \qquad (3.8)$$

Having defined the basis of sound power assessment, the various bandwidth typologies are described.

First of all, the bandwidth is defined as the whole interval between the minimum and the maximum frequency occupied by a signal in the spectrum, as expressed in formula 3.9.

$$\Delta f = f_1 - f_2 \qquad (3.9)$$

The second concept to be introduced is the centre frequency, or "average frequency", that is expressed by the formula 3.10.

$$f_c = \sqrt{f_1 f_2} \hspace{4cm} (3.10)$$

In acoustics, generally, the entire bandwidth of a signal is considered constant, thus indicating that all the bands in which the noise frequency spectrum is subdivided are wide the same. On the other hand, the term proportional bandwidth is used when the ratio of upper frequency to the lower one is constant. In addition, a one octave bandwidth definition is exploited when the relationship 3.11 is verified:

$$f_2 = 2 * f_1 \hspace{4cm} (3.11)$$

While a half octave bandwidth is related to the expression 3.12:

$$f_2 = 2^{1/2} * f_1 \hspace{4cm} (3.12)$$

3.1.1 The dB weighting

Considering the human perception of the acoustic power, the human ear sensitivity to sound is higher in the 1-4 kHz range than at very low or very high frequencies [19]; thus, talking about noise, higher sound pressures are therefore more acceptable at lower and higher frequencies than in this defined mid-range interval.

Indeed, the proper physical characteristics of the human ear are of paramount importance in acoustic design and sound measurement; hence, to compensate for the human hearing, filters adapting the measured sound response to the human sense of sound are usually applied to sound meters, most common ones being:

- *dB(A)*
- *dB(B)*
- *dB(C)*

These A,B,C weightings are frequency dependent curves often fitted to sound pressure microphone measurements to mimic the effects of human hearing.

Among the several factors affecting the difference between the human hearing and the microphone recordings, the presence of human head, torso and outer ear interfering with and alter the sound field is one of the main ones, other differences are due to the cochlea hearing organ and psychological effects; in fact, sounds at low frequencies and very high frequencies are more difficultly detected by it.

About these main filters, most widely used is the dB(A) one, which roughly corresponds to the inverse of the *40 dB* (at *1 kHz*) equal-loudness curve for the human ear. Actually, fitting the dB(A) filter involves a less sensitive sound level meter relatively to very high and very low frequencies.

Instead, the decibel C filter is practically linear over several octaves and is suitable for subjective measurements at very high sound pressure levels, while the decibel B

filter is between C and A; actually the use of B and C decibel filters is merely occasional.

The relative response of these dB filters is depicted in Figure 3.x while Table 3.y shows their quantitative frequency dependent comparison.

Figure 3.3: dB filters criteria.
(From [19]).
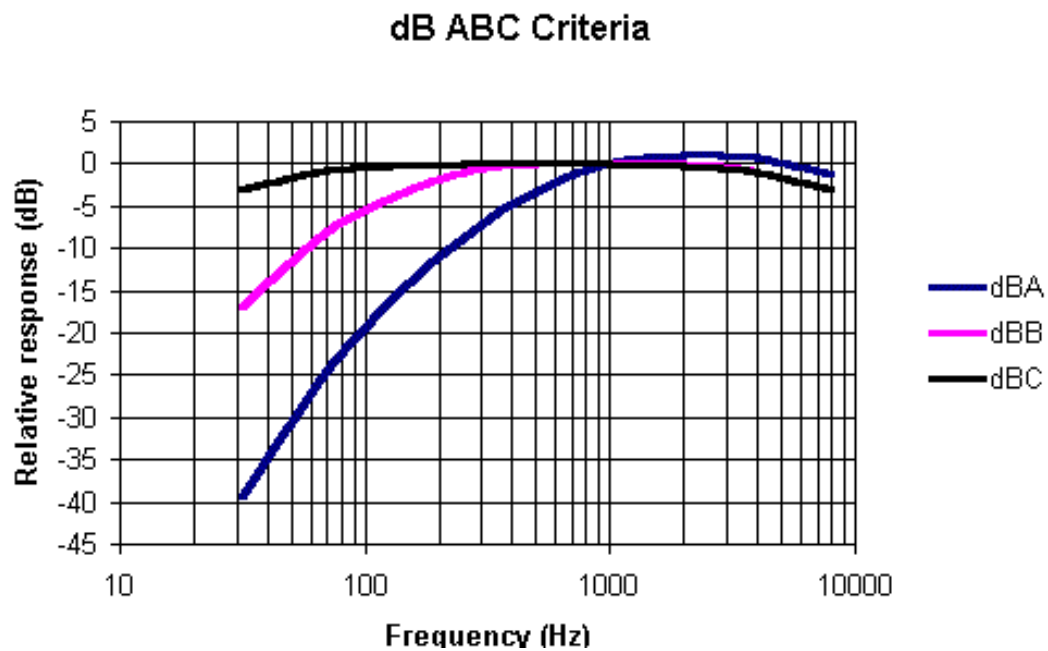
Table 3.2: Main dB filters frequency relative response.
(Derived from [19]).

Relative Response (dB)	Frequency (Hz)								
	31.25	62.5	125	250	500	1000	2000	4000	8000
dB(A)	-39.4	-26.2	-16.1	-8.6	-3.2	0	1.2	1	-1.1
dB(B)	-17	-9	-4	-1	0	0	0	-1	-3

dB(C)	-3	-0.8	-0.2	0	0	0	-0.2	-0.8	-3

3.2 Superposition of pure sounds and critical bands

When two different pure sounds are superposed, several effects take place, which can be grouped in two different categories: the 1st order effects are those elaborated by the internal ear, related to the mechanic elaboration, while the 2nd order effects are typically elaborated in a subsequent stage, linked to the neural elaboration.

The 1st order effects appear when, being the hearing stimulus constituted by two pure sounds with the same frequency and phase, the frequency of one of the two stimuli is gradually varied. A comprehensive overview on these phenomena has been provided by D. Drioli and N. Orio [18].

Considering two sounds of frequency respectively f_1 and f_2, being initially $f_1 = f_2$, till the frequencies and phases of the two sounds are identical, the basilar membrane shows an excitation in correspondence of the common frequency position, with an amplitude equal to the sum of the amplitudes of the two stimuli.

Then, when the frequency of one of the two stimuli starts to grow ($f_2 = f_1 + \Delta f$) and till Δf is less than a certain value Δf_d, the listener perceives a unique sound having frequency $f = (f_1 + f_2)/2$ amplitude modulated. This amplitude modulation is named 1st order beat, where the 1st order beat frequency is equal to $f_b = (f_2 - f_1)$, since the expression of the two sounds sum is:

$$\sin \omega_1 t + \sin \omega_2 t = 2 \sin \frac{(\omega_1 + \omega_2)t}{2} \cos \frac{(\omega_1 - \omega_2)t}{2}$$

(3.13)

Being $\omega t = 2\pi f t$, it is possible to observe that the argument of the sine determines the pitch of the sound:

$$f = \frac{f_1 + f_2}{2} = f_1 + \frac{\Delta_f}{2} \tag{3.14}$$

while the argument of the cosine is related to the beat frequency:

$$f_b = 2 \left(\frac{f_2 - f_1}{2} \right) = f_2 - f_1 = \Delta_f$$
(3.15)

Beats are thus considerable as phenomena of interference in time, since during a certain time there is an alternation of instants in which the waves sum in phase or in counter phase. A graphical representation of 1st order beats is depicted in Figure 3.4.
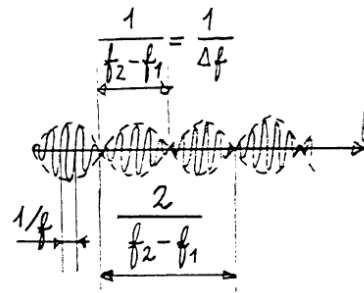
Figure 3.4: 1st order beats, beat frequency.

With the rising of Δf over the value of 15 Hz, the beat sensation disappear, being substituted by an unpleasant roughness feeling, conversely, when Δf overcomes the magnitude Δf_D, (discrimination threshold), the two sounds become distinguishable, even if the roughness is still present. Only when the module of Δf grows larger than a second threshold Δf_{CB}, the sensation of two different sounds is clear and pleasing.

The magnitude $2\Delta f_{CB}$ is defined as critical band, as is described in Figure 3.5, while Figure 3.6 shows the dependency of the pitch discrimination threshold Δf_D and the critical band threshold Δf_{CB} on the central frequency.
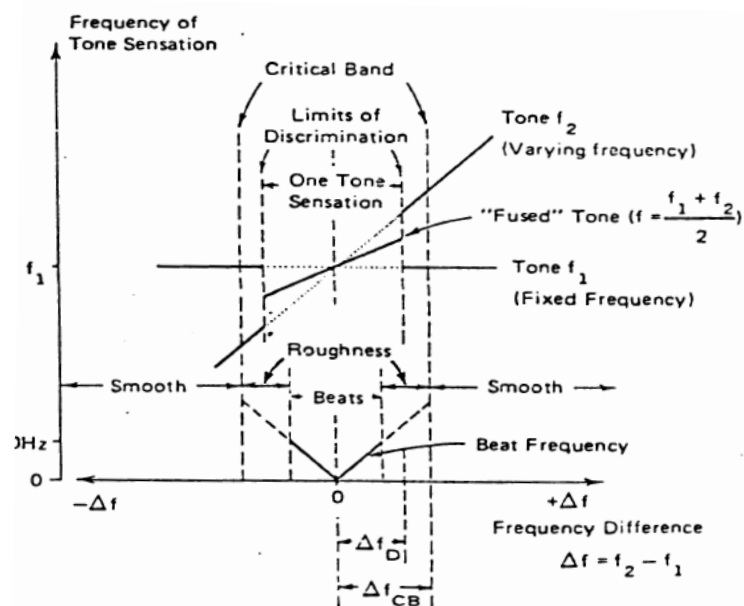
Figure 3.5: Hearing sensations trends varying the frequency.
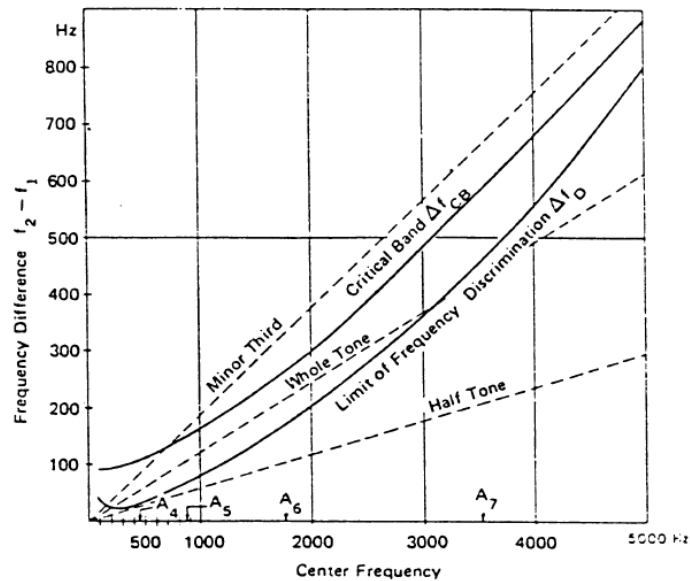
Figure 3.6: Critical band and pitch discrimination varying the central frequency.

In general, healthy, young people can hear sounds comprised in frequencies between 20 Hz - 20 KHz. Actually, while receiving the acoustic waves, the ear splits up sounds in this range into 26 unequal, overlapping partitions called critical bands which are logarithmically distributed and represent the physiological basis for masking effects.
 The evolution of the frequency and amplitude of the several bands along the Cochlea uncoiled length is depicted in Figure 3.7.
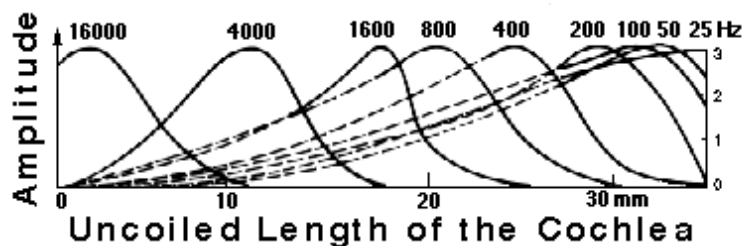
Figure 3.7: The bulging of the basilar membrane as a function of frequency.
(From [20])

3.2.1 The Bark frequency scale

Based on the results of many psychoacoustic experiments, the Bark scale is defined so that the critical bands of human hearing have each a width of one Bark. By representing spectral energy in dB over the Bark scale, a closer correspondence is obtained with spectral information processing in the ear.
The Bark scale ranges from 1 to 24 Barks, corresponding to the first 24 critical bands of hearing [21]. The published Bark band edges and band centre frequency are expressed in Table 3.3.

Table 3.3: Critical Bands.

Critical band	1	2	3	4	5	6	7	8
Centre Frequency [Hz]	50	150	250	350	450	570	700	840
Bandwidth [Hz]	100	100	100	100	100	120	140	150
Critical band	9	10	11	12	13	14	15	16
Centre Frequency [Hz]	1000	1170	1370	160	1850	2150	2500	2900
Bandwidth [Hz]	160	190	210	240	280	320	380	450
Critical band	17	18	19	20	21	22	23	24
Centre Frequency [Hz]	3400	4000	4800	5800	7000	8500	10500	13500
Bandwidth[Hz]	550	700	900	110	1300	1800	2500	3500

These centre-frequencies and bandwidths are to be interpreted as samplings of a continuous variation in the frequency response of the ear to a sinusoid or narrow-band noise process. That is, critical-band-shaped masking patterns should be seen as forming around specific stimuli in the ear rather than being associated with a specific fixed filter bank in the ear.

Note that since the Bark scale is defined only up to 15.5 kHz, the highest sampling rate for which the Bark scale is defined up to the Nyquist limit, without requiring extrapolation, is 31 kHz.

While human hearing generally does not extend above 20 kHz, audio sampling rates as high as 48 kHz or higher are common in practice.

The Bark scale is defined above in terms of frequency in Hz versus Bark number. For computing optimal bilinear transformations, it is preferable to optimize the fit to the inverse of this map, i.e., Barks versus Hz, so that the mapping error will be measured in Barks rather than Hz.

In Figure 3.8 the trend of the Bark scale bands in relation to the frequency is represented.
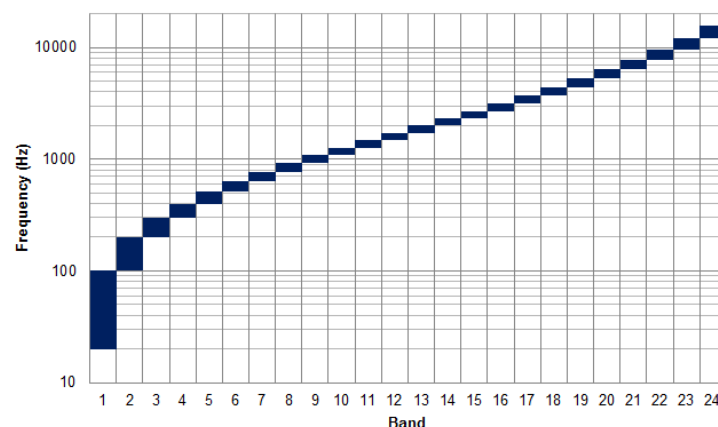
Figure 3.8: Bark scale.

3.3 Modern psychoacoustics and related magnitudes

In the modern psychoacoustic, the first approach consists in the production of acoustic stimuli, generally with the help of sophisticated digital techniques and algorithm for the signal elaboration. Then, following the DA conversion, the resulting signals are presented to the subjects by means of headphones or loudspeakers.

Afterwards, the subjects are invited to judge the attributes of the perceived sounds, such as the pitch, the volume, the tone, etc.

By these procedures, along the years, several psychoacoustic parameters were modelled, such as the loudness, the sharpness, the roughness, the fluctuation strength and the relative approach.

Usually, during extended psychoacoustic studies a particular sound is defined, which constitutes the optimal sound for a specific product, the so called target sound.

Essentially, product engineers task is to act on the physical characteristics of sound generation in order to get a result as near as possible with respect to the sound target previously defined. Several features of the signal can affect the acoustic environment evaluation: physical, psychoacoustic, binaural, cognitive ones.

Concerning the soundscape evaluation, as a first step binaural recordings are accomplished, then the sounds are analyzed and the psychoacoustic parameters are obtained together with the sound pressure levels.

Subsequently, the sounds are presented to a sample of subjects that express subjective judgments, at the end, possible correlation-ship between the psychoacoustic parameters and the subjective evaluations are researched.

Among the leader companies developing tools and software dedicated also to the acoustic analysis for vehicle testing, Siemens constitutes a major competitor, thanks to its product LMS Test.Lab, which has been exploited for this project along with the documentation about sound metrics and sound quality, that contributed in a deep manner to collect the information concerning this field of knowledge.

Moreover, relevant information has been collected from the study led by ARPA Piemonte about acoustics [22].

3.3.1 Loudness

Loudness expresses the volume sensation of a sound, correlated to the perceived energetic content of the sound. The evaluation criteria introduced by H. Fletcher is based on a binary comparison between pure tones, where a fixed frequency tone at 1000 Hz constitutes the reference one [23].

As a relevant observation, to define two sounds having equal intensity is not the same thing to state that they have equal loudness; indeed, since the human hearing sensitivity varies with frequency, it is useful to plot equal loudness curves which show that variation for the average human ear. If 1000 Hz is chosen as a standard

frequency, then each equal loudness curve can be referenced to the decibel level at 1000 Hz. This is the basis for the measurement of loudness in phons. If a given sound is perceived to be as loud as a 60 dB sound at 1000 Hz, then it is said to have a loudness of 60 phons [24].

 The criteria is the following: at 1000 Hz, the scale of the objective values L, in dB, coincides with the scale of the subjective levels P, in phon; first of all, listening tests allow to draw the isophonic curves; then, the results are collected in the audiogram normal diagram, whose shape depends on the listening conditions. The use of the phon as a unit of loudness has been an improvement over just quoting the level in decibels, though, was not a measurement directly proportional to loudness; thus, the sone scale was created to provide such a linear scale of loudness. It is usually presumed that the standard range for orchestral music is about 40 to 100 phons. If the lower end of that range is arbitrarily assigned a loudness of one sone, then 50 phons would have a loudness of 2 sones, 60 phons would be 4 sones, etc.

The relationship between loudness S in son and the perceived level P in phon is established by the ISO-131 [25] norm as follows:

$$S = 2^{(P-40)/10} \ [sone] \tag{3.13}$$

$$P = 40 + 10 * log_2(S) \ [phon] \tag{3.14}$$

Where 1 sone expresses the loudness of a pure tone at the frequency of 1 kHz and with an acoustic pressure level of 40 dB It can also be noted that the dependency of the loudness on the acoustic pressure is exponential. Figure 3.9 reports an example of isophonic curves diagram.
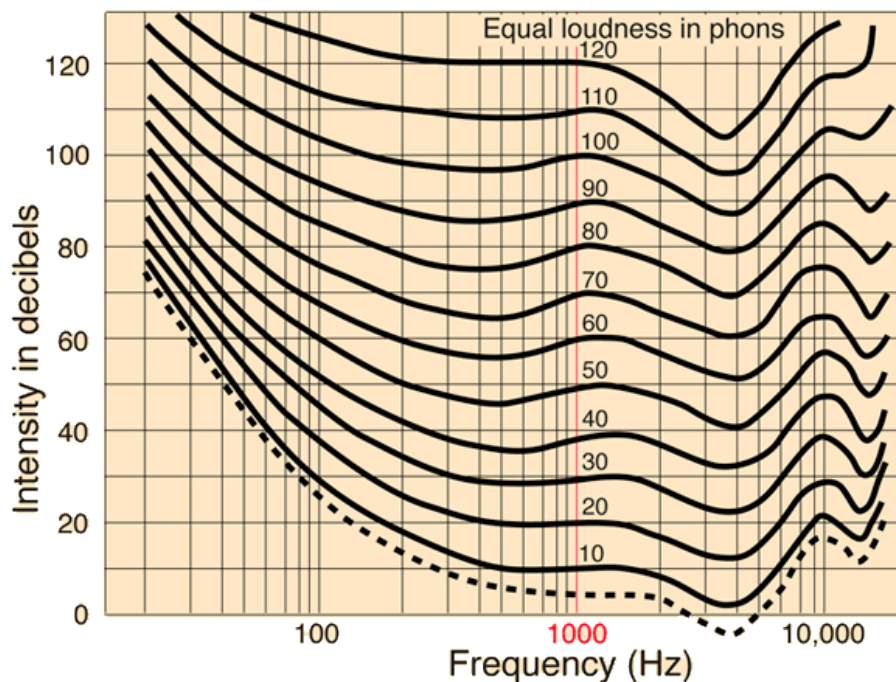
Figure 3.9: Isophonic curves, binaural listening in free field.

Considering sound loudness, a relevant factor to consider is the masking effect. Indeed, masking is the phenomenon according to which the perception of a determined acoustic signal results more difficult in presence of extraneous sounds that hide the signal intended to be listened. Taking into account these assumptions, complex sound loudness evaluation is not trivial, thus, ISO-R 532 [26]suggests two procedure about this issue, the Method A by Stevens and the Method B by Zwicker. In particular, Stevens method is based on the following hypotheses:

- The spectral component falling within the same critical band are summed in power with respect to the same subjective level; thus summing two contributes with same power the result is an increase of 3 phons.
- The spectral component falling within different critical bands are directly summed in terms of loudness, thus in S.

Besides, the process is composed of three main steps: firstly, the sound spectrum is analyzed by bands of 1/3 octave or 1 octave; then, for each band k, the loudness index S_k is determined from the graph; afterwards, the various bands contributes are summed taking into account the masking effect by exploiting the 3.1 formula.

$$S = S_{max} + F(\sum_{k=1}^{N} S_k - S_{max}) \ [son] \tag{3.15}$$

Where:
- S is the loudness of the complex sound [sone],
- S_{max} = max value of the N values of S_k, F corresponds to 0.15 for 1/3 octave bands and to 0.30 for 1 octave bands
- S_k represents the loudness index corresponding to the k band (k = 1:N)

Then, subjective level of the complex sound is computed with the formula 3.14.

$$P = 40 + 10 * log_2(S) \ [phon] \tag{3.14}$$

In Figure 3.10, the diagram provided by ISO 532 for calculating loudness is represented.
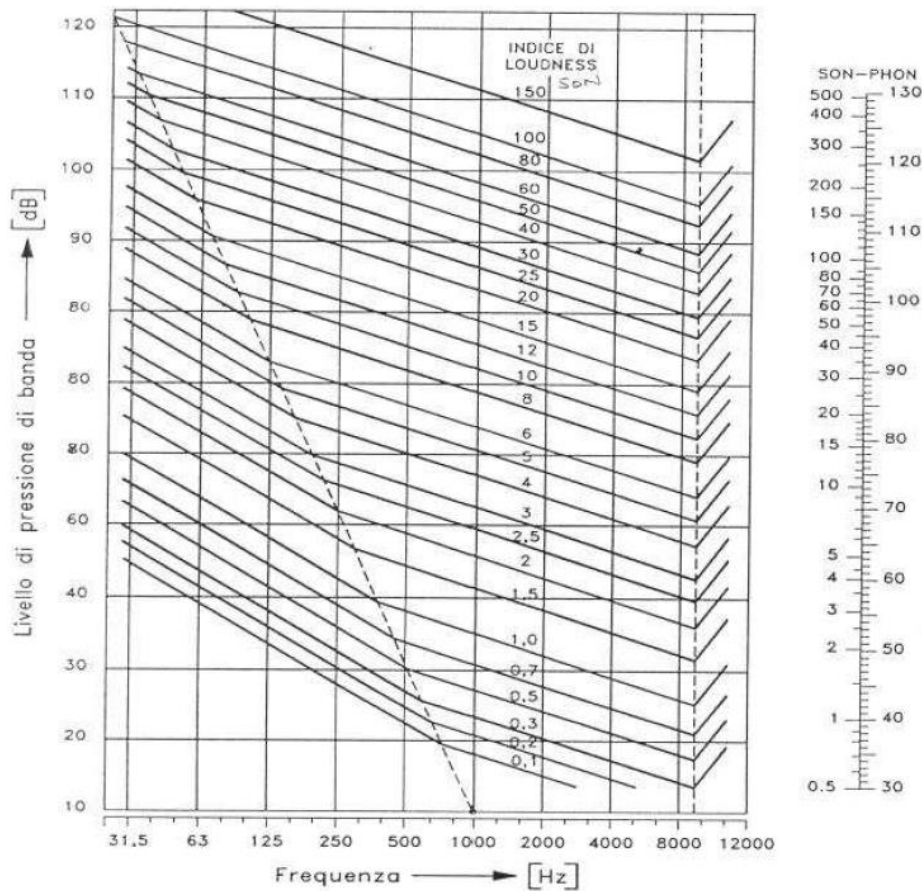
Figure 3.10: Diagram for the loudness computing according to ISO 532.

On the other hand, even if it is common to consider in acoustics the loudness expressed in dB, a better perceived loudness measure is obtainable by properly applying the critical bandwidths. In this case, the specific loudness is computable from the dB level of each third octave band, according to the assumption by Zwicker and Fastl [27] that "a relative change in loudness is proportional to a relative change in intensity". Thus, values of specific loudness N' expressed sone-per-Bark can be calculated using a power law; whereas masking curves can be constructed around these levels representing the effect of critical bands.

The final value for loudness N is then calculated as the integral, i.e. the area under the curve, presented in sones.

$$N = \int_0^{24 Bark} N' \, dz \tag{3.17}$$

3.3.2 Sharpness

Sharpness can be considered as a measure of the colour of the tone, denoting a certain aggressiveness and a feeling of power depending on the degree of the magnitude. The sharpness sensation is strongly related to the spectral content and centre frequency of narrow-band sounds and is not dependent on loudness level or

the detailed spectral content of the sound. Essentially, sharpness is the value of sensation caused by the high frequency of a noise, thus corresponding to the first spectral moment of the specific loudness, with a pre-emphasis for higher frequencies. The unit measure is the *acum*; one acum is related to a 1 kHz narrow band noise wide 150 Hz with a level of 60 dB. For narrow band noise, the sharpness rises with the value of the centre frequency and with the increment in dB level.

The specific sharpness calculation *S'(z)* is made according to

$$S'(z) = \frac{0.11 * N'(z)g(z)z}{\sum_{0Bark}^{24Bark} N'(z)\Delta z} \tag{3.18}$$

where:
- *N'(z)* is the specific *Zwicker* loudness
- *g(z)* a weighting function that pre-stresses higher frequency components
- *g(z)* has unit value below 16 Bark, (Figure 3.12), and rises exponentially as:

$$g(z) = 0.066e^{0.171z} \tag{3.19}$$
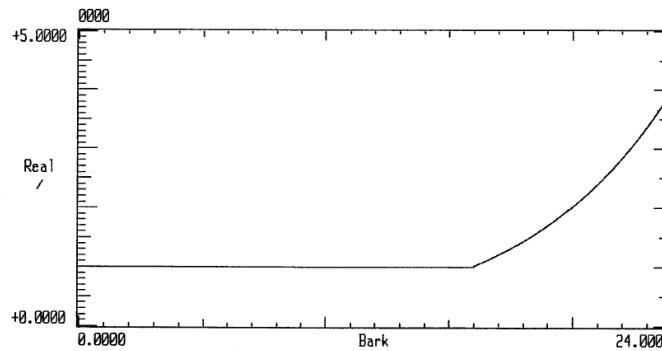
Figure 3.11: Weighting function for sharpness calculation

The total sharpness *S* expressed in acums is obtained by integrating the specific sharpness.

$$S = \sum_{0Bark}^{24Bark} S'(z)\Delta z \tag{3.20}$$

3.3.3 Roughness

Roughness is a magnitude useful to express the sportiness characteristic of automotive engine sounds. It is a hearing system feeling produced by relatively fast modifications caused by the modulation frequencies in the region 15 – 300 Hz.
The unit measure is the *asper*. Roughness *R* of a sound can be described by the product between the modulation depth ΔL and the modulation frequency f_{mod}:

$$R \approx \Delta L * f_{mod} \tag{3.21}$$

The value is expressed in dB/s, so the roughness is proportional to the speed of variation of the temporal masking model.
An example of the roughness model signal is depicted in figure 3.12.
The hatched part corresponds to the modulated signal in dB(level L_T).
The black curve is a sinusoid-like curve on which the masking depth(ΔL) and the modulation frequency (f_{mod}) can be measured to calculate the fluctuation strength according to equation 3.22.
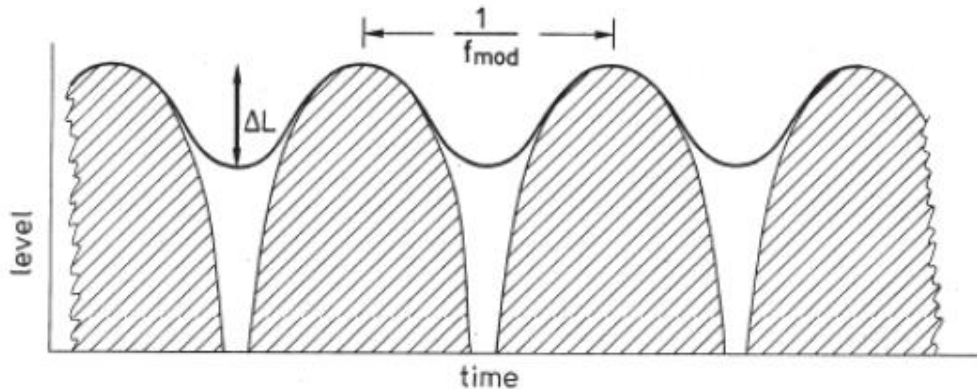
Figure 3.12: Graphical model of the roughness signal.

3.3.4 Fluctuation Strength

This magnitude is similar to the roughness, but reaches maximum peak at modulation frequency around 4 Hz. The unit measure is the *vacil*; in addition, fluctuation strength is particularly relevant for the speech, as 4 Hz is equal to the frequency of the envelope oscillation during a human speech. The expression 3.22 shows the dependency of fluctuation strength on f_{mod}.

$$F \approx \frac{\Delta L}{{}^{4Hz}/_{f_{mod}} + {}^{f_{mod}}/_{4Hz}} \tag{3.22}$$

3.3.5 Relative Approach

Nowadays it is a consolidated knowledge the fact that our hearing judges sounds based on relative comparison between the different characteristics on which it concentrates, instead of exploiting an absolute measure criteria, it works in an adaptive way. In fact, human hearing system creates a specific series of references based on recently heard sounds and subsequently compares new sounds with these reference models.
The relative approach model has been developed to implement an accurate analysis concerning the phonetic profile. Such model of relative analysis is available as function of the time (2D) and as function of the time and the frequency (3D).

The essential idea of this model is to determine an estimation of the signal by extrapolating the signal known history before the current instant, then subtracting the estimated value from the actual signal value.

The difference between the actual value and the estimated one is a measure of the signal variation. This analysis, thus, produces relative values; however, if an acoustic signal does not include characteristics distinct in time or in frequency, the relative analysis model will produce only very low values.

The unit measure is the compressed pressure quantity (Compressed Pascal).

3.3.6 Pitch

Pitch is defined as the sound attribute that help to classify different sounds from low to high; generally, when considering pure tones, it is strictly related to the tone's frequency, other than to is level, whereas taking into account complex tones it is possible to detect several pitches, which are correlated in large part to the frequencies of the many spectral components. Though, a relevant influence is exerted also by the masking effect, that can make certain pitches more prevalent than others. Moreover, both in case of pure and complex tones, pitches derivable from the signals spectral content are named spectral pitches.

On the other hand, virtual pitch is present when, considering complex tone characterized by a fundamental frequency and a number of harmonics, a pitch corresponding to the fundamental frequency is perceived, thus not relating anymore to the actual spectral components, but to the difference between higher harmonics.

Therefore, to determine how prominently pitch is perceived, the weight attribute has been introduced, calculating the true pitch if the tone level effect has been considered, or the nominal pitch if instead it has been neglected.

In 1937, Stevens, Volkmann and Newmann proposed a new unit measure, the "mel", defining the Mel scale as a scale of pitches judged by listeners to be equal in distance one from another. The reference in this scale is determined by equating a 1000 Hz tone, 40 dB above the listener's threshold, with a pitch of 1000 mels; besides, below about 500 Hz the mel and hertz scales coincide; conversely, above that, larger and larger intervals are judged by listeners to produce equal pitch increments. As a result, four octaves on the hertz scale above 500 Hz are judged to comprise about two octaves on the mel scale.

To measure the different pitch level, Pitch Unit scale is adopted, where the Pitch Units are strictly linked to frequencies and Pitch Shifts represent small variations of a specific frequency when the perceived pitch of a tonal sound is studied.

These variations are affected by the tone amplitude/level and by the masking pattern, when complex tones are taken into account.

Figure 3.13 illustrates the mapping between the linear frequency scale and the Mel scale, while Figure 3.14 depicts the mel scale as function of frequency.
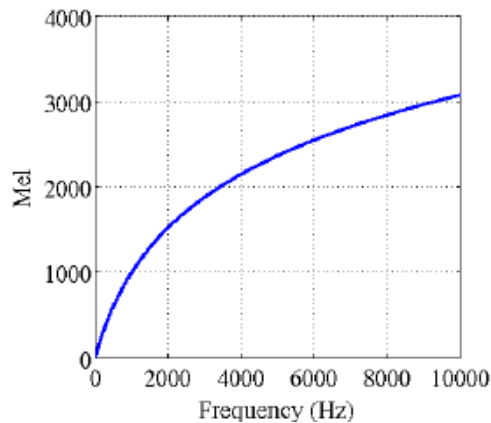
Figure 3.13: Mapping between the linear frequency scale and the Mel scale.
(From https://www.researchgate.net/figure/229087891_fig6_Figure-8-Mapping-between-the-linear-frequency-scale-and-the-Mel-scale)
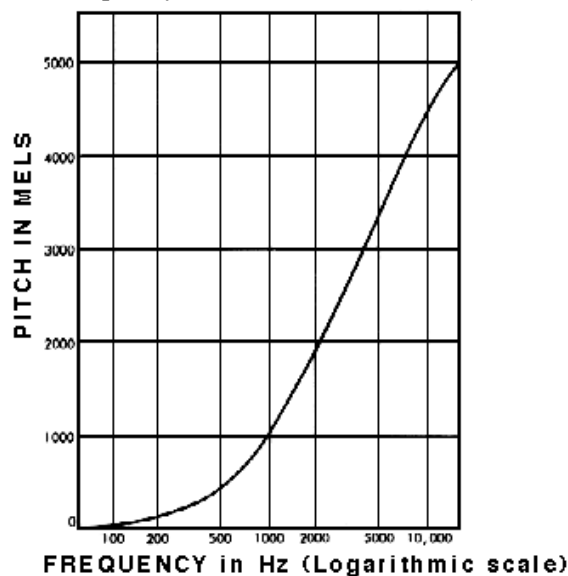
Figure 3.14: Mapping between the linear frequency scale and the Mel scale.
(From Appleton and Perera, eds., The Development and Practice of Electronic Music, Prentice-Hall, 1975, p. 56; Stevens and Davis, Hearing)

3.3.7 Tonality

Tonality is a metric regarding the tonal prominence of a sound, whose purpose is the evaluation of the possible presence of tones in the spectrum of a noisy sound.
In this regard, it is worth of notice that in a noise spectrum, the maximum tonality impression is given by a tone contribution at about 700Hz.
Therefore, it is logical that tonality is represented as a frequency dependent function. Conversely, the tonal attribute is applicable also to narrow-band noises, in these cases, the smaller the bandwidth is, the more tonal the noise seems.

The tonality metric is built from the model of W. Aures (PhD dissertation, TU Munich, 1984), while to identify tonal components, the model uses the method developed by Terhardt (J. Acoust. Soc. Am., vol.71, pp.679-688, 1982) for pitch extraction.

First, the spectral lines that are at least 7dB higher than their two lower and higher neighbours are isolated. A new spectrum, free of tonal components, is built by removing the detected sequences of five spectral lines, considered as pure tones. From both spectra, the fraction of the total loudness due to tonal components is calculated, which is denoted by W_N.

An extra weighting function, W_T, is determined from the pitch weights of the tonal components relevant to the pitch perception. This is a frequency dependent function such that at 700Hz the perception of tonality is maximal. Subsequently, a constant value C is added to scale the tonality results to standardize the result, i.e. such that a 1kHz sine tone at 60dB gives a tonality of 1 t.u. (tonality unit).

Finally the tonality is calculated in expression 3.23 as the combination of the three functions described above:

$$K = C * W_T^{0.29} * W_N^{0.79} \tag{3.23}$$

3.4 Recording techniques and equalization process

In psychoacoustic field, sound recording is performed by means of a binaural dummy, or artificial head; in fact, head is an obstacle for the mid-high frequencies, as from the far side respect to the sound source head shield the high frequency, while from the near side respect to the source there's an increase of the sound pressure at the mid-high frequency. Moreover, the shape of the external auricle causes sound reflections, that can cause phase destructive interferences at specific frequency.

To sum up, head and auricle cause peaks and attenuation of the frequency response of the sound received that vary depending on the angle of incidence of the sound and the source position. When the signals of the artificial head microphones are reproduced by the headphones, the same inter-aural differences perceived by the artificial head are listened to. Such realism cannot be obtained with conventional single omnidirectional microphones with linear frequency response.

After the recording phase, it may be desirable to reconstruct the binaural recording as if it was the original sound (as recorded by microphones in the sound field) and not as it is heard inside the head. In this case, you will need to 'undo' the modifications that were caused by the presence of the head.

To do this as accurately as possible, you need to "correct" with the inverse of the frequency response function of the head.

Applying this correction is called 'equalization'. Unfortunately, this transfer function depends on the type of field in which the measurement was done.

Typically the best approximation will be done based on one or a few of known equalization curves: 'free-field equalization' and 'diffuse field equalization'.

The third equalization method involves characteristics that are independent of direction, as usually the direction from which the sound comes is not really defined. When equalizing, the equalization curve that corresponds the best with the measurement situation should be chosen.

A free field (FF) refers to an idealized situation where the sound flows directly out from the source to the ears at normal incidence. There are no reflections. The measurement of a free-field equalization curve can be performed in an anechoic chamber or in a real free field as illustrated in Figure 3.15; this equalization curve should be used if the sound is in the free field and the source is in front of the head.
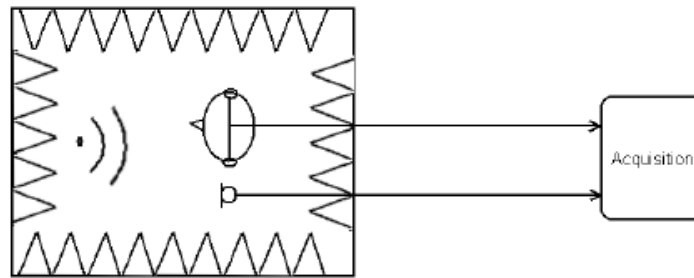
Figure 3.15: Free Field equalization: The ratio of the record from the microphone (at the head location but without the head present) upon the record from the artificial head (without equalization applied)) yields the free field equalization FRF.

Conversely, diffuse field (DF) occupies a smaller space and the sound is reflected many times, as depicted in Figure 3.16.
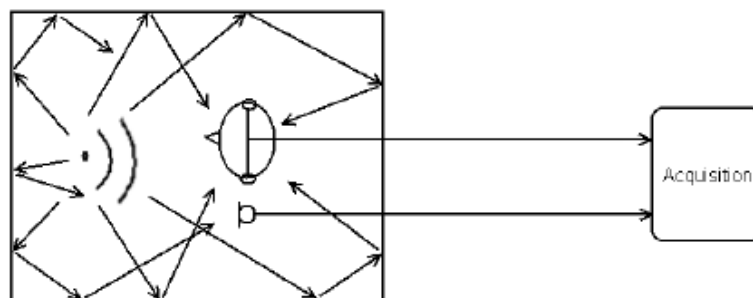
Figure 3.16: Diffuse Field equalization: The ratio of the record from the microphone (at the head location but without the head present) upon the record from the artificial head (without equalization applied)) yields the diffuse field equalization FRF.

On the other hand, the equalization typology independent of direction is a curve where the characteristics that are dependent on the direction of the source are removed. An equalization 'Independent of direction' is typically used if the sound field is neither free field nor diffuse field. This may happen in situations with several sources one cannot localize in a complex environment. Such kind of process is based on the modelling of the resonances in the ear canal and the Cavum Conchae, which are independent of direction.

3.5 Subjective evaluation methods in the listening tests

Among the several methods for evaluating in a subjective way the sounds during listening tests, the most commonly exploited are the random access classification method, which shows if a product has a better sound than a competitor, the semantic differential method, that gives indications on which sounds are suitable for transmitting a certain message, the category scaling and the magnitude estimation methods, helping to define how much the sound quality varies between different products.

Concerning the random access classification method, the subject job is to classify the sound in relation to a certain feature, e.g., ordering them considering their quality, as is depicted in Figure 3.17.

Figure 3.17: Example of the sound quality ordering by means of the random access classification method.

On the other hand, concerning the semantic differential method, a usual procedure consists in assigning specific attributes to a listened sound, that can be related to the suitability of a determined sound for a pre-set purpose, as an alarm signal, like it is reported in Table 3.4.

As far as the category scaling is concerned, such a method aims at the evaluation of the loudness. Generally, five to seven categories are considered, even though a numerical scale consisting of five classes subdivided in ten subcategories with score from zero to fifty points can also be exploited, as is represented in Table 3.5.

Table 3.4: Semantic differential table from an international study on alarm signals.

ADJECTIVE SCALES	
loud	soft
deep	shrill
frightening	not frightening
pleasant	unpleasant
dangerous	safe
hard	soft
calm	exciting
bright	dark
weak	powerful

busy	tranquil
conspicuous	inconspicuous
slow	fast
distinct	vague
weak	strong
tense	relaxed
pleasing	unpleasing

Table 3.5: Category scaling with seven categories on the right, five categories at centre, fifty subcategories on the left.

Too loud	5 categories	7 categories
50	Very loud	Very loud
-	loud	loud
-		slightly loud
25	neither soft nor loud	neither soft nor loud
-		slightly soft
-	soft	soft
0	very soft	very soft
Inaudible		

Considering the magnitude estimation method, its advantages are that it has an infinite resolution, without uncertainties on the maximum values.

Often, the magnitude estimation related with reference sounds is exploited to evaluate the sound quality of an audio device. As an example, two sounds are considered, A, defined the reference sound, B being the test sound.

During the test, the reference sound is maintained constant, while the test sound is varied; then, a numerical value is assigned to a psychoacoustic entity of the ref sound, as loudness; the job of the subject is to assign a numerical value to the test sound B, as depicted in Figure 3.18. This value should represent the correlation between the psychophysical entity of the test sound evaluated with respect to the reference sound. In some cases, the reference sound choice can affect the result of the magnitude estimation in a significant way, therefore, it is recommended to use at least two reference sounds, on with a large high value of the psychophysical entity examined, the other with a very low value.
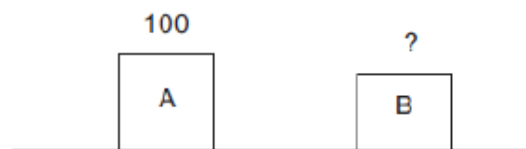
Figure 3.18: Graphical example of magnitude estimation.

3.6 Semantic and cognitive perspectives

During the sound evaluation, the meaning assigned to it while listening can affect the judgment. As the example reported in Figure 3.19, the same sound can be perceived differently by subjects with different cultural back-grounds.
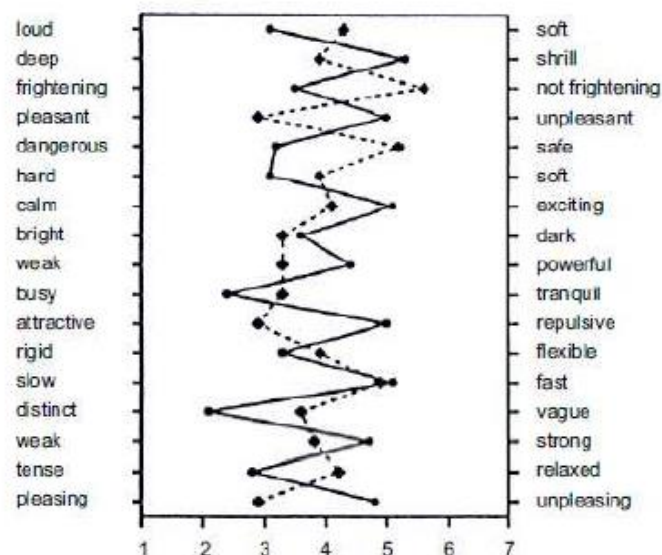
Figure 3.19: Semantic differential applied to a bell sound, data from Japanese sample study are linked by a solid line, data from German sample study are linked by dashed line.
(From [22])

To solve this inconsistency, a procedure to remove the majority of the information bounded to a stimulus has been developed.

From an original noise, the spectral analysis is executed by means of a FTT transformed, a technique using a temporal window corresponding to a frequency dependent on the bandwidth that simulates the frequency resolution of the human hearing system. In the subsequent phases, after the spectral broadening, consequently obscuring the spectral data, the sound is re-synthetized by means of an inverse FTT.

In such a way it is created a sound with the same spectral and temporal envelope and with the same loudness temporal trend but in which the information on the sound source have been removed.

It is worth of notice that some signals, as the FTT elaboration of the human speech, still maintain a large resemblance with the original sound.

Conversely, the evaluation of the sound quality can also depend on other senses solicitation, as the sight.

The procedure for spectral data obscuring can be observed in Table 3.6.

Table 3.5: Block diagram illustrating the procedure adopted to obscure information on the acoustic source.

Original sound
↓
FTT (Analysis)
↓
Spectral broadening
↓
Inverse FTT (Synthesis)
↓
Sound with same envelope, same loudness-time function, but whose source cannot be identified
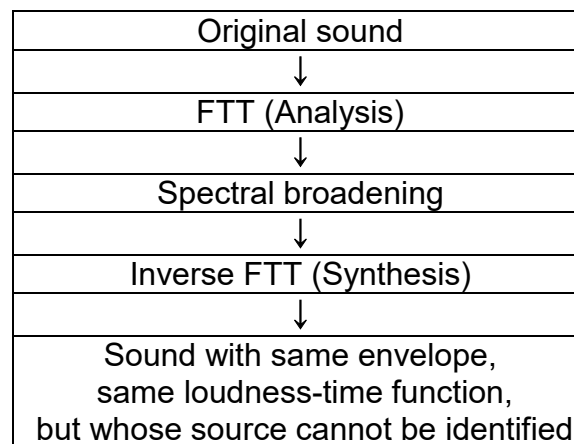
3.6.1 Disturb evaluation through the loudness

First step was the measurement of the SPL level weighted A with relatively cheap equipment, a better method was introduced by ISO with the regulation 532 [26], defining two methods for the subjective intensity evaluation.

The former method put in relation the loudness with the critical frequency bands, the latter procedure is function of the temporal evolution of the total subjective intensity, usually only measured by loudness meters.

Since loudness often depends strongly on time, a cumulative distribution is usually adopted, which can show the time percentage in which a certain loudness level is reached or overcome. The use of the calculus procedure for the loudness calculus is effective for the noise reduction.

Figure 3.20 shows a comparison between the perceived loudness sensation and an indicator of the measured pressure levels.
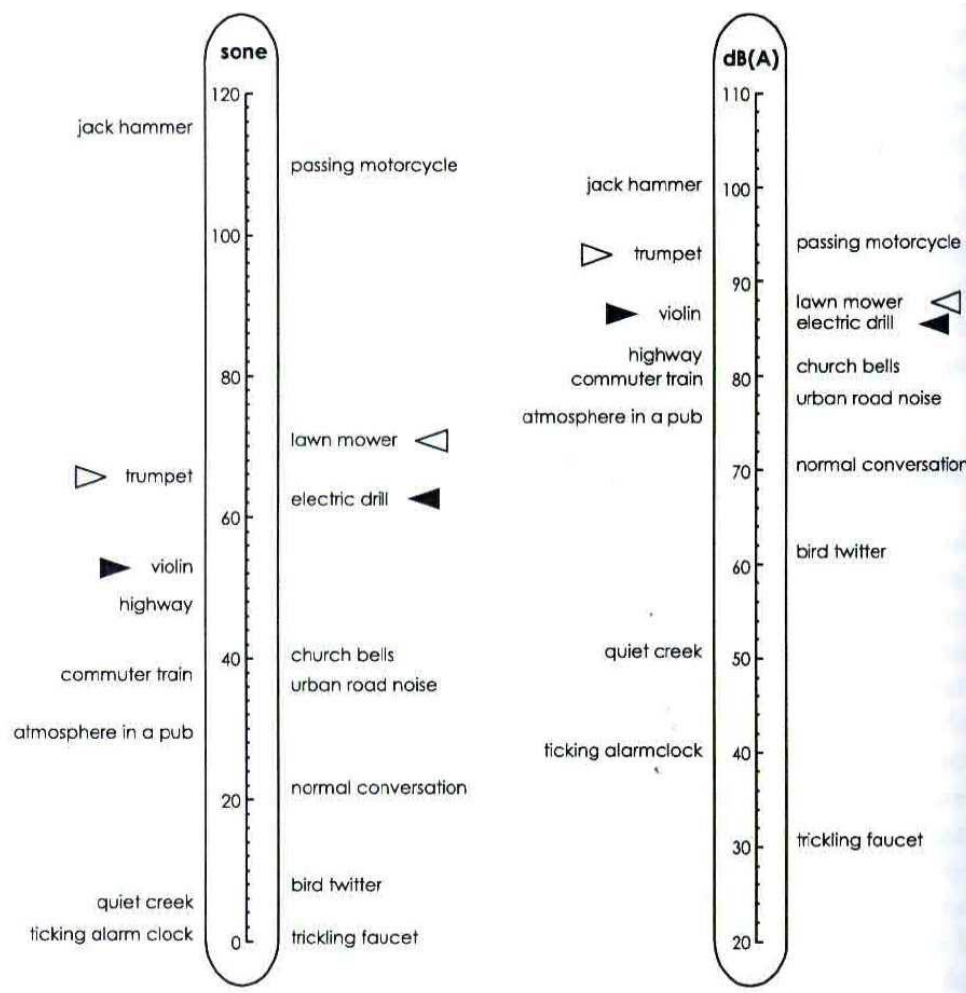
Figure 3.20: Perceived loudness(on the left), compared with the acoustic pressure levels(on the right). (From [22])

3.6.2 Noise emissions evaluation

The noise emitted from the different sound source can be subjectively evaluated by means of psychoacoustic experiments other than physically assessed by the use of noise measurement devices, as loudness meters.
For the subjective evaluations, usually the magnitude estimation method by means of a ref sound is exploited; for the physical measurement of the noise emission, it is recommended to consider the loudness percentile N5, even if, for a big number of emissions, the maximum loudness N_{max} provides almost the same values.
In synthesis, the loudness of acoustic emissions can be physically measured by a loudness meter in line with the subjective evaluations for the various noise typologies; on the other hand, the acoustic power weighted A, despite being often used for advertising, usually overestimates in a substantial way the differences in loudness.

3.6.3 Noise insertion evaluation

In psychoacoustic experiment, noise insertions often are evaluated by presenting to the chosen subjects specific acoustic stimuli 15 minutes long including a subtle background noise, together with a series of stronger events.

During these tests the subject has to indicate the instantaneous loudness varying the length of a bar showed on a pc monitor. At the conclusion of the test, the person is asked to fill a questionnaire in which the global loudness during the last 15 minutes must be indicted by assigning a length to a line.

In many cases the global loudness perceived corresponds to the N5 percentile of a loudness meter, thus to the loudness level reached or exceeded for the 5% of the measurement time. Another relevant feature from the perspective of noise insertions in environmental field is the sound propagation in external environment.

Figure 3.21 illustrates the trend of the different psychoacoustic parameters as function of the distance in free field, on the basis of the tonal noise and of broad band. it is clearly noticeable the different behaviour of these parameters decreasing the SPL-A.
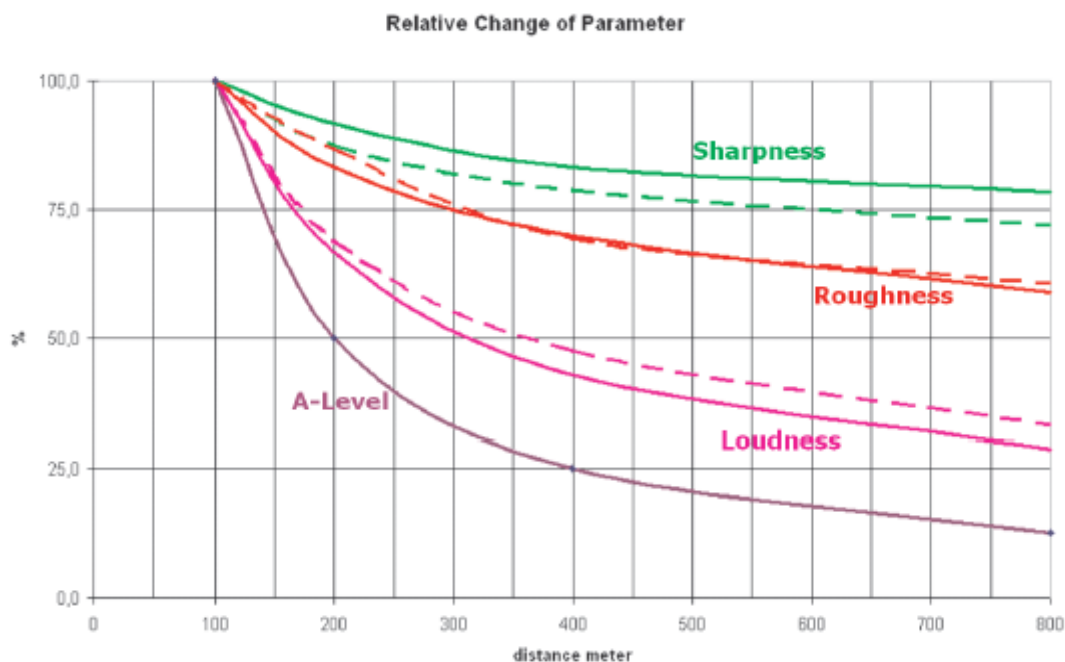
Figure 3.21: Evolution of the psychoacoustic parameters and of the SPL-A as function of the distance, for a pure tone (solid line) and of a broad band noise (dashed line).

3.6.4 Sound quality evaluation

As far as the sound quality is concerned, other than the acoustic features of the signal, the aesthetics and the cognitive effects can play an essential role. The psychoacoustic elements of the sounds considered as annoying can be described as a combination of hearing sensations called psychoacoustic disturb. More in detail, according to the studies performed by ARPA Piemonte concerning the best practices in the psychoacoustics field **[22]**, the psychoacoustic disturb magnitude, named *PA*, can describe quantitatively the judgments obtained in the psychoacoustic experiments. Essentially, the *PA* disturb depends on the loudness, the tonality and the temporal structure of sounds. According to the study performed by ARPA following empirical relationship between the psychoacoustic disturb , the loudness perception N, the sharpness S, the fluctuation strength F and the roughness R can be defined as in formula 3.23:

$$PA \approx N_5(1 + \sqrt{w^2(S) + w^2(F,R)}) \tag{3.23}$$

Where:

- N_5 is the percentile of the loudness in son

- $w(S) = (1.75 * S) * 0.25 \log(N + 10) \, for \, S > 1.75 \, acum$

- $w(F,R) = \frac{2.18}{N_5^{0.4}} * (0.4 * F + 0.6 * R)$

This formula enhances the correlation of the psychoacoustic disturb magnitude with the contributes of the sharpness, the roughness and the fluctuation strength that have to be taken into account by calculating an RMS average.

3.6.5 Articulation index

The Articulation Index is a parameter originally developed with a view to assuring speech privacy. Speech privacy can be defined as the lack of intrusion of recognizable speech into an area when background sound or noise then provides a positive quality of privacy. The measure of interference caused by noise to the masking of speech can be calculated by weighting the noise spectrum, in 1/3 octave bands, according to its importance to the understanding of speech.
From this weighted spectrum, the Articulation Index is derived. In Figure 3.22 a graphical description of Articulation Index is depicted.
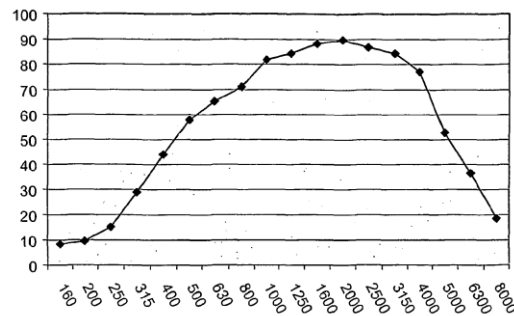
Figure 3.22: Graphical representation of the Articulation Index importance function values for average speech at 1/3 octave centre frequency [Hz], the sum of importance values is 1000. (From [28])

This index can then be related to a percentage of syllables understood. For complete privacy, an AI of 0.05 is the limit, for semi-privacy to discuss non-confidential matters, an AI of 0.1 is acceptable. In Figure 3.23, intelligibility of sentences as a function of articulation index is represented.
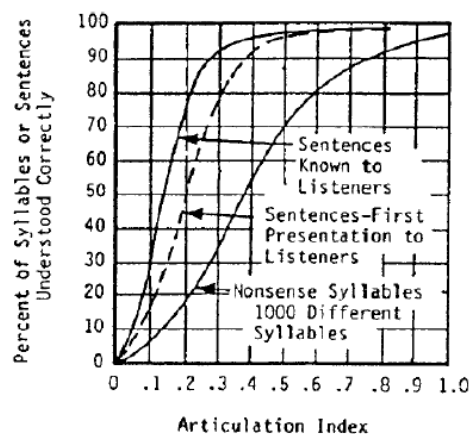
Figure 3.23: Intelligibility of sentences as a function of articulation index.

A quantitative measure of the intelligibility of speech consists in computing the percentage of speech items correctly perceived and recorded. An articulation index of 100% means that all speech can be understood, while a value corresponding to 0% means that no speech can be understood.

Articulation Index is commonly calculated from the 1/3 octave band levels between 200Hz and 4000 Hz centre frequencies, even though sometimes the max frequency considered is 6300 Hz. Each of the 1/3 octave dB(A) levels are weighted according to the following criteria:

- If A-weighted 1/3 octave level lies between upper and lower limits then it will be a linear value between 0 and 1.
- If value falls above the upper limit then result is equal to 0 for that particular 1/3 octave band.
- If value falls below the lower limit then result is equal to 1 for that particular 1/3 octave band.
- Multiply all of the calculated values by the AI weighting and sum all the values to get the AI in percentage terms.

In Table 3.6 below the reference table for assessing AI is reported:

Table 3.6: Intelligibility of sentences as a function of articulation index.

1/3 Octave Centre Frequency Hz	AI lower level dB(A)	AI upper level dB(A)	AI Weighting
200	23.1	53.1	1.0
250	30.4	60.4	2.0
315	34.4	64.4	3.25
400	38.2	68.2	4.25
600	41.8	71.8	4.5
630	43.1	73.1	5.25
800	44.2	74.2	6.5
1000	44.0	74.0	7.25
1250	42.6	72.6	8.5
1600	41.0	71.0	11.5
2000	38.2	68.2	11
2500	36.3	66.3	9.5
3150	34.2	64.2	9.0
4000	31.0	61.2	7.75
5000	26.5	56.5	6.25
6300	20.9	50.9	2.5

In automotive specific testing, A.I. is adopted to verify the quality of the noise in cabin, allowing to quantify the disturb caused by a determined noise on a conversation in the vehicle. In many cases, the band considered by automotive sector magazines is the one corresponding to the 200 – 5000 Hz range, while the A.I. assumes value from 0 to 100, corresponding respectively to the maximum disturb and to the minimum one.

Figure 3.24 below represents a comparison between the several A.I measured for different vehicles varying the speed, as obvious, the trend is decreasing increasing the velocity, due to the aerodynamic and rolling resistance prevalence.
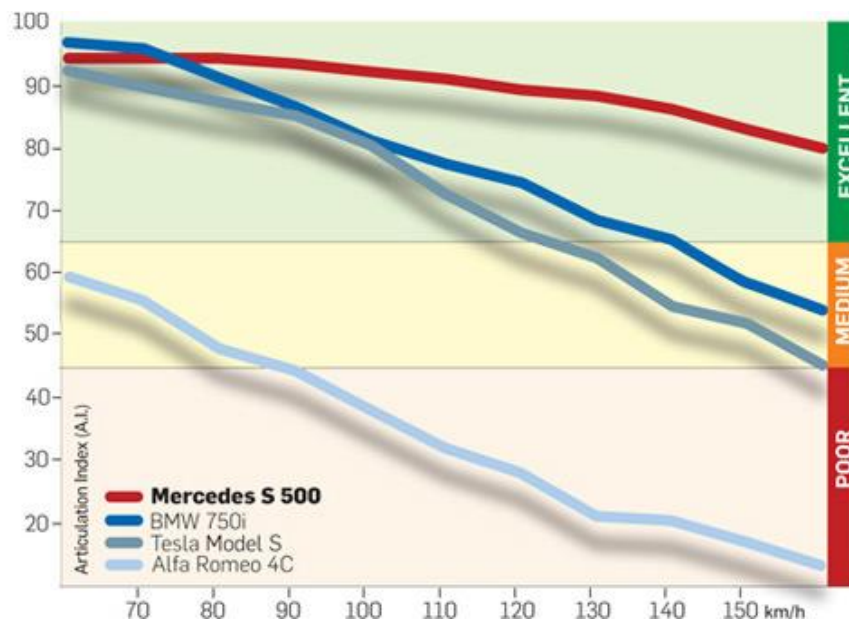
Figure 3.24: Articulation index comparison between four different cars.
(From: Travelling in Silence – Mercedes S500, by Alessio Viola on Quattroruote, October 1, 2014)
(Available from https://www.autox.in/quattroruote/mercedes-s-500/)

3.6.6 Speech interference level (SIL, PSIL)

When the comprehension of speech is the goal, background sound or noise has the negative quality of interference. It can cause annoyance, and even be hazardous in a working environment where instructions need to be correctly understood; therefore, a noise rating called 'Speech Interference Level' (SIL) was developed.

Beranek originally defined it as the arithmetic average of the sound pressure levels in the bands 600-1200, 1200-2400 and 2400-4800 Hz [29].

Since the definition of the new preferred octave band limits, this definition was changed to the Preferred Speech Interference Level' or PSIL, defined as the average sound pressure level in the 500, 1000 and 2000 Hz octave bands.

In 1977, Speech Interference level was standardized as ANSI S3.14-1977(R-1986).

The application of the SIL to the actual understanding of speech has been presented in several graphs and tables, which show the relationship between SIL and the conditions under which speech can be understood.

As an example, Figure 3.23 shows the relationship between ease of face-to-face conversation with ambient noise level in PSIL, and separation distance in meters.
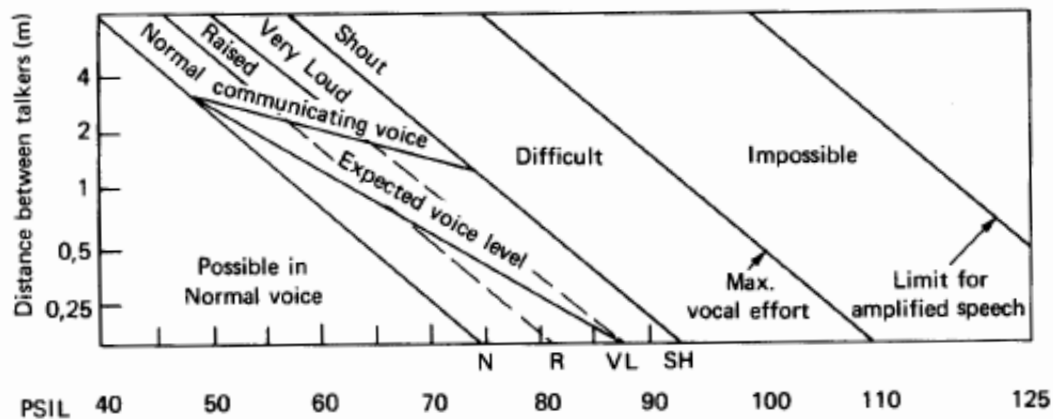
Figure 3.25: Communication limits in the presence of background noise.

4 Experimental setup and techniques for NVH analysis

As a first assumption, it is important to consider that internal vehicle noise does not depend only on the acoustic and vibration sources; key roles are also played by the different transmission paths between the sources and the receivers.

As mentioned before, the two different categories of transmission paths in a vehicle are related to completely different mechanisms of energy transmission: structure-borne and air-borne paths. Commonly in a car, the structure-borne noise transmission path dominates at low frequency (<200 Hz), while the air-borne noise transmission path dominates above 500 Hz. In the mid-frequency range, both transmission paths have usually the same level of importance.

In order to implement an improvement process of NVH performance of a vehicle, the knowledge of the main noise sources and the transmission paths represents a fundamental aspect.

4.1 Common procedures for human vibration assessment

Taking into account the measurement flow, there is a sequence of steps in between the mechanical oscillation and the final numeric values forming a measurement [1]. The simplest way of considering these steps is to group them into a "black box" with the input of the physical quantity and the output of the desired measurement presented on a display (Figure 4.1a). Such of an ideal utopian black box consist of a transducer, some signal conditioning and at least some basic signal processing.

A practical system is illustrated in Figure 4.1b.

First, a transducer must be attached to the vibrating surface, then this transducer, in most cases being an accelerometer, converts the mechanical oscillation into an electrical property, as a variation in the electrical resistance of the accelerometer.

Afterwards, the signal conditioning, which is attached to the transducer by a cable, converts the electrical property into a voltage that can be processed.

Subsequently, modern vibration-measuring equipment converts the voltage into a digital signal on which complex calculations can be carried out.

Actually, when a human vibration assessment is made, the final measurement depends on a reliable flow of the signal.

This includes not only the main components of the system but also the connections, as mistakes can be made even before the vibration affects the electromechanical properties of the accelerometer if it is not mounted to the vibrating surface adequately, or if the wrong surface is measured.

In order to avoid this issue, the accelerometer must be appropriate so that the important frequencies are properly measured: low frequency vibration should be measured for motion-sickness assessments; intermediate frequencies should be analyzed for whole-body vibration assessments; high frequencies should be examined for hand-transmitted vibration assessments.

A good quality cable should be used to connect the accelerometer to the signal conditioning; otherwise, unwanted electrical noise can be inadvertently added to the wanted signal, reducing the fidelity of the measurement.

Moreover, care should be taken to reduce any unnecessary cable movement as this can also interfere with the signal due to phenomenon known as the "triboelectric effect." Signal conditioning must be matched to the accelerometer type, and signal processing must be matched to the signal conditioning.

Although it is possible to combine some elements of vibration-measuring components into "single-box" solutions, as the human vibration meter in Figure 4.1c, these still internally contain the same components as the full expanded system. Conversely, the user must still ensure that each part is set up appropriately, which can mean navigating through multilayer menus within the device software.
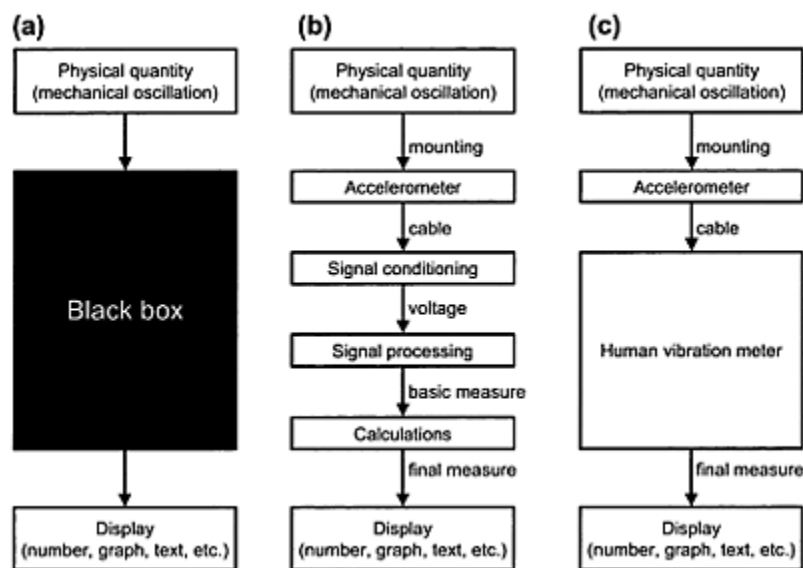
Figure 4.1: Component parts of human vibration measurement systems represented as (a) an idealistic "black box" solution, (b) a modular system constructed from component parts, and (c) a system using an integrated human vibration meter.

Talking about general methods about WBV evaluation in vehicles, most recurrent procedures are based on the acceleration measurements at three main zones on the driver's seat, by exploiting accelerometers to compute the vertical vibration on the floor below the seat, the longitudinal, lateral and vertical excitation on the seat cushion and the fore and aft vibrational stress on the backrest of the driver seat. According to ISO 10326-1 [20], measurements are usually performed at the driver seat interface by installing mutually perpendicular accelerometers in a semi-rigid mounting disc, to measure tri-axial excitation on the seat, whereas another accelerometer is mounted inside a similar disc to assess longitudinal vibrations on the seat backrest. The signals from the accelerometers can be acquired into a digital computer-based data acquisition and analysis system.

 Afterwards, the acceleration waveforms may be low-pass filtered at 100 Hz via anti-aliasing filters with an elliptical characteristic and then digitized, as with a PCL-818 analogue to digital converter, with a certain sampling rate.

It is important to have always in mind that the test vehicles should necessarily be operated in the normal work appropriate to each vehicle. A practical guideline about human vibration analysis process is contained in the Mansfield's compendium [1].

4.1.1 Human vibration meters

In most cases, the critical focus of the attention is on the vibration transmission from the vehicle floor, at the seat base, to the seated driver via the driver's seat and the driver's buttocks. Regarding this topic, it is simple to observe that, generally, both translational and rotational vibration components are present, though, the most often evaluated components are the former ones, located in mutually perpendicular axes.

For attended measurements, companies dealing with vibrational analysis provide the so-called human vibrometers, which constitute special-purpose vibration measuring instruments having to comply with the ISO 8041:2005 standard [6].

An increasing number of "human vibration meters" have come onto the market since the 1990s. Their development has been prompted by an increased demand for basic vibration measurement, largely in response to the development and implementation of the European Union Physical Agents (Vibration) Directive.

Some meters are designed for assessment of hand-transmitted vibration only, while others are more generally applicable. Many are based on sound-level-meter technology and it is possible to purchase a single device that can be simply converted from a sound-level-meter to a hand-transmitted vibration meter. Most meters are not able to store the acceleration waveform, and so the user is unable to examine the nature of the signal and the fidelity of the measurement.

Although meters can be easy to use, it is important to guarantee that their configuration is correct, cause frequency weightings, axis multipliers, calibration factors, analysis methods and many other possible variables must all be programmed appropriately for a valid assessment to be carried out.

 For basic measurements, meters might be simpler than modular systems, but there is still scope for methodological errors. As the waveform is not stored on the meter, it is impossible to investigate why some measures might be abnormally high or low, thus, it is fundamental to avoid measuring non-vibration artifacts such as mounting or repositioning of the accelerometers or events such as drivers occupying or leaving the seat. Regarding the current state of the art for field vibration acquisition systems, tri-axial ICP accelerometers are preferred; usually, one is applied under the seat, while another one, whose purpose is to measure the vibratory input with respect to the seated person, is put in a specifically designed seat pad, respecting the ISO 10326-1:2016 [20] regulation, that is the reference standard also for EN 30326-1:1994 normative. The meters should include the appropriate frequency weightings: at least W_h for hand-transmitted vibration; W_d, W_k, and possibly W_b for whole-body vibration; W_f for motion sickness.

 On the other hand, if the meter is only required for one type of assessment, then it is unnecessary to purchase a device with frequency weightings suitable for all types of environments.

Among the different instruments available, some meters allow to measure more than one direction of vibration simultaneously, while others are restricted to making multi-axis assessments by sequentially measuring each direction. As a matter of fact, tri-axial assessments is required by the standards to be made for both hand-transmitted and whole-body vibration.

Therefore, it is possible to substantially reduce the testing time required by exploiting a multichannel meter suitable for measuring at least three axes simultaneously.

Actually, for non-stationary signals, it is not appropriate to measure each direction separately. In most cases, indeed, the capability to measure six channels simultaneously is really useful: referring to hand-transmitted vibration assessments, this allows for measurement of both hands at the same time; while for whole-body vibration assessments, measurements can be made both on the seat surface and base, allowing for calculation of the SEAT value.

Finally, the capital requirement for a measure instrument is to be usable by the operator, as in some cases ergonomic principles for good software design can be overlooked by some manufacturers. Regarding this issues, when considering an instrument for purchase, practical experience may be really important for making an assessment of the ease of use; hence, all common tasks should be simulated, including setting up, calibration, measurement, and data transfer.

4.1.2 Data acquisition systems

If a system more flexible than a vibration meter is required, then a modular data acquisition system can be assembled. Within a modular system, the output from the accelerometer is converted to a voltage signal using appropriate signal conditioning. This voltage is the property that the system can measure and analyze.

Data-acquisition systems are usually computer based, although some stand-alone data loggers are available. These have the capability of sampling a voltage, i.e., the conditioned acceleration, at discrete time intervals such that the waveform of the voltage can be stored on a computer. The stored waveform can then be analyzed using any compatible software. If any anomalies have occurred within the measurement, then these can be viewed to help provide an explanation.

Usually, devices are capable of sampling on more than one channel simultaneously; many are 8 or 16 channel systems, allowing for 8 or 16 vibration measurements to be made simultaneously. For each tri-axial measurement, three channels are required.

Most computers require an additional interface to measure voltage with the precision required for vibration analysis. These interfaces can be internal, e.g., PCI cards and PCMCIA cards, or external, e.g., USB, parallel and serial.

Generally, a pocket Personal Digital Assistant (PDA) with an auxiliary battery pack and an extended memory may be used together with an external PCMCIA data acquisition card. Moreover, in case positional data for the use in laboratory are required, a Global Positioning System(GPS) is used, usually integrated within the PDA.

The typical process consists in storing the continuous data streams acquired in various test runs in the PDA, then downloading to a PC equipped with a proper post-processing and elaboration software after each testing to process the raw collected

data according to the standards used in the assessment of the human body vibration influence and in the seating dynamics research.

4.1.3 Strategic planning of approach and collation and calibration of equipment

The first step of the overall vibration measurement and assessment procedure is to confirm an appropriate strategy. An assessment might be for a motion sickness, hand-transmitted vibration, or whole-body vibration application, or a combination of more than one of these. The frequency range of the vibration to be assessed depends on the application area, and this often dictates the type of accelerometer and hardware to be used. It is essential that the correct
frequency weightings are available. The assessment might be a simple check to establish compliance with a guidance or regulation, in which case a simple human vibration meter might be adequate, or the assessment might need more in depth analysis whereby a data acquisition system will be required.

At this strategic stage of the measurement process, it is useful to clearly identify which methodology in which version of which standards are to be used for the assessment. Once the appropriate measurement strategy has been decided, the required measuring instrumentation will need collation and calibration.

A preliminary calibration can be carried out at the office or laboratory.

This approach has the advantage of giving the investigator confidence that hardware and software settings are nominally correct, thereby reducing time on-site for configuring equipment. It also has the practical benefit of functionally testing all equipment prior to leaving for the site visit. Calibration should also be checked immediately prior to the measurement itself on site, where minor adjustments might be necessary.

4.1.4 Mounting of accelerometers

For whole-body vibration field measurements, accelerometers should be mounted on the seat surface and possibly on the floor, beneath the seat or at the feet, and at the backrest. If measures are to be made on the surface of a compliant seat, then seat accelerometers should be mounted in a flexible disc, (Figure 4.2). This disc is sometimes referred to as an "SAE pad" due to its first appearance in a Society for Automotive Engineers standard (SAE, 1973), although it is now also defined elsewhere [30].
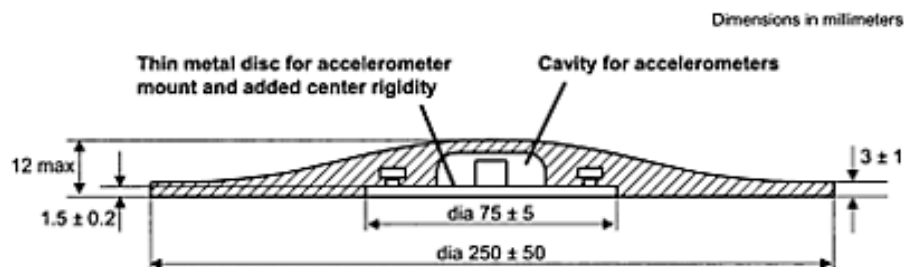
Figure 4.2: Design of flexible disc for mounting seat accelerometers as defined in ISO 10326-1.

The disc has a diameter of 25 cm and the accelerometer is mounted onto a 7.5 cm diameter thin metal disc in the centre of the device. The mounting device is placed onto the centre of the seat cushion, as represented in Figure 4.3.

Figure 4.3: Flexible disc containing accelerometers mounted on a forestry machine seat.

When the seat occupant sits on the disc, his or her body weight presses the metal part of the disc onto the surface of the seat so that the accelerometer measures the vibration in the seat centre. The flexible part of the disc deforms to the contour of the occupied seat and allows for the accelerometer to be sat on without causing excessive discomfort. The same pad is also sometimes used for measurement of backrest vibration, where it is fixed to the seat back.

 Several discs contain a tri-axial accelerometer set, in which case the disc must be orientated such that the x-accelerometer is aligned in the x-direction.

To measure seat transmissibility, accelerometers must also be mounted beneath the seat. Ideally, these should be mounted on the floor directly beneath the seat pad on which the seat occupant sits. However, for many vehicles there are practical difficulties with mounting on the floor beneath the seat.

Therefore, accelerometers are sometimes mounted on seat guides and at seat mounting points. Ideally, measurements should be made at many points and mathematical techniques used to calculate the vibration beneath the centre of the seat. However, if it can be assumed that the floor is rigid and that there is negligible pitch and roll vibration, then a mounting point on one seat guide will suffice.

Nevertheless, as many vehicles have trim and covers that must be removed to gain access beneath the seat, this can prove to be a really challenging process.

Regarding joining and mounting techniques, floor accelerometers can be mounted using cyanoacrylate adhesive, double-sided adhesive tape, magnetic fixings, beeswax, or clamping using hose clips. The essential quality of the fixing method is that it must be rigid in the frequency range of interest.

For hand-transmitted vibration exposures, measurements should be made at the hands, ideally in the middle of the grip. Some tools have two clearly defined handles, whereas other one only have one handle, where a trigger might be located, and require the other hand to guide the tool by holding the tool body.

In some situations, the vibration is transmitted to the operator through the work piece and not through the tool itself, e.g., pedestal grinding.

The general principle of measurement at the centre of the hand contact surface should be applied wherever possible, although practical difficulties might require a compromise of mounting accelerometers adjacent to the contact point.

Suggested measurement locations are published in ISO 8662-2 to ISO 8662-14 and ISO 5349-2, as illustrated in Figure 4.4.
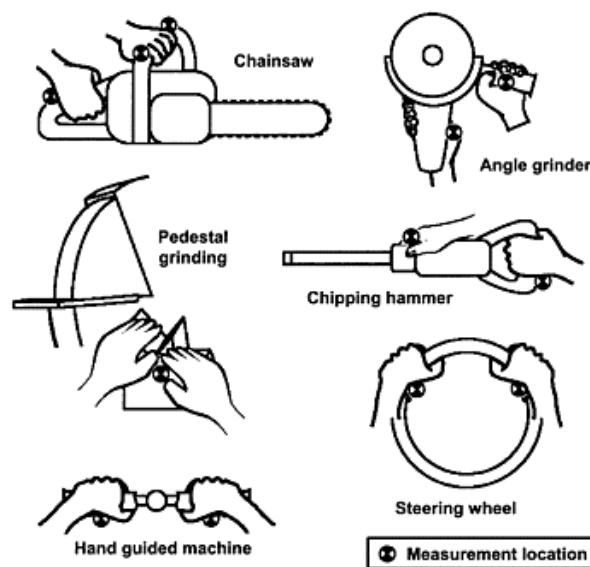
Figure 4.4: Examples of practical measurement locations for some common power tool types.
(From BS EN ISO 5349-2, 2002)

In the field of HTV analysis, special care must be taken to ensure that transducers, mountings and their associated cables do not compromise the safety of the tool operation.

The physical mounting of the accelerometers for hand-transmitted vibration applications can be achieved by a variety of methods.

Essentially, the accelerometers can either be mounted to the tool (or work piece) or they can be mounted onto handheld adapters that are located between the operator's hands and tool. Some methods of fixing to the tool can cause minor damage to the tool handle but provide a convenient mounting point.

These include using a threaded mounting stud screwed into the tool and accelerometer or using cement, possibly in combination with a disposable mounting stud; see Figure 4.5.
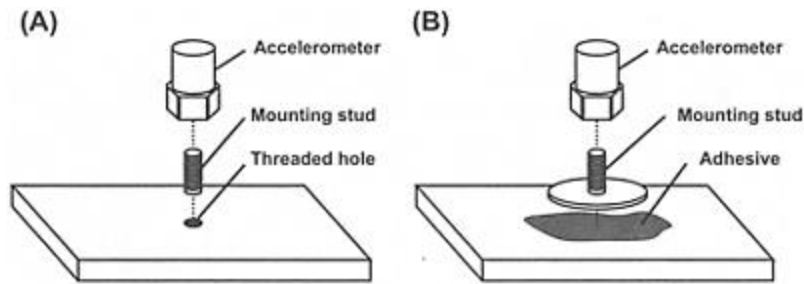
Figure 4.5: Methods of mounting an accelerometer to a tool using a stud A, or glue/wax (B).

An alternative, but more bulky, method of fixing accelerometers to the tool is to use mounting blocks clamped in place using hose clips, see Figure 4.6.
 Handheld adapters can be used in situations where fixing to the tool is inappropriate , e.g., the handle of the tool might be covered in a compliant hand-grip).
The adapters either contain an accelerometer or an accelerometer mounting point and are pushed onto the tool by the gripping force of the operator. For instance, the "palm adapter" used for measurement of the dynamic properties of anti-vibration gloves can be used as a handheld adapter.
 Considering common issues related to measurement, it is quite common that high-frequency high-magnitude impulsive vibration can affect the materials from which the accelerometer is constructed, this is a peculiar issue especially for measurements of vibration on impulsive and percussive tools. These specific phenomena are defined as "DC shifts", which may be observed in the time domain either as instantaneous changes in the offset of the accelerometer or as an exponential decay, due to the functioning of band-pass filters in the signal conditioning, see Figure 4.7.
If DC shifts occur, then a low-frequency artefact will occur in the measurement and this will severely affect the values obtained in the vibration assessment, especially when the signal is W_h weighted. To reduce the occurrence of DC shifts, a mechanical filter should be mounted between the accelerometer and the mounting point, such vibration isolation devices are exploited for transmitting the low frequencies of interest to the accelerometer but protecting it from the shocks, see Figure 4.6C
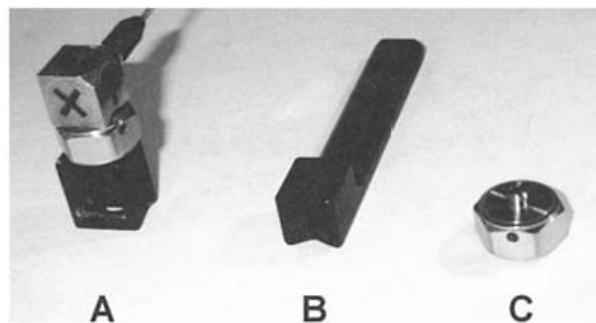
Figure 4.6: Methods of clamping an accelerometer to a tool. By using a hose clip (A), by the gripping force using a hand-adapter (B). or using a mechanical filter in case of DC shifts risk (C).
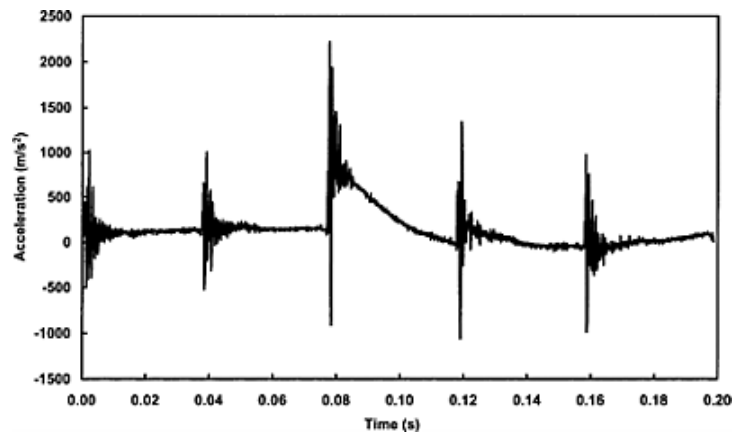
Figure 4.7: Acceleration measured on the handle of a pick hammer showing a DC shift at about 0.08 s followed by an exponential decay due to the characteristics of the filter in the signal conditioning.

4.1.5 Measurement of the vibration

Once all equipment is calibrated, mounted, and connected, the measurement itself has to be investigated, first of all by checking that all settings and configurations are correct, then verifying that the appropriate frequency weighting has been selected and that antialiasing filters are set correctly, as these might have been switched off during the calibration process.

As far as human vibration meters are concerned, the internal memory buffer should be reset so that previous measurements are not inadvertently included in the new analysis. During the measurement, indeed, the meter's display should be monitored to ensure a good signal and that no overloads occur.

Conversely, gain settings might need adjustment if the signal level is too high or too low. After each measurement, the results should be noted and stored in the meter. Then, concerning data-acquisition systems, the signal should be checked to ensure that the full range of the measurement hardware is used and that the signal has not been clipped. Subsequently, the data should be saved within the system and notes made to ensure unique identification of each measurement.

Furthermore, as a final step it is recommended to use one of the several systems for implementing descriptors to be added to each file.

Figure 4.8 depicts sensors and computing tools part of a compact measurement system for automotive applications.

Figure 4.8: Photo of measurement sensors (a) and the of box with laptop (b).
(From [31])

Analysing the different set-ups for the transducers installation adopted in the NVH analysis in passenger vehicles, a relevant example of mounting position is reported in Figure 4.9, which describes a model exploited in an experimental study by Isfahan University and Kebangsaan University, Malaysia [32].

This diagram illustrates how the tri-axial accelerometer can be mounted on the passenger seat surface, where a torso is located, to measure vertical, fore-aft, and lateral accelerations, whereas vertical and fore-aft vibrations at the seat base can be measured using two single-axis accelerometers placed on a rigid beam and mounted on the front, left seat rail.

In addition, also for measuring for-aft vibration at the seat backrest, it is possible to install another single axis accelerometer inside an additional mounting support, which has to be properly attached to the backrest top.

On the other hand, to evaluate the vertical acceleration of the floor, an additional single axis accelerometer may be placed on a plate mounted on the floor beneath the front edge and centreline of the seat.
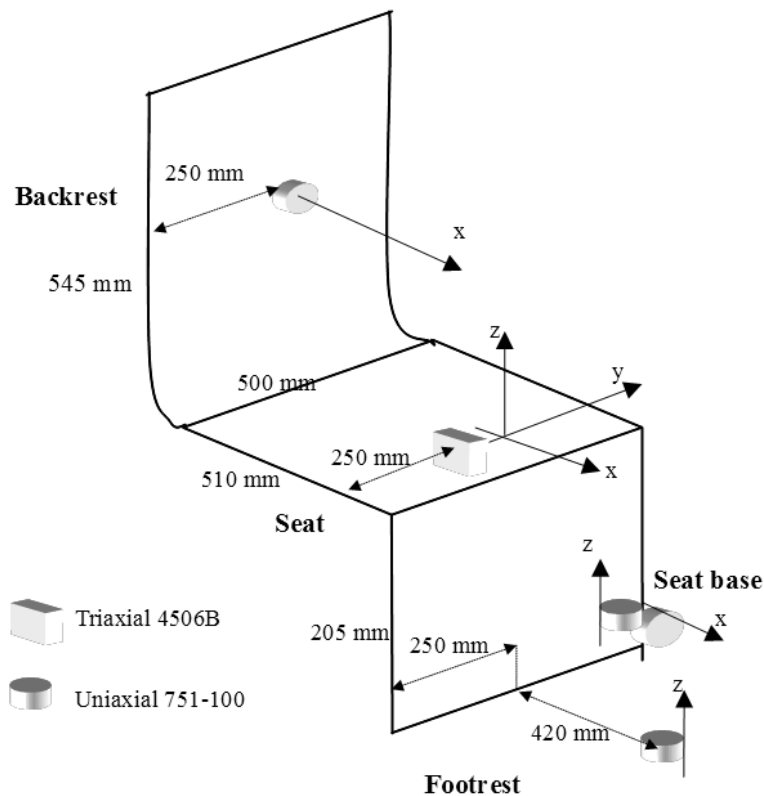
Figure 4.9: Schematic diagram of the experiment assembly and transducer mounting positions. From [32]

Following this sample procedure, the collected signals can be acquired by a multi-channel data acquisition and analysis system, by pre-setting a proper recording period and considering as relevant for WBV studies only the excitations up to a certain specific frequency, usually 80 Hz.

At this point, depending on the chosen frequency span of measurements, the sampling frequency can be directly derived according to Nyquist rule; for instance, considering a frequency span of 100 Hz, the obtained sampling frequency would correspond to 256 Hz.

As a further remark, a band pass filter is usually applied to isolate the spectrum on the signals actually worth to be considered; this implies in most cases to consider only filtered signals in the range 0.5-80 Hz [3].

4.2 Experimental Evaluation of Vehicle Cabin Noise using Subjective and Objective Psychoacoustic Analysis Techniques

Sound generation and transmission in a vehicle takes place in terms of small pressure waves that travel in air, representing the so called airborne noise, together with vibrations that travel in vehicle structures, constituting the structure-borne noise. While air-borne noise involves a physical mechanism from which sound is generated and radiated, structure-borne noise is caused from a vibrating source that induces the acoustic energy to travel through solid structures and to be then released as air-borne noise. The main targets of NVH experimental techniques are to determine the characteristics of these two types of noise in a vehicle, as well as the transmission paths to driver and passengers.

Considering the several noise mapping techniques, sound intensity, acoustic holography and beam forming, Transfer Path Analysis, modal analysis and order tracking are considered the most relevant experimental techniques to analyze and identify NVH sources in a vehicle. On the other hand, it is important to take into account that some of these techniques employ instrumentation which requires specifically constructed rooms such as anechoic or reverberant chambers.

Figure 4.10 depicts the semi-anechoic room equipped with a 4WD dynamometer at Brüel & Kjær Application Research Centre (ARC) in Canton, Michigan, USA.

Figure 4.10: 4WD dynamometer ARC anechoic chamber.

(From [33])

In fact, only in these particular controlled sound fields the noisiness of a sound source can be easily related to the measured sound pressure ensuring sufficient accuracy. It is the case, for instance, of a typical condenser microphone, that if used in rooms that are neither anechoic nor reverberant could provide incorrect results, whether positioned too close to the sound source, at a distance less than the wavelength of the lowest frequency emitted from the source, that is the near field, or too far away from the source, where reflections from walls and other objects may considerably alter the measurement accuracy.

Other measurement devices that need to be employed in free field conditions are the sound level meter and the traditional pressure-pressure sound intensity probe. Actually, thanks to the development of more innovative measurement techniques, sound intensity in-situ tests are now possible also where anechoic conditions are not applicable, like in an engine bay or car interior.

This kind of methodology can be successfully used also for other applications related to mapping and analyzing automotive noise and vibration.

Among the others, Panel Noise Contribution Analysis is a well-known methodology for an air-borne Transfer Path Analysis (TPA) in car interior, through which pressure contribution from the individual panels at a reference point can be very accurately calculated, whereas Near Field Acoustic Camera for sound source localization during transients can be even used in non-anechoic conditions [34].

Another methodology is In-Situ Absorption method for the measurement of the acoustic properties of materials. All these procedures are typical tools employed for increasing the acoustic comfort quality in a car. Given the complexity of such acoustic studies, it is always fundamental to have in mind that structural measurement techniques play a key role in the vehicle development process, as well.

A typical procedure for evaluating vehicle cabin noise develops on four main phases: recording, analysis, averaging and post processing.

Usually, acoustic pressure measurements inside vehicle cabin can be performed by exploiting normal microphones located next to the driver's left ear position, or by installing a binaural head at the passenger's ears position, (Figure 4.11). After the decision on the acquisition sensors, the recording time is set, together with the testing environment.

Concerning this issue, a common choice is to run the acquisition in anechoic or hemi-anechoic chambers while the tested vehicle is driven and motored on a 4WD dynamometer. Moreover, to get additional information, it is possible to install microphones outside the car near the driver front side wheel.

Figure 4.11: Artificial torso and related instruments position inside the car.

According to this procedure, a lot of information can be collected by using both a binaural head installed on a stand at passenger seat position and two conventional microphones at the driver side, one near to its left ear, the other outside the cabin next to the front wheel. Examples of acoustics recording equipment are illustrated in Figure 4.12.

Figure 4.12: (Left) passenger's seat with binaural head; (Middle) driver's seat with conventional microphone; (Right) microphone next to the front wheel.

As far as the testing dynamometers are concerned, their function is to simulate the typical rolling resistance experienced by a vehicle when driven on the road, whereas testing rooms have to ensure accurate sound measurement with minimal background noise; therefore, anechoic or hemi anechoic chambers are usually chosen. In both these typologies, the walls are treated by applying sound absorbing edges aiming at minimizing ambient noise and reflections, characterizing the room with a specific cut-off frequency, semi-anechoic rooms having only the floor as a reflecting surface.

The opposite of these chamber typologies is represented by the reverberation ones; indeed, a reverberation room may be considered as a closed environment in which the surrounding walls reflect the acoustic energy, instead of absorbing it, with the aim to create a measuring environment which is widely diffused, within which the acoustic energy can freely flow across all directions. Figure 4.13 illustrates a semi-anechoic room and a reverberation room.

Figure 4.13: Semi-anechoic chamber (left), Reverberation chamber (right).

For cases of self-driven and motored vehicle, the testing speed, engine load, air circulation and exhausts emissions can be controlled remotely from the controlling room located next to the test cell, whereas data acquisition is typically performed during motored and driven conditions.

Talking about the classical operating conditions followed during testing, the most common are :

- idling/ambient.
- steady speeds measurement, usually from 20 to 80 km/h with pace 20.
- acceleration run-up measurement from 0 to 80 km/h.

4.2.1 Technic for single motor vehicles noise emission detection

Among the practical empirical methods to evaluate noise issues concerning a vehicle, recommended test procedures adopted by automotive specialized magazines include:

- vehicle driving by the receiver microphone at 70 km/h steady
- vehicle approaching at 50 km/h steady, starting to brake at 25 m, come to a full stop in front of the microphone, drive away at moderate acceleration, simulating the traffic light scenario

In Europe, several communitarian regulations have been decreed to indicate criteria and methodologies for the vehicles homologation, which also include simplified verifications for the periodic and occasional noisiness control.

In particular, procedures for noisiness detection at stand still vehicle have been established by the Council directive CEE 92/97 on 10th November 1992, resumed in the followings:

- Any area not subject to significant acoustic disturbance may be used as a test site. Flat surfaces which are covered in concrete, asphalt or any other hard surfacing and possess a high degree of reflectivity are particularly suitable ; surfaces consisting of earth which has been tamped down must not be used. The test site must be in the form of a rectangle, the sides of which are at least 3 m from the sides of the vehicle. This rectangle must not contain any significant obstacles, e.g. an individual other than the observer and the driver. The vehicle must be positioned within the abovementioned rectangle so that the microphone is at least 1 m from any kerbstone.

- Measurements must not be made in poor atmospheric conditions. It must be ensured that the results are not affected by gusts of wind. For measurements, the A-weighted sound level of sound sources other than those of the vehicle to be tested and of wind effects must be at least 10 dB (A) below the sound level produced by the vehicle.

- The microphone must be located level with the exhaust outlet or 0,2 m above the test-track surface, whichever is the higher. The microphone diaphragm must face the exhaust outlet at a distance of 0,5 m from the latter. The axis of maximum sensitivity of the microphone must be parallel to the track surface at an angle of 45° ± 10° to the vertical plane defined by the direction in which the exhaust gases are emitted. The microphone must be positioned to the side of this vertical plane which gives the greatest possible distance between the microphone and the vehicle contour. If the exhaust system has several outlets, the centres of which are not more than 0,3 m apart, and which are connected to the same silencer, the microphone must face the outlet closest to the vehicle contour or the outlet which is the highest above the track surface. In all

other cases separate measurements must be taken at each of them, the highest figure recorded being taken as the test value.

- The vehicle engine must be brought to normal running temperature before measurements commence. If the vehicle is fitted with fan(s) having an automatic actuating mechanism, this system must not be interfered with during the sound-level measurements. Engine speed must be stabilized at three-quarters of the speed (S) at which the engine develops rated maximum power. When constant engine speed is reached, the throttle must be rapidly returned to the idling position. The sound level must be measured over an operating period comprising brief maintenance of constant engine speed and the entire deceleration period, the maximum sound-level meter reading being taken as the test result.
- Readings, rounded off to the nearest decibel, shall be taken from the measuring instrument. Only those values obtained from three consecutive measurements which do not differ by more than 2 dB(A) respectively are taken into consideration. The highest of these three values shall constitute the test results. During measurements, the gear lever must be in the neutral position.

As enhanced by the several criteria and procedures listed above, it is clear how motor vehicle noise assessment is really a very complex task. An example of road traffic noise analysis is depicted in Figure 4.14.

Figure 4.14: Road traffic noise assessment

(From: http://www.acoustics.ie/transport/)

5 Main threshold guidelines

5.1 Vibrational comfort guidelines according to main standards

Concerning whole-body vibration, assessments are based on the daily exposure which is calculated as the most severe axis of vibration at the seat (or floor for a standing worker; as stated in the previous chapters, assessments include axes multipliers as specified in ISO 2631 (1997).

In order to minimize the risk of vibration-induced adverse health effects, action levels and threshold limit values (TLVs) for vibration exposure have been proposed by several committees or organizations.

In particular, American Conference of Governmental Industrial Hygienists 2016 conference refers to the ISO Standard 2631-1 "Mechanical vibration and shock - Evaluation of human exposure to whole-body vibration" [3], which focuses on the possible effects of vibration on health, comfort and perception, and on the incidence of motion sickness, taking into account that vibration is often complex, contains many frequencies, occurs in several directions and changes over time. Moreover, other limit values are proposed by the EU Physical Agents Directive 2002/44/EC.

In Figure 5.1, the exposure limits curves according to BS 6841 [4] and ISO 2631-1 [3] for vibrational excitation on x, y, z axes are represented.
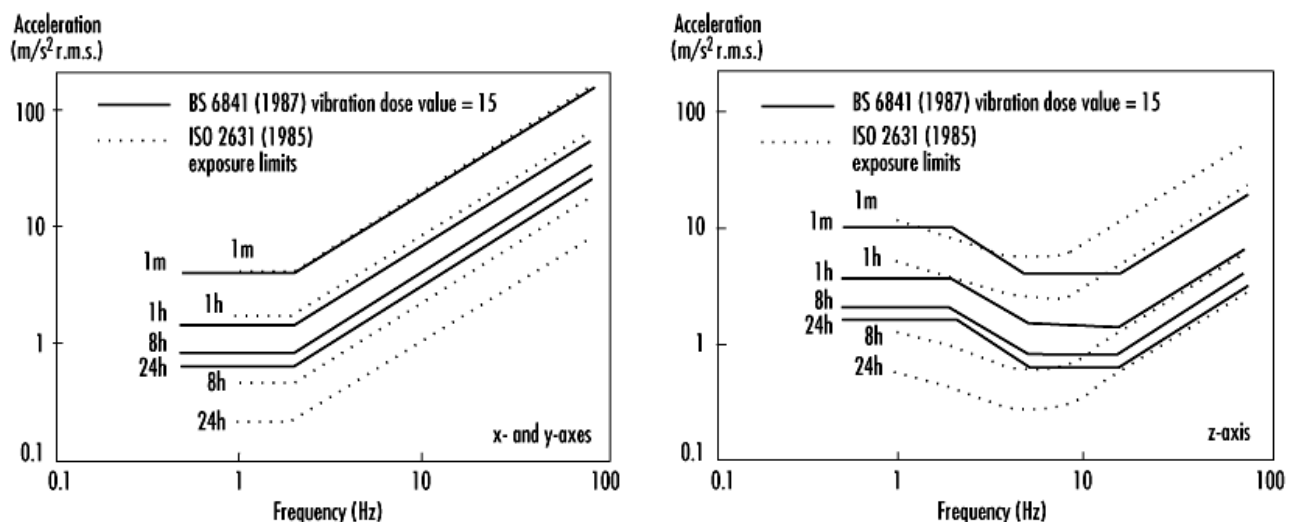
Figure 5.1: Frequency dependencies for human response to whole-body vibration, thresholds for x-y axes (left), thresholds for z-axis (right).
(From [35])

Moreover, the ACGIH TLVs use a curve which compares ISO 2631 Health Guidance Caution Zones, the weighted acceleration and the exposure time, as well as a series of calculations to assist users. As a general advice, direct use of the ACGIH and/or ISO prescriptions is recommended; in this regard ISO 2631 and European Commission guideline levels for an eight hour per day WBV excitation are reported in Table 5.x

Table 5.1: Whole-Body Vibration Exposure Limits according to ACGIH and EU Physical Agents (Vibration) Directive 2002.

Standard	Limit Values (likely healthy risk)	Action Values (Caution)
ACGIH ISO 2631	A(8) = 0.9 m/s^2 VDV = 17 m/s$^{1.75}$	A(8) = 0.5 m/s^2 VDV = 8.5 m/s$^{1.75}$
EU Directive 2002/44/EC	A(8) = 1.15 m/s^2 VDV = 21 m/s$^{1.75}$	A(8) = 0.5 m/s^2 VDV = 9.1 m/s$^{1.75}$

Also, it is important to remember that people vary in their susceptibility to effects of exposure to vibration; hence, such exposure limits should be considered as guidelines in controlling exposure, but they should not be considered as an upper safe limit of exposure or a boundary between safe and harmful levels.

Indeed, since acceptable values of vibration magnitude vary with each application, a unique limit is not always defined; however, approximate indication values are often provided as information of likely reactions to various magnitudes of the overall total vibrational values in the transport field, as expressed by recommended scale of discomfort suggested by BS 6841 [4] and ISO 2631 [3] in Table 5.3:

Table 5.2: Scale of vibration discomfort suggested in BS 6841 and ISO 2631.

Overall r.m.s weighted acceleration total value	Degree of discomfort
Less than 0.315 m/s^2	Not uncomfortable
0.315 – 0.63 m/s^2	A little uncomfortable
0.5 – 1 m/s^2	Fairly uncomfortable
0.8 – 1.6 m/s^2	Uncomfortable
1.25 – 2.5 m/s^2	Very uncomfortable
Greater than 2 m/s^2	Extremely uncomfortable

Talking about vibration exposure measurement, vibration dose values are also exploited to generally express the severity of the vibration exposures which caused them. Nevertheless, there is currently no consensus of opinion on the precise relation between vibration dose values and the risk of injury.

According to the guidelines contained in the BS 6841 standard, it is recognised that vibration magnitudes and durations which produce vibration dose values in the region of 15 m/s$^{1.75}$ will usually cause severe discomfort, thus, it is reasonable to assume that increased exposure to vibration implies an increased risk of injury [4]. In other words, the vibration dose value provides a measure by which highly variable and complex exposures can be compared, this way, organizations may use it to define limits or action levels. Indeed, the exposure period required for the vibration dose value to reach a tentative action level of 15 m/s$^{1.75}$ can be calculated as:

$$T_{15} = \left(\frac{15}{VDV_t}\right)^4 * t \qquad\qquad (5.1)$$

where:

- T_{15} is the time (in seconds) required to reach a VDV value of 15 m/s$^{1.75}$
- VDV_t is the VDV measured over the period of t seconds.

About multi-axis vibration British Standard 6841 specifies that when evaluating multi-axis vibration, the forth root of the sum of the fourth powers of the VDVs in each axis should be determined to give the total vibration dose value, VDV_{total}, for the environment

$$VDV_{total} = \left(VDV_{xs}^4 + VDV_{ys}^4 + VDV_{zs}^4\right)^{1/4} \tag{5.2}$$

Where: VDV_{xs}, VDV_{ys} and VDV_{zs} are the VDV in the x, y and z-axis on the seat,

As an example, in some countries, a vibration dose value of 15 m/s$^{1.75}$ is defined as a provisional action level, but it may be appropriate to limit vibration or repeated shock exposures to higher or lower values depending on the situation; actually, with current understanding, an action level merely serves to indicate the approximate values that might be excessive. Conversely, any exposure to continuous vibration, intermittent vibration, or repeated shock may be compared with the action level by calculating the vibration dose value. Figure 5.2 illustrates the advised root-mean-square accelerations threshold corresponding to a vibration dose value of 15 m/s$^{1.75}$ for exposures between one second and 24 hours.
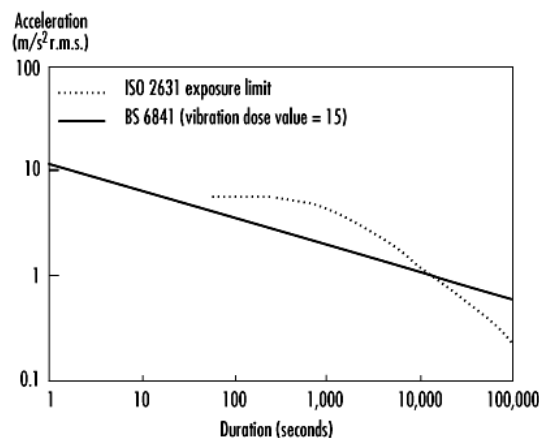
Figure 5.2: Time dependencies for human response to a whole-body vibration.
(From [35])

Regarding human discomfort correlated to vibrations, the curves describing different exposing time period of vibrations look like each other in terms of their characteristics and the minimum region of these curves represents the zone in which people are affected negatively at the most affected way.

This region is defined as a discomfort region where the vibrations are at the frequency interval of about 4-8 Hz. The most important reason determining this frequency range is a resonance situation that origins from the coincidence of the natural frequencies of certain human body structures and the vibration frequencies originating from the vehicle [36].

Since the main irritating range sits between 4 and 8 Hz for discomfort, human exposed to those resonance frequencies can suffer a relevant annoyance and experiment the worst case of ride comfort; such ride comfort can be improved by either keeping the frequencies higher at about 15-20 Hz or lower than 4 Hz.

Figure 5.3 and Figure 5.4 show the correlation between acceleration values, frequency range and conditions of discomfort.
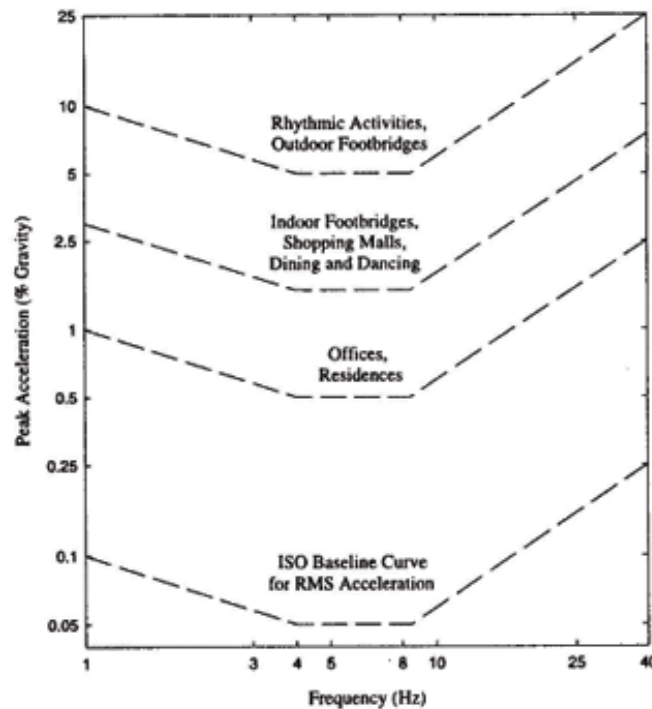
Figure 5.3: Values of peak accelerations for checking the human discomfort due to vibrations generated by human activities.
(From [3])
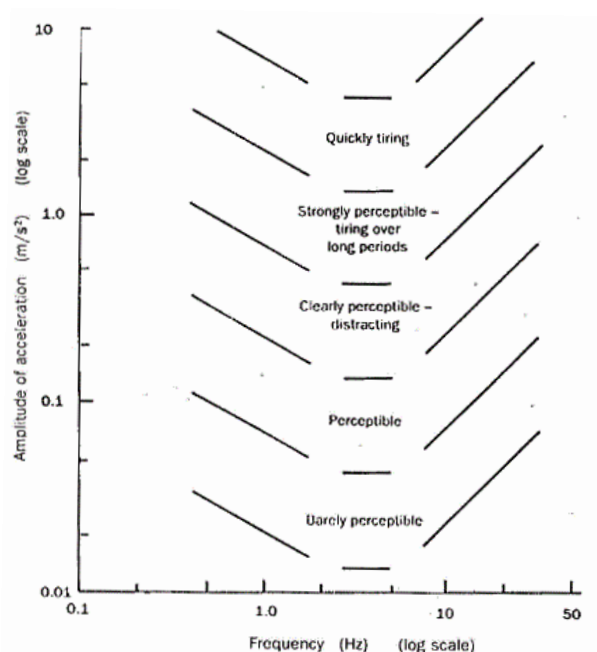
Figure 5.4: Qualitative description of human reaction to sustained steady oscillation.
(From [37])

Obviously, being such a frequency excitation range the most critical one, it involves strictly the time a person could stand in an acceptable way the specific oscillation, (Figure 5.5).
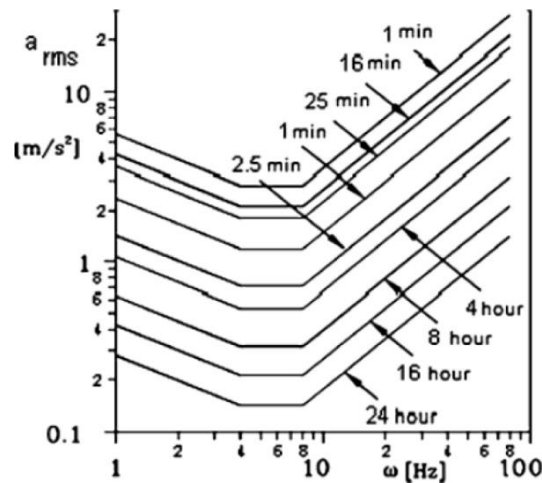
Figure 5.5: Human vibration discomfort curves related to tolerability time and time frequency. (From [3])

On the other hand, concerning hand-arm vibration, assessments are based on the daily exposure which is calculated as the root sum of the squares of the orthogonal frequency weighted vibration at the hands normalized to an 8-h reference period [$A(8)$]; in this case measurements should be made according to ISO 5349–1 (2001), using the W_h frequency weighting.

Regarding HTV prescriptions, the American Conference of Government Industrial Hygienists (ACGIH) has published TLVs for hand-transmitted vibration measured according to the ISO frequency-weighting procedure, (Table 5.1).

Table 5.3: Threshold limit values for hand-transmitted vibration according to the American Conference of Government Industrial Hygienists 1992.

Total daily exposure (hours)	Frequency-weighted r.m.s. acceleration in the dominant direction that should not be exceeded	
	g (1g = 9.81 m/s^2)	m/s^2
4-8	0.40	4
2-4	0.61	6
1-2	0.81	8
1	1.22	12

According to ACGIH, the proposal TLVs concern vibration exposure to which "nearly all workers may be exposed repeatedly without progressing beyond Stage 1 of the Stockholm Workshop Classification System for VWF", (Table 5.4), where VWF stands for vibration-induced white finger; such disease is characterized by episodes of white or pale fingers caused by spastic closure of the digital arteries, whose attacks are usually triggered by cold and last from 5 to 30/40 minutes.
This is a severe disease, since a complete loss of tactile sensitivity may be experienced during an attack.

Table 5.4: The Stockholm Workshop scale for staging cold-induced Raynaud's phenomenon in the hand-arm vibration syndrome. (Derived from [35])

Stage	Grade	Symptoms
0	—	No attacks
1	Mild	Occasional attacks affecting only the tips of one or more fingers
2	Moderate	Occasional attacks affecting distal and middle (rarely also proximal) phalanges of one or more fingers
3	Severe	Frequent attacks affecting all phalanges of most fingers
4	Very severe	As in stage 3, with trophic skin changes in the finger tips

As far as the minimum health and safety requirements regarding the exposure of workers to the risks arising from physical agents are concerned, the Directive 2002/44/EC of the European Parliament and of the Council of 25 June 2002 establishes the following guidelines collected in Table 5.5:

Table 5.5: EU Physical Agents Directive Daily Limit and Action Levels in relation to HTV. (Derived from [38])

EU Directive 2002/44/EC Limit and Action Levels		
Daily Exposure Duration	Daily Limit	Daily Action Level
8 hours	5 m/s^2	2.5 m/s^2

As a fundamental remark, it is recommended to have in mind that many human organs are subjected to resonance frequency in the common vibrational range, thus causing relevant discomfort, as observable in Table 5.4:

Table 5.6: Frequency of resonance of main human body organs and parts. (Derived from [39])

HUMAN ORGAN	RESONANCE FREQUENCY [Hz]
Head	4-5
Jaw	6-8
Eyes	60-90
Chest Organs	5-9
Upper Limb	3
Stomach Organs	4.5-10
Bladder	10-18
Pelvis	5-9
Muscles	13-20
Liver	3-4
Spinal Column	8
Chest Wall	60
Abdominal	4-8
Shoulders	4-8
Lungs	4-8
Hands/arms	20-70
Maxilla	100-200

5.2 Noise exposure guidelines according to OMS, OSHA and other standards

As far as the acoustic field is concerned, several guidelines about threshold limit exposure have been developed; in this regard, a fundamental achievement was the determination of the main acoustic range in which it is highly advised to stay in: a range comprised between 0 dB and 120 dB, values corresponding respectively to the audibility limit (10^{-12} W) and to the threshold pain (1000 W).

Considering the definition of an exposure indicator, the most appropriate exposure measurement for occupational noise is the A-weighted decibel, dB(A), usually averaged over an 8-hour working day (L_{Aeq},8h). Actually, there is a strong correlation between this parameter and the ability of the noise hazard to damage human hearing, hence, being the most commonly used epidemiological measurement of exposure, it is frequently adopted in the workplace.

In addition, it is worth to observe that, despite exposure being often measured as a continuous variable, many surveys report exposure above and below cut-off values, rather than as a distribution, thus making this tendency quite impractical in assessing the burden of disease. As a general method, the following categories are widely applied because they correspond to regulatory limits in some developed and many developing countries for an 8-hour day; in the majority of cases, the reference thresholds correspond respectively to 85 dB(A) and 90 dB(A) [40]:

- minimum noise exposure: 85 dB(A).
- moderately high noise exposure: 85−90 dB(A)
- high noise exposure: >90 dB(A).

Conversely, several other standards have been established to suggest safe exposure level to noise phenomena [41]. In this regard, Figure 5.5 summarizes the different permissible exposure times corresponding to the various continuous sound intensity levels in dB according to NIOSH and CDC recommendations [42] [43].

Continuous dB	Permissible Exposure Time
85 dB	8 Hours
88 dB	4 hours
91 dB	2 hours
94 dB	1 hour
97 dB	30 minutes
100 dB	15 minutes
103 dB	7.5 minutes
106 dB	3.75 minutes (< 4 min)
109 dB	1.875 minutes (< 2 min)
112 dB	.9375 min (~ 1 min)
115 dB	.46875 min (~ 30 sec)
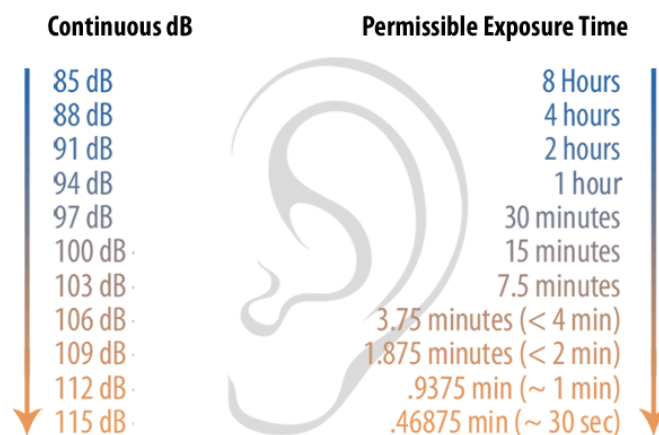
Figure 5.6: Accepted standards concerning recommended permissible exposure time for continuous time weighted average noise, according to NIOSH. For every 3 dB(A) over 85 dB(A), the permissible exposure time before possible damage can occur is cut in half.

Despite the suggested thresholds, it is important to consider that even a level of 90 dB is just critical for possible damages to the hearing system, especially if the exposure time is not instantaneous, but prolonged.

About this issues, WHO recommends average maximum values in order to avoid several disturbs related to noise exposure:

- 55 dB(A) during daytime   6 AM – 10 PM
- 45 dB(A) during night   10 PM – 6 AM

Occupational Safety and Health Administration(OSHA), National institute for Occupational Safety and Health Administration(NIOSH) and the United Health Group(UGH) association provided a guidelines concerning the acoustic exposure thresholds and hearing safety charts [44], [45], with the purpose to define the Permissible Exposure Limit (PEL), as the maximum noise level allowed beyond which protective measures are mandated. Such PEL is also named the Criterion Level. In current OSHA regulations, the Permissible Exposure Limit is 90 dB(A) of noise exposure over an 8-hour time-weighted average.

Workers exposed continuously at this level throughout a work shift will have a dose of 100%. Exposures over this PEL warrant protective actions, administrative or engineering controls, or mandatory use of hearing protection, the so called HPD, Hearing Protection Devices. Table 5.5 and Table 5.6 collect the recommended reference values regarding the acoustic exposure according to these standards:

Table 5.7: OSHA recommended permissible noise exposures depending on a daily base duration.

OSHA's Permissible Noise Exposures	
Duration per day, hours	Sound level dB(A) slow response
8	90
6	92
4	95
3	97
2	100
1.5	102
1	105
0.5	110
<0.25	115

Table 5.8: NIOSH maximum duration thresholds for acoustic exposure depending on dB SPL.

LEVEL	NIOSH MAX TIME
>115 dB SPL	none
115 dB SPL	28 seconds
112 dB SPL	56 seconds
109 dB SPL	1 minute 52 seconds
106 dB SPL	3 minutes 45 seconds
103 dB SPL	7 minutes 30 seconds
100 dB SPL	15 minutes
97 dB SPL	30 minutes
94 dB SPL	1 hour
91 dB SPL	2 hours
88 dB SPL	4 hours
85 dB SPL	8 hours
82 dB SPL	16 hours
80 dB SPL	24 hours (continuous)

As the sound level increases above the Criterion Level, the allowed exposure time must be decreased, this is calculated by using an exchange rate, also called a "dose-trading relation" or "trading ratio."

The exchange rate is the amount by which the permitted sound level may increase if the exposure time is halved. There are two types of exchange rates currently in use: 3 dB(A) exchange rate, also called, "3 dB rule," and 5 dB(A) exchange rate, also known as "5 dB rule." These two exchange rates, with criterion levels of 85 dB(A) and 90 dB(A), give two different sets of exposure guidelines, as Table 5.7 shows.

The 3 dB(A) exchange rate is more stringent. Indeed, with criterion levels of 85 dB(A) the maximum permitted duration for a 100 dB(A) noise exposure in the 3 dB(A) exchange rate is 15 minutes. With the 5 dB(A) exchange rate, it is one hour.

Actually, many experts recognize the 3 dB rule as more logical, arguing that it is logical that if the sound level is doubled, then the allowable exposure time should be cut in half. It follows, then, that the allowable time should be halved for every 3 dB(A) increase in sound level [46].

Table 5.7 reports the allowable exposure time versus TWA, that is the eight-hour time-weighted average sound exposure level, for an eight hours work-shift with the noise level constant over the entire shift, the TWA is equal to the measured sound level .

Table 5.9: NIOSH maximum duration thresholds for acoustic exposure depending on dB SPL.

ALLOWABLE EXPOSURE TIME (H)	5 dB(A) EXCHANGE RATE AND 90 dB(A) 8 HOUR LIMIT	3 dB(A) EXCHANGE RATE AND 90 dB(A) 8 HOUR LIMIT	3 dB(A) EXCHANGE RATE AND 85 dB(A) 8 HOUR LIMIT
8	90	90	85
4	95	93	88
2	100	96	91
1	105	99	94
0.5	110	102	97
0.25	115	105	100

5.3 Noise emission limits in European automotive field

The external noise emitted by passenger cars has been controlled since 1929 when the Motor Cars Excessive Noise regulations were introduced. Since then, new cars homologated in EU are now required to meet Europe-wide noise limits, whose values have been progressively reduced from 82 dB(A) in 1978 to the limit of 74 dB(A) established in 1996, quite a long time ago, considering the environmental and traffic change across the world. It is important to consider that noise levels quoted above are the maximum levels that are permitted for new vehicle types. Many vehicles produce lower levels of noise, and it is illegal to modify the exhaust system of a vehicle to make it noisier than the level recorded for that model at type approval.

Afterwards, in December 2011, the European Commission adopted a proposal for a new regulation aimed at tightening noise emissions standards for cars, vans, lorries and buses. The Commission proposal had foreseen a four-decibel reduction in noise emissions from cars and a three-decibel reduction from lorries that would have entered into force five years after the regulation receives final approval, i.e. not before 2017. Unfortunately, the Commission's proposal was significantly weakened, adding unnecessary delay and a less ambitious level noise reduction.

In November 2013 a new law agreed between the Commission, Parliament and member states extended a 15 year delay before new vehicle standard are fully introduced, compared to the Commission proposal which would have them introduced in 7 years.

Subsequently, a new EU regulation has been introduced from July 2016, Regulation (EU) No 540/2014, which will phase in tighter noise limits over 10 years, together with a revised, more representative test procedure. By 2026 the limit for most new passenger cars will be 68 dB(A).The 2013 European agreement main features of the agreement included the setting of noise limit values for the different vehicle categories and a timeframe for implementation, labelling and consumer information, the development of acoustic alert systems and the impact of the road surface.

The industry is developing acoustic systems to compensate for the lack of audible signals in electric and hybrid electric vehicles to increase awareness of road users and, in particular, of blind and visually impaired pedestrians and cyclists. To this end, such vehicles will be equipped in the coming years with Acoustic Vehicle Alerting Systems (AVAS).

Under the agreement, the sound level would have not exceed the following limits, listed in Table 5.8.

Table 5.10: Limit values according to provisional agreement reached on 5 November between the Lithuanian Presidency of the Council and the European Parliament representatives for the reduction of the sound level of motor vehicles (From [47])

Vehicle category	Description of vehicle category	Limit values expressed in dB(A)		
		Limit values for Type-approval of new vehicle types	Limit values for Type-approval of new vehicle types/new vehicles	Limit values For Type-approval of new vehicle types/ new vehicles
		Phase 1 applicable from date of application specified in Article 16(2) [after 2 years]	Phase 2 applicable from 4/6 years after the date of application specified in Article 16(2) [after 6/8years]	Phase 3applicable from 8/10 years after the date of application specified in Article 16(2) [after 10/12 years]
M	**Vehicles used for the carriage of passengers**			
M1	power to mass ratio ≤ 120 kW/1000kg	72 [1]	70 [1]	68 [1]
M1	120 Kw/1000kg < power to mass ratio ≤ 160 kW/1000kg	73	71	69
M1	160 Kw/1000kg < power to mass ratio	75	73	71
M1	power to mass ratio > 200 Kw/1000kg: n seats ≤ 4 R point of driver seat ≤ 450 mm from the ground	75	74	72
M2	mass ≤ 2500 kg	72	70	69
M2	2500 kg < mass ≤ 3500 kg	74	72	71
M2	3500 kg < mass ≤ 5000 kg; rated engine power ≤ 135 kW	75	73	72
M3	3500 kg < mass ≤ 5000 kg; rated engine power > 135 kW	75	74	72
M2	rated engine power ≤ 150 kW	76	74	73 [2]
M2	150 kW <rated engine power ≤ 250 kW	78	77	76 [2]
M2	rated engine power > 250 kW	80	78	77 [2]

1) M1 vehicles derived from N1 vehicles:

M1 vehicles with a R point > 850 mm from the ground and a total permissible laden mass more than 2500 kg have to fulfil the limit values of N1 (2500 kg < mass ≤ 3500 kg).

2) + 2 years for new vehicle type and + 1 year for new vehicles registration

Limit values shall be increased by 1dB (2 dB(A) for N3 and M3 categories) for vehicles that meet the relevant definition for off-road vehicles set out in point 4 of Section A of Annex II to EU Directive 2007/46/EC. For M1 vehicles the increased limit values for off-road vehicles are only valid if the technically permissible maximum laden mass > 2 tonnes. Limit values shall be increased by 2 dB(A) for wheelchair accessible vehicles and armoured vehicles, as defined in Annex II of Directive 2007/46/EC.

Reducing noise emission from motor vehicles in all but an easy task, as source of acoustic waves are really many and widely distributed, in addition, Every system is composed of several interdependent components so any modification to reduce noise requires fundamental redesign of other parts. Figure 5.7 resumes in a scheme the different components producing noise in automotive scope.
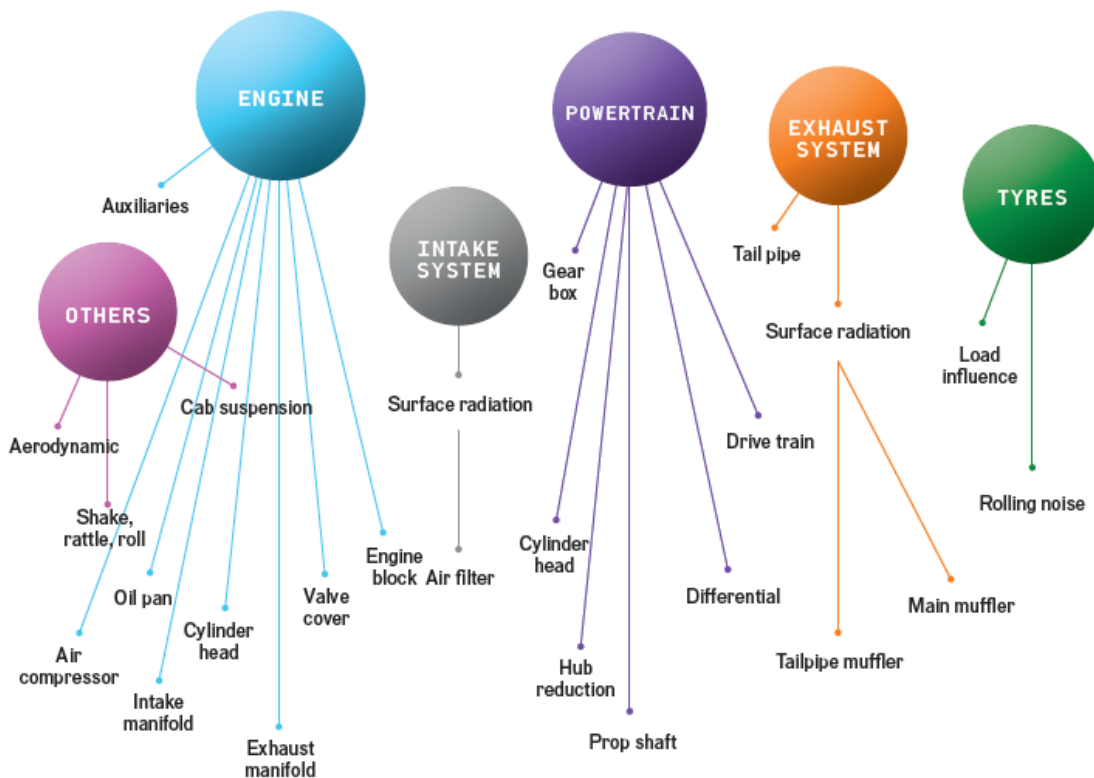
Figure 5.7: Scheme of different acoustic annoyance source and components in a motor vehicle. (From [48])

6 Experimental project methodology

6.1 Motor vehicles utilized technical specifications

The two car models adopted for this experimental project are the Mazda CX-5 first generation and the Fiat Panda second generation, referred in the following chapters respectively as vehicle A and vehicle B. Both the cars were equipped with summer tyres during all the tests executed. The main characteristics of the two vehicles are reported in Table 6.1, while their external shape is illustrated in Figure 6.1:

Table 6.1: Technical data concerning the two examined car models.

Vehicle	A	B
Class	Compact Crossover SUV	City car
Layout	Front engine, AWD	Front engine, FWD
Body style	5-door SUV	3-door hatchback
Engine	2.2 L I4 (diesel), 150 CV	1.2 L I4 (petrol), 69 CV
Transmission	6-speed automatic	5-speed manual
Wheelbase	2.700	2.299 m
Length	4.540	3.538 m
Width	1.840	1.590 m
Height	1.670	1.578 m
Curb Weight	1530 Kg	860 Kg
Tyres	225/55 R 19	165/65 R 14

Among the several differences between the two cars, a focus point is related to the transmission design utilized: vehicle A is equipped with a 6-speed automatic gearbox, whereas vehicle B exploits a 5-speed manual transmission system.
In particular, the automatic gearbox constitutes an excellent vibration insulator, thanks to the torque converter presence and to the absence of a mechanical linkage between the gear-stick and the intermediate command, effectively reducing vibration propagation. Conversely, the 4WD layout implemented in vehicle A may generate more NVH related head-scratchers with respect to the FWD system of vehicle B.

Figure 6.1: Vehicle A, (left), Vehicle B, (right).

6.2 Equipment and instrumentation

Concerning the vibration assessment, the acceleration represented the measured quantity; in this regard, for both the cars, 3 PCB Piezoelectronics ICP tri-axial accelerometers has been exploited, mounted respectively on the seat guide and cushion on the passenger side and on the steering wheel to evaluate hand-transmitted vibration. The accelerometers at the seat guide and at the steering wheel have been mounted using special petro-wax, assuring their proper positioning during the various tests by applying strips of adhesive tape, useful to retain cables from moving around in the vehicle cabin too. On the other hand, to measure accelerations at the interface hip-cushion, a seat pad accelerometer purposely designed has been mounted with the proper direction on the cushion. All the sensors have been connected to the LMS SCADAS acquisition hardware, linked to a laptop for the elaboration and management of the interface software-hardware.

The specification of the two PCB ICP tri-axial accelerometers applied to the seat guide and to the steering wheel are listed in the following:

- Serial number: LW226919
- Positioning axes: -X seat rail, -Y seat rail, +Z seat rail, passenger side
- Nominal sensitivity @ 100 Hz: 100 mV/g
- Actual sensitivity for reference direction:
  - -X 102.5 mV/g ;
  - -Y 97.5 mV/g ;
  - +Z 98.6 mV/g ;

Figure 6.2 and Figure 6.3 depict the position for the accelerometer mounted on the seat rails respectively on the vehicle A and the vehicle B.

Figure 6.2: Detail of the installation for the seat rail accelerometer on vehicle A .

Figure 6.3: Detail of the installation for the seat rail accelerometer on vehicle B.

Considering the positioning of the accelerometers dedicated to hand-arm transmitted vibration measurement, this represented a tricky procedure, because, being the two cars different, it has been impossible to replicate the same position in both cases; thus, the attention has been on trying to achieve the best position in relation to the correct axes reference directions for the measurements, to obtain results as comparable as possible. The specification of the PCB ICP tri-axial accelerometer applied to the steering wheel zone are listed in the following:

- Model: 356A15, serial number: LW226918
- Positioning axes: -X steering wheel, -Y steering wheel, +Z steering wheel
- Nominal sensitivity @ 100 Hz: 100 mV/g
- Frequency range: 2 to 5000 Hz (error ±5%); 1.4 to 6500 Hz (error ±10%)
- Actual sensitivity for reference direction:
  - -X 102   mV/g ;
  - -Y 102.1 mV/g ;
  - +Z 102.3 mV/g ;

Figure 6.4-6.5 illustrate the accelerometer position on the steering-wheel respectively of vehicles A and B, for the latter in particular, the position has been chosen taking into account the most flat surface available in the steering wheel zone.

Figure 6.4: Detail of the installation for the steering wheel accelerometer on vehicle A.

Figure 6.5: Detail of the installation for the steering wheel accelerometer on vehicle B.

Conversely, in measuring the vibration excitation at the hip-seat interface, the focus has been on installing the sensor trying to make it maintain the correct initial position relative to the main axes directions, even during the running of the tests, in order to avoid possible movements and readjustment by the passenger.

Specifications of the PCB ICP seat pad accelerometer, conforms to ISO 10326-1, are listed below:

- Model: 356B4, serial number: 226779
- Positioning axes: X cushion, Y cushion, Z cushion, passenger side
- Range: 0.5 to 1000 Hz, (±5%)
- Nominal sensitivity @ 100 Hz: 100 mV/g
- Actual sensitivity for reference direction:
- +X – 101.7 mV/g ;
- +Y – 101.9 mV/g ;
- +Z – 101.3 mV/g ;

Figure 6.6 and Figure 6.7 show the position for the seat-pad accelerometer respectively on the vehicles A and B.

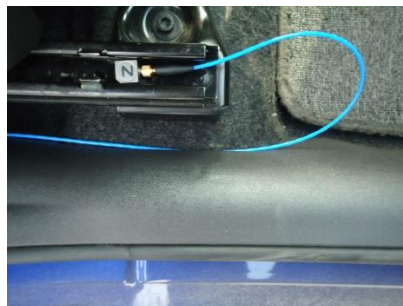**Figure 6.6**: Detail of the installation for the seat pad accelerometer on vehicle A.

Figure 6.7:Detail of the installation for the steering wheel accelerometer on vehicle B.

Conversely, regarding the psychoacoustic analysis; the Siemens FRF LMS 3D Headset ABH04 has been utilized, being applied on the passenger head to collect and record the acoustic information during the tests.

The specification of the Siemens FRF LMS 3D Headset ABH04 with ICP input are listed in the following:

- Serial number: 31924
- Positioning: passenger head
- Measured quantity: Pressure
- Nominal sensitivity @ 100 Hz: 100 mV/Pa
- Actual sensitivity for reference direction:
    - LEFT – 31.698 mV/Pa ;
    - RIGHT – 31.698 mV/Pa ;

In Figure 6.8 and 6.9 the headset and the laptop used during the tests are depicted.

Figure 6.8: Detail of the passenger wearing the headset and using the laptop during the tests.
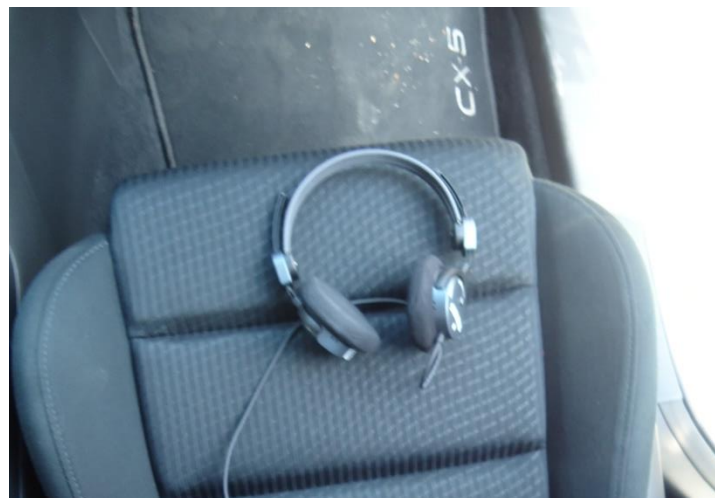

Figure 6.9: Headset on the passenger seat.

The acquisition hardware Siemens LMS SCADAS Mobile 02 Mainframe specifications are reported in the list below:

- Serial number 52122621
- Type SCM02
- Acquisition Channels: 16
- Frequency cut-off: 0.5 Hz (HP), 102.4 kHz (LP)
- Acquisition channels exploited: 11
- 1: x rail passenger seat
- 2: y rail passenger seat
- 3: z rail passenger seat
- 4: x steering wheel
- 5: y steering wheel
- 6: z steering wheel
- 7: x cushion passenger seat
- 8: y cushion passenger seat
- 9: z cushion passenger seat
- 10: passenger head Left
- 11: passenger head Right

During the running of the tests, the SCADAS hardware has been put on the rear seats, then all the cables arranged in the cabin to link each sensor and the laptop connected through the Ethernet port, (Figure 6.10).

Figure 6.10: LMS SCADAS Mobile acquisition system position in vehicle cabin.

Furthermore, regarding the tests performed on both the vehicles, it is worth of notice that in the advanced options of the Test.Lab acquisition and post processing software the cut-off frequency of the high pass filter has been fixed on 0.5 Hz, whereas the Butterworth, 6th order high pass filter cut-off frequency has been leaved on the default value: 102 kHz.

6.3 Testing procedure and acquisition methodology

The two cars were driven in two consecutive days, in similar climatic condition and on the same roads, trying to follow an almost equal path to perform recordings in a way as accurate as possible in regard of the road conditions (Table 6.2).

Table 6.2: List of runs with manoeuvres executed (Vibration)

Driving Manoeuvres (Vibrations)	
Vehicle A	**Vehicle B**
Run 2 single wide speed bump 20 km/h	Run 2 single wide speed bump 20 km/h
Run 4 urban road 40 km/h	Run 4 urban road 40 km/h
Run 5 urban road 70 km/h	Run 5 urban road 70 km/h
Run 9 mixed tarmac extra-urban road 70 km/h	Run 9 mixed tarmac extra-urban road 70 km/h
Run 12 smooth tarmac extra-urban road 70 km/h	Run 16 smooth tarmac extra-urban road 70 km/h
Run 19 off-road 30	Run 20 off-road 20
Run 20 off-road 40	Run 21 off-road 30
Run 21 off-road 50	Run 22 off-road 40
Run 22 severe off-road	Run 23 severe off-road
Run 23 paved urban road 20 km/h	Run 27 paved urban road 20 km/h
Run 24 paved urban road 30 km/h	Run 28 paved urban road 30 km/h
Run 25 urban bumps 20 km/h	Run 26b urban bumps 30 km/h
Run 26 urban bumps 30 km/h	Run 26a urban bumps 40 km/h

Driving Manoeuvres (Psychoacoustics)	
Vehicle A	**Vehicle B**
Run 4 urban road 40 km/h	Run 4 urban road 40 km/h
Run 5 urban road 70 km/h	Run 5 urban road 70 km/h
Run 7 run up 70-120 km/h	Run 7 run up 70-120 km/h
Run 12 extra urban road 70 km/h	Run 16 extra urban road 70 km/h
Run 14 run up 70-110 km/h	Run 15 run up 70-110 km/h
Run 15 up-hill road trait 80 km/h	Run 14 up-hill road trait 80 km/h
Run 16 Racconigi main road course 60 km/h	Run 19 Racconigi main road course 60 km/h
Run 18 run up 50-130 km/h	Run 18 run up 50-130 km/h
Run 24 paved urban road 30 km/h	Run 28 paved urban road 30 km/h

The testing route included several different kind of roads, ranging from urban roads, extra-urban roads, countryside paths and city centre paved stone courses.

In the following figures, graphical representation of the paths and routes travelled during the several tests have been collected by exploiting online Google Maps application, inserting the proper addresses and selecting the specific route calculations to get an indicative visualization of the different road segments encountered along the recording and driving procedures.

In detail, most of the urban and extra-urban cycle testing have been accomplished on the road traits between Carmagnola and Racconigi towns, in proximity of the borderline between the two provinces of Torino and Cuneo (Figure 6.11 and Figure 6.12), travelling also in the city centre areas for the recordings of the urban runs and the bumps sequences (Figure 6.13 and Figure 6.14), then on the Racconigi bypass for the mid-high speed recordings. Rural off-road paths testing have been executed in the countryside surroundings of Carmagnola and near hamlets. (Figure 6.15).
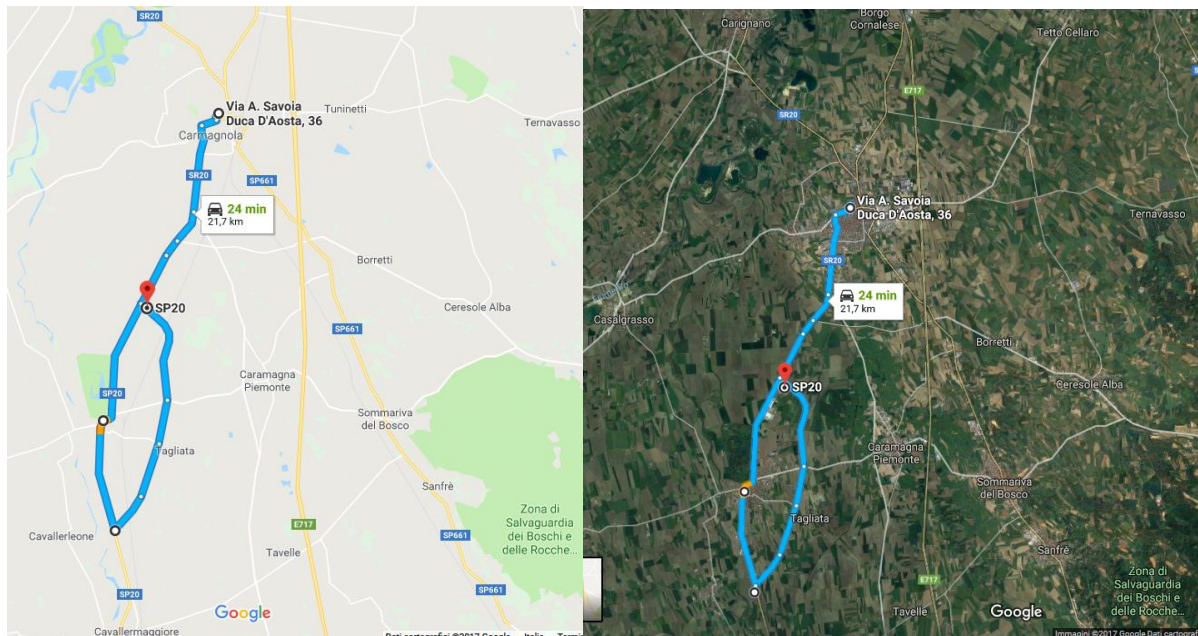

Figure 6.11: Overview of the driving route followed during the extra-urban tests.

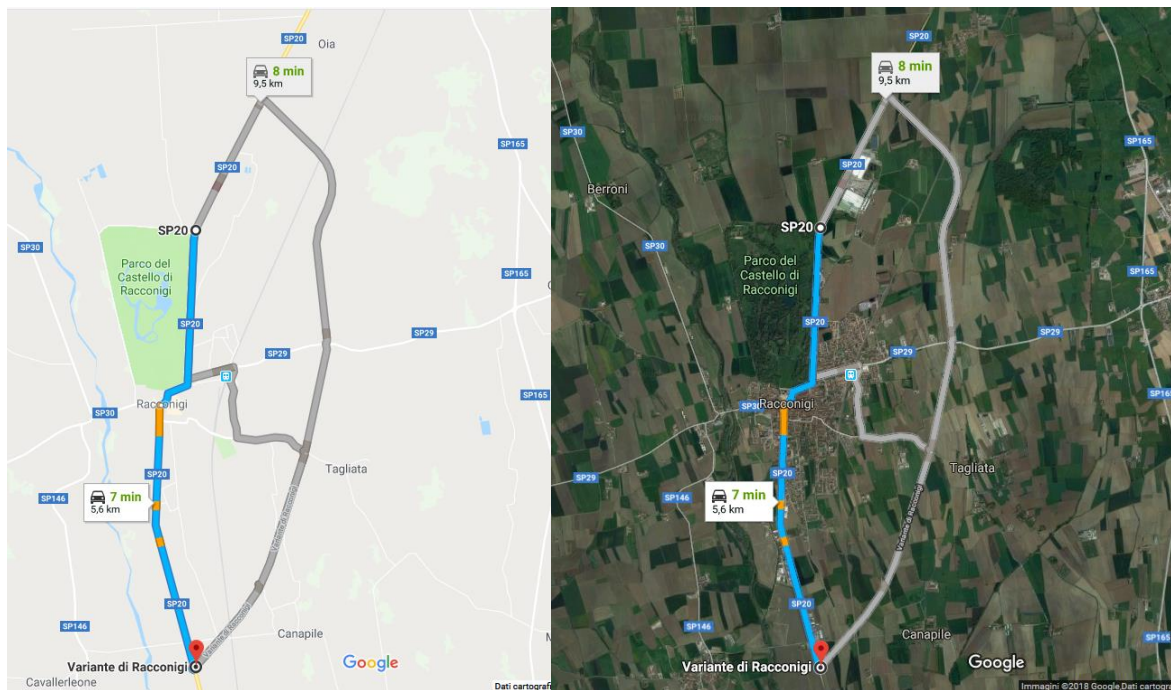**Figure 6.12**: Detail of the driving route followed during the urban and extra-urban tests in Racconigi.
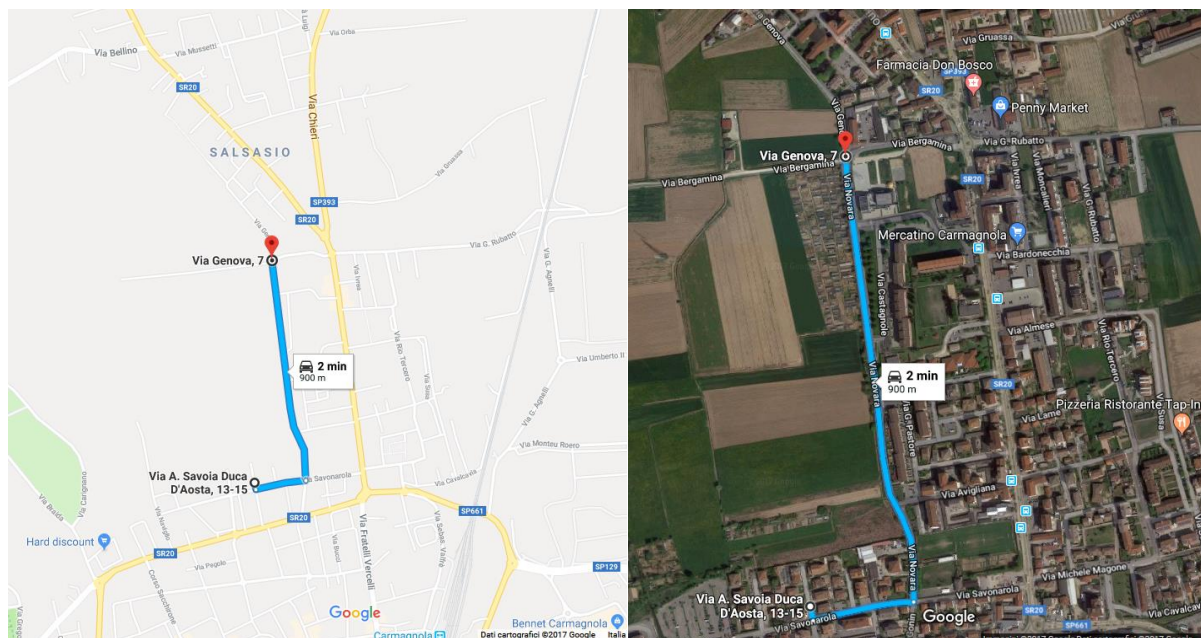

Figure 6.13: Overview of the driving route followed during the urban bumps sequence runs.
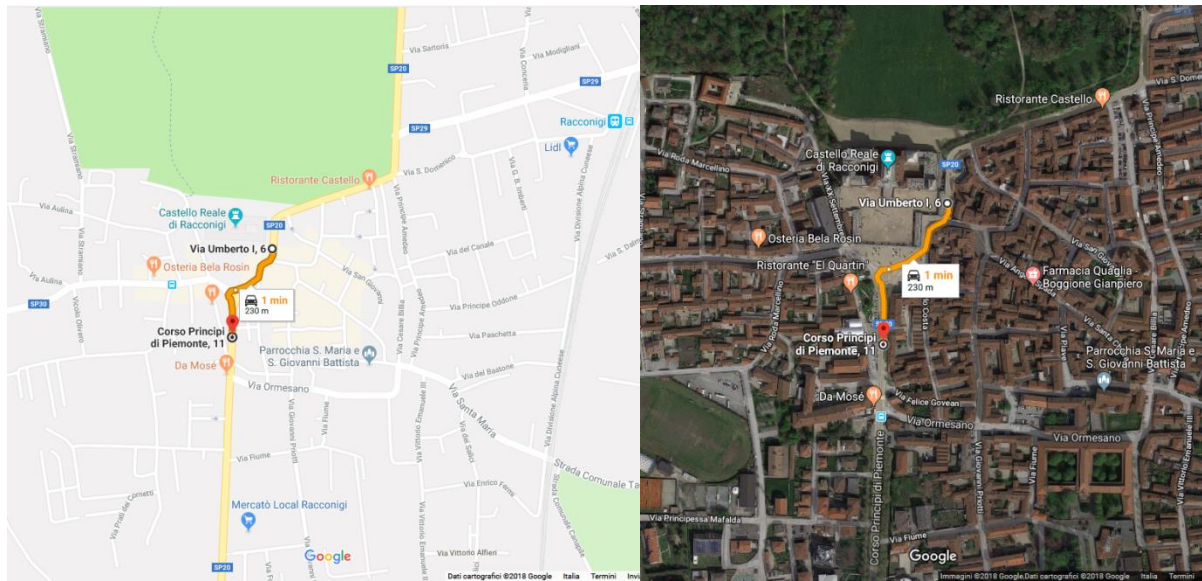
Figure 6.14: Overview of the driving route followed during the Racconigi urban paved road run.
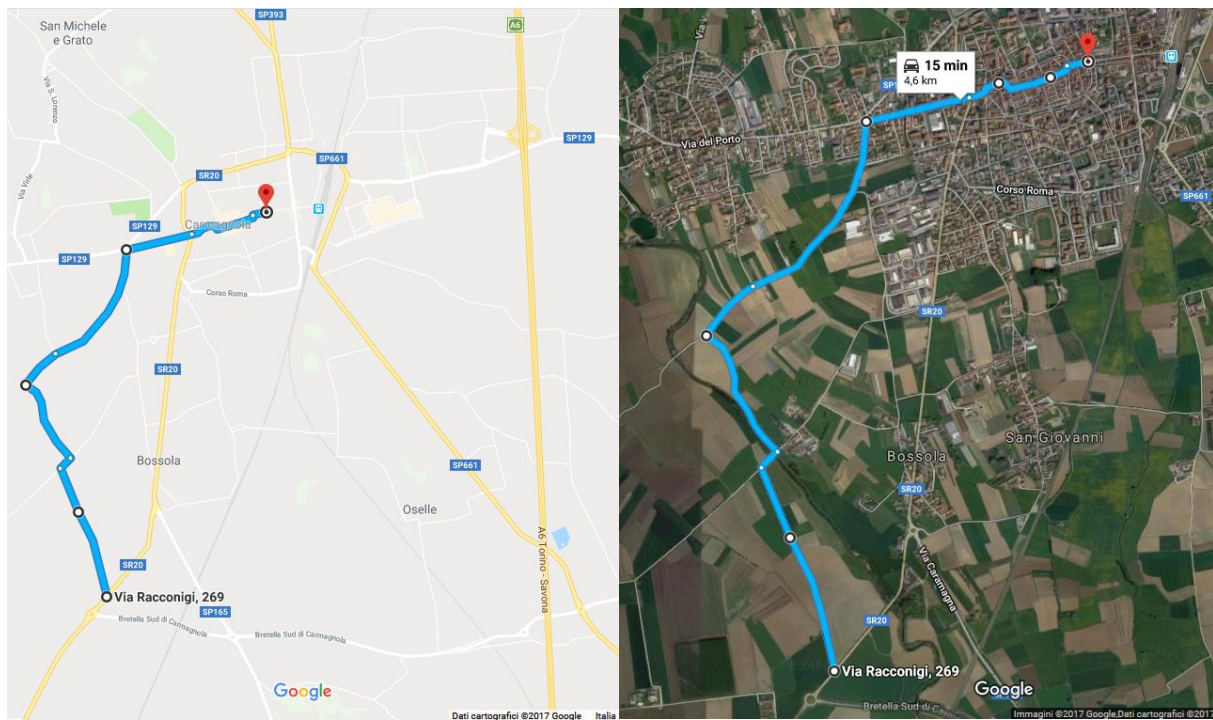
Figure 6.15: Overview of the driving route followed during the rural off-road tests and urban paved road runs near Carmagnola.

Regarding the information elaboration, the data acquisition has been performed with the aid of the Signature Acquisition LMS Test.Lab dedicated tool, whose interface is reported in Figure 6.16.
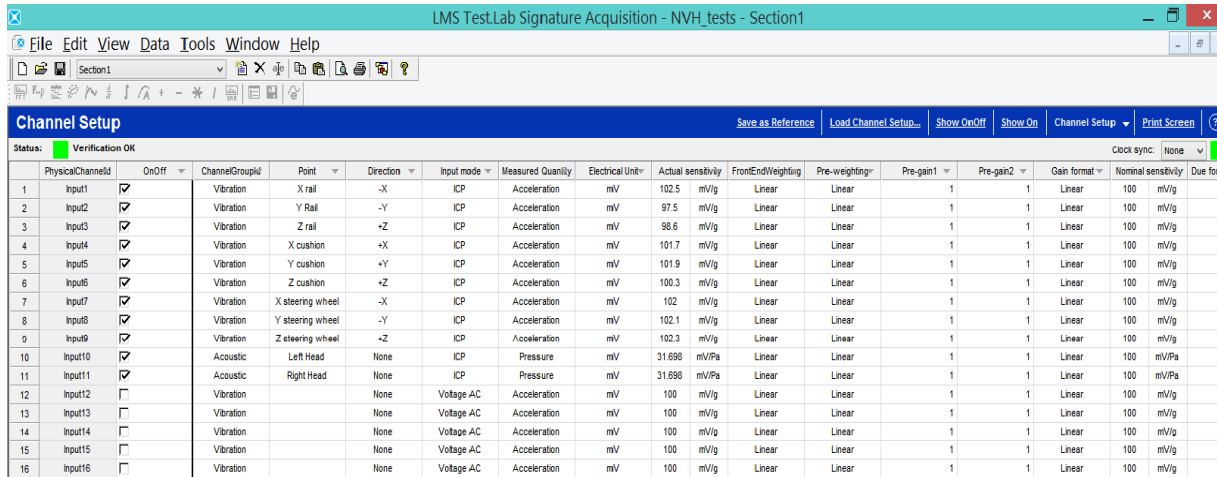
Figure 6.16: Channel Setup interface in Test.Lab Signature Acquisition.

Then, the sensors channels calibration has been performed, using the calibration pack, included in the Signature Acquisition tool, (Figure 6.17).
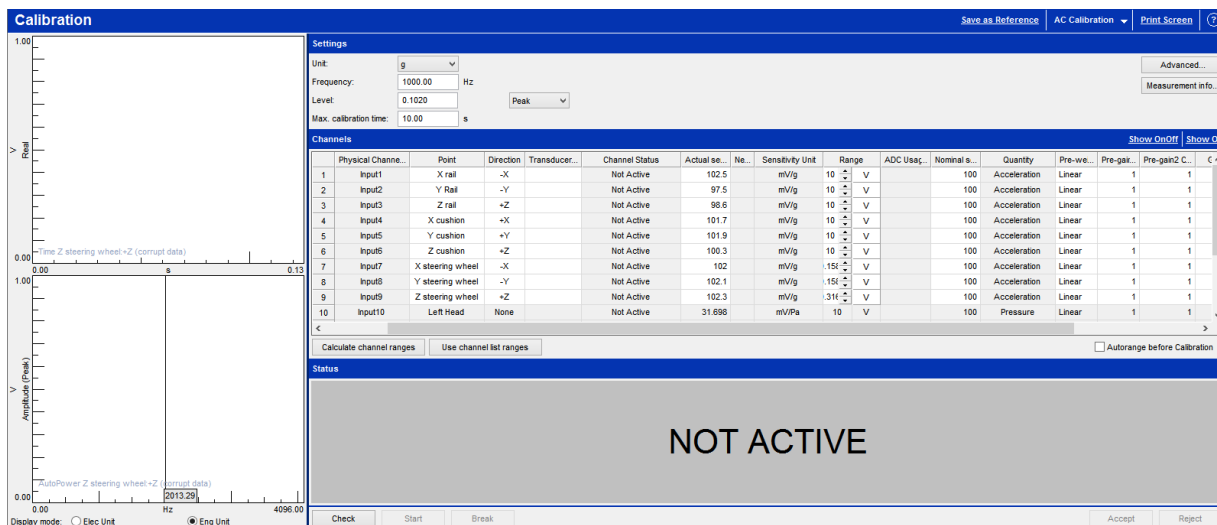
Figure 6.17: Calibration interface in Test.Lab Signature Acquisition, (offline).

Afterwards, the proper options have been selected in the Tracking and Acquisition Setup tools, (Figure 6.18 and Figure 6.19 respectively), to obtain a correct measuring.
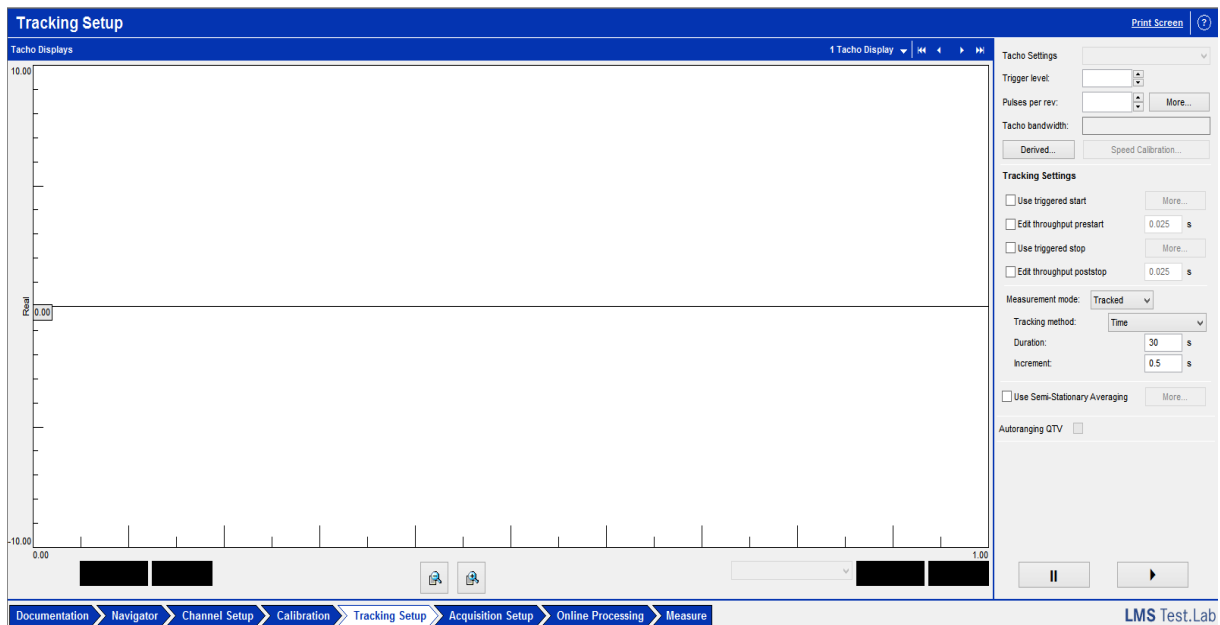
Figure 6.18: Tracking Setup interface in Test.Lab Signature Acquisition, (offline).

Figure 6.19: Acquisition Setup interface in Test.Lab Signature Acquisition, (offline).

Moreover, before to actually start the measures, the Online Processing pack has been exploited, in order to manage the different settings concerning channel processing and the sections options, relative to both the acoustics and vibration parts, (Figure 6.20).
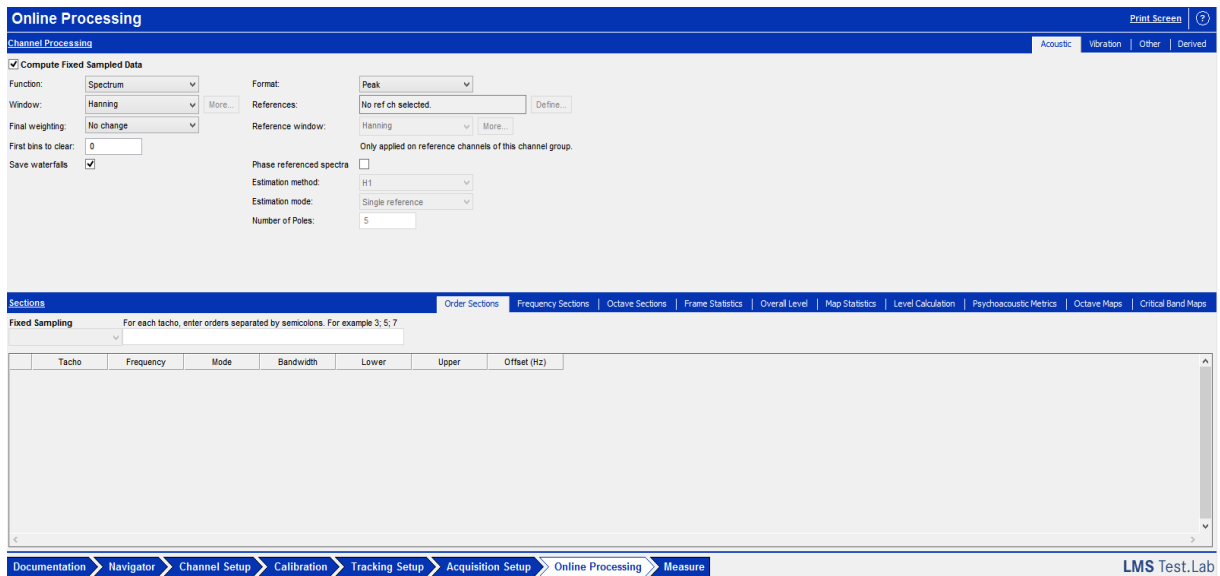
Figure 6.20: Online Processing interface in Test.Lab Signature Acquisition, (offline).

Subsequently, as a last step regarding the acquisition software management, all the previous options have been considered in the Measure pack, the tool dedicated to actively perform the collection of the external acoustics and vibrational inputs, which involves a comprehensive overview on channels, including the settings for ranging, tracking, acquiring, together with the general project and the specific measure options, providing also notifications in case of overload from one or more channels. Figure 6.21 depicts the interface of the last tool in Signature Acquisition.
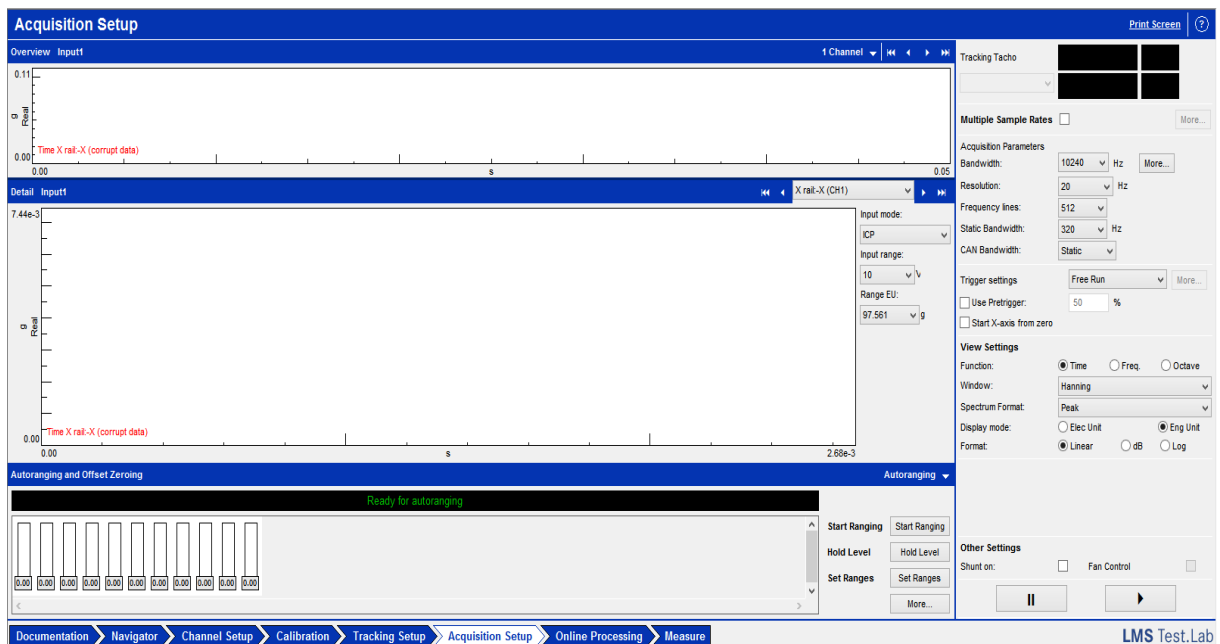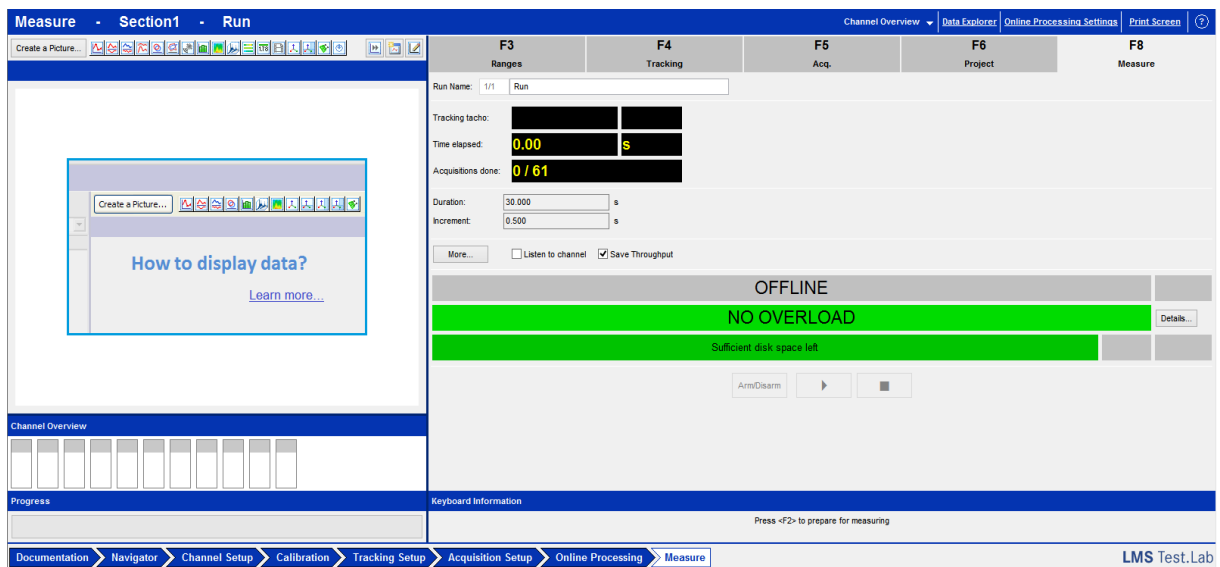

Figure 6.21: Measure interface in Test.Lab Signature Acquisition, (offline).

In the following part, the acquired data have been analyzed and processed by exploiting the Signature Throughput Processing tool, which includes several add-ins suitable for examining, manipulating, elaborating and post-processing the different information so that the desired computations and results have been obtained.

The several folder and files containing the data recordings of the tests on the two selected cars have been loaded on the software, to allow a quick and simple exploration between the various items, within the internal environment of the Navigator interface, helpful for changing the actual section, the run on which the elaborations are executed and suitable for creating pictures describing the different results, (Figure 6.22).
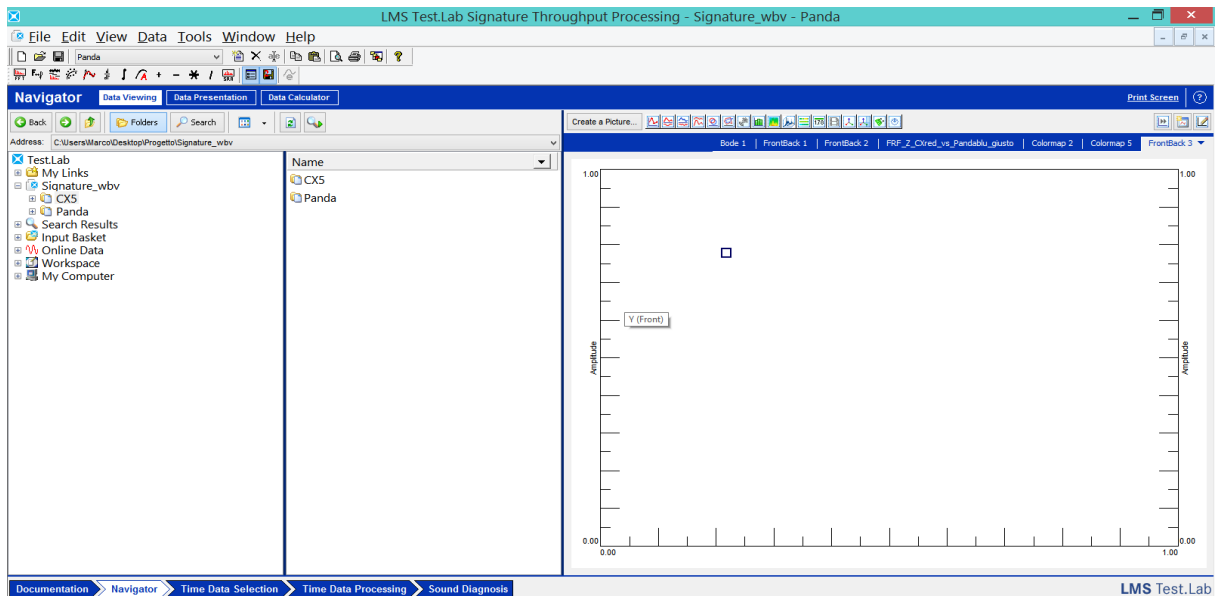
Figure 6.22: Navigator interface in Test.Lab Signature Throughput Processing.

In addition, to actuate the specific computations, the several runs of each data source have been selected in the Time Data Selection toolbox, (Figure 6.23).
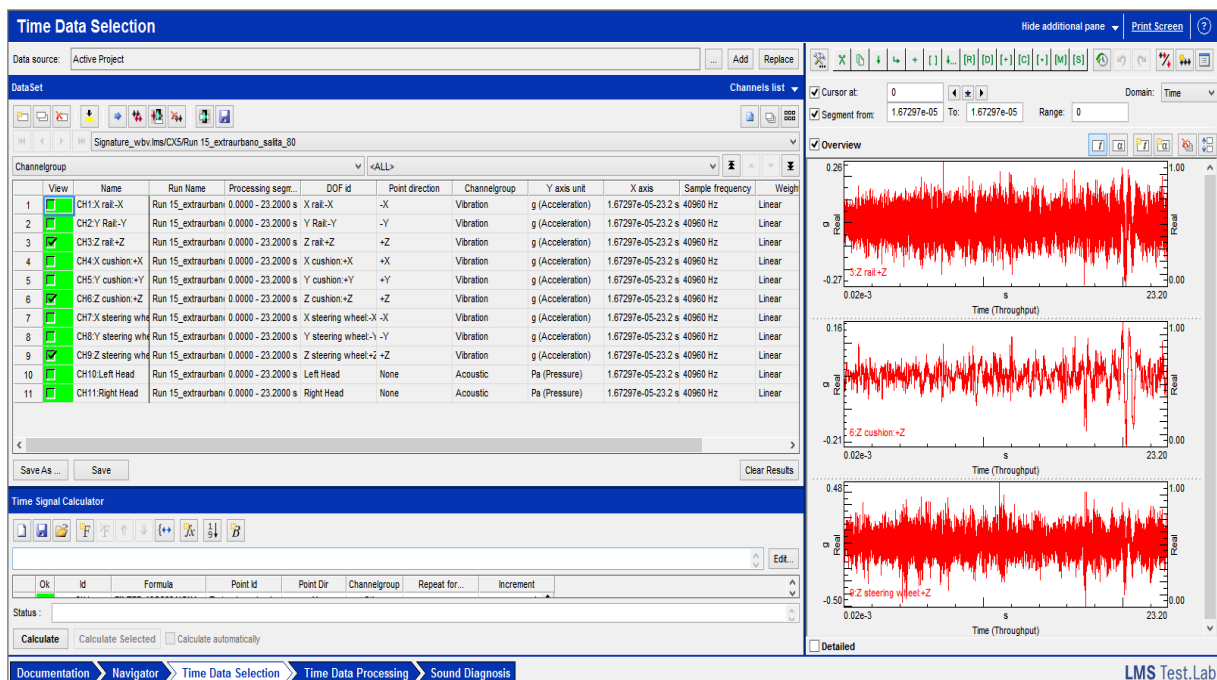
Figure 6.23: Time Data Selection interface in Test.Lab Signature Throughput Processing.

Such an interface provided also the specific Time Signal Calculator add-in, that has been adopted to manage the resampling and the weighting/filtering of the data chosen to perform the WBV and HTV analysis.

Indeed, both the resampling and the vibration analysis formulas have been chosen between the conditioning functions in the function selection panel, (Figure 6.24).
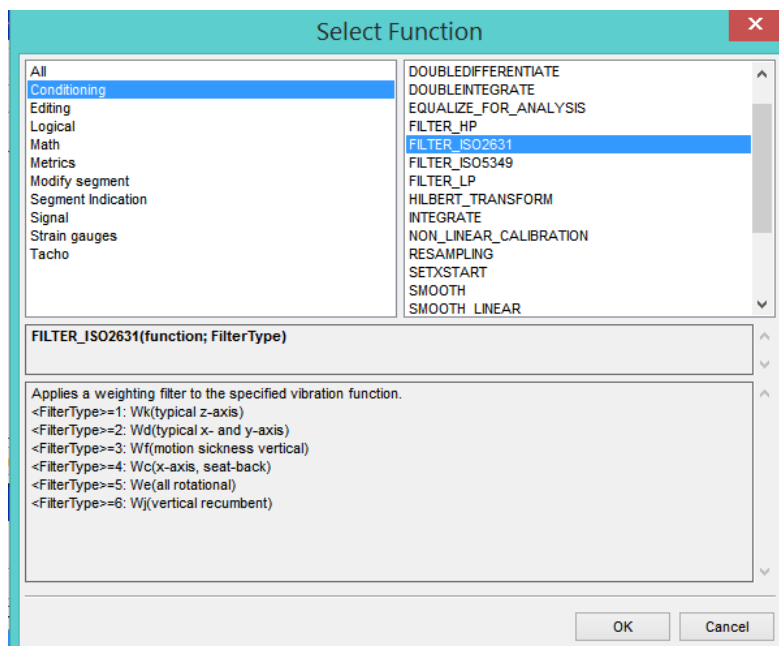
Figure 6.24: Function selection tooltip, to insert the WBV and HTV filtering formulas.

In particular, the formulas for ISO-2631 and ISO-5349 filtering have been managed in the formula editing option included , (Figure 6.25 and Figure 6.26).
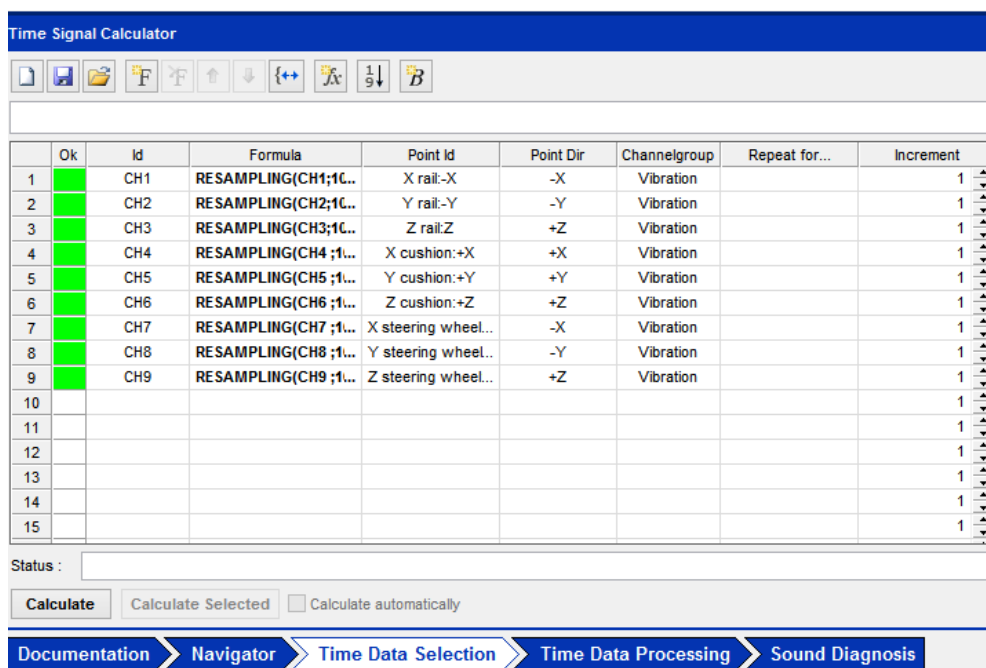
Figure 6.25: Time Signal Calculator resampling functions template in Time Data Selection tool.

Figure 6.26: Time Signal Calculator ISO weighting functions template in Time Data Selection tool.

After, the specific weighting indexes relative to the channel measuring directions have been chosen: concerning the HTV channels, W_h is valid for all the directions; conversely, regarding the WBV channels, the W_k index have been considered for the Z-axis direction channels, while the W_d one have been opted for the x-y axes directions channels(Figure 6.27).

Figure 6.27: Time Signal Calculator formula editing for ISO-2631 and ISO 5349 weighting.

Subsequently, as a former step, the desired channels have been enabled each time, depending on the computations, (Figure 6.28), thus, the selected data have been processed and the proper settings chosen in the Time Data Processing interface, which comprises the various options concerning the acquisition, section, channel parameters, (Figure 6.29).
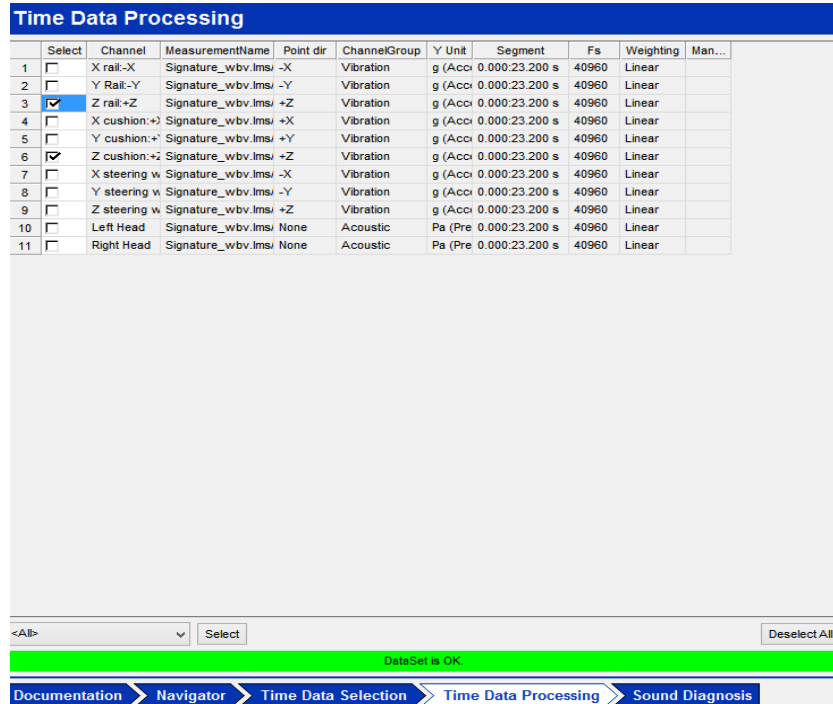
Figure 6.28: Channel selection panel in Time Data processing toolbox.
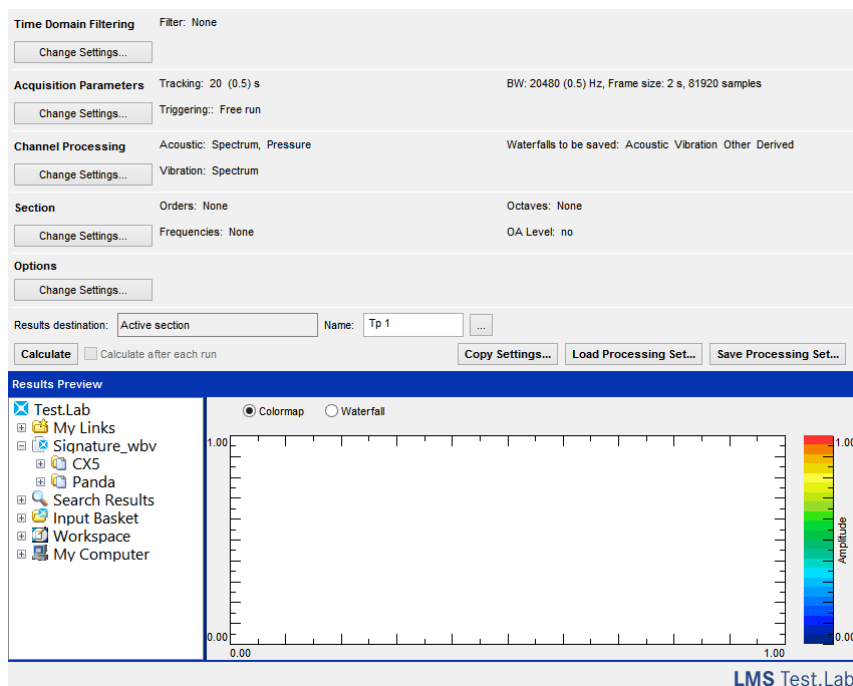
Figure 6.29: Processing option panel in Time Data processing toolbox.

As the different computation has been based on different sources and different settings, a non-little effort has been produced in looking for the best possible settings to obtain in every case the most accurate and representative results, both from a graphical and a numerical point of view, (Figure 6.30).

Moreover, in the channel processing settings, the desired magnitudes to be calculated for the acoustics and vibration fields have been chosen from time to time, together with the possible reference channel to be considered, as in the case of the FRF calculations, (Figure 6.31).
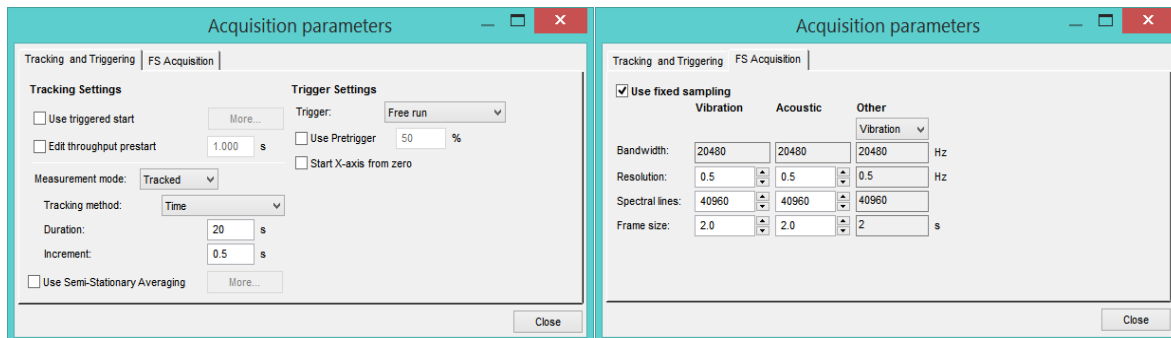
Figure 6.30: Acquisition parameters option menu included in Time Data Processing interface.
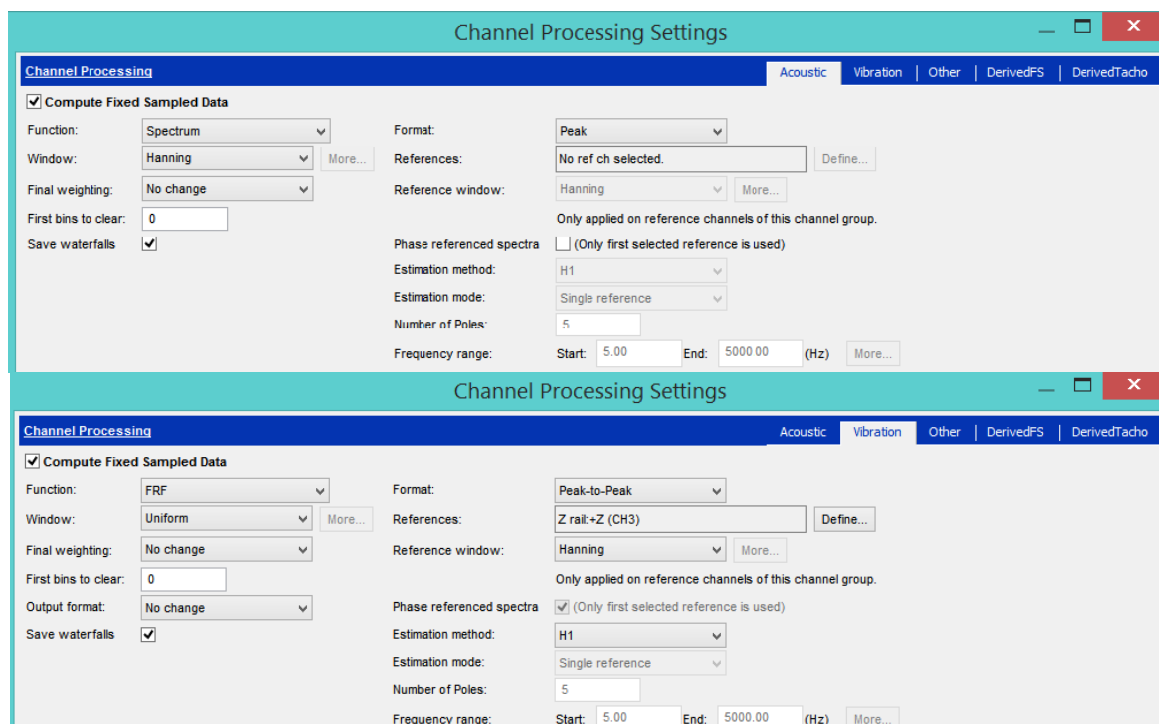
Figure 6.31: Acoustics and Vibration channel processing settings in Time Data processing interface.

Furthermore, concerning the assessment of wbv and htv parameters for the discrete manouvre tests, as the bumps sequence runs performed in Carmagnola, specific temporal segements have been defined within the chosen runs, (Figure 6.32, Figure 6.33 and Figure 6.34), together with proper settings related to resolution, sampling and time duration selection, in order to get results as accurate as possible even considering the particular characteristics of the considered segments.
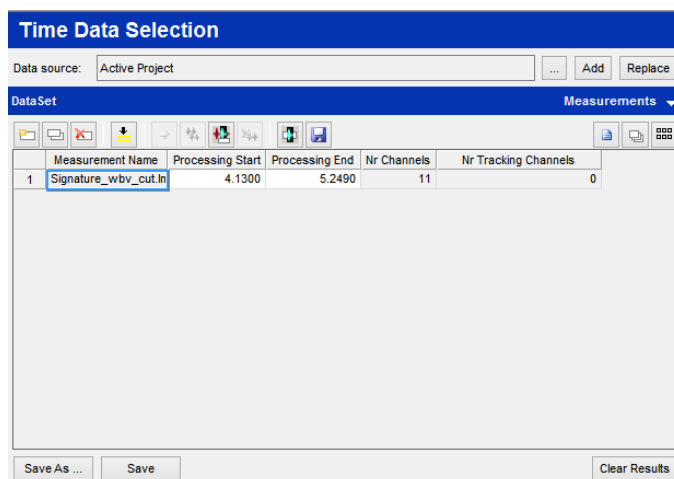
Figure 6.32: Example of a segment temporal definition inside a selected run.
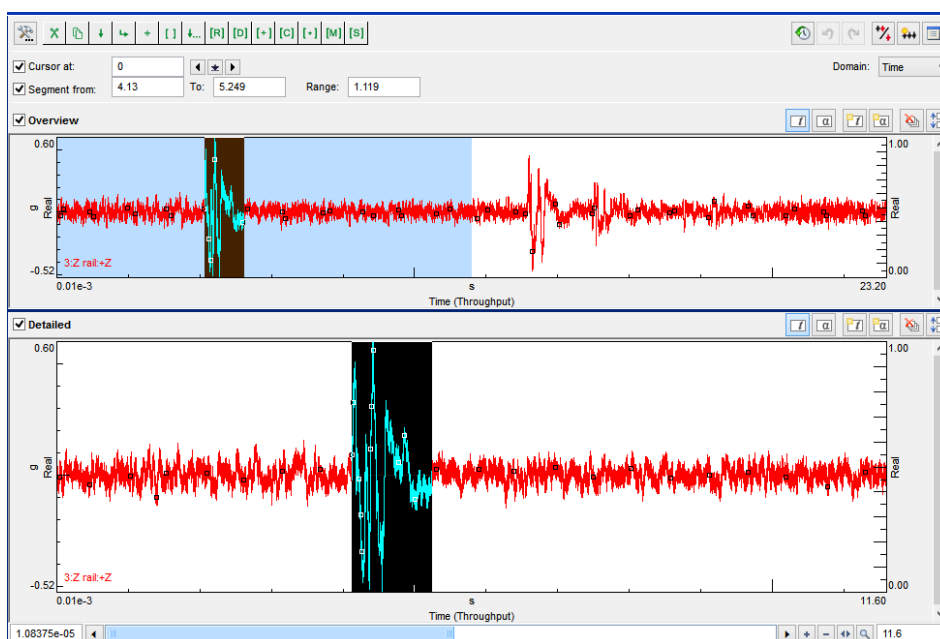
Figure 6.33: Graphical methodology for the selection of the specific temporal segment duration.
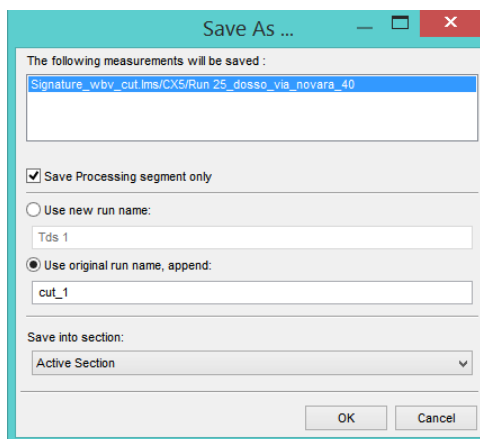
Figure 6.34: Saving procedure for the specific run segment.

Moreover, being the bumps related to descrete phenomena of excitation, from a general duration about 20 seconds the frame size and time have been changed to values giving proper results in case of recording durations often in the proximity of 1 second, thus requiring several trials and errors procedure to understand the correct settings in order to have non-null, realistic outcomings (Figure 6.35 and figure 6.36).

Figure 6.35: FS acquisition parameter for discrete manouvres vibrational assessment.

Figure 6.36: Tracking and Triggering acquisition parameter for discrete manoeuvres vibrational assessment, with a sample time duration.

As a last tool exploited in the Signature Throughput Processing software, the Sound Diagnosis add-in has been properly exploited to perform the psychoacoustic analysis, other than listening and comparing the several recordings, also extracting the main sound quality metrics of interest, creating pictures and graphs representing the different magnitudes. A representation of the main interface of Sound Diagnosis main menu is provided in Figure 6.37.
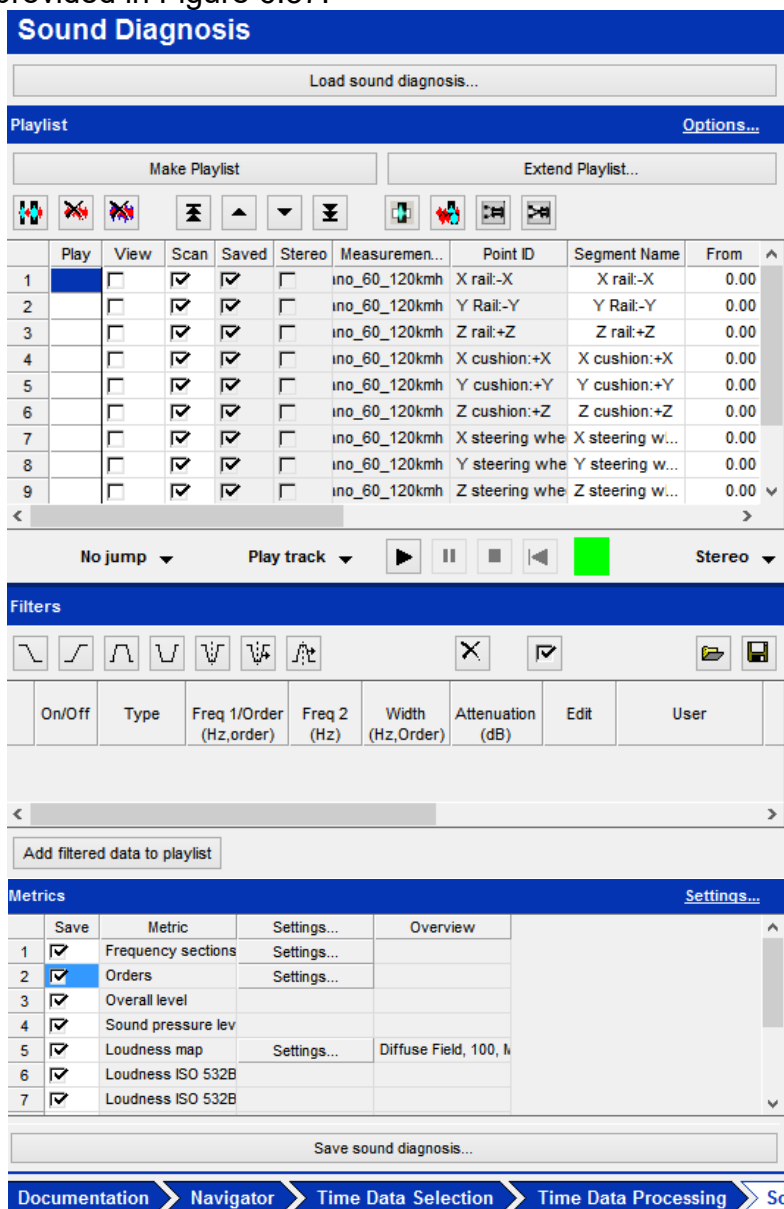
Figure 6.37: Play set and sound quality metrics menu in Sound Diagnosis interface.

On the other hand, the management of the different data folders, the creation of diagrams and the working on the various wave shapes relied on the functions provided by the strip chart display, the data display and the picture editor, (Figure 6.38).
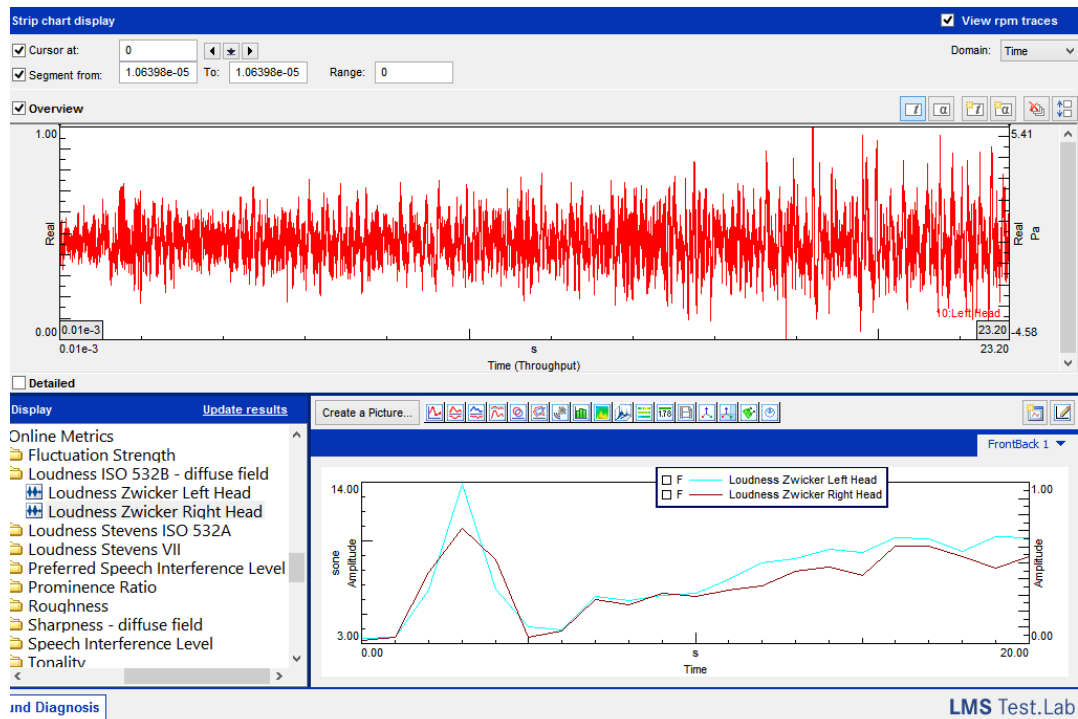
Figure 6.38: Picture editor, results and strip chart displays included in Sound Diagnosis interface.

Furthermore, when dealing with audio-spectrum colour-maps, the specific frequency and acoustic power boundaries have been selected, choosing a frequency range suitable to distinguish the different colour shades and an orientation useful to make better understandable the trend of the considered entities. In Figure 6.x a rough example of colour-map relative to an audio spectrum is depicted, whereas Figure 6.y illustrates the option screen in which the axes orientation have been changed.
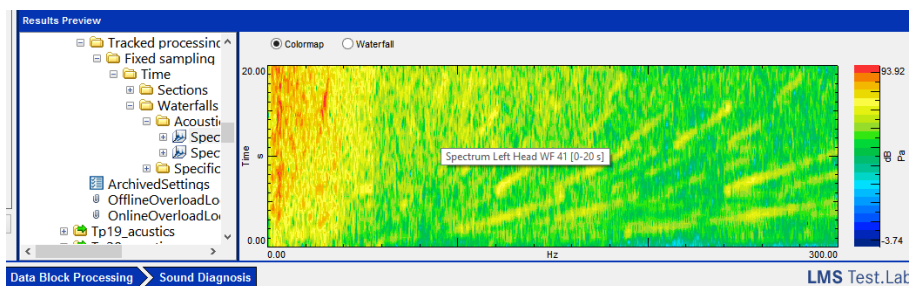
Figure 6.39: Sound Diagnosis Colour-map display, relative to a CX.5 run audio-spectrum.
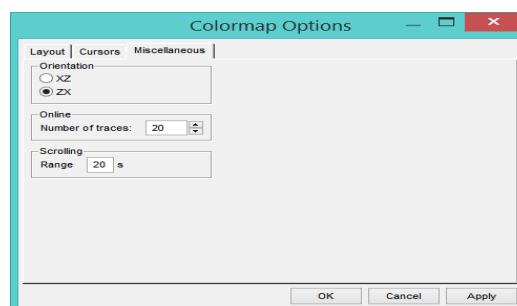
Figure 6.40: Colour-map option toolbox, with the preferred axis orientation.

7 Vibration analysis results

7.1 General Z-axis test acceleration profile at the seat rail

Concerning the vibration parameters assessment, a first step in the distinction and representation of the several tests is based on presenting the temporal trend of the acceleration level at the seat guide on the Z axis, to have a first glance on the generic excitation characteristic fore faced by the vehicle.

The graphs refer to real data recorded with a sample frequency of 40960 Hz, by exploiting the accelerometer corresponding to the user channel ID: seat z rail.

Moreover, the limited and defined temporal segments, related to the bump sequence runs, are included too, as they have been specifically utilized in the whole-body vibration assessment to determine the RMS and VDV levels.

In Figures 7.11 - 7.20 the vehicle A related a_z seat rail diagrams are illustrated.

7.1.1 Vehicle A seat rail acceleration on z-axis
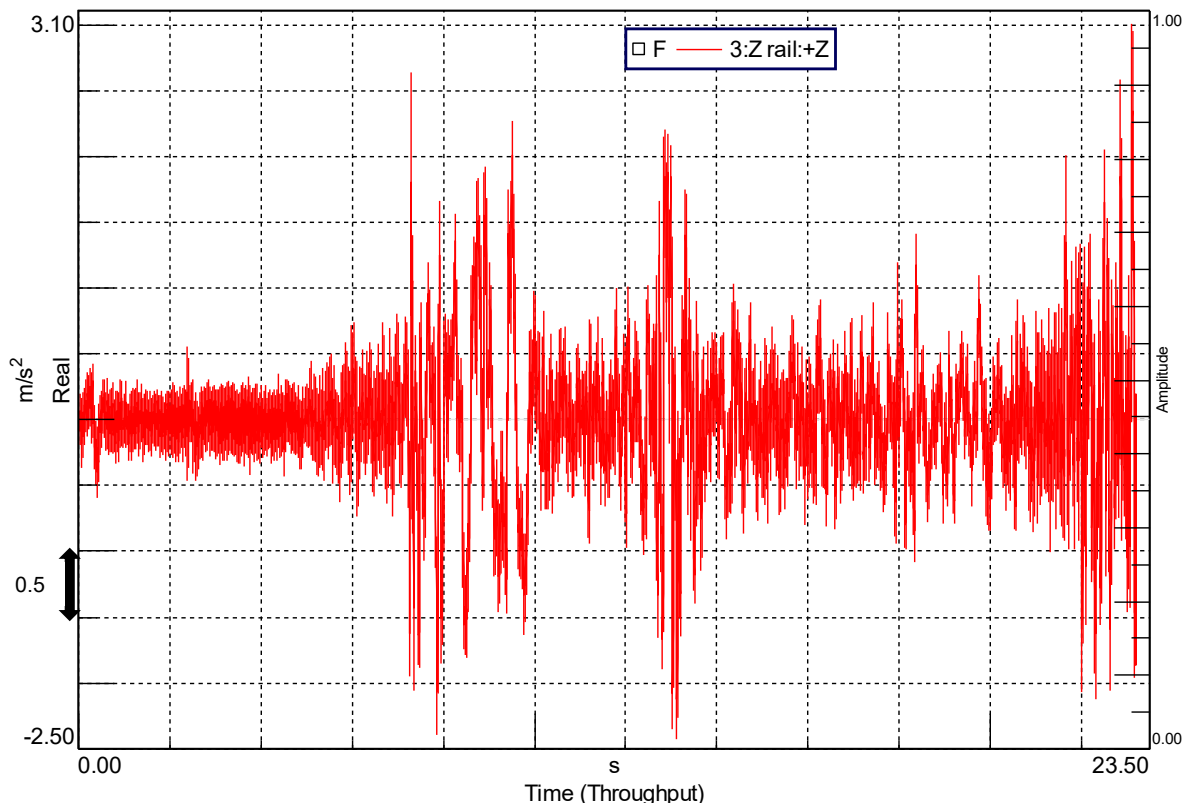
Figure 7.1: Run 2 single wide speed bump 20 km/h, (vehicle A).
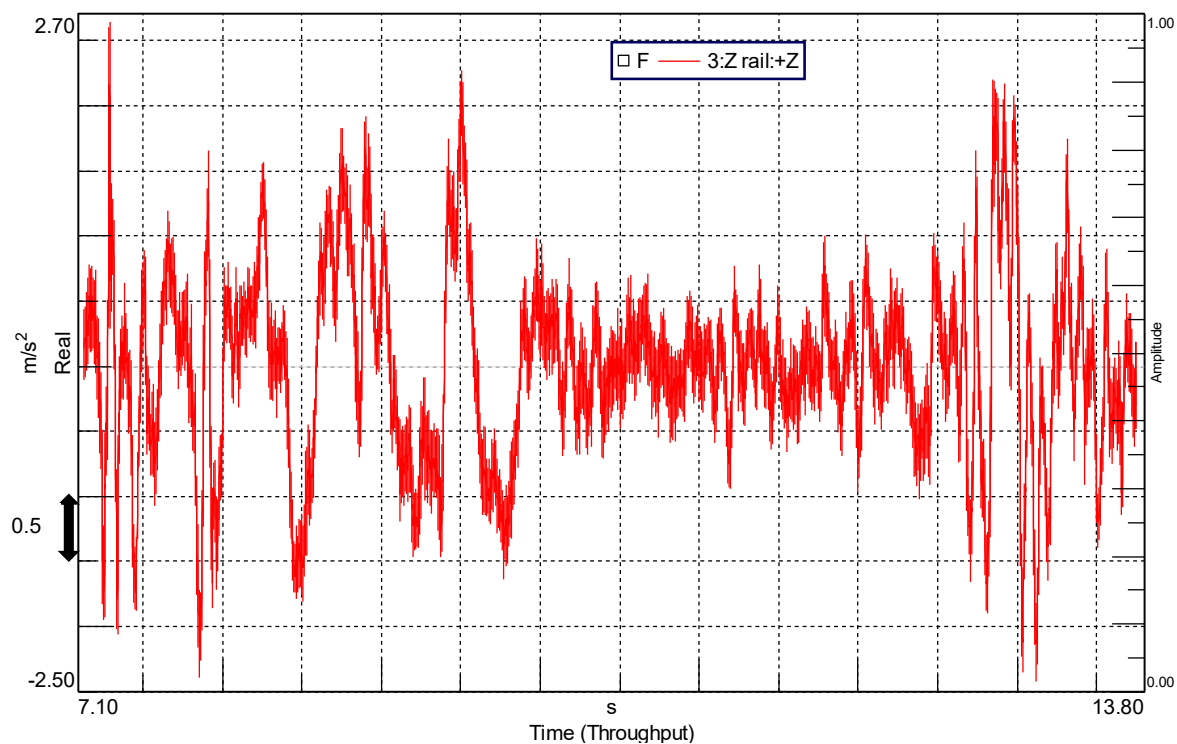
Figure 7.2: Run 2 single wide speed bump 20 km/h cut, (vehicle A).
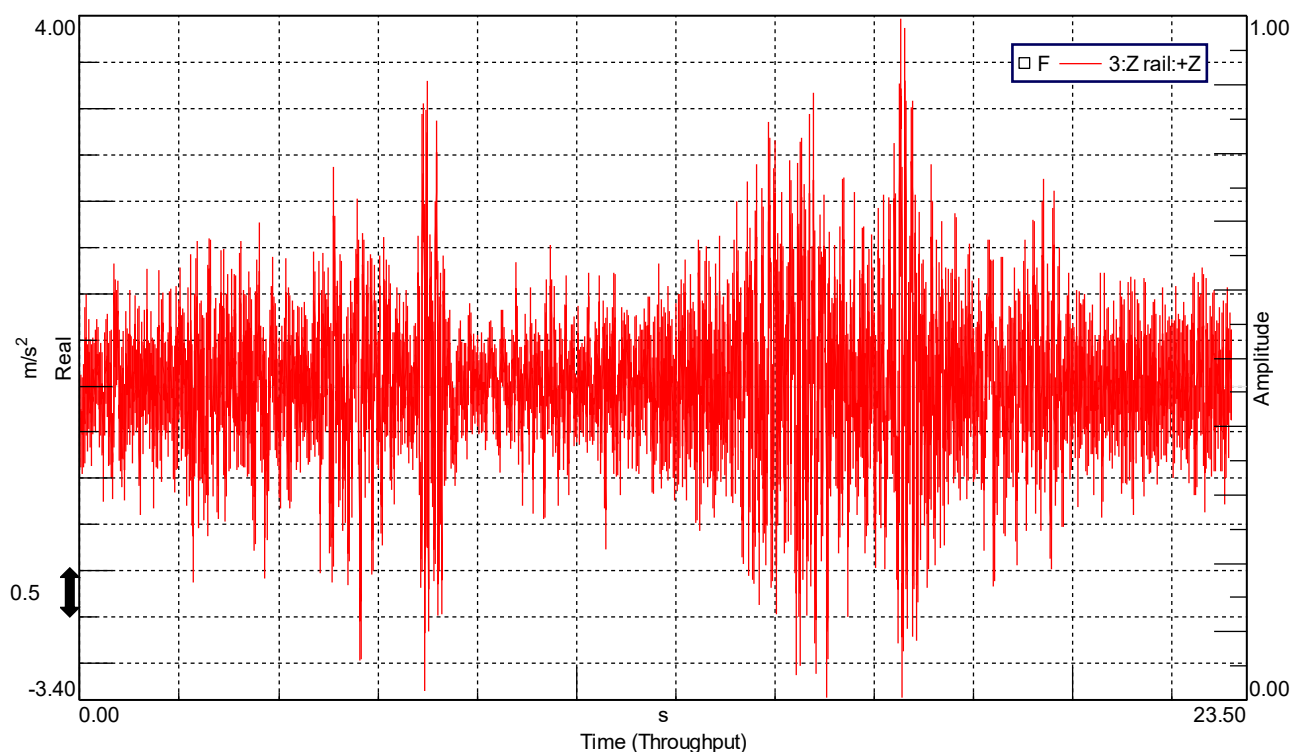
Figure 7.3: Run 4 urban road 40 km/h, (vehicle A).
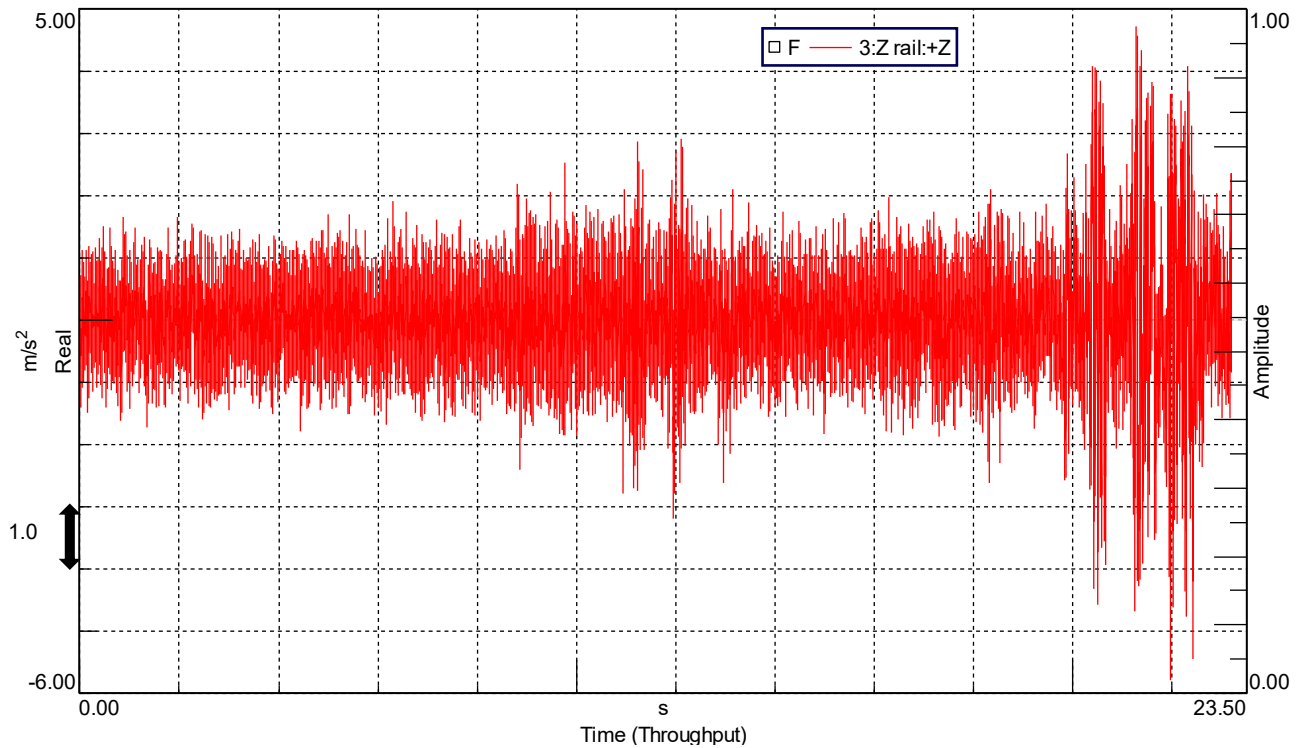
Figure 7.4: Run 5 urban road 70 km/h, (vehicle A).
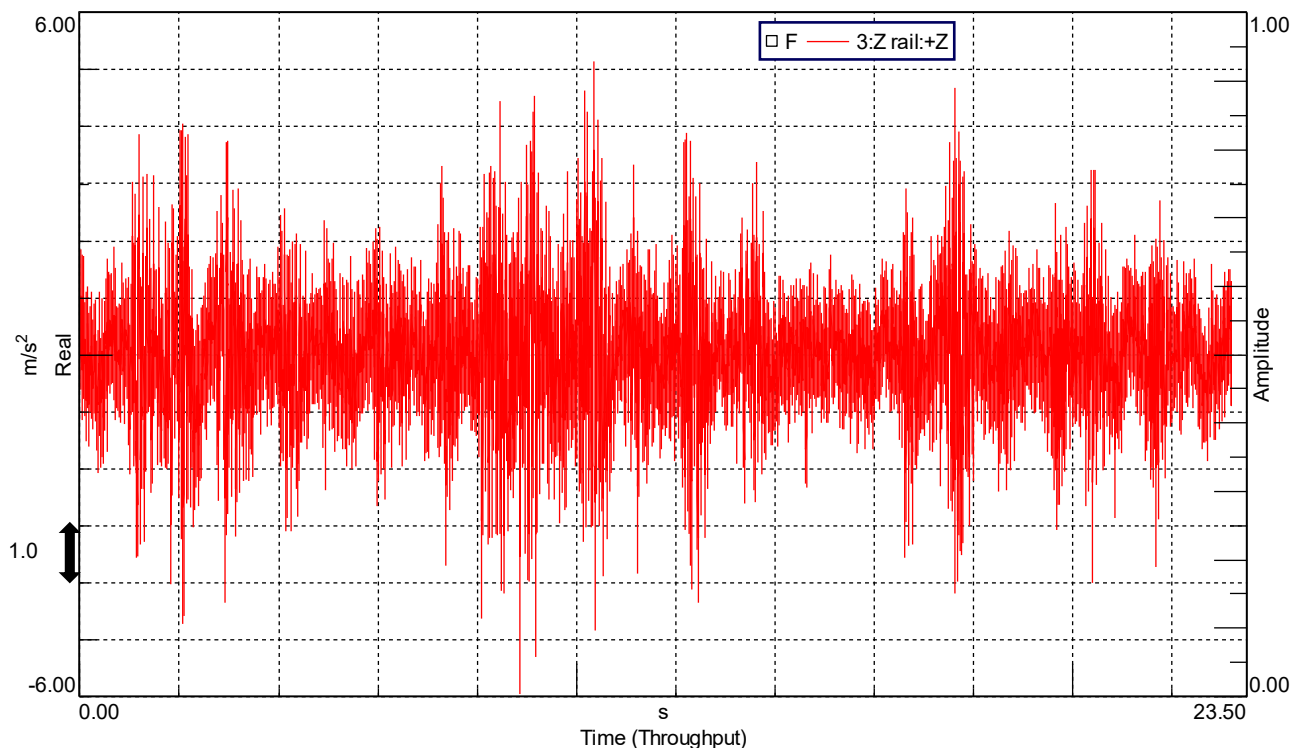
Figure 7.5: Run 9 uneven tarmac extra-urban road 70 km/h, (vehicle A).
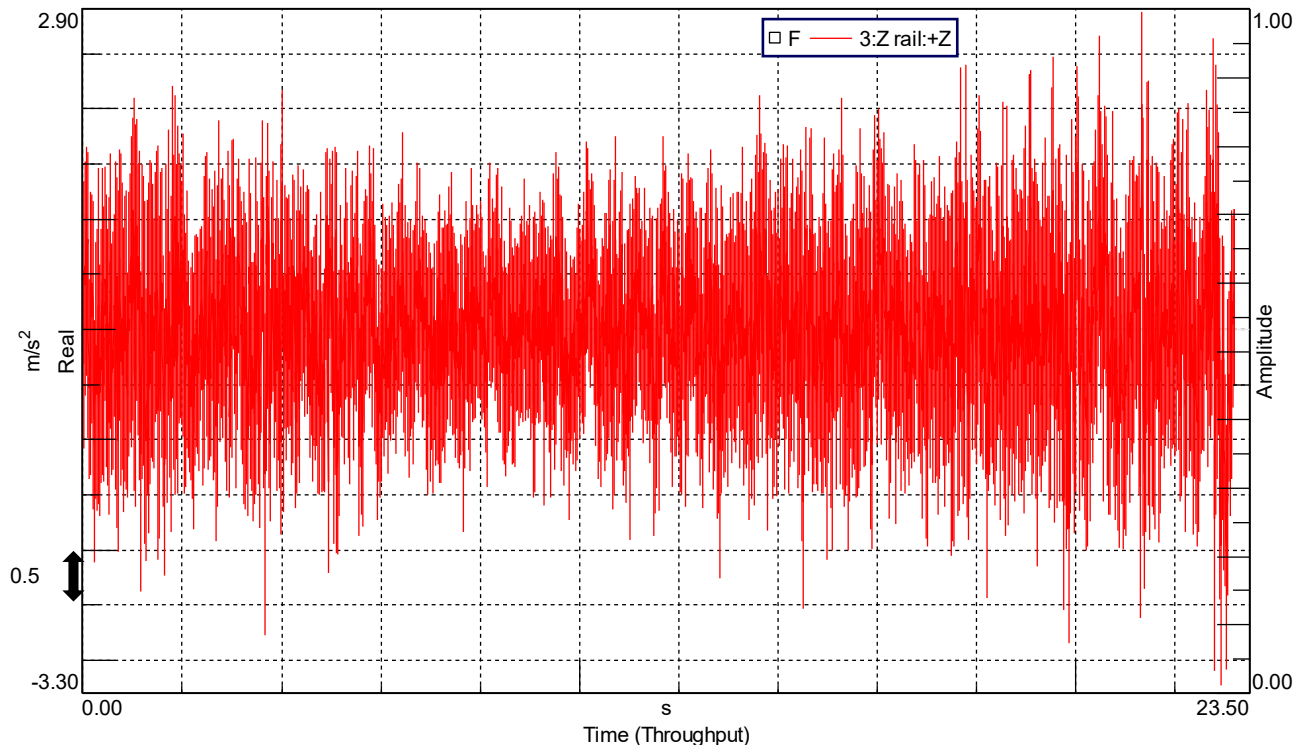
Figure 7.6: Run 11 smooth tarmac extra-urban road 90 km/h, (vehicle A)..
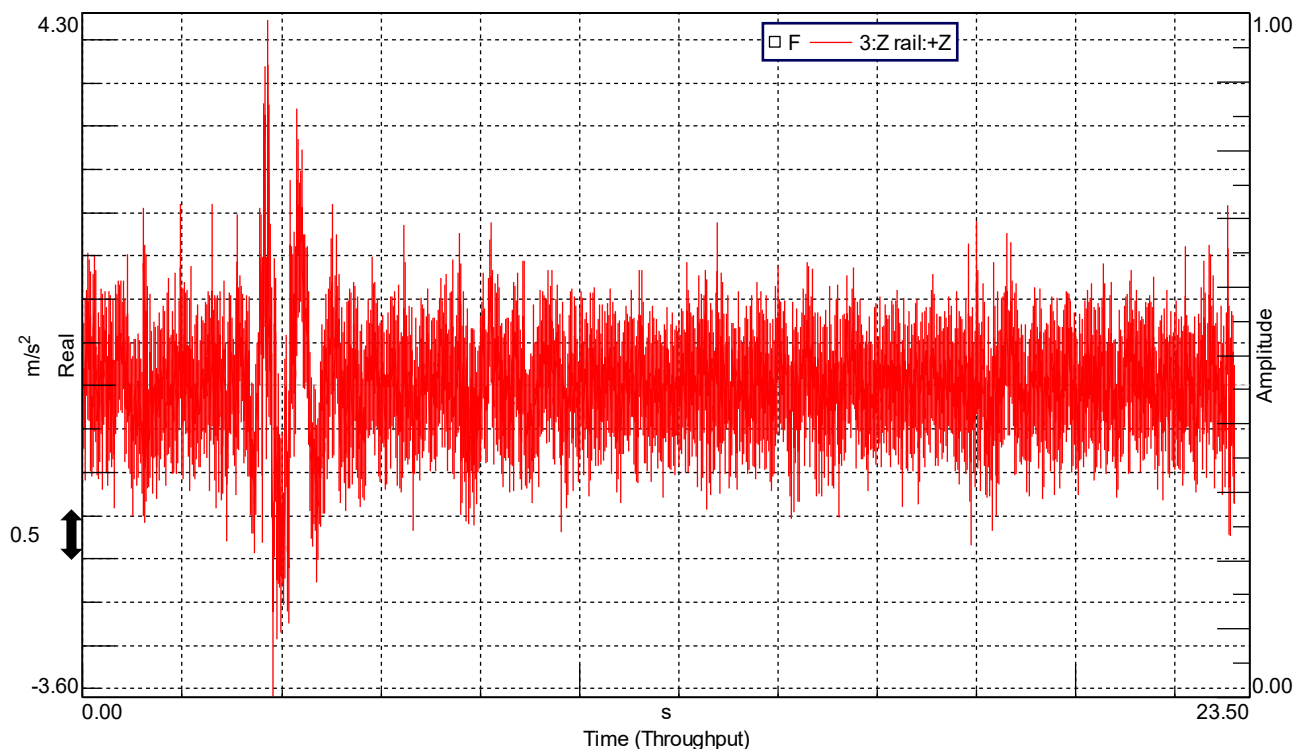
Figure 7.7: Run 12 mixed extra urban-road 70 km/h, (vehicle A).
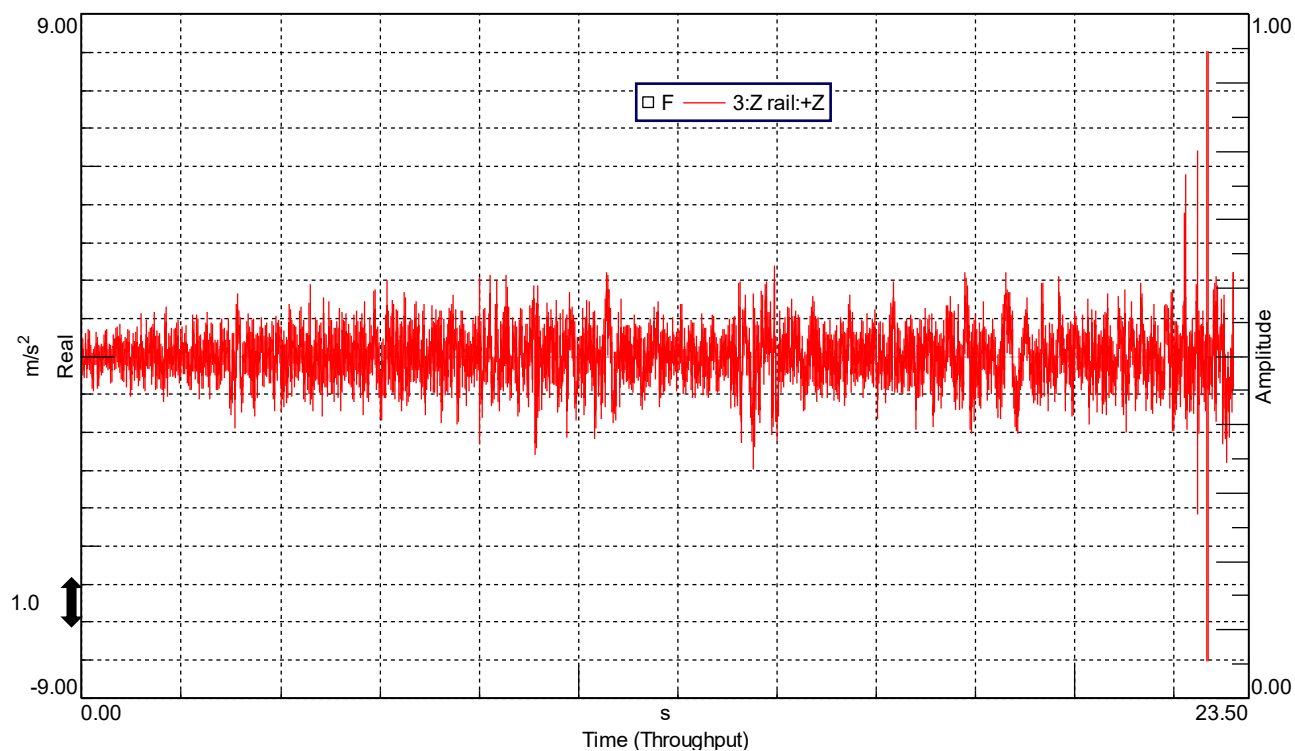
Figure 7.8: Run 19 off-road 30 km/h, (vehicle A).
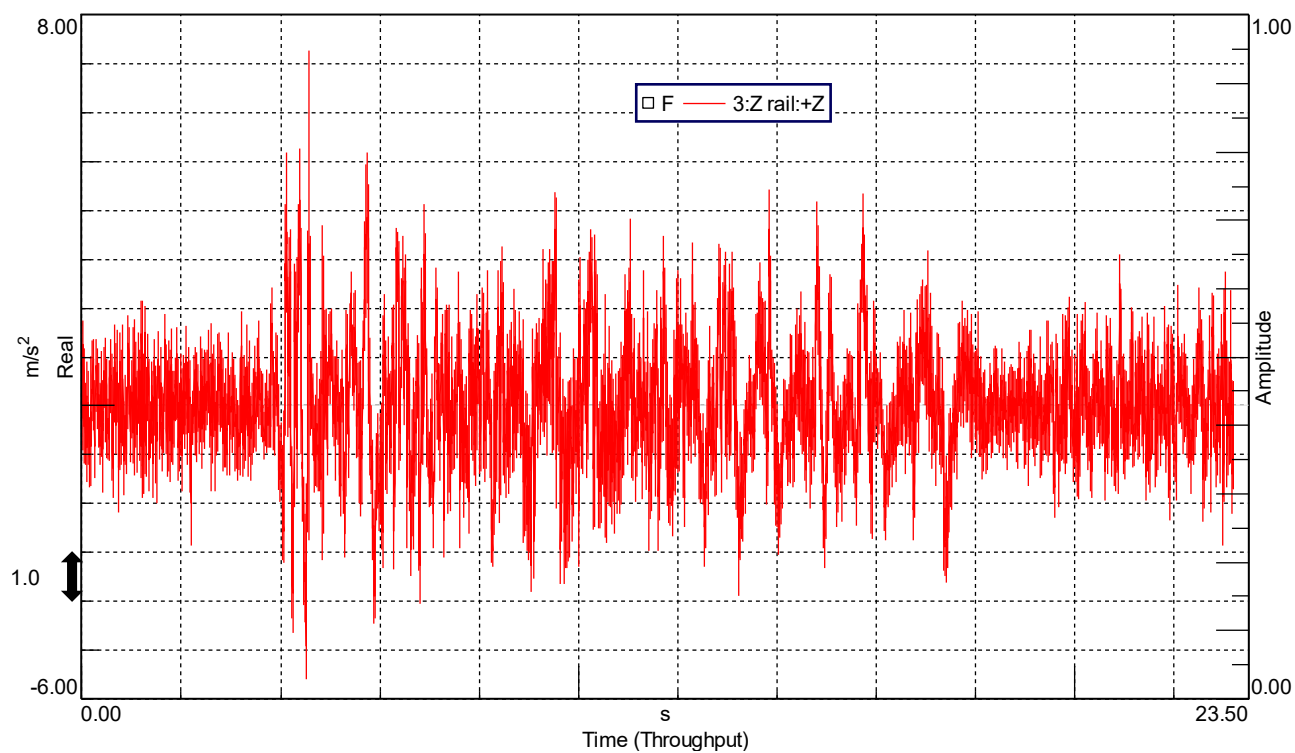
Figure 7.9: Run 20 off-road 40 km/h, (vehicle A).
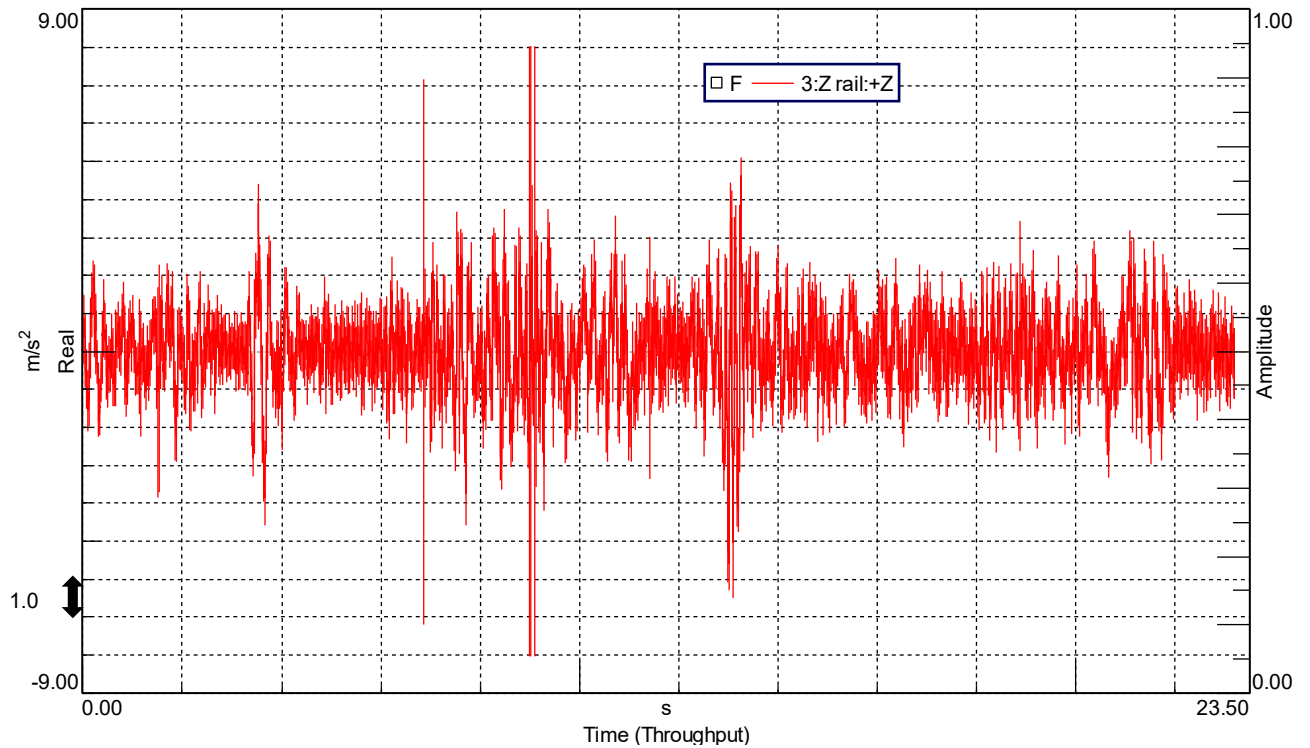
Figure 7.10: Run 21 off-road 50 km/h, (vehicle A).
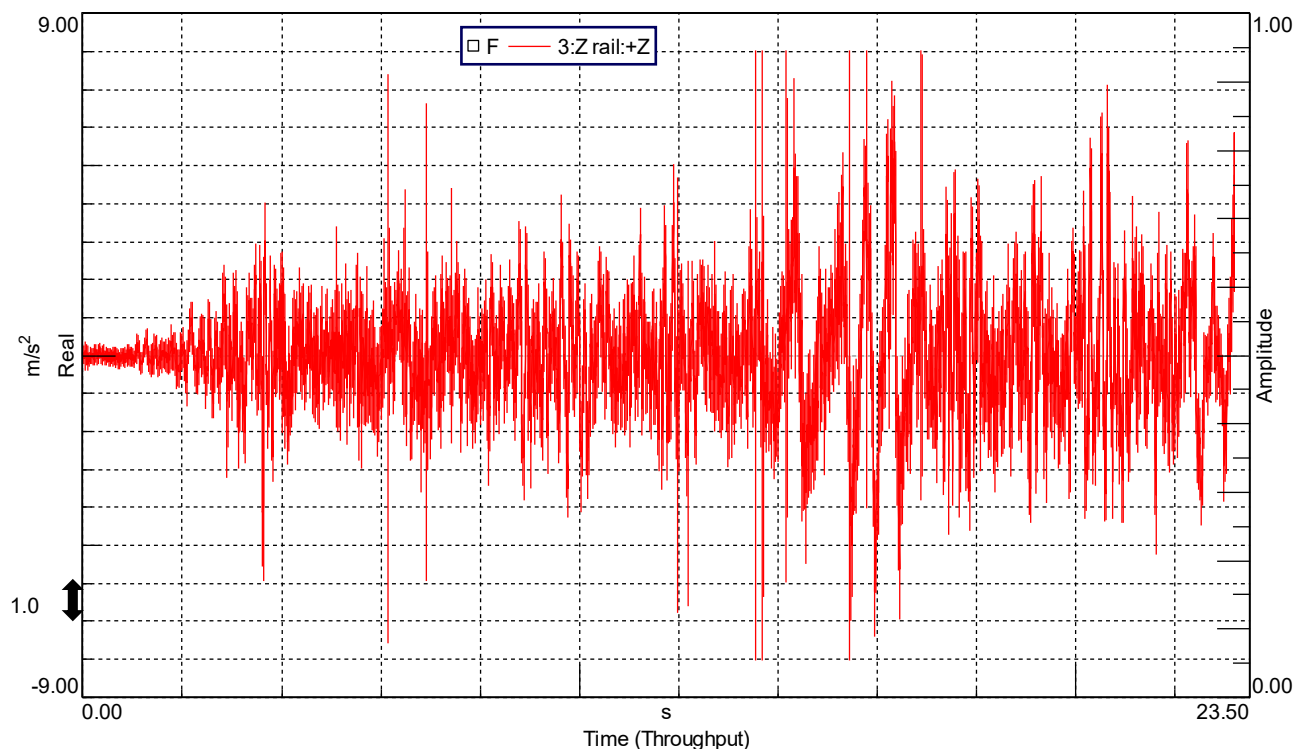
Figure 7.11: Run 22 severe off-road, (vehicle A).
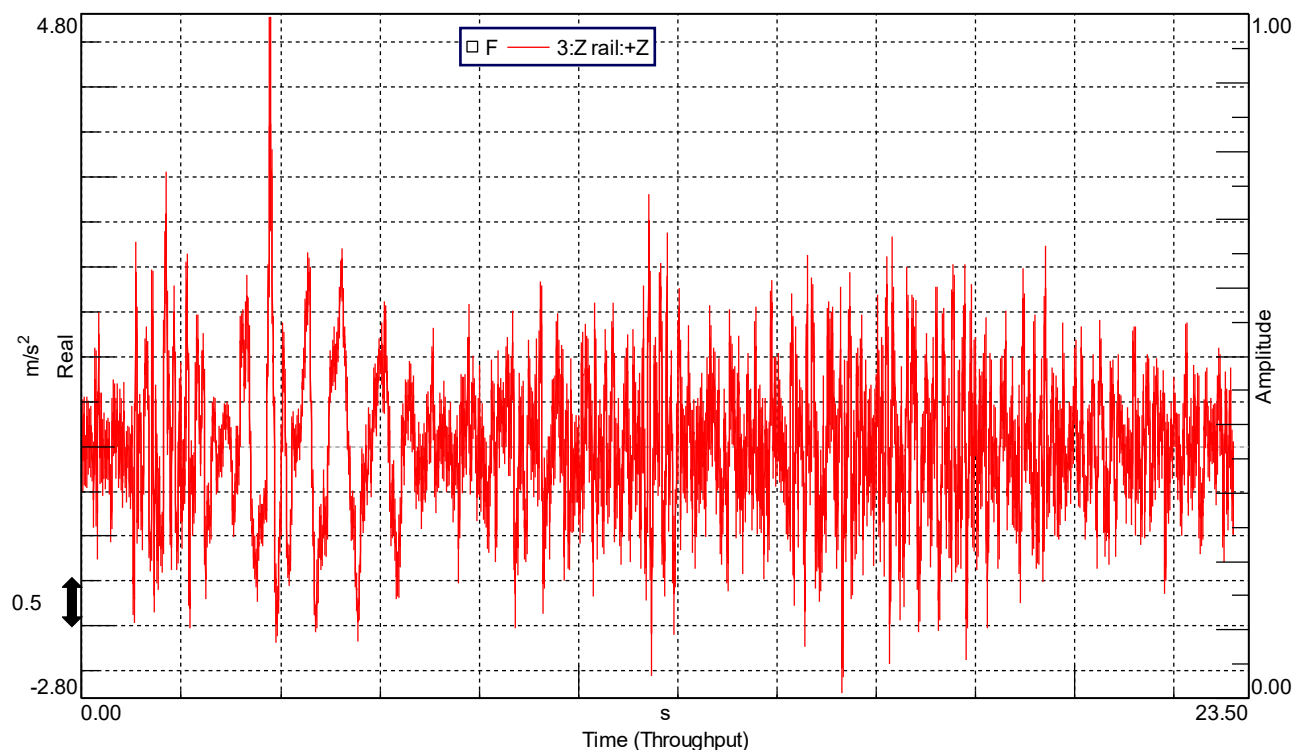
Figure 7.12: Run 23 paved urban road 20 km/h, (vehicle A).
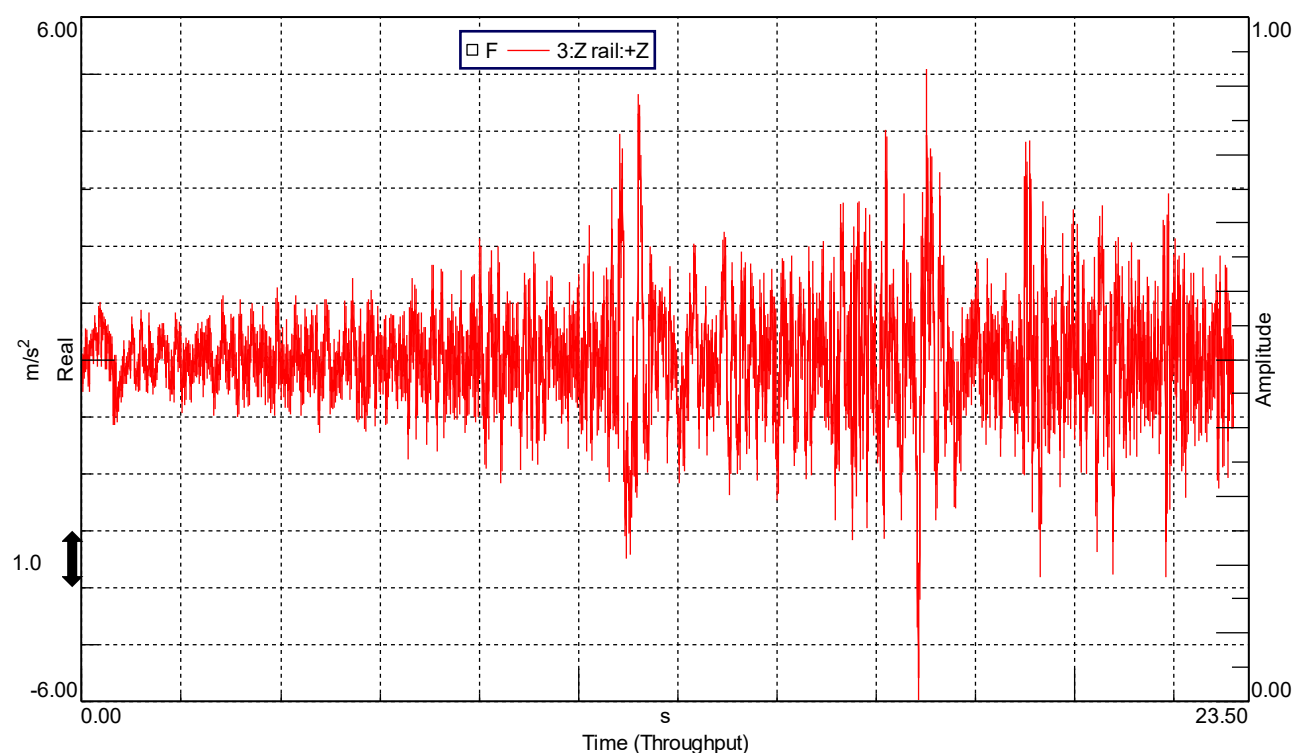
Figure 7.13: Run 24 paved urban road 30 km/h, (vehicle A).
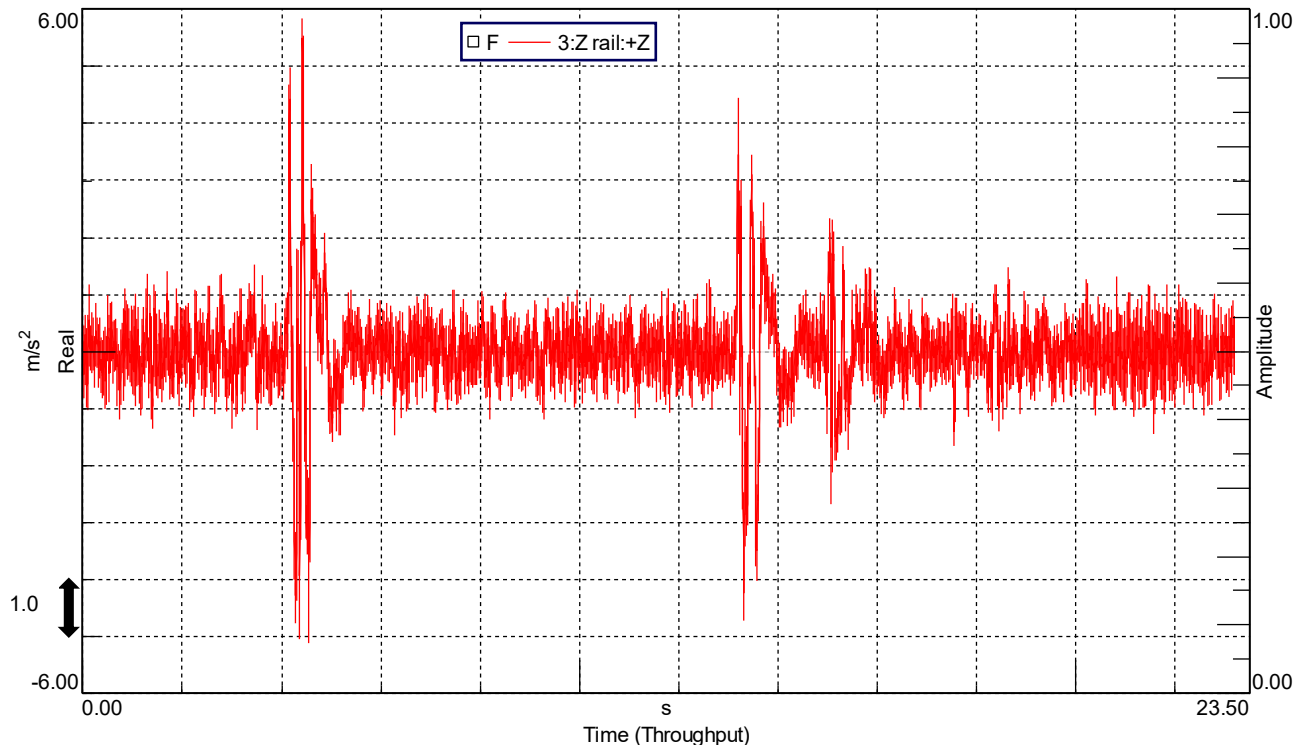
Figure 7.14: Run 25 urban bumps 40 km/h, (vehicle A).
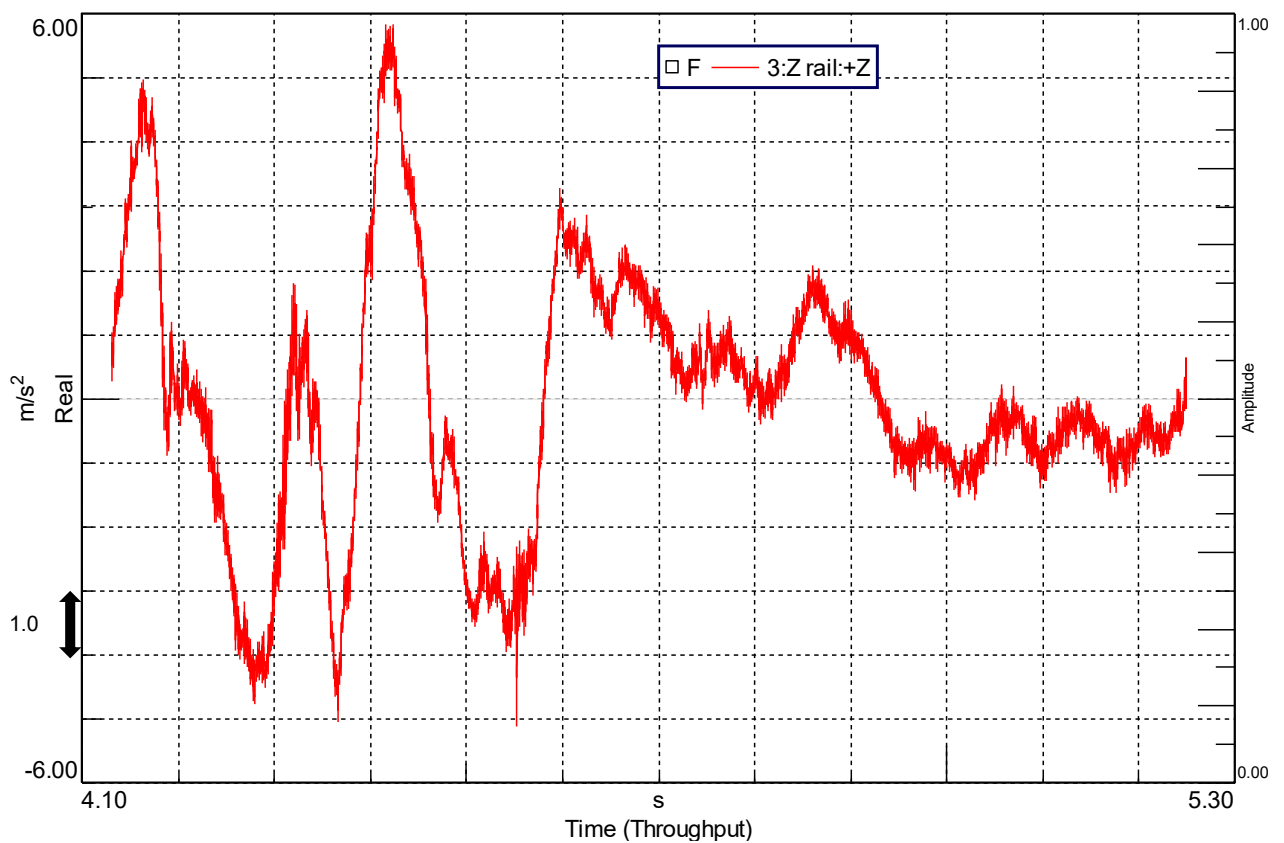
Figure 7.15: Run 25 urban bumps 40 km/h cut1, (vehicle A).
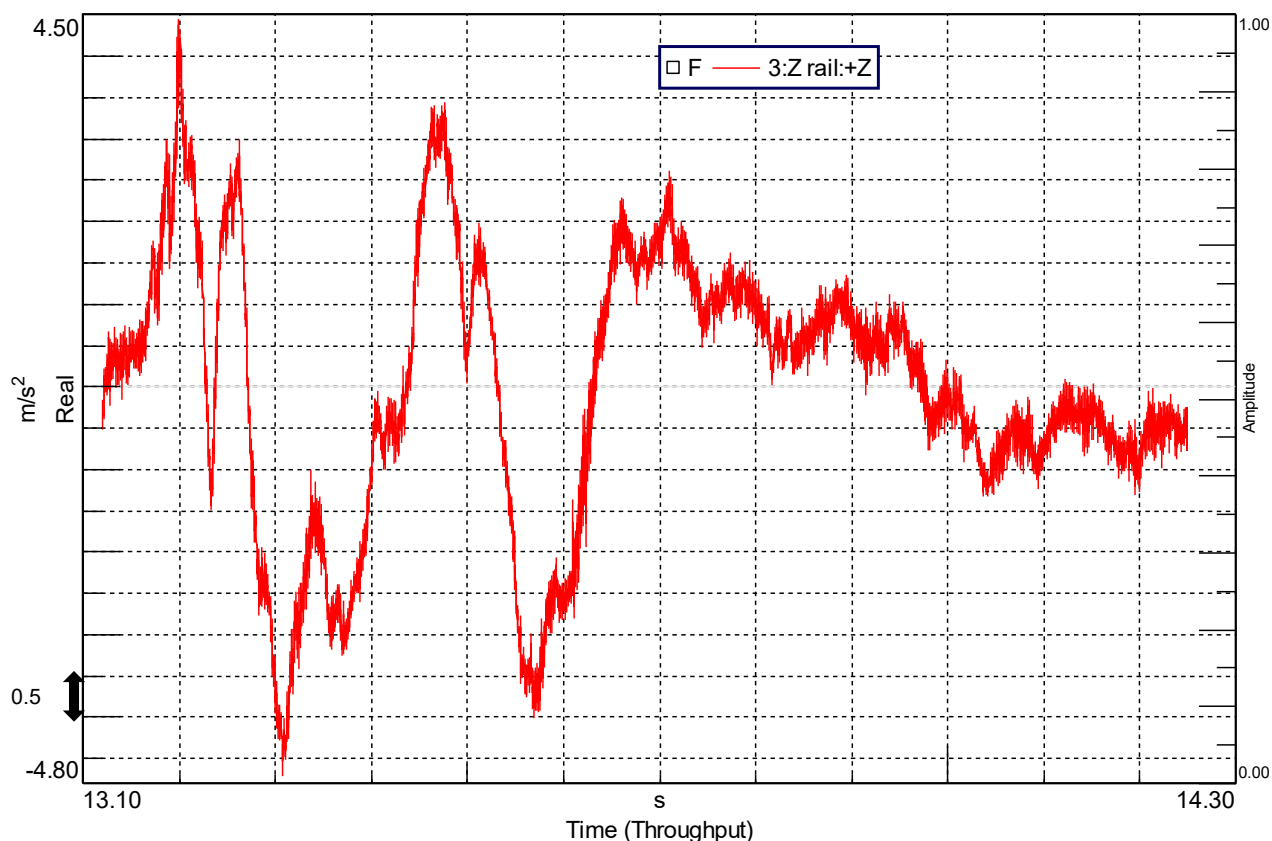
Figure 7.16: Run 25 urban bumps 40 km/h cut2, (vehicle A).
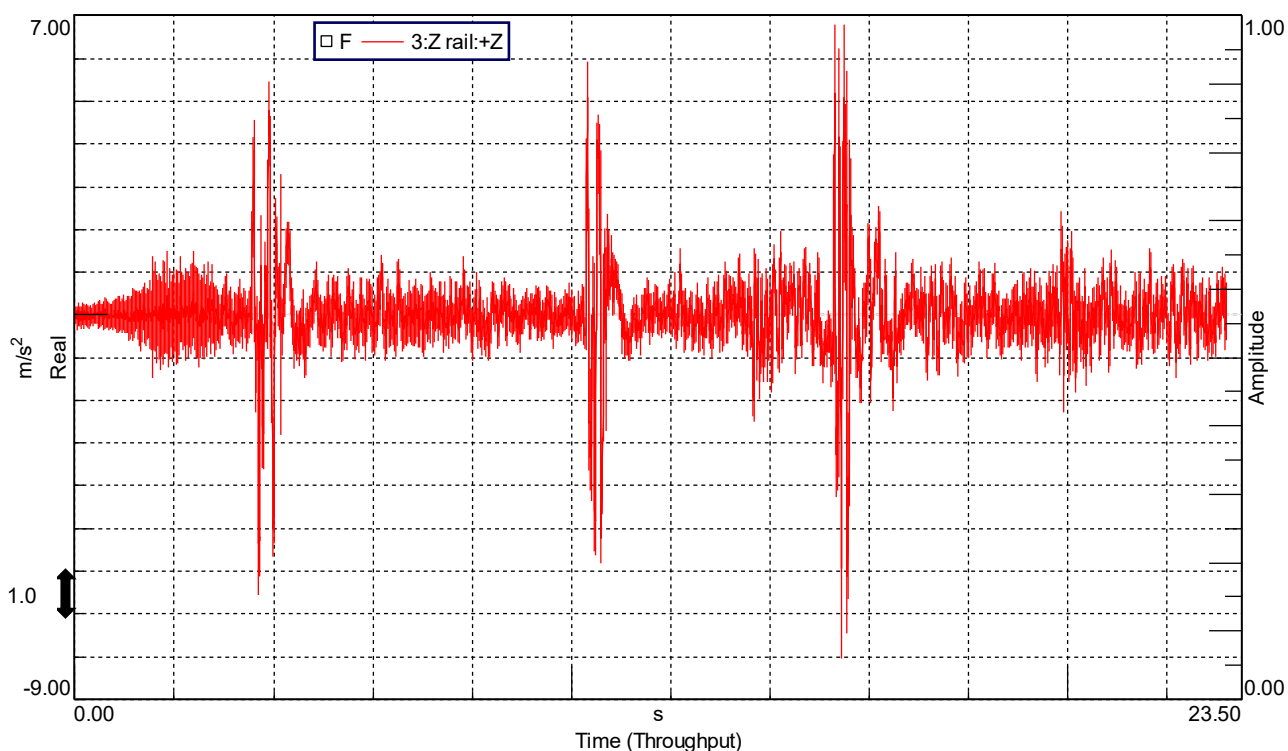
Figure 7.17: Run 26 urban bumps 50 km/h, (vehicle A).
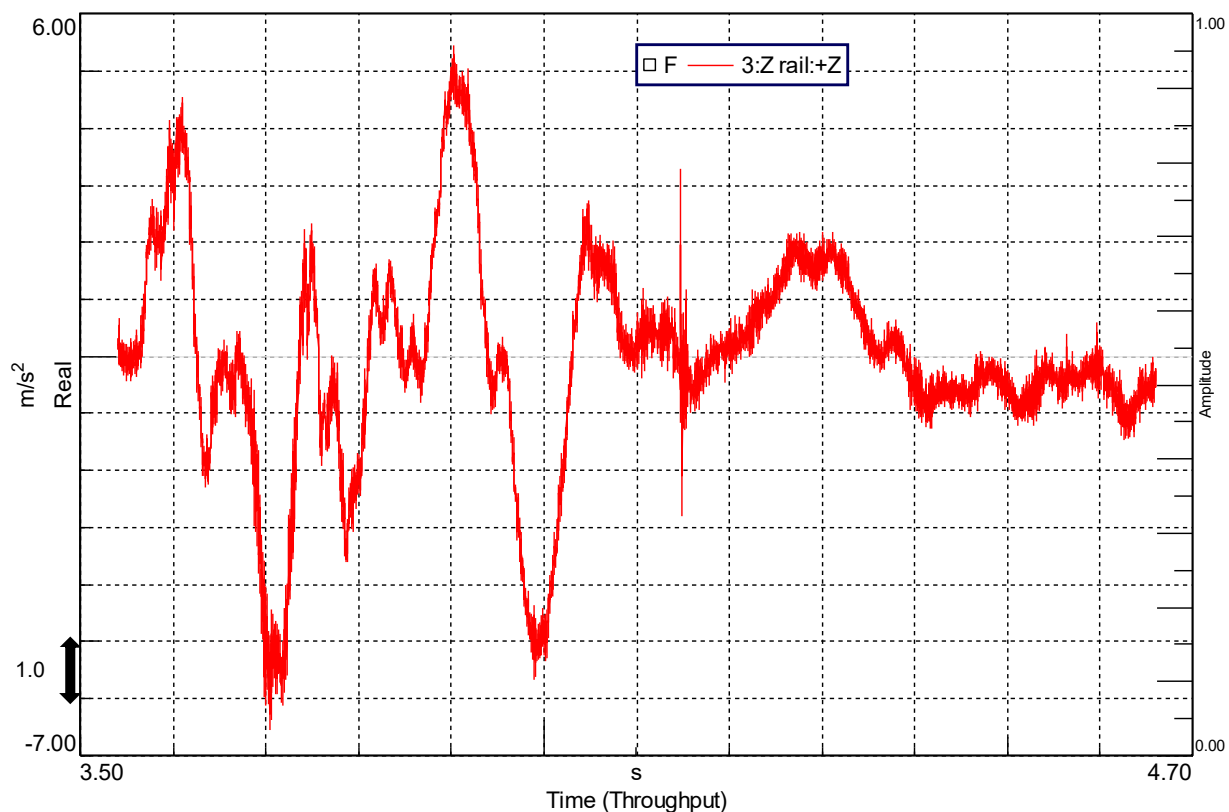
Figure 7.18: Run 26 urban bumps 50 km/h cut1, (vehicle A).
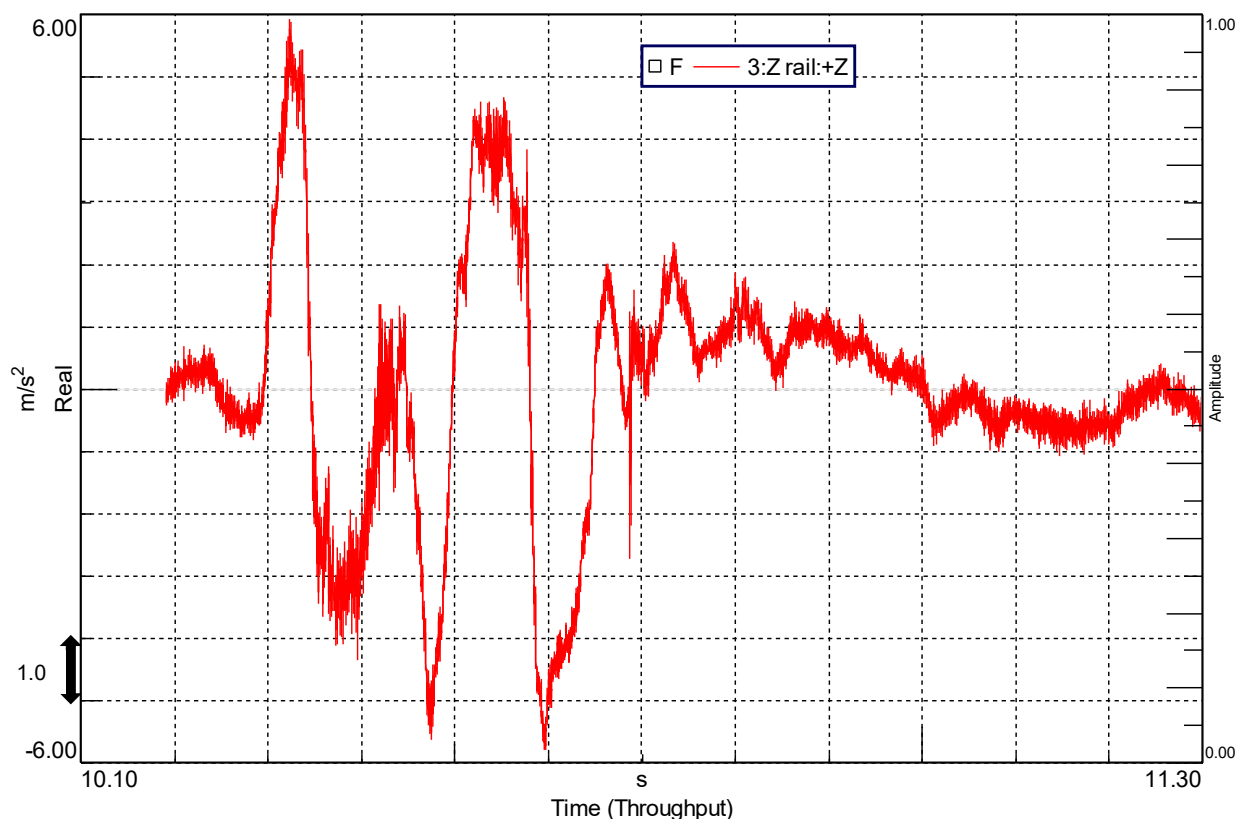
Figure 7.19: Run 26 urban bumps 50 km/h cut2, (vehicle A).
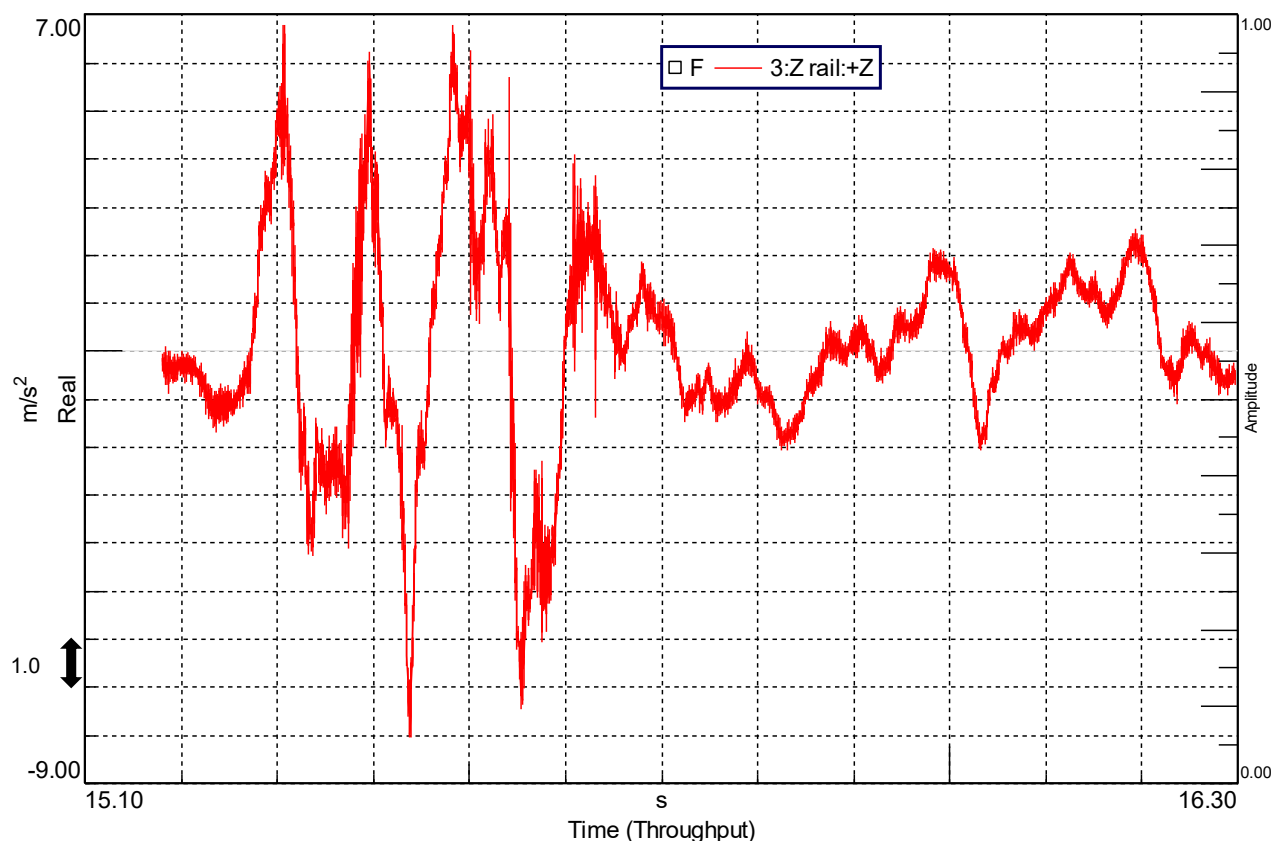
Figure 7.20: Run 26 urban bumps 50 km/h cut3, (vehicle A).

In Figures 7.21 - 7.40 the vehicle B related a_z seat rail diagrams are illustrated.

7.1.2 Vehicle B seat rail acceleration on z-axis
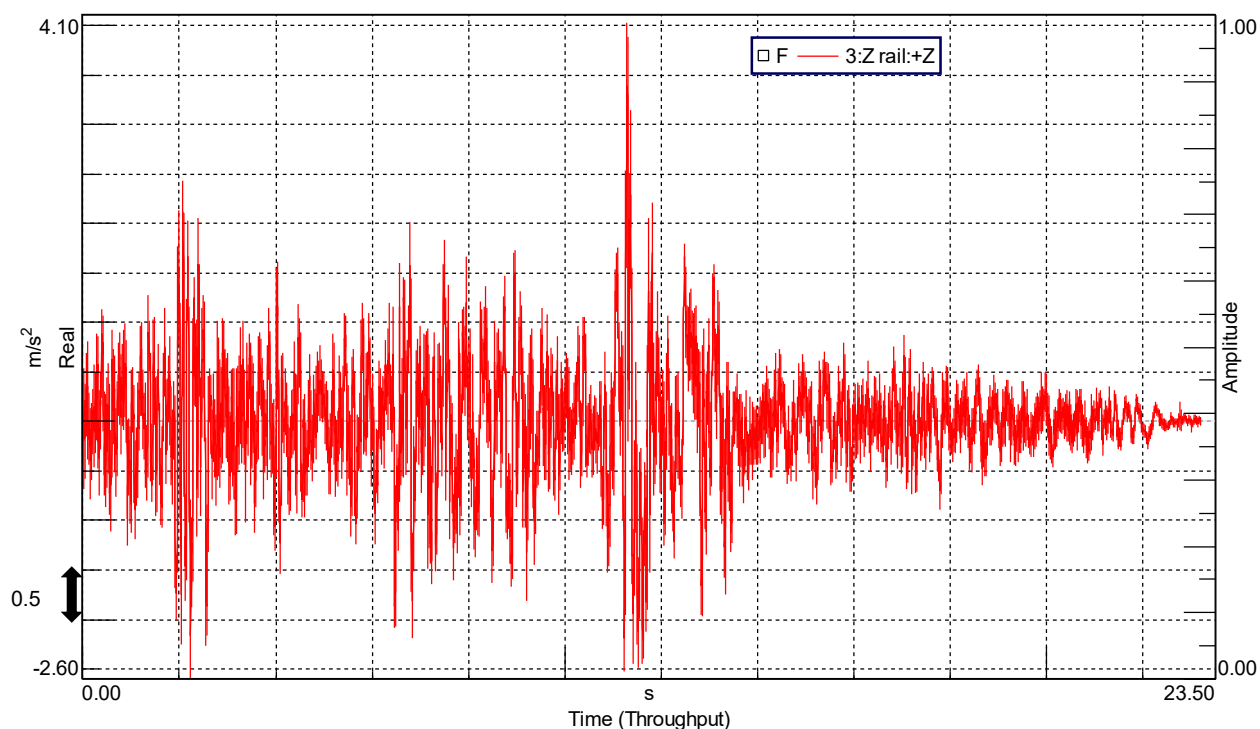
Figure 7.21: Run 2 single wide speed bump 20 km/h, (vehicle B).
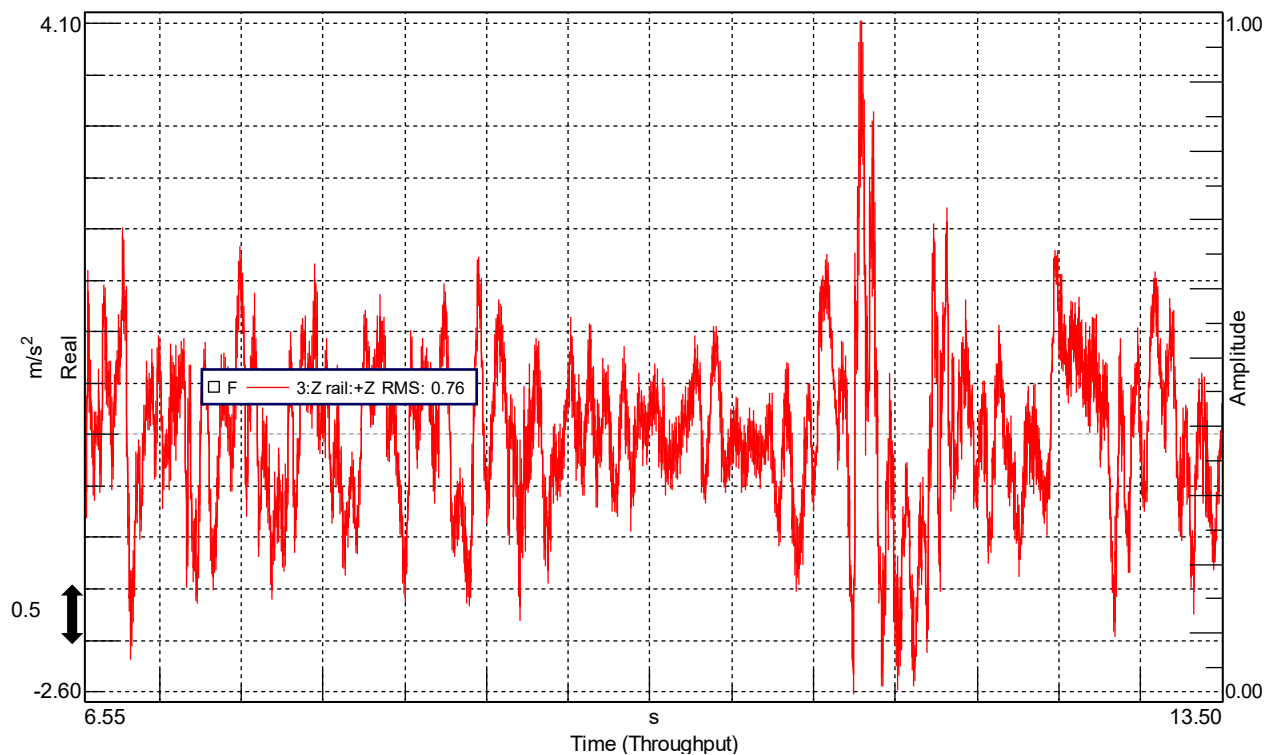
Figure 7.22: Run 2 single wide speed bump 20 km/h cut, (vehicle B).
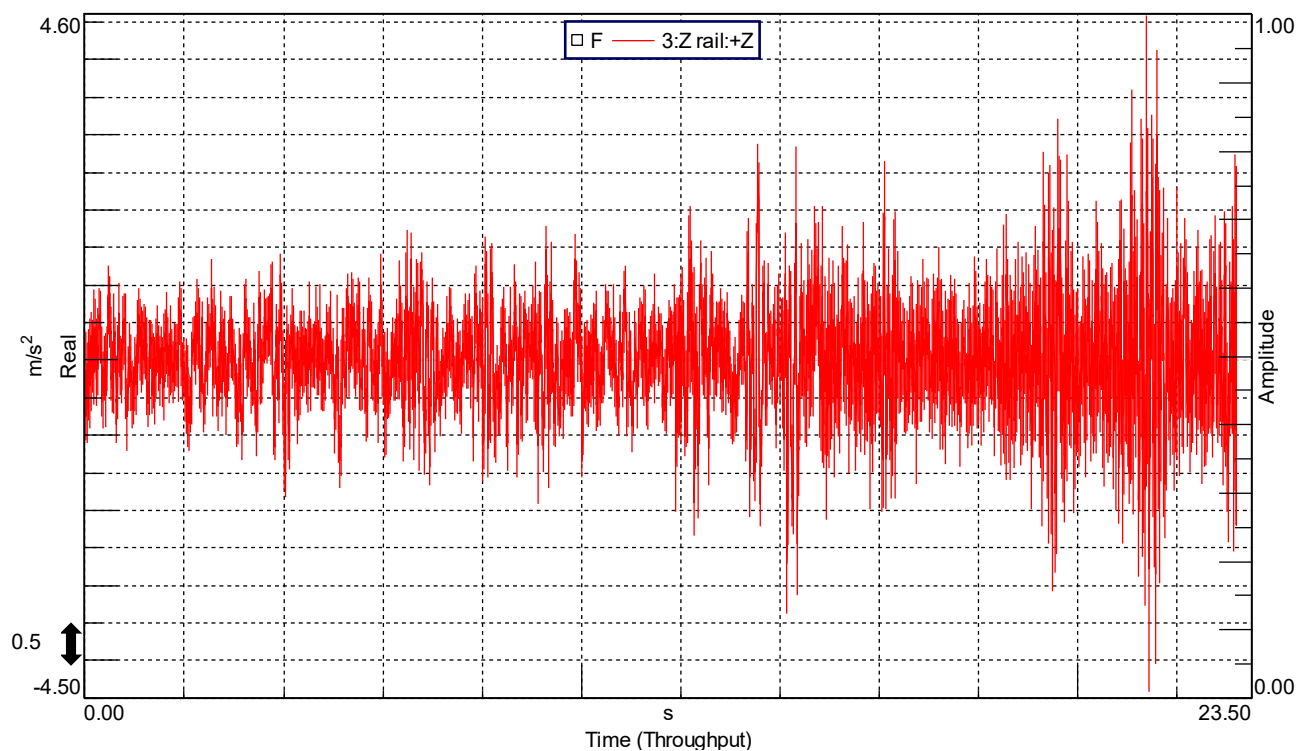
Figure 7.23: Run 4 urban road 40 km/h, (vehicle B).
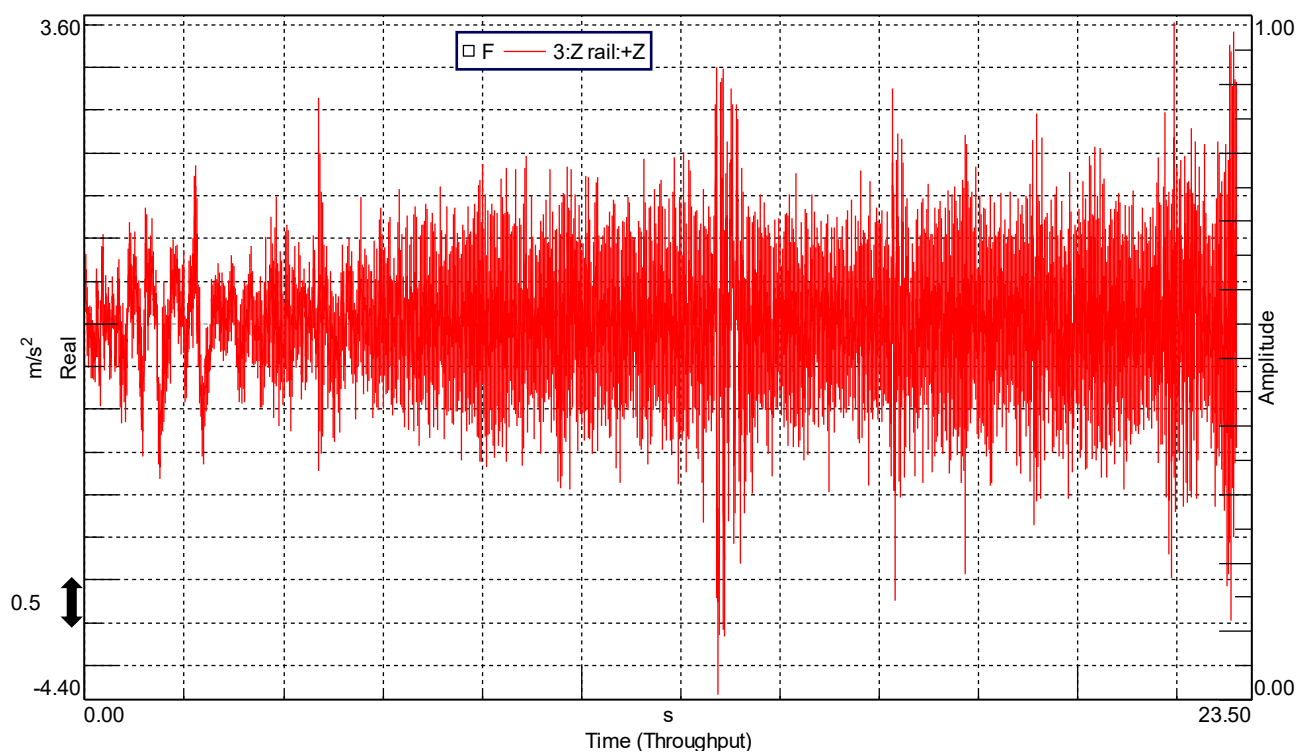
Figure 7.24: Run 5 urban road 70 km/h, (vehicle B).
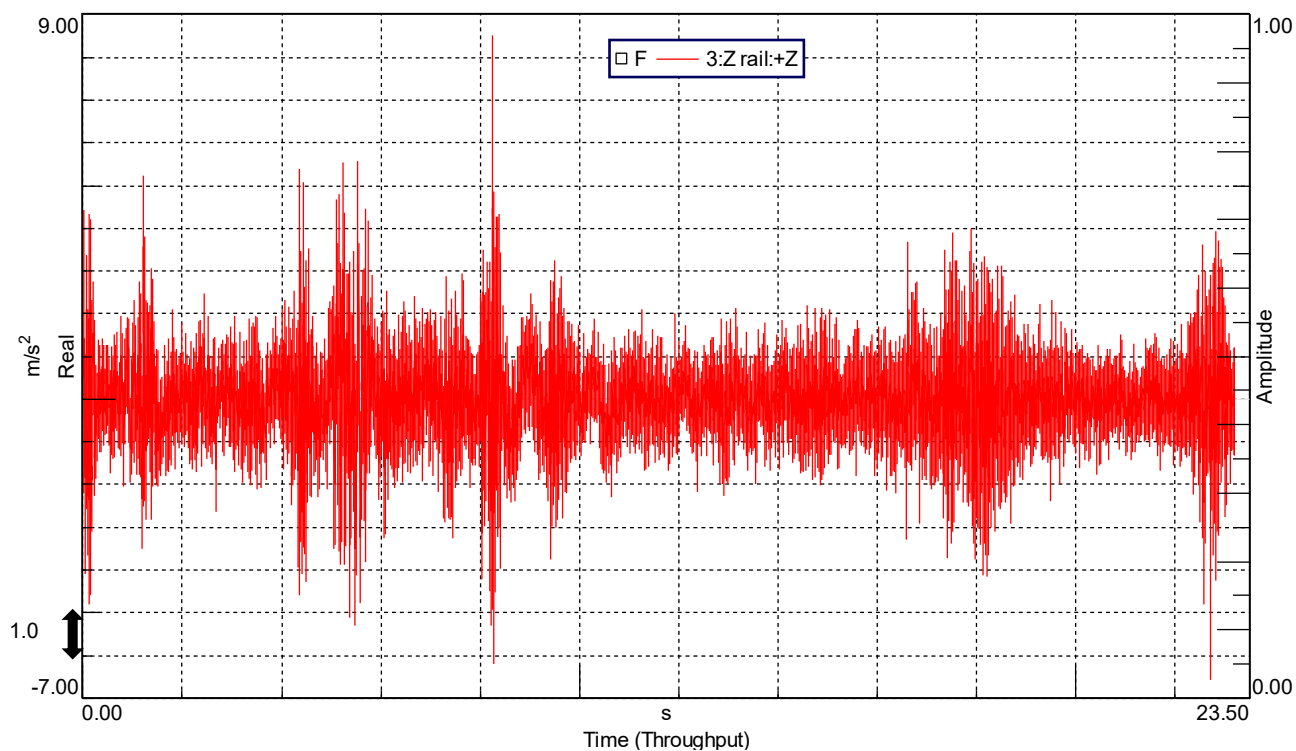
Figure 7.25: Run 9 mixed extra-urban road 70 km/h, (vehicle B).
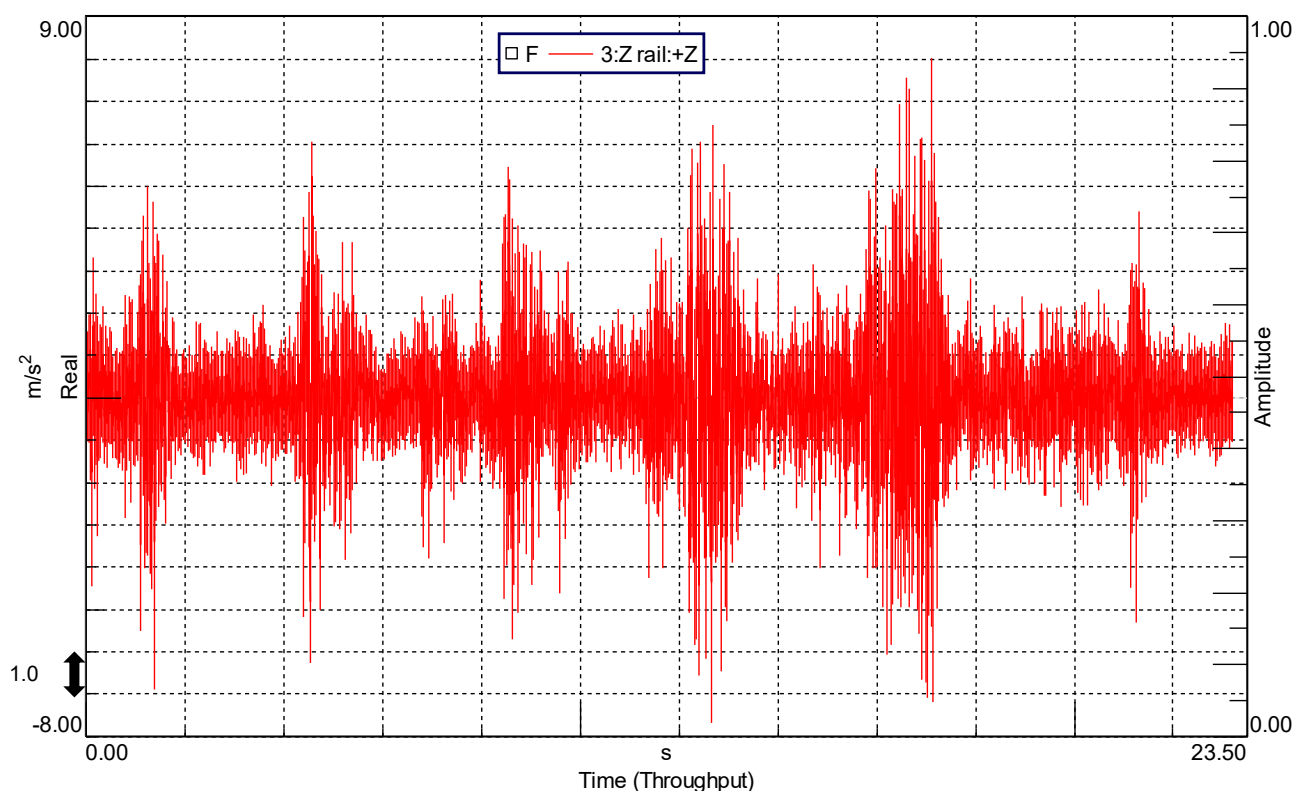
Figure 7.26: Run 13 uneven extra-urban road 70 km/h, (vehicle B).
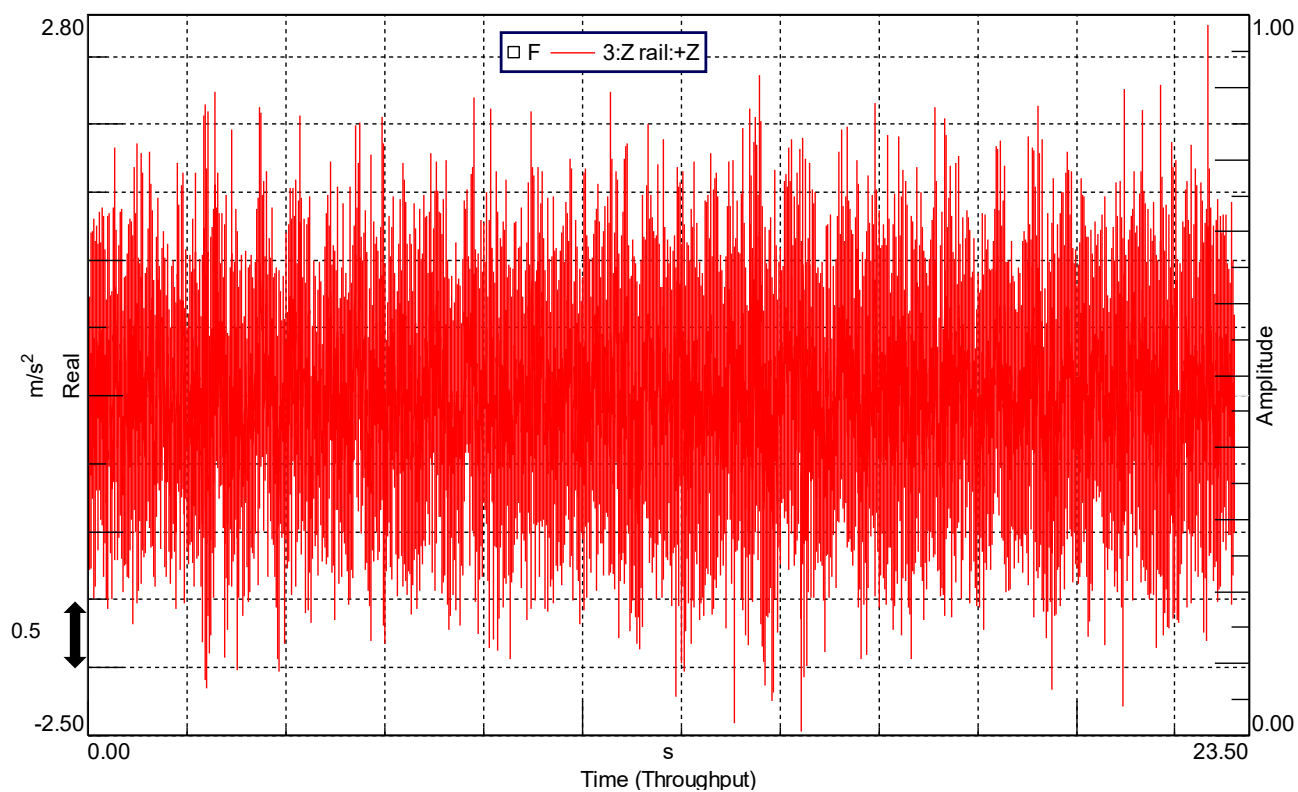
Figure 7.27: Run 16 smooth tarmac extra-urban road 70 km/h, (vehicle B).
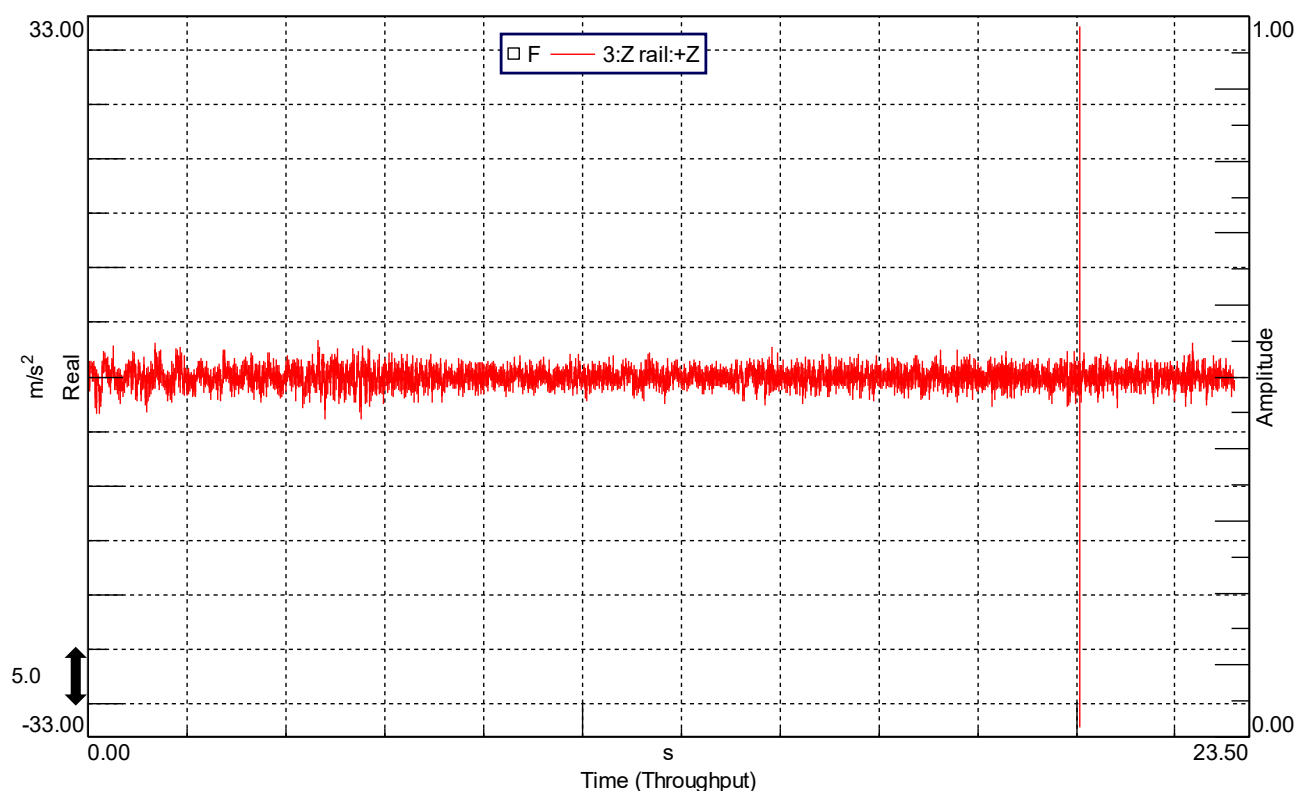
Figure 7.28: Run 20 off-road 20 km/h, (vehicle B).
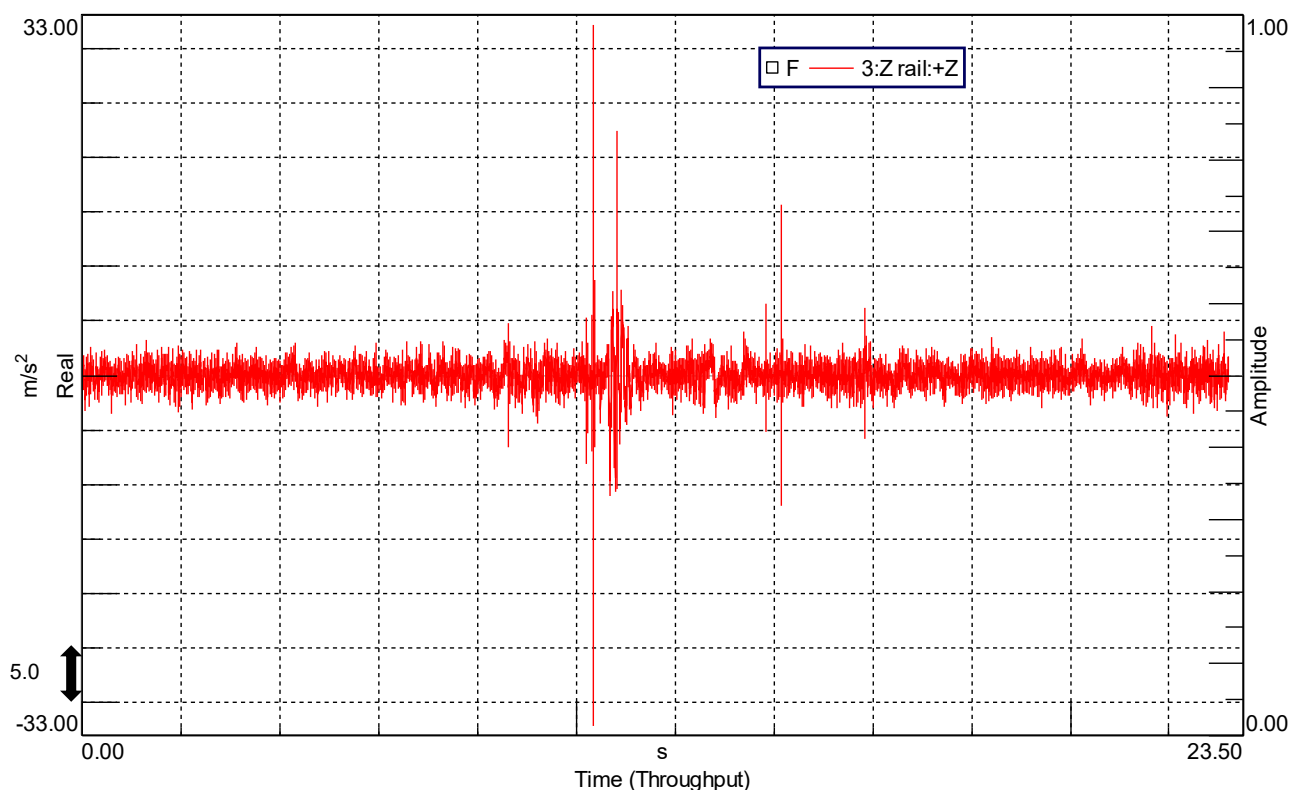
Figure 7.29: Run 21 off-road 30 km/h, (vehicle B).
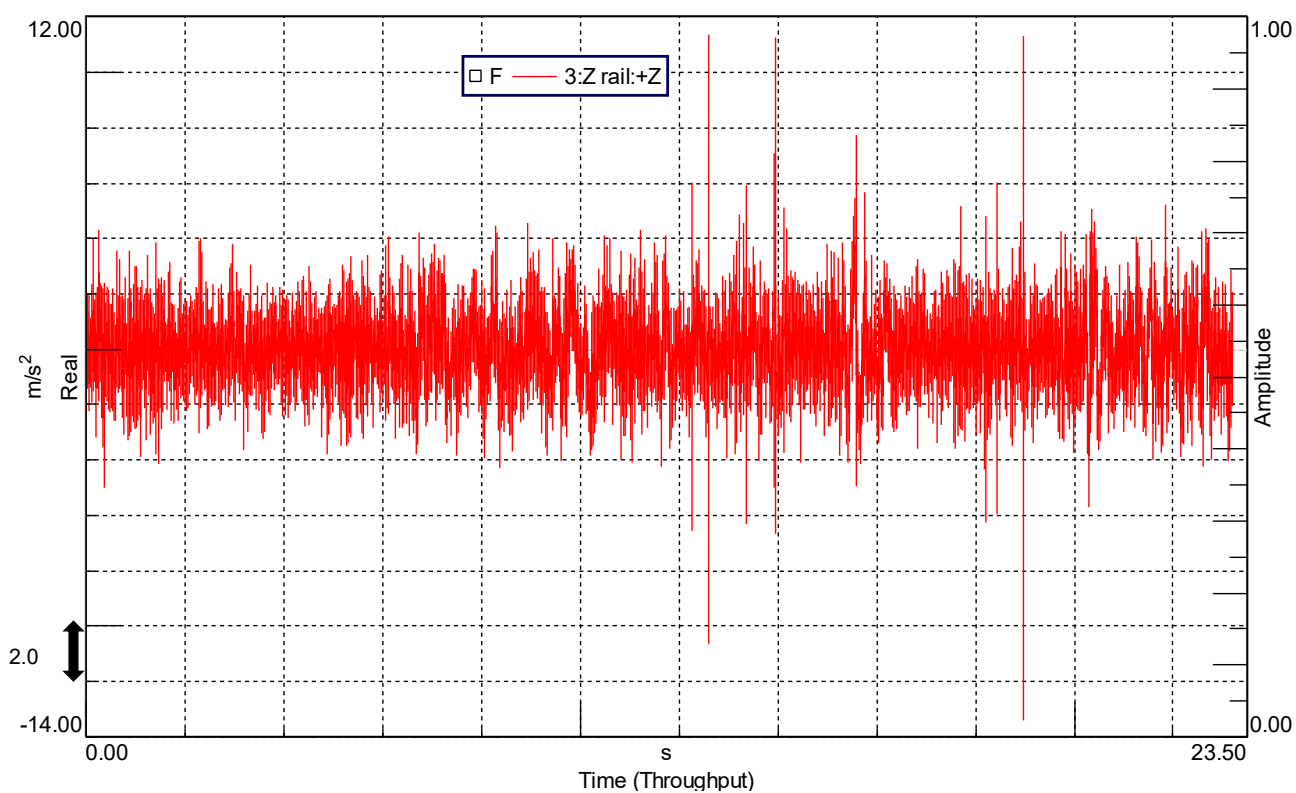
Figure 7.30: Run 22 off-road 40 km/h, (vehicle B).
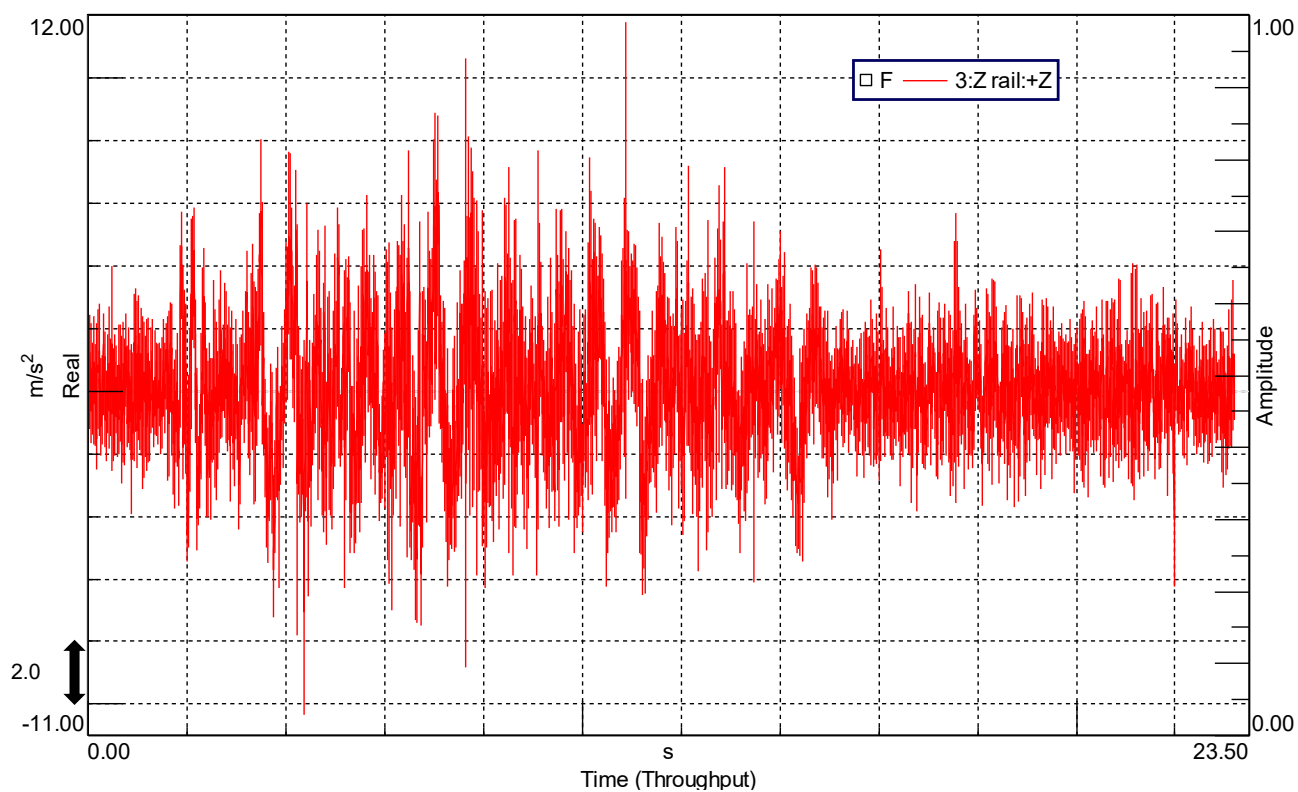
Figure 7.31: Run 23 severe off-road, (vehicle B).
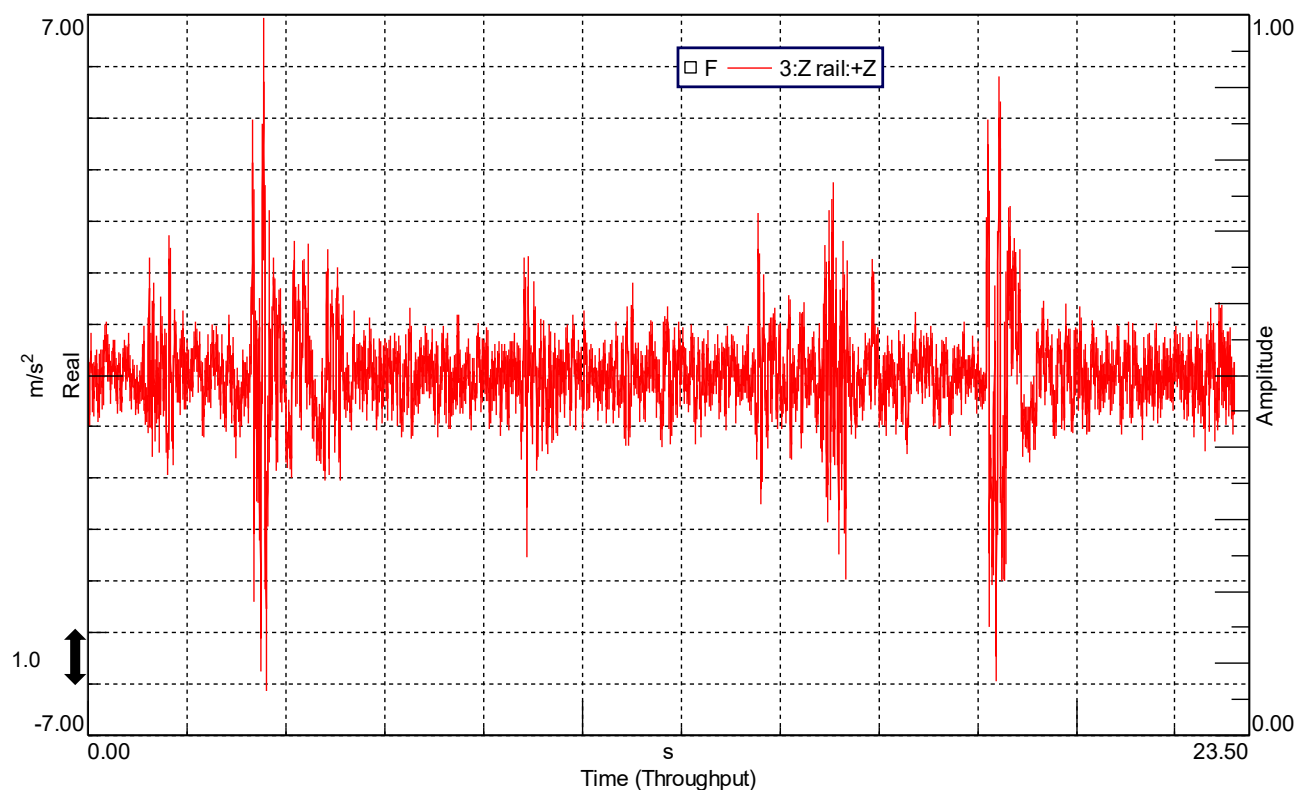
Figure 7.32: Run 26a urban bumps 40 km/h, (vehicle B).
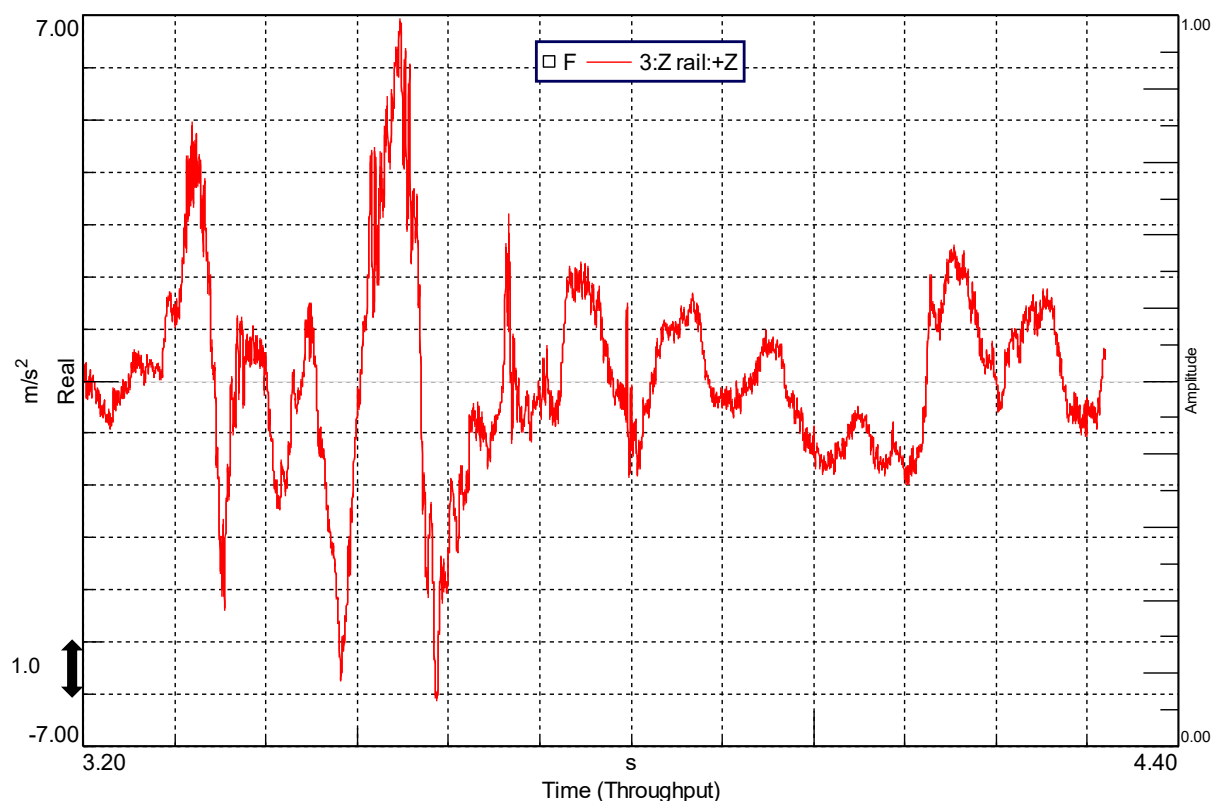
Figure 7.33: Run 26a urban bumps 40 km/h cut1, (vehicle B).
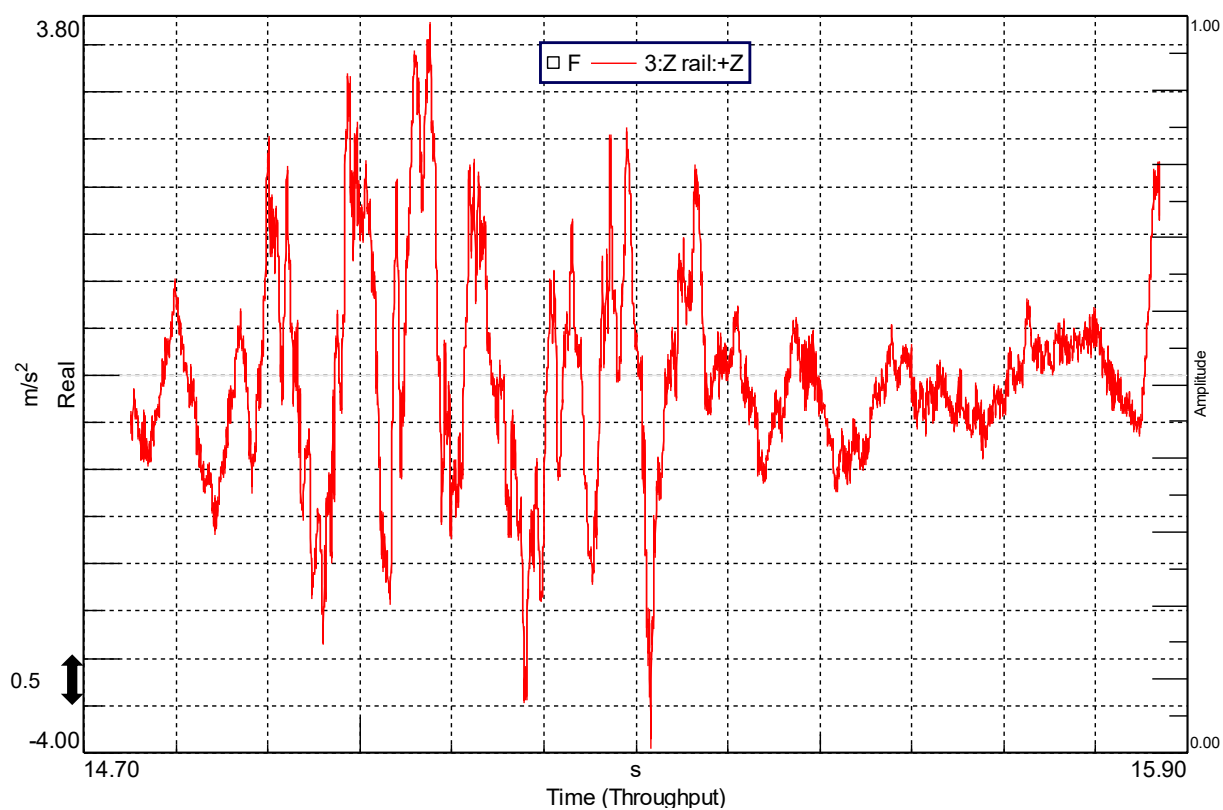
Figure 7.34: Run 26a urban bumps 40 km/h cut2, (vehicle B).
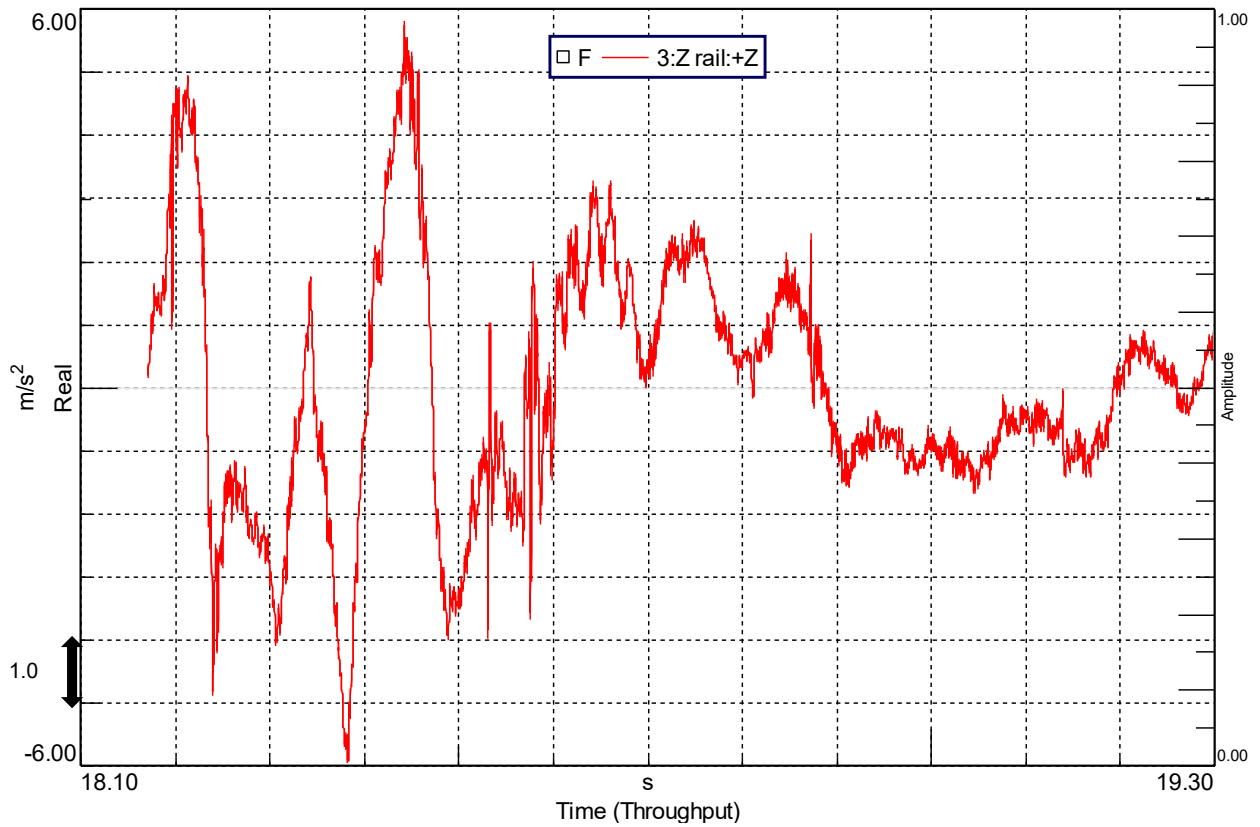
Figure 7.35: Run 26a urban bumps 40 km/h cut3, (vehicle B).
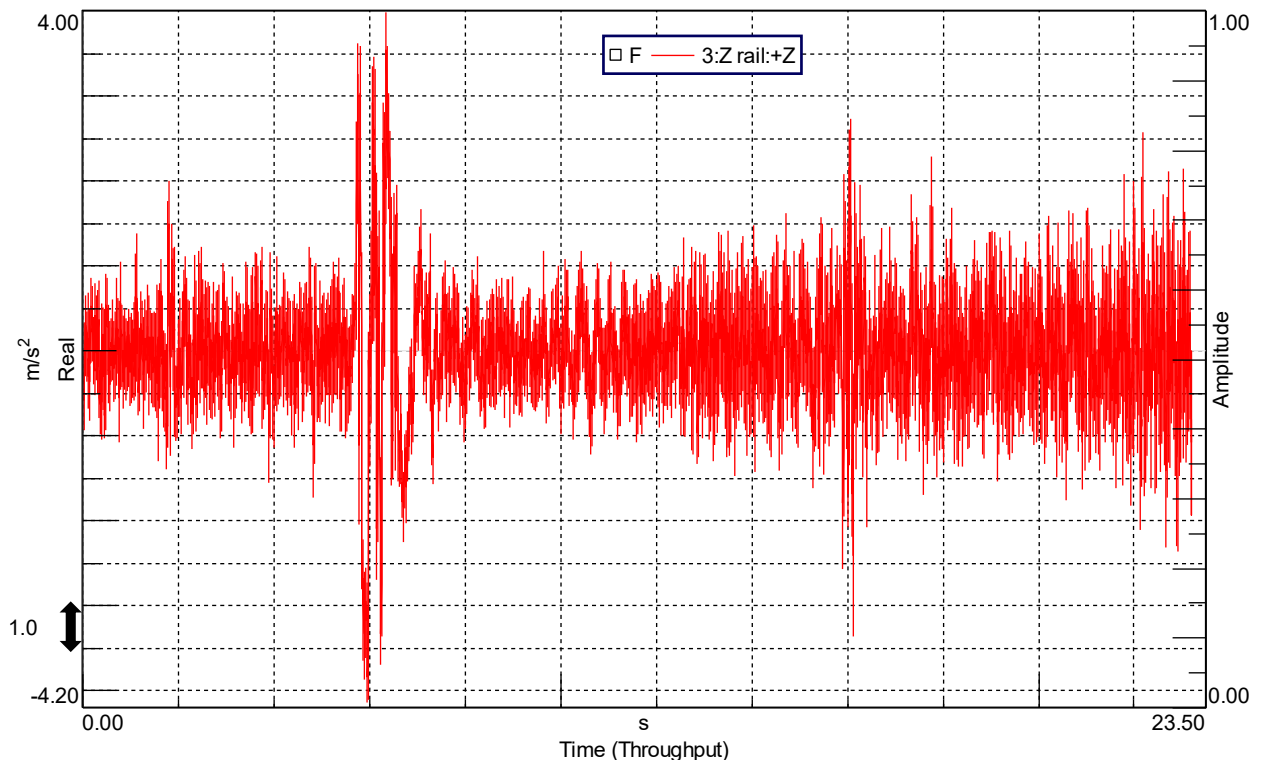
Figure 7.36: Run 26b urban bumps 30 km/h, (vehicle B).
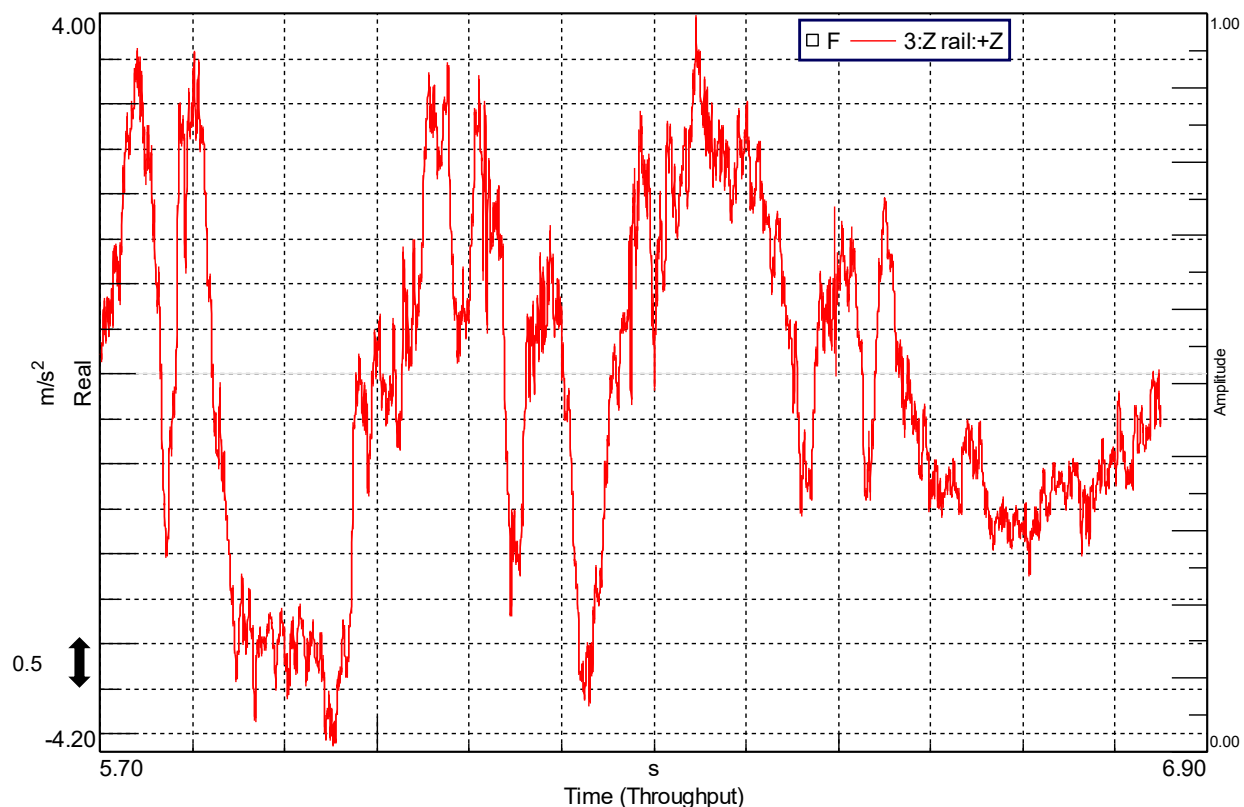
Figure 7.37: Run 26b urban bumps 30 km/h cut1, (vehicle B).
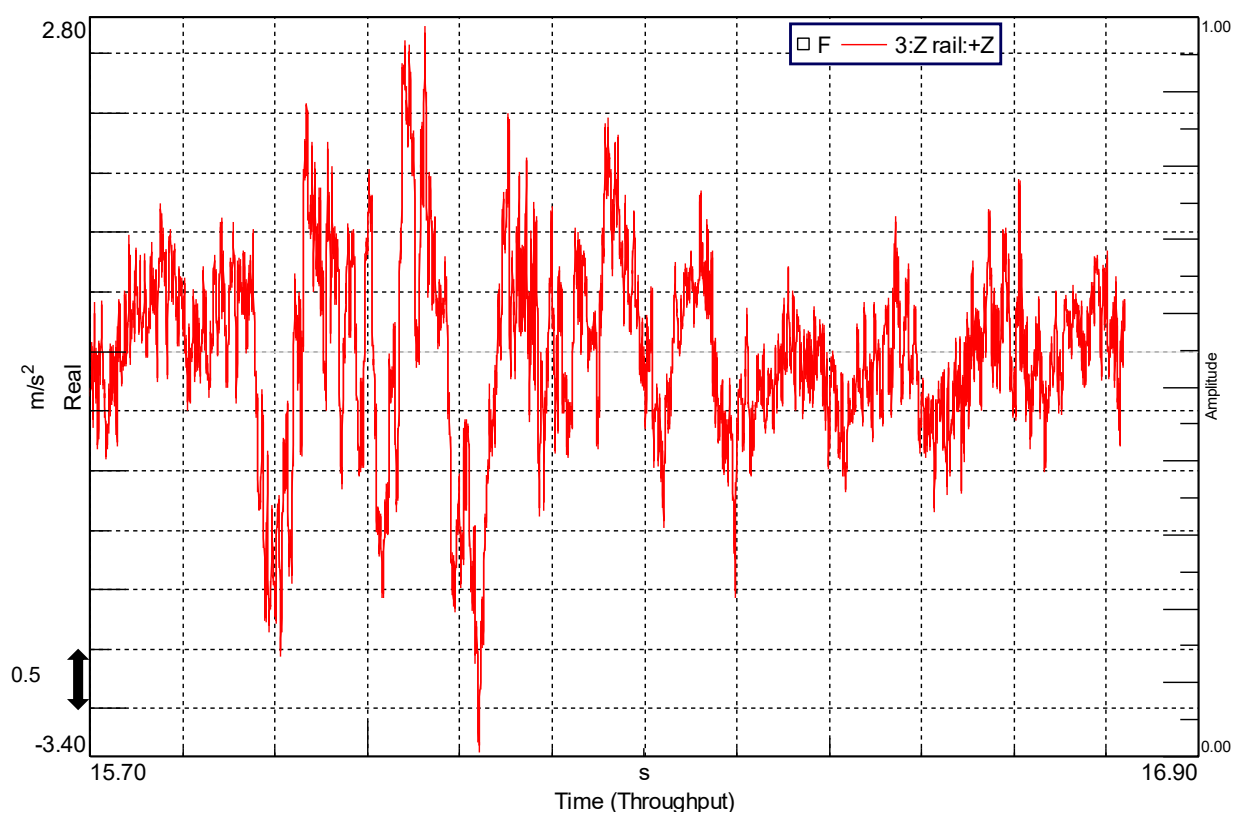
Figure 7.38: Run 26b urban bumps 30 km/h cut2, (vehicle B).
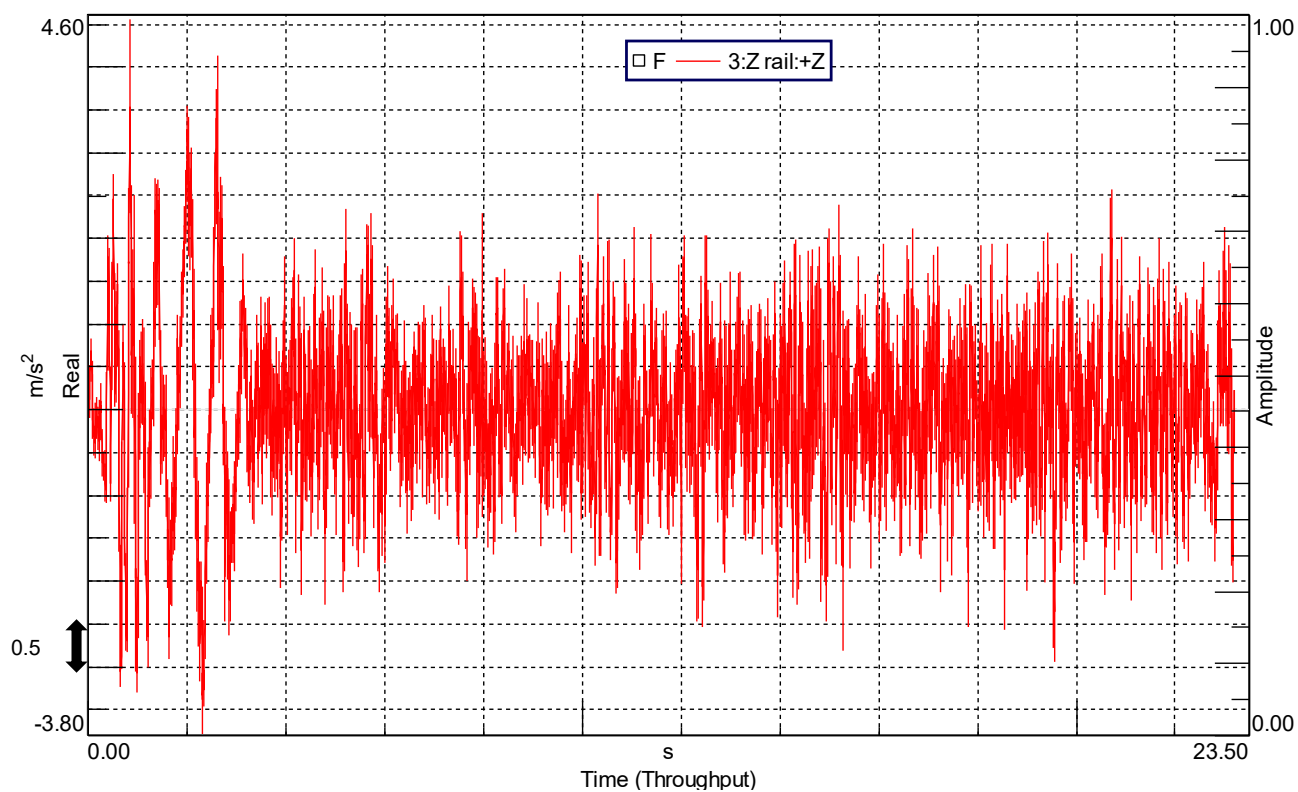
Figure 7.39: Run 27 paved urban road 20 km/h, (vehicle B).
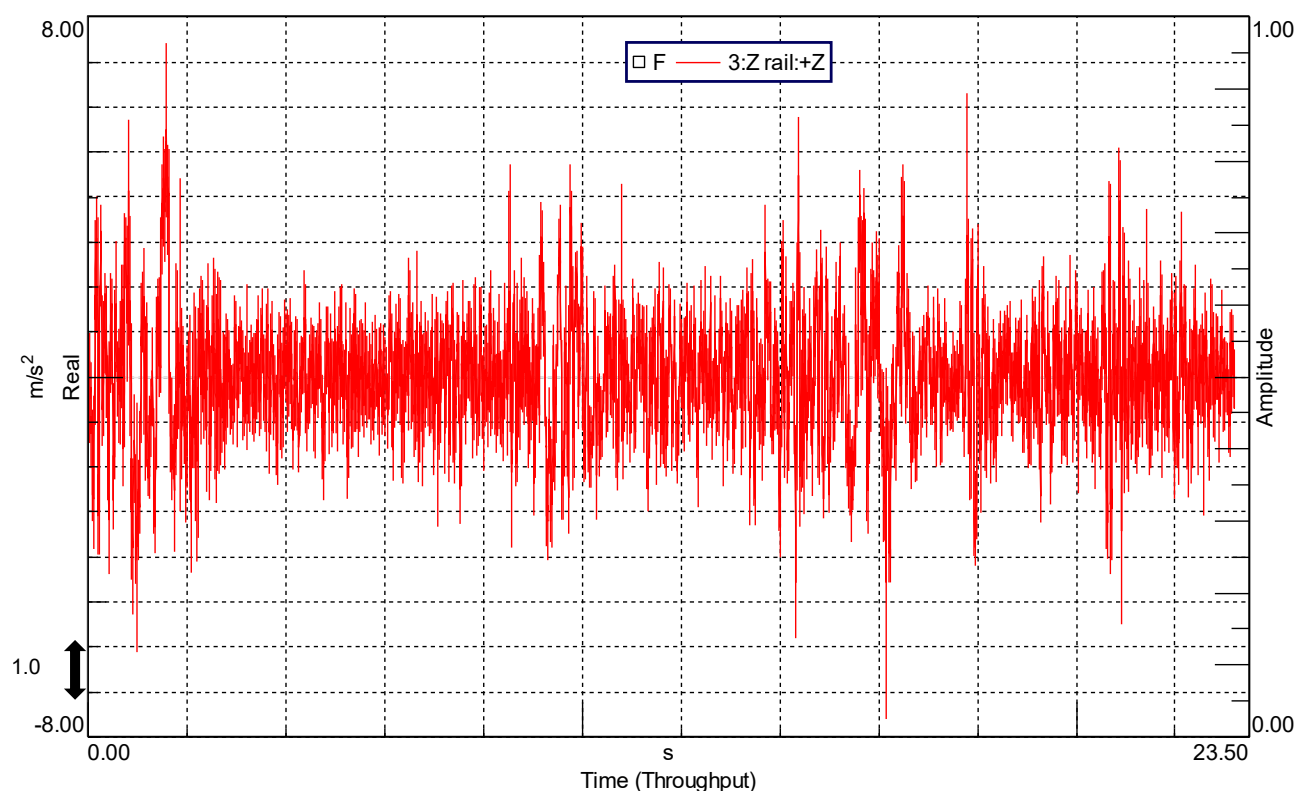
Figure 7.40: Run 28 paved urban road 30 km/h, (vehicle B).

7.2 WBV & HTV assessment

Considering the whole-body vibration and the hand-transmitted vibration metrics computation, the software required a resampling of the data with a sample frequency equal to 1000 Hz. The settings selected are strictly linked to the requirements and well-functioning of the program, having been chosen after several trials to get results as far as possible optimized.

As previously explained, when applying the standard filtering to the several channel axes involved in the measurement, the specific comfort axis multiplying factors (k_x, k_y, k_z) have been considered and the proper weighting functions have been taken activated from the dedicated toolbox:

- WBV Vibration Weighting - W_d for X,Y axes; W_k for Z axis;
- HTV Vibration Weighting - W_h for all axes.

In both cases, linear weighting was applied by the Test.Lab application, with pre-defined time constant values for the Running RMS and VDV levels respectively equal to 1 s and 0 s. In addition, the acquisition parameters and the tracking setting have been varied depending on the measurement of continuous manoeuvres tests or discrete manoeuvres ones, i.e. the bump sequence segments, as expressed below.

- Continuous:
  - Frame size 2 s;
  - Bandwidth 20480 Hz;
  - Resolution 0.5 Hz;
  - Spectral Lines 40960;
  - Time tracking duration 20 s;
  - Time tracking increment 0.5 s.
- Discrete:
  - Frame size 0.1 s;
  - Bandwidth 20480 Hz;
  - Resolution 10 Hz;
  - Spectral Lines 2048;
  - Time tracking duration: variable s
  - Time tracking increment: 0.1 s

The reference time period for the continuous manoeuvres corresponds to 20 seconds, whereas, regarding the discrete manoeuvres, the various single temporal segments have been defined and the average duration and excitation values computed:

- CX-5 Discrete :run 2- 6.619 s; run 25 - 1.124 s; run 26 - 1,140 s;
- Panda Discrete: run 2- 6.949 s; run 26a – 1.119 s; run 26b - 1,1340 s;

In Tables 7.1 – 7.4, the several WBV measurement levels for each of the two vehicles are reported, computed with the Test.Lab dedicated tools and sensed by the seat pad accelerometer placed with the correct orientation on the passenger seat cushion.

Table 7.1: Vehicle A runs RMS acceleration values at seat cushion.

Vehicle A	RMS_X [m/s^2]	RMS_Y [m/s^2]	RMS_Z [m/s^2]	Vector sum RMS [m/s^2]
Test	k_x=1	k_y=1	k_z=1	
Run 2 single wide speed bump 20 km/h	0,19	0,12	0,47	0,521
Run 4 urban road 40 km/h	0,07	0,09	0,41	0,426
Run 5 urban road 70 km/h	0,06	0,06	0,22	0,236
Run 9 mixed tarmac extra-urban road 70 km/h	0,10	0,11	0,39	0,417
Run 11 smooth tarmac extra-urban road 90 km/h	0,07	0,07	0,27	0,288
Run 12 extra urban-road 70 km/h	0,09	0,07	0,30	0,321
Run 19 off-road 30	0,07	0,15	0,36	0,396
Run 20 off-road 40	0,22	0,28	0,77	0,848
Run 21 off-road 50	0,13	0,17	0,72	0,751
Run 22 severe off-road	0,32	0,25	0,88	0,969
Run 23 paved urban road 20 km/h	0,23	0,32	0,53	0,660
Run 24 paved urban road 30 km/h	0,21	0,16	0,69	0,739
Run 25 urban bumps 40 km/h	0,13	0,02	0,41	0,424
Run 26 urban bumps 50 km/h	0,11	0,05	0,45	0,466

Table 7.2: Vehicle A runs VDV values at seat cushion.

Vehicle A	VDV_X [m/s$^{1.75}$]	VDV_Y [m/s$^{1.75}$]	VDV_Z [m/s$^{1.75}$]	Vector sum VDV [m/s$^{1.75}$]
Test	$k_x=1$	$k_y=1$	$k_z=1$	
Run 2 single wide speed bump 20 km/h	0,49	0,33	1,20	1,210
Run 4 urban road 40 km/h	0,22	0,27	1,30	1,301
Run 5 urban road 70 km/h	0,19	0,21	0,95	0,951
Run 9 uneven tarmac extra-urban road 70 km/h	0,31	0,32	1,24	1,243
Run 11 smooth tarmac extra-urban road 90 km/h	0,25	0,21	0,80	0,803
Run 12 mixed extra urban road 70 km/h	0,38	0,25	1,24	1,243
Run 19 off-road 30	0,23	0,48	1,05	1,062
Run 20 off-road 40	0,63	0,85	2,52	2,531
Run 21 off-road 50	0,39	0,56	2,30	2,302
Run 22 severe off-road	1,11	0,81	2,79	2,812
Run 23 paved urban road 20 km/h	0,77	1,06	1,62	1,708
Run 24 paved urban road 30 km/h	0,75	0,50	2,39	2,397
Run 25 urban bumps 40 km/h	0,68	0,13	2,34	2,344
Run 26 urban bumps 50 km/h	0,52	0,21	2,34	2,341

Table 7.3: Vehicle B runs RMS acceleration values at seat cushion.

Vehicle B	RMS_X [m/s²]	RMS_Y [m/s²]	RMS_Z [m/s²]	Vector sum RMS [m/s²]
Test	$k_x=1$	$k_y=1$	$k_z=1$	
Run 2 single wide speed bump 20 km/h	0,19	0,15	0,51	0,565
Run 4 urban road 40 km/h	0,07	0,10	0,33	0,352
Run 5 urban road 70 km/h	0,34	0,16	0,27	0,463
Run 9 mixed extra-urban road 70 km/h	0,10	0,10	0,26	0,296
Run 16 smooth tarmac extra-urban road 70 km/h	0,14	0,05	0,17	0,226
Run 13 uneven extra-urban road 70 km/h	0,06	0,09	0,37	0,385
Run 20 off-road 20	0,08	0,12	0,31	0,342
Run 21 off-road 30	0,11	0,13	0,54	0,566
Run 22 off-road 40	0,10	0,16	0,58	0,610
Run 23 severe off-road	0,38	0,41	1,01	1,154
Run 27 paved urban road 20 km/h	0,18	0,22	0,51	0,584
Run 28 paved urban road 30 km/h	0,23	0,16	0,90	0,943
Run 26b urban bumps 30 km/h	0,07	0,05	0,38	0,390
Run 26a urban bumps 40 km/h	0,01	0,05	0,25	0,255

Table 7.4: Vehicle B runs VDV values at seat cushion.

Vehicle B	VDV_X [m/s$^{1.75}$]	VDV_Y [m/s$^{1.75}$]	VDV_Z [m/s$^{1.75}$]	Vector sum VDV [m/s$^{1.75}$]
Test	$k_x=1$	$k_y=1$	$k_z=1$	
Run 2 single wide speed bump 20 km/h	0,44	0,37	1,25	1,257
Run 4 urban road 40 km/h	0,22	0,30	1,06	1,062
Run 5 urban road 70 km/h	1,28	0,61	1,09	1,434
Run 9 mixed extra-urban road 70 km/h	0,43	0,29	0,90	0,914
Run 16 smooth tarmac extra-urban road 70 km/h	0,62	0,15	0,50	0,678
Run 13 uneven extra-urban road 70 km/h	0,20	0,30	1,28	1,281
Run 20 off-road 20	0,23	0,35	0,94	0,945
Run 21 off-road 30	0,39	0,43	2,30	2,301
Run 22 off-road 40	0,32	0,48	2,08	2,082
Run 23 severe off-road	1,19	1,44	3,12	3,171
Run 27 paved urban road 20 km/h	0,72	0,83	1,65	1,690
Run 28 paved urban road 30 km/h	0,80	0,47	3,16	3,164
Run 26b urban bumps 30 km/h	0,40	0,26	2,57	2,570
Run 26a urban bumps 40 km/h	0,39	0,26	1,42	1,422

Considering the RMS excitation values, in Tables 7.5 and 7.6, the different discomfort parameters according to the main regulations described in chapter 5 are represented for each test performed on the two vehicles. These parametric assessments are based on the recommended Threshold Limit Values (TLVs) established by the American Conference of Governmental Industrial Hygienists (ACGIH), other than the advised vibration levels included in the EU Directive 2002/44/EC; whereas the generic comfort classification is define depending on the ISO 2631-1 guidance.

Table 7.5: Vehicle A WBV RMS acceleration discomfort levels.

Vehicle A	Dominant axis a_w r.m.s. [m/s^2]	Degree of discomfort according to ACGIH TLVs	Degree of discomfort according to EU Directive 2002/44/EC	Vector sum RMS [m/s^2]	Degree of discomfort (according to ISO 2631-1 guidelines)
Test					
Run 5 urban 70 km/h	0,22	Below action value	Below action value	0,236	A little uncomfortable
Run 11 extra 90 smooth	0,27	Below action value	Below action value	0,288	A little uncomfortable
Run 12 extra 70 mixed	0,30	Below action value	Below action value	0,321	A little uncomfortable
Run 19 off-road 30	0,36	Below action value	Below action value	0,396	A little uncomfortable
Run 9 uneven extra 70	0,39	Below action value	Below action value	0,417	A little uncomfortable
Run 25 bump 40	0.41	Below action value	Below action value	0.424	Fairly uncomfortable
Run 4 urban 40	0,41	Below action value	Below action value	0,426	A little uncomfortable
Run 26 bump 50	0,45	Below action value	Below action value	0,466	A little uncomfortable
Run 2 wide bump 20	0,47	Below action value	Below action value	0,521	Fairly uncomfortable
Run 23 paved road 20	0,53	Above the action value, below limit value	Above the action value, below limit value	0,660	Fairly uncomfortable
Run 24 paved road 30	0,69	Above the action value, below limit value	Above the action value, below limit value	0,739	Fairly uncomfortable
Run 21 off-road 50	0,72	Above the action value, below limit value	Above the action value, below limit value	0,751	Fairly uncomfortable
Run 20 off-road 40	0,77	Above the action value, below limit value	Above the action value, below limit value	0,848	Fairly uncomfortable
Run 22 severe off-road	0,88	Above the action value, below limit value	Above the action value, below limit value	0,969	Uncomfortable

Table 7.6: Vehicle B WBV RMS acceleration discomfort levels.

Vehicle B	Dominant axis a_w r.m.s. [m/s²]	Degree of discomfort according to ACGIH TLVs	Degree of discomfort according to EU Directive 2002/44/EC	Vector sum RMS [m/s²]	Degree of discomfort according to ISO 2631-1 guidelines
Test					
Run 16 extra 70 smooth	0,17	Below action value	Below action value	0,226	A little uncomfortable
Run 26b bump 30	0.25	Below action value	Below action value	0.255	A little uncomfortable
Run 9 extra 70 mixed	0,26	Below action value	Below action value	0,296	A little uncomfortable
Run 20 off-road 20	0,31	Below action value	Below action value	0,342	A little uncomfortable
Run 4 urban 40	0,33	Below action value	Below action value	0,352	A little uncomfortable
Run 5 urban 70	0,34	Below action value	Below action value	0,463	A little uncomfortable
Run 13 uneven 70	0,37	Below action value	Below action value	0,385	A little uncomfortable
Run 26a bump 40	0.38	Below action value	Below action value	0.390	A little uncomfortable
Run 2 wide bump 20	0.51	Above the action value, below limit value	Above the action value, below limit value	0.565	Fairly uncomfortable
Run 27 paved road 20	0,51	Above the action value, below limit value	Above the action value, below limit value	0,584	Fairly uncomfortable
Run 21 off-road 30	0,54	Above the action value, below limit value	Above the action value, below limit value	0,566	Fairly uncomfortable
Run 22 off-road 40	0,58	Above the action value, below limit value	Above the action value, below limit value	0,610	Fairly uncomfortable
Run 28 paved road 30	0,90	Equal to the limit value	Above the action value, below limit value	0,943	Uncomfortable
Run 23 severe off-road	1,01	Above the limit value	Above the action value, below limit value	1,154	Uncomfortable

Analysing the weighted acceleration r.m.s. at the seat cushion, it is possible to observe that, considering vehicle A, whenever the total vector sum of the aw r.m.s. is such that the overall degree of discomfort according to ISO 2631-1 is in the range " a little uncomfortable", the dominant a_w r.m.s. component is always below the action value according to both ACGIH TLVs and EU Directive 2002/44/EC,

On the other hand, considering test conditions classified as "fairly uncomfortable" and "uncomfortable", the dominant aw component in all cases is "above the action value, below the limit value", according to both the recommended regulations.

Furthermore, regarding the absolute r.m.s. vibration values, the less severe test condition has been represented by the run 5, urban road at constant speed 70 km, while the most critical test condition is the one encountered during run 22, in highly uneven off-road ground.

As a further remark, it is worth of notice that in none of the selected cases for the analysed vehicle, the RMS dominant component, which is mostly represented by the Z-axis), trespassed the daily exposure limit value.

Concerning the vehicle B analysis, both the regulations classify the dominant a_w component as "above the action value, below the limit value" in all the conditions defined as "fairly uncomfortable". Though, differently from the vehicle A situation, in some particularly critical test, where the vector sum RMS indicated an "uncomfortable" definition concerning the degree of discomfort, the dominant aw r.m.s. value has been found equal or superior the daily exposure limit threshold.

Specifically, regarding the absolute r.m.s. vibration values, the less severe test condition has been spotted in the run 16, extra-urban road with smooth tarmac ground at constant speed 70 km/h, while the most critical test condition is the one detected during run 23, in highly uneven off-road ground; in addition, considering ACGIH TLVs, a_w r.m.s. component is equal to the critical limit value for run 28 too, corresponding to a rough paved urban ground, with significant road irregularities.

All the previous considerations above action and limit values are to be taken as a pure indicative reference concerning continuous daily excitation thresholds, as these evaluation parameters have been developed to assess vibration issues regarding the workplace, thus involving average periods of 8 hours. Therefore, even though they've been adopted to generally classify al the run tests, the first remarks is that each of the ordinary test, taken as a single phenomenon, would never affect substantially the health of the vehicle's occupants, as it is reasonable to be.

Taking into account the VDV levels, in Tables 7.7 and 7.8 show the different discomfort parameters according to the main regulations described in chapter 5 for each test performed on the two vehicles.

Table 7.7: Vehicle A VDV WBV discomfort levels.

Vehicle A	Dominant component VDV [m/s$^{1.75}$]	Degree of discomfort according to ISO 2631-1	Degree of discomfort according to EU Directive 2002/44/EC	Vector sum 4thpower VDV$_{TOT}$ [m/s$^{1.75}$]	Allowed exposure period T$_{15}$ [h]	Max. # of allowed iterations during T$_{15}$
Test						
Run 11 extra 90 smooth	0,80	Below action value	Below action value	0,803	676,98	
Run 5 urban 70	0,95	Below action value	Below action value	0,951	343,93	
Run 19 off-road 30	1,05	Below action value	Below action value	1,062	221,21	
Run 9 uneven 70	1,24	Below action value	Below action value	1,243	117,98	
Run 12 extra 70 mixed	1,24	Below action value	Below action value	1,243	117,73	
Run 4 urban 40	1,30	Below action value	Below action value	1,300	98,21	
Run 2 wide bump 20	1,20	Below action value	Below action value	1,210		23622
Run 23 paved road 20	1,62	Below action value	Below action value	1,708	33,08	
Run 21 off-road 50	2,30	Below action value	Below action value	2,302	10,01	
Run 24 paved road 30	2,39	Below action value	Below action value	2,397	8,52	
Run 20 off-road 40	2,52	Below action value	Below action value	2,531	6,86	
Run 22 severe off-road	2,79	Below action value	Below action value	2,812	4,50	
Run 26 bump 50	2,34	Below action value	Below action value	2,341		1684
Run 25 bump 40	2,34	Below action value	Below action value	2,344		1676

Table 7.8: Vehicle B VDV WBV discomfort levels.

Vehicle B	Dominant component VDV [m/s$^{1.75}$]	Degree of discomfort according to ISO 2631-1	Degree of discomfort according to EU Directive 2002/44/EC	Vector sum 4thpower VDV$_{TOT}$ [m/s$^{1.75}$]	Allowed exposure period T$_{15}$ [h]	Max. # of allowed iterations during T$_{15}$
Test						
Run 16 extra 70 smooth	0,50	Below action value	Below action value	0,678	1334,40	
Run 9 extra 70 mixed	0,90	Below action value	Below action value	0,914	403,31	
Run 20 off-road 20	0,94	Below action value	Below action value	0,945	352,20	
Run 4 urban 40	1,06	Below action value	Below action value	1,062	220,95	
Run 13 uneven extra 70	1,28	Below action value	Below action value	1,281	104,40	
Run 5 urban 70	1,28	Below action value	Below action value	1,434	66,42	
Run 2 wide bump 20	1,25	Below action value	Below action value	1,257	41,10	20269
Run 27 paved road 20	1,65	Below action value	Below action value	1,690	34,49	
Run 22 off-road 40	2,08	Below action value	Below action value	2,082	14,97	
Run 21 off-road 30	2,30	Below action value	Below action value	2,301	10,03	
Run 26b bump 30	1,42	Below action value	Below action value	1,422	3,90	12366
Run 28 paved road 30	3,16	Below action value	Below action value	3,164	2,81	
Run 23 severe off-road	3,12	Below action value	Below action value	3,171	2,78	
Run 26a bump 40	2,57	Below action value	Below action value	2,570	0,36	1159

Concerning Vibration Dose Value assessment, the table indicates that the recommended thresholds of action and limit exposure have never been overcome in each single test, as expected, due to the fact that the several verifications have reduced duration and mostly executed on typical road paths, also taking into account that, unless being in exceptional conditions, the daily routine driving should never imply excessive physical stress and health implications as in the case of heavy duty situations that may be encountered in particular working or racing conditions.

Conversely, despite all the VDV dominant axis being always below the action value, the repetition of sequences of single tests may very well exceed the advised prescriptions based on annoyance and health issues possibility.

In detail, having chosen the 15 m/s$^{1.75}$ VDV value as a general indicative threshold according to the BS 6841 regulation, the maximum time of tolerance T_{15} has been computed or continuous manoeuvres, while the maximum numbers of consecutive iteration of each discrete proof have been computed, by performing the vector sum of the tri-axial VDV components. In this regard, as stated in the standard, it should be reminded that the 15 VDV limit is not constituting a border line between the safe and unsafe region, but only as an indicator above which severe discomfort occurs.

About vehicle A, the run 22, representing a severe off-road test, together with the run 25 for the bump travelled at 40 km/h has been classified as the most critical.

In contrast, the most comfortable situation is represented by the smooth extra-urban tarmac test of run 11.

As far as the vehicle B VDV assessment is concerned, from the table it is possible to observe that the recommended thresholds of action and limit exposure have never been overcome in each single test, as expected, similarly to the vehicle A verification.

Again, the maximum numbers of consecutive iteration of each single proof have been computed, by performing the vector sum of the tri-axial VDV components.

As a first observation, in comparison with vehicle A, the overall maximum allowed times for the selected tests is generally lower, due to the higher average VDV level along the several components.

Observing the relative table, it is simple to recognize that the less severe test conditions are represented by the constant speed smooth tarmac test of run 16, together with the extra-urban test at constant speed 70 km/h corresponding to run 9. Oppositely, worst situations are detected in run 23, relative to the most severe off-road conditions, together with the run 28, characterized by a roughly paved urban ground travelled at 30 km/h and the run 26a representing bump travelled at 40 km/h.

Considering both vehicles, best comfort has been achieved on pretty-smooth extra-urban tarmac road, while worst situations are represented by the severe off-road test at relevant speed and by the discrete urban bumps run recorded at the higher speed adopted for each car. In Table 7.9, a summary of the WBV comfort situation in relationship with the specific continuous manoeuvre run for each vehicle is reported.

Table 7.9: Summary of best and worst WBV comfort test runs.

WBV	Vehicle	A	B
Continuous Manoeuvre Tests			
RMS	Best comfort	Run 5 urban 70 km/h	Run 16 extra 70 smooth
RMS	Worst comfort	Run 22 severe off-road	Run 23 severe off-road
VDV	Best comfort	Run 11 extra 90 smooth	Run 16 extra 70 smooth
VDV	Worst comfort	Run 22 severe off-road	Run 23 severe off-road

On the other hand, looking at HTV assessment, the analysis of the various RMS and VDV levels considered the vector sum of the tri-axial components to get an indicative parameter of discomfort, again referring to the degree of allowable exposure according to the Association Advancing Occupational and Environmental Health ACGIH TLVs and the degree of discomfort according to EU Directive 2002/44/EC.

Tables 7.10 – 7.13 show the various HTV measured excitation for both the two vehicles, while Tables 7.14 – 7.17 report the RMS and VDV HTV discomfort levels.

Table 7.10: Vehicle A runs RMS acceleration values at steering wheel.

Vehicle A	RMS_X [m/s²]	RMS_Y [m/s²]	RMS_Z [m/s²]	Vector sum RMS [m/s²]
Test	$k_x=1$	$k_y=1$	$k_z=1$	
Run 2 single wide speed bump 20 km/h	0,24	0,46	0,32	0,610
Run 4 urban road 40 km/h	0,22	0,54	0,54	0,795
Run 5 urban road 70 km/h	0,14	0,35	0,48	0,610
Run 9 mixed extra-urban road 70 km/h	0,27	0,64	0,66	0,958
Run 11 smooth extra-urban road 90 km/h	0,13	0,29	0,40	0,511
Run 12 extra urban-road 70 km/h	0,13	0,33	0,45	0,573
Run 19 off-road 30	0,31	0,56	0,64	0,905
Run 20 off-road 40	0,47	1,02	0,99	1,497
Run 21 off-road 50	0,30	0,56	0,75	0,983
Run 22 severe off-road	0,42	0,86	1,01	1,391
Run 23 paved urban road 20 km/h	0,35	0,91	0,63	1,161
Run 24 paved urban road 30 km/h	0,38	0,93	0,69	1,219
Run 25 urban bumps 40 km/h	0,13	0,15	0,22	0,296
Run 26 urban bumps 50 km/h	0,32	0,24	0,43	0,587

Table 7.11: Vehicle A runs VDV values at steering wheel

Vehicle A	VDV_X [m/s¹·⁷⁵]	VDV_Y [m/s¹·⁷⁵]	VDV_Z [m/s¹·⁷⁵]	Vector sum VDV [m/s¹·⁷⁵]
Test	$k_x=1$	$k_y=1$	$k_z=1$	
Run 2 single wide speed bump 20 km/h	1,04	1,34	0,99	1,521
Run 4 urban road 40 km/h	0,77	2,05	1,65	2,246
Run 5 urban road 70 km/h	0,58	1,59	1,62	1,913
Run 9 mixed extra-urban road 70 km/h	0,96	2,18	2,21	2,622
Run 11 smooth extra-urban road 90 km/h	0,36	0,87	1,19	1,269
Run 12 extra urban-road 70 km/h	0,57	1,32	1,55	1,728
Run 19 off-road 30	0,90	1,65	1,84	2,102
Run 20 off-road 40	1,57	3,28	3,06	3,804
Run 21 off-road 50	0,93	1,73	2,40	2,559
Run 22 severe off-road	1,80	3,04	3,43	3,912
Run 23 paved urban road 20 km/h	1,15	3,11	2,15	3,287
Run 24 paved urban road 30 km/h	1,18	3,28	2,11	3,424
Run 25 urban bumps 40 km/h	0,87	0,99	1,41	1,530
Run 26 urban bumps 50 km/h	1,85	1,32	2,37	2,609

Table 7.12: Vehicle B runs RMS acceleration values at steering wheel.

Vehicle B	RMS_X [m/s^2]	RMS_Y [m/s^2]	RMS_Z [m/s^2]	Vector sum RMS [m/s^2]
Test	k_x=1	k_y=1	k_z=1	
Run 2 single wide speed bump 20 km/h	0,49	0,38	0,61	0,870
Run 4 urban road 40 km/h	0,37	0,31	0,65	0,810
Run 5 urban road 70 km/h	0,38	0,36	0,65	0,835
Run 9 mixed extra-urban road 70 km/h	0,19	0,15	0,23	0,334
Run 16 tarmac extra-urban road 70 km/h	0,26	0,19	0,49	0,586
Run 13 uneven extra-urban road 70 km/h	0,67	0,50	1,00	1,303
Run 20 off-road 20	0,57	0,41	1,21	0,939
Run 21 off-road 30	0,76	0,59	1,20	1,399
Run 22 off-road 40	0,61	0,50	0,97	1,538
Run 23 severe off-road	0,92	0,73	1,15	1,250
Run 27 paved urban road 20 km/h	0,59	0,77	1,15	1,644
Run 28 paved urban road 30 km/h	0,76	0,60	0,91	1,504
Run 26b urban bumps 30 km/h	0,36	0,24	0,47	1,329
Run 26a urban bumps 40 km/h	0,18	0,11	0,21	0,639

Table 7.13: Vehicle B runs VDV values at steering wheel.

Vehicle B	VDV_X [m/s$^{1.75}$]	VDV_Y [m/s$^{1.75}$]	VDV_Z [m/s$^{1.75}$]	Vector sum VDV [m/s$^{1.75}$]
Test	k_x=1	k_y=1	k_z=1	
Run 2 single wide speed bump 20 km/h	1,63	1,15	1,84	2,122
Run 4 urban road 40 km/h	1,29	1,18	2,57	2,637
Run 5 urban road 70 km/h	1,56	1,25	2,31	2,464
Run 9 mixed extra-urban road 70 km/h	1,57	1,31	1,86	2,140
Run 16 tarmac extra-urban road 70 km/h	0,76	0,57	1,48	1,513
Run 13 uneven extra-urban road 70 km/h	2,43	1,78	3,54	3,770
Run 20 off-road 20	1,72	1,19	3,61	3,666
Run 21 off-road 30	3,42	2,28	5,34	5,591
Run 22 off-road 40	1,75	1,46	2,82	2,964
Run 23 severe off-road	2,70	2,19	3,50	3,878
Run 27 paved urban road 20 km/h	1,73	2,81	3,27	3,691
Run 28 paved urban road 30 km/h	2,35	1,74	2,95	3,278
Run 26b urban bumps 30 km/h	2,58	1,64	3,42	3,705
Run 26a urban bumps 40 km/h	1,12	0,70	1,39	1,535

Table 7.14: Vehicle A HTV RMS acceleration discomfort levels.

Vehicle A	Dominant component a_w rms	Vector sum RMS [m/s²]	Degree of allowable exposure according ACGIH TLVs	Degree of discomfort according to EU Directive 2002/44/EC
Test				
Run 25 bump 40	0,22	0,296	More than 8 hours	Below daily action level
Run 11 extra 90 smooth	0,40	0,511	More than 8 hours	Below daily action level
Run 12 extra 70 mixed	0,45	0,573	More than 8 hours	Below daily action level
Run 26 bump 50	0,43	0,587	More than 8 hours	Below daily action level
Run 2 wide bump 20	0,46	0,610	More than 8 hours	Below daily action level
Run 5 urban 70 km/h	0.48	0,610	More than 8 hours	Below daily action level
Run 4 urban 40	0.54	0,795	More than 8 hours	Below daily action level
Run 19 off-road 30	0,64	0,905	More than 8 hours	Below daily action level
Run 9 uneven extra 70	0,66	0,958	More than 8 hours	Below daily action level
Run 21 off-road 50	0,75	0,983	More than 8 hours	Below daily action level
Run 23 paved road 20	0,91	1,161	More than 8 hours	Below daily action level
Run 24 paved road 30	0,93	1,219	More than 8 hours	Below daily action level
Run 22 severe off-road	1,01	1,391	More than 8 hours	Below daily action level
Run 20 off-road 40	0,99	1,497	More than 8 hours	Below daily action level

Table 7.15: Vehicle B HTV RMS acceleration discomfort levels.

Vehicle B	Dominant component a_w r.m.s.	Vector sum RMS [m/s^2]	Degree of allowable exposure according ACGIH TLVs	Degree of discomfort according to EU Directive 2002/44/EC
Test				
Run 26b bump 30	0,21	0,298	More than 8 hours	Below daily action level
Run 9 extra 70 mixed	0,23	0,334	More than 8 hours	Below daily action level
Run 16 extra 70 smooth	0,49	0,586	More than 8 hours	Below daily action level
Run 26a bump 40	0,47	0,639	More than 8 hours	Below daily action level
Run 4 urban 40	0,65	0,810	More than 8 hours	Below daily action level
Run 2 wide bump 20	0,61	0,870	More than 8 hours	Below daily action level
Run 22 off-road 40	0,97	1,250	More than 8 hours	Below daily action level
Run 13 uneven 70	1,00	1,303	More than 8 hours	Below daily action level
Run 28 paved road 30	0,91	1,329	More than 8 hours	Below daily action level
Run 20 off-road 20	1,21	1,399	More than 8 hours	Below daily action level
Run 27 paved road 20	1,15	1,504	More than 8 hours	Below daily action level
Run 21 off-road 30	1,20	1,538	More than 8 hours	Below daily action level
Run 23 severe off-road	1,15	1,644	More than 8 hours	Below daily action level

About hand-transmitted vibration, the vector sum of the tri-axial acceleration components on the steering-wheel position has been compared for each run with the typical recommended levels included in ACGIH prescriptions and EU Directive 2002/44/EC dogmas.

The general result of vehicle A investigation indicates that, considering the totality of the runs, the daily exposure action level is never trespassed; as a consequence, all of the tests are characterized by an allowable exposure time to the hand-transmitted excitation longer than 8 hours/day.

Such outcomes are quite predictable, since these specific standards are mostly adopted to assess the health and safety risks connected to HTV diseases as the hand-arm vibration syndrome (HAVS), which is a typical industrial injury triggered by continuous use of vibrating hand-held machinery, thus involving much harder conditions with respect to those encountered during normal daily driving. In detail, the most comfortable situation is the same of WBV assessment is the run 25 single bump recording at 40 km/h, while the most critical one is the off-road terrain travelled at 40 km/h speed in run 22.

On the other hand, considering the table relative to vehicle B results, the same observations about ACGIH prescriptions and EU Directive 2002/44/EC thresholds apply; though, the maximum peak of vector sum r.m.s. is lower with respect to vehicle A one. Here the highest excitation is reached in run 23, where a the severe off-road ground has produced high vibrations on steering wheel.

Instead, most reduced excitations are detectable in run 9, featuring an extra-urban road with low irregularities travelled at 70 km/h.

All the previous considerations above action and limit values are to be taken as a pure indicative reference concerning continuous daily excitation thresholds, as these evaluation parameters have been developed to assess vibration issues regarding the workplace, thus involving average periods of 8 hours. Therefore, even though they've been adopted to generally classify al the run tests, the first remarks is that each of the ordinary test, taken as a single phenomenon, would never affect substantially the health of the vehicle's occupants, as it is reasonable to be.

Table 7.16: Vehicle A HTV VDV acceleration discomfort levels.

Vehicle A	Dominant component VDV	Vector sum VDV[m/s$^{1.75}$]
Test		
Run 11 extra 90 smooth	1,19	1,269
Run 2 wide bump 20	1,34	1,521
Run 25 bump 40	1,41	1.530
Run 12 extra 70 mixed	1,55	1,728
Run 5 urban 70	1,62	1,913
Run 19 off-road 30	1,84	2,102
Run 4 urban 40	2,05	2,246
Run 21 off-road 50	2,40	2,559
Run 26 bump 50	2.37	2.609
Run 9 uneven 70	2,21	2,622
Run 23 paved road 20	3,11	3,287
Run 24 paved road 30	3,28	3,424
Run 20 off-road 40	3,28	3,804
Run 22 severe off-road	3,43	3,912

Table 7.17: Vehicle B HTV VDV acceleration discomfort levels.

Vehicle B	Dominant component VDV	Vector sum VDV [m/s$^{1.75}$]
Test		
Run 16 extra 70 smooth	1,48	1,513
Run 26b bump 30	1,33	1,535
Run 9 extra 70 mixed	1,86	2,140
Run 2 wide bump 20	1,84	2,122
Run 5 urban 70	2,31	2,464
Run 4 urban 40	2,57	2,637
Run 22 off-road 40	2,82	2,964
Run 28 paved road 30	2.95	3.278
Run 20 off-road 20	3,61	3,666
Run 27 paved road 20	3,27	3,691
Run 26a bump 40	3,42	3,705
Run 13 uneven extra 70	3,54	3,770
Run 23 severe off-road	3,50	3,878
Run 21 off-road 30	5,34	5,591

Taking into account VDV, general prescriptions usually prefer to make reference to r.m.s. acceleration vector sum only, though, in order to have an overview on vibration dose value relative to hand-transmitted vibration and to compare the results with those obtained with the r.m.s. acceleration inspection, the VDV dominant component and the vector sum have been computed, collected and reported for completeness.

At a first glance, it is possible to observe that the VDV level is generally higher for the Panda, with significantly larger values in both the columns of the table, while the CX-5 table put in evidence more limited peaks.

In particular, the less severe test condition for the vehicle A is still the run 11, characterized by smooth tarmac travelled at 90 km/h, which represents the best ideal condition amongst all the ones examined, while the most critical one is represented by the run 23, corresponding to severely uneven off-road.

Actually, it is worth to observe that these run 11 constitutes the best test conditions for whole body vibration VDV assessment too.

Alternatively, looking at the vehicle B results, the same considerations can be done in regards of the maximum VDV level, as the worst excitation situation is verified in run 21. Instead, the best condition is achieved in run 16, featuring extra-urban smooth tarmac road, travelled at 70 km/h.

In Table 7.18, a summary of the best and worst hand-transmitted vibration comfort situation in relationship with the specific run for each vehicle is reported.

Table 7.18: Summary of best and worst WBV comfort test runs.

HTV	Vehicle	A	B
Test			
RMS	Best comfort	Run 25 single bump 40	Run 9 extra 70
RMS	Worst comfort	Run 20 off-road 40	Run 23 bad off-road
VDV	Best comfort	Run 11 extra 90 smooth	Run 16 extra 70 smooth
VDV	Worst comfort	Run 22 bad off-road	Run 21 off-road 30

7.3 Seat effective amplitude transmissibility assessment

As expressed in chapter 2, SEAT contribution represents the ratio of the vibration experienced on the top of the seat and the vibration that a subject would withstand when sitting directly on the vibrating floor, therefore constituting a numerical index computed as the weighted vibration ratio between Z_f of the floor and Z_s of the hip perfectly adequate to assess the vibrational attenuation of a seat with respect to excitations from the floor. In the specific case, the SEAT values corresponding to the several runs recorded with each vehicle have been calculated taking into account both RMS and VDV vibration levels, to have a wide overview on the seat filtering capability, which is mainly represented by its cushion design and features.

In detail, the ratios between the acceleration measured on the Z-axis at the seat cushion and at the seat rail have been considered, in order to have the best possible data recording from vehicle floor in a fixed and stable position.

Also in this case, the reference time for continuous manoeuvres is equal to approximately 20 seconds, while the discrete manoeuvres runs have a time dependent on the effective excitation duration of the bumps, the other settings and option in Test.Lab being maintained from the previous WBV and HTV calculations.

Figure 7.41 – 7.44 depicts some sample diagrams containing the vehicles A and B acceleration RMS and VDV levels exploited to derive the final numerical SEAT indexes, showing the Maximum Transient Vibration Value for each run too.
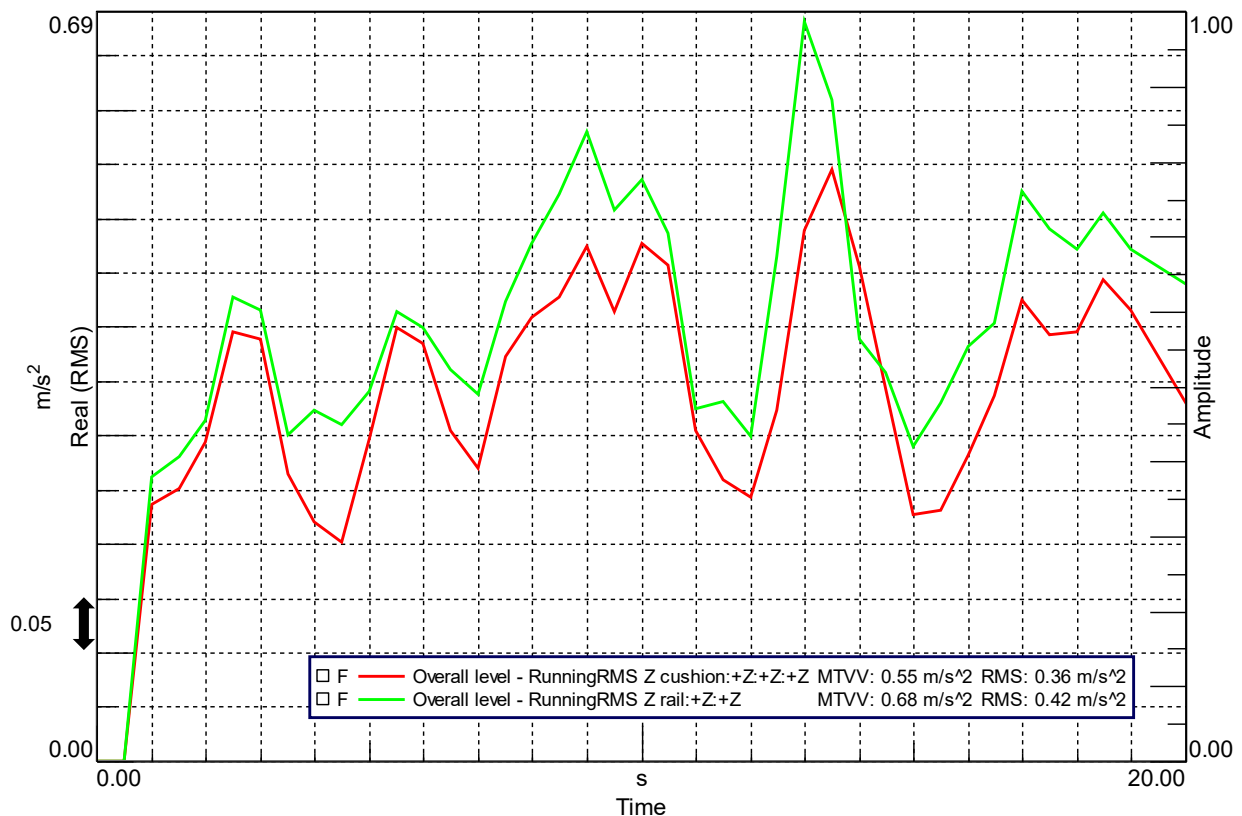

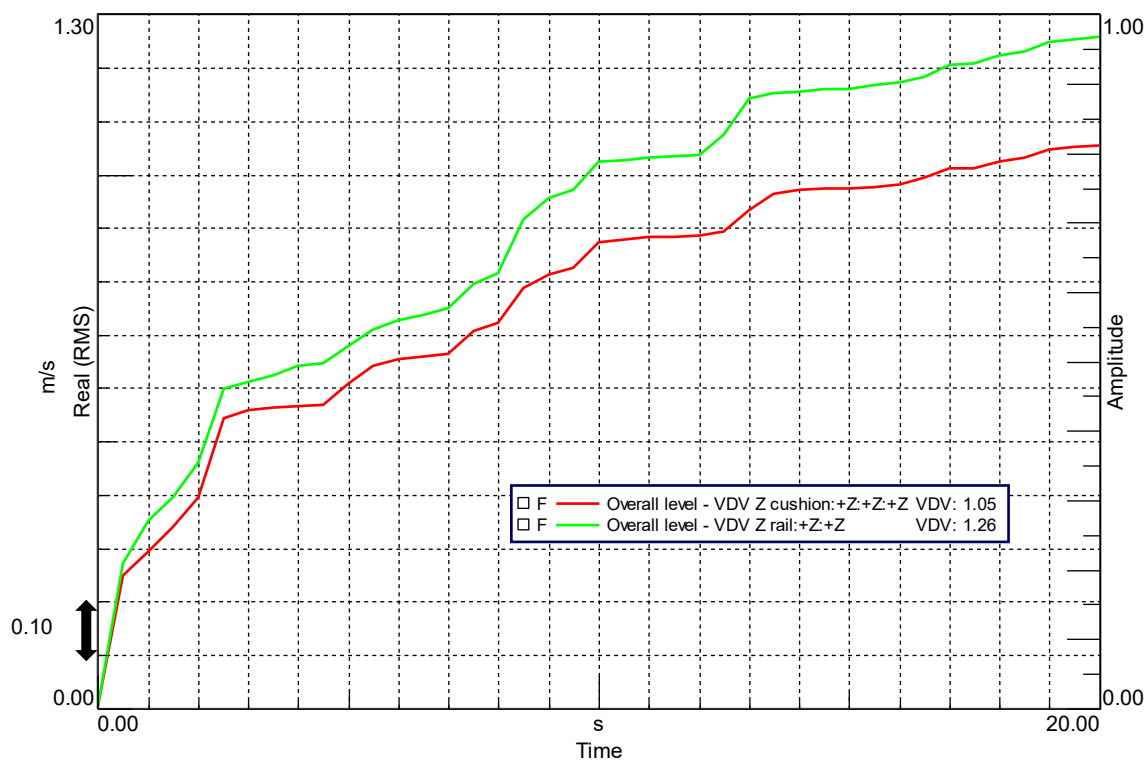**Figure 7.41**: Run 19 off-road 30 km/h SEAT RMS diagram, (vehicle A).

Figure 7.42: Run 19 off-road 30 km/h SEAT VDV diagram, (vehicle A).
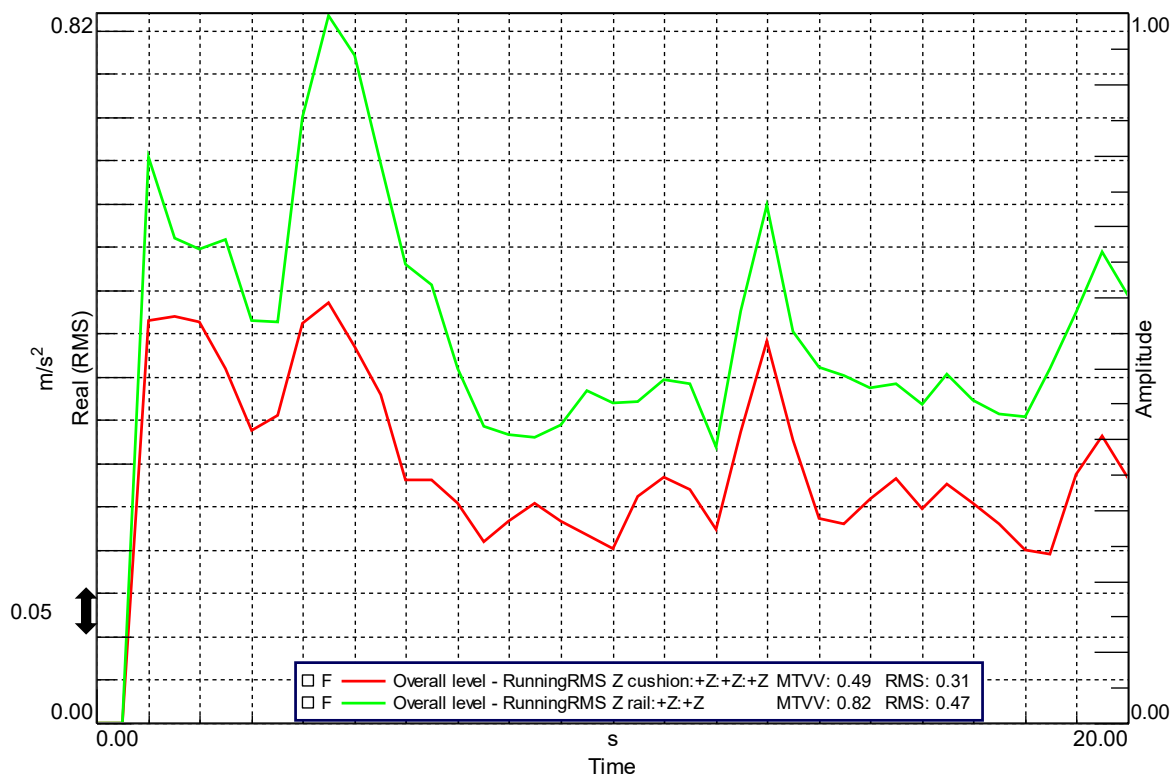

Figure 7.43: Run 20 off-road 20 km/h SEAT RMS diagram, (vehicle B).
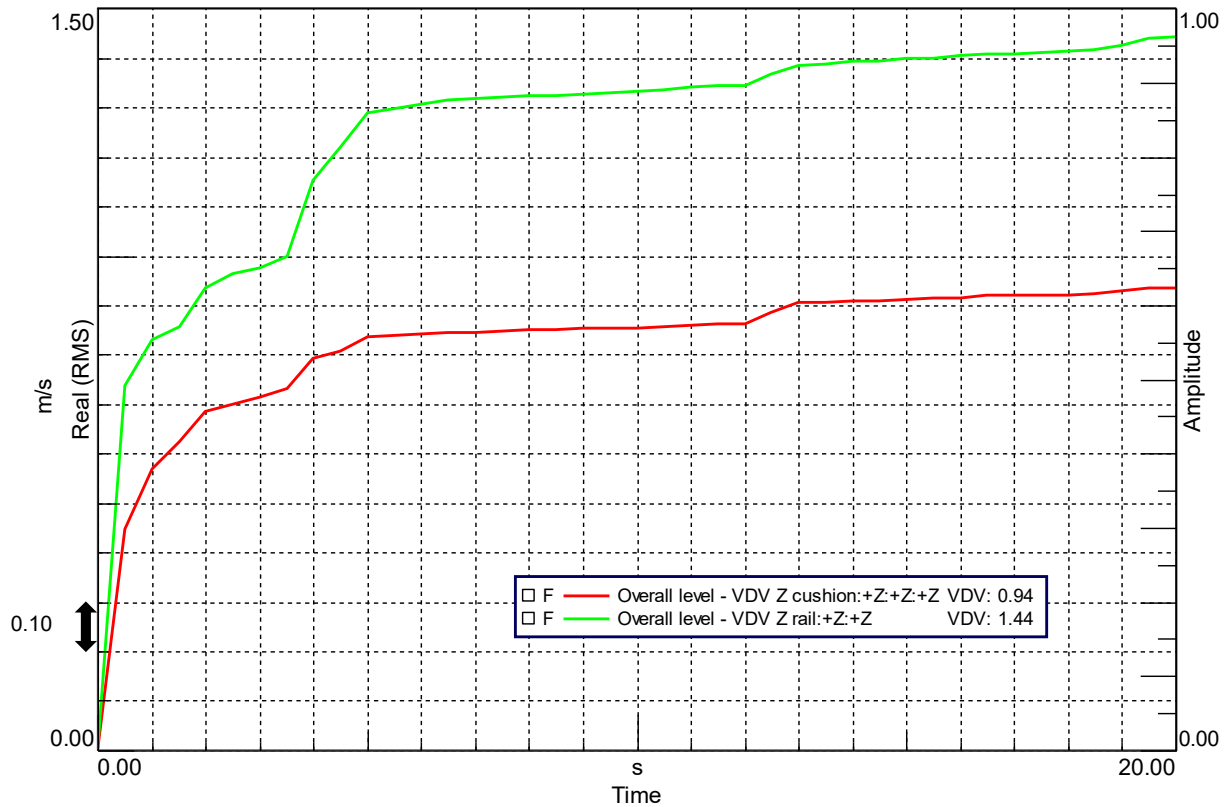
Figure 7.44: Run 20 off-road 20 km/h SEAT VDV diagram, (vehicle B).

To get a wide glance on the difference between the several testing condition, other than making a comparison between the seat filtering effectiveness of each car, the SEAT indexes from all the several tests executed in the two chosen vehicles have been reported in Tables 7.19 – 7.22, including both the $SEAT_{RMS}$ and $SEAT_{VDV}$ categories, the former being computed from the frequency-weighted r.m.s. acceleration on the seat surface and seat base, $a_{seat,w}$ and $a_{base,w;}$ the latter, strongly recommended in case of input motion shocks, is related to the VDV amount at the seat surface and at the seat base, respectively VDV_{seat} and VDV_{base}.

Table 7.19: Vehicle A SEAT RMS computed data.

Vehicle A	RMS seat [m/s²]	RMS rail [m/s²]	SEAT_RMS
Test			
Run 5 urban 70	0,22	0,35	62,86%
Run 9 mixed extra-urban 70	0,39	0,62	62,90%
Run 4 urban 40	0,41	0,59	69,49%
Run 11 extra-urban 90 smooth	0,27	0,33	81,82%
Run 21 off-road 50	0,72	0,87	82,76%
Run 22 bad off-road	0,88	1,05	83,81%
Run 23 urban paved 20	0,53	0,62	85,48%
Run 19 off-road 30	0,36	0,42	85,71%
Run 12 extra-urban 70	0,30	0,34	88,24%
Run 26 bump 50	0,45	0,51	88,24%
Run 20 off-road 40	0,77	0,86	89,53%
Run 24 urban paved 30	0,69	0,75	92,00%
Run 2 wide bump 20	0,47	0,46	102,17%
Run 25 bump 40	0,41	0,36	112,50%

Table 7.20: Vehicle A SEAT VDV computed data.

Vehicle A	VDV seat [m/s^1.75]	VDV rail [m/s^1.75]	Seat_VDV
Test			
Run 5 urban 70	0,95	1,71	55,56%
Run 9 mixed extra-urban 70	1,24	2,05	60,49%
Run 4 urban 40	1,30	1,97	65,99%
Run 22 bad off-road	2,79	3,55	78,59%
Run 21 off-road 50	2,30	2,91	79,04%
Run 11 extra-urban 90 smooth	0,80	0,98	81,63%
Run 19 off-road 30	1,05	1,26	83,33%
Run 26 bump 50	2,34	2,70	86,67%
Run 23 urban paved 20	1,62	1,87	86,63%
Run 20 off-road 40	2,52	2,77	90,97%
Run 2 wide bump 20	0,70	0,76	92,11%
Run 24 urban paved 30	2,39	2,54	94,09%
Run 12 extra-urban 70	1,24	1,28	96,88%
Run 25 bump 40	2,34	2,21	106,12%

Table 7.21: Vehicle B SEAT RMS computed data.

Vehicle B	RMS seat [m/s^2]	RMS rail [m/s^2]	SEAT$_{RMS}$
Test			
Run 13 extra-urban 70	0,37	0,70	52,86%
Run 9 mixed extra-urban 70	0,26	0,46	56,52%
Run 20 off-road 20	0,31	0,47	65,96%
Run 16 extra-urban 70 smooth	0,17	0,25	68,00%
Run 21 off-road 30	0,54	0,75	72,00%
Run 5 urban 70	0,27	0,36	75,00%
Run 4 urban 40	0,33	0,43	76,74%
Run 27 urban paved 20	0,51	0,58	87,93%
Run 22 off-road 40	0,58	0,65	89,23%
Run 23 bad off-road	1,01	1,12	90,18%
Run 2 wide bump 20	0,51	0,56	91,07%
Run 26a bump 40	0,38	0,39	97,44%
Run 28 urban paved 30	0,90	0,91	98,90%
Run 26b bump 30	0,25	0,23	108,70%

Table 7.22: Vehicle B SEAT VDV computed data.

Vehicle B	VDV seat [m/s$^{1.75}$]	VDV rail [m/s$^{1.75}$]	Seat$_{VDV}$
Test			
Run 9 mixed extra-urban 70	0,90	1,74	51,72%
Run 13 extra-urban 70	1,28	2,47	51,82%
Run 21 off-road 30	2,30	3,60	63,89%
Run 20 off-road 20	0,94	1,44	65,28%
Run16 extra-urban 70 smooth	0,50	0,74	67,57%
Run 4 urban 40	1,06	1,44	73,61%
Run 5 urban 70	1,09	1,47	74,15%
Run 2 wide bump 20	1,25	1,43	87,41%
Run 23 bad off-road	3,12	3,45	90,43%
Run 22 off-road 40	2,08	2,18	95,41%
Run 27 urban paved 20	1,65	1,72	95,93%
Run 26b bump 30	1,42	1,33	106,39%
Run 26a bump 40	2,62	2,39	109,62%
Run 28 urban paved 30	3,16	2,87	110,10%

Looking at the results in such tables below in general, for both vehicles considered it is possible to recognize a worsening trend that, from extra-urban and urban roads, passing though off-road conditions, leads to less and less filtering capability going towards paved road and bumps sequences.

In detail concerning SEAT$_{RMS}$ index, regarding vehicle A, highest transmissibility, with amplification of the excitation, is noticed in run 25 (SEAT RMS 112.50%), representing urban bumps at 40 km/h, together with run 2 (SEAT RMS 102.17%), consisting in a wide speed bump at 20 km/h with pedestrian crossing, whereas best seat cushion filtering is provided in run 5 and run 9, representing urban and extra-urban roads at 70 km/h (SEAT RMS respectively 62.86% and 62.90%).

Conversely, considering vehicle B case, worst isolation goodness, with amplification of the excitation, is noticed in run 26b (SEAT RMS 108.70%), representing urban bumps at 30 km/h, while best seat isolation property, with attenuation of the excitation, is observable in run 13 and run 9, representing extra-urban mixed roads at 70 km/h (SEAT RMS respectively 52.86% and 56.52%).

About SEAT$_{VDV}$, considering vehicle A, amplification of the excitation is again detected in run 25 (SEAT VDV 106.12%), and best seat cushion filtering is witnessed in run 5 and run 9, (SEAT VDV respectively 55.56% and 60.49%). Instead, taking into account vehicle B, similarly to before, amplification of the excitation is mainly noted in paved and bumps tests as run 28, (SEAT VDV 110.10, run 26a (SEAT VDV 109.62%) and run 26b (SEAT VDV 106.39%), respectively corresponding to urban bumps at 40 km/h and 30 km/h, moreover, run 13 and run 9 extra-urban mixed roads at 70 km/h still constitute the best filtering property test conditions, (SEAT VDV respectively 51.72% and 51.82%).

Vehicle B shows a better behaviour on the wide speed bump at low speed, keeping a certain attenuation degree, whereas vehicle A overcomes the 100% SEAT$_{RMS}$ threshold. Then, taking into account urban road tests at moderate speed, vehicle A skills stand out, denoting a better seat filtering in regards of both RMS and VDV sides. Conversely, in the response on smooth and mixed tarmac at higher speed in extra-urban conditions, vehicle B highlights a larger isolation at higher frequency for more pronounced road irregularities; as an overall tendency, increasing the speed, the seat transmissibility grows up; indeed the attenuation capability drops downs while the SEAT level tends to increase, still avoiding to reach the amplification zone.

On the other hand, looking at off-road tests, both vehicles demonstrate a certain attenuation, which is better on the whole for vehicle A at higher speed and for the vehicle B at very low ones. In addition, about the bumps sequences, for vehicle B a relevant worsening of the filtering property is detected when speed rises, breaching the critical VDV threshold already at 30 km/h, whereas vehicle A does the same for a velocity of 40 km/h, to a lesser extent.

Furthermore, its seat effectively filters vibrations during the bump test at 50 km/h, attenuating the solicitation, which would be a highly severe proof for vehicle B, causing excessive strong mechanical stresses and peaks of excitation.

Moreover, considering the urban paved road in Carmagnola, vehicle A shows the better SEAT characteristic, stably remaining below the critical level both for RMS and VDV, while vehicle B exhibits a worse attenuation, displaying an overrun of the SEAT$_{VDV}$ 100 % value at 30 km/h.

Summarizing these results, it is possible to observe that vehicle B seat behaves better on bumps and speed bump at low speed, on mixed extra-urban roads and off-road paths at low speed.

Contrariwise, vehicle A seat has proven to outperform on mixed urban road at moderate speed, on off-road paths at higher speed and with severe terrain deformations, on urban paved road with significant irregularities and bumps travelled at relevant speed. Overall, the assessment leads to suppose that vehicle B seat, softer, is prone to damp the vibration transmission from the seat rails during bumps tests at very low speed and with a wide width, as well as well filtering the limited irregularities encountered during low speed off-road and extra-urban roads.

However, due to its specific design characteristics, the seat cushion struggles to attenuate effectively more wearing irregularities, present in the bad stoned pave road, severe off-road and short bumps sequences travelled at higher speed, putting in evidence a poor isolation of the system resonances, whereas vehicle A seat, although tougher, succeeds in providing a more adequate filtering thanks to its specific building characteristics. In this concern, vehicle B shows larger RMS acceleration levels on the seat rail, mainly related to the different tyres and suspension, partly compensated in the previously described conditions by a seat designed in order to obtain a good filtering whereby the strain is not excessive.

Indeed, this is the field in which, especially at higher speeds, the vehicle A suspensions and the seat cushion excel, leading to reduced RMS levels at seat guide and an optimum filtering.

7.4 Frequency Response Function analysis

After having looked at the a_z rail profiles of each test, considering the whole-body and hand-transmitted vibration metrics, together with the Seat Effective Amplitude Transmissibility indexes, the focus shifts now on studying the Frequency Response Function curves, again obtained by exploiting the LMS Test.Lab software dedicated tools. In this case, within the Time Data Processing tooltip, the following settings have been chosen to compute the FRFs.

- Channel processing data:
    - Function: FRF;
    - Reference: Variable, X rail/ Y rail/ Z rail;
- Acquisition parameters:
    - Measurement mode: Stationary;
    - Method: Free run;
    - Averaging type: Linear average;
    - Overlap: 50%;
    - Bandwidth: 20480 Hz:
    - Resolution: 0.2 Hz;
    - Spectral lines: 102400;
    - Frame size: 5 s.

As a first remark, it is worth of notice that the Frequency Response Function represented in the following are all based on the relationship between the vibration excitation at the seat cushion and the vibration stimulus at the seat rail.

Actually, these results are partly linked to the damping capability of the seat cushion, even if in a more generic way with respect to the ad-hoc SEAT indexes mentioned in the previous paragraph. On the other hand, the results obtained are pretty interesting to observe the overall trend of these functions in relation with the type of test performed and the car utilized. A quick legend to recall the various runs performed in the two vehicles and utilized in this assessment is reported in Table 7.23.

Concerning these computations, particular consideration has been dedicated to the specific frequency filtering characteristics of the acquisition hardware and the accelerometers. Indeed, the cut-off frequency of the SCADAS acquisition tool is equal to 0.5 Hz in HP, whereas the PCB accelerometers exploited have a working frequency range comprised between 1.4 - 6500 Hz, (error ± 5%) and within 2 – 5000 Hz, (error ± 10%), thus the signals with frequency under 0.5 Hz have been excluded as wrong, the signals with frequency in between 0.5-1.4 Hz are considered as intermediately reliable, with an error not always lower than 10%, the ones with frequency between 1.4 and 2 Hz are subjected to an error varying between 5-10% and the signals above 2 Hz are more than reliable, with error lower than 5%.

Table 7.23: List of considered tests in FRF study.

Vehicle A	Vehicle B
FRF STUDY TESTS	
Run 2 single wide speed bump 20 km/h	Run 2 single wide speed bump 20 km/h
Run 19 off-road 30 km/h	Run 20 off-road 20 km/h
Run 20 off-road 40 km/h	Run 21 off-road 30 km/h
Run 21 off-road 50 km/h	Run 22 off-road 40 km/h
Run 22 severe off-road	Run 23 severe off-road
Run 23 paved urban road 20 km/h	Run 27 paved urban road 20 km/h
Run 24 paved urban road 30 km/h	Run 28 paved urban road 30 km/h
Run 25 urban bumps 40 km/h	Run 26b urban bumps 30 km/h
Run 26 urban bumps 50 km/h	Run 26a urban bumps 40 km/h

In Figures 7.45 - 7.56 the several FRF curves relative to Z, X, Y axes for vehicle A and vehicle B runs are depicted; the FRF_z representing the most interesting typology for the conducted study, the other two being included for completeness, even though they do not constitute a real interest, as the seat is designed to filter vibrations acting mainly on the cushion vertical axis, while on X,Y axes its function is mainly to restrain the occupants. The FRF functions trends are computed by the software and depicted in amplitude with unit measure dB and in phase.

The critical threshold between amplification and attenuation is located in correspondence of the 0 dB line, chosen as a clear border line between the two zones, avoiding complex constraints related to the different cut-off frequency definition, more bounded to the electronics field. Instead, the main range considered in this whole-body vibration FRF study corresponds to the range 0.5 – 80 Hz.

Moreover, diagrams reporting the functions in a more detailed view adopt a range in between 0.5 – 20 Hz. As a further remark, it is worth to have in mind that according to ISO 2631-1 specified WBV vertical weighting class W_k (seated/standing/recumbent person, z direction), most uncomfortable frequency range for human body subjected to excitation is comprised in the interval 4-8 Hz, as put in evidence by Figure 2.10; therefore, analysing the seat cushion transmissibility FRFs, this range represents a key focus as far as human comfort is concerned.
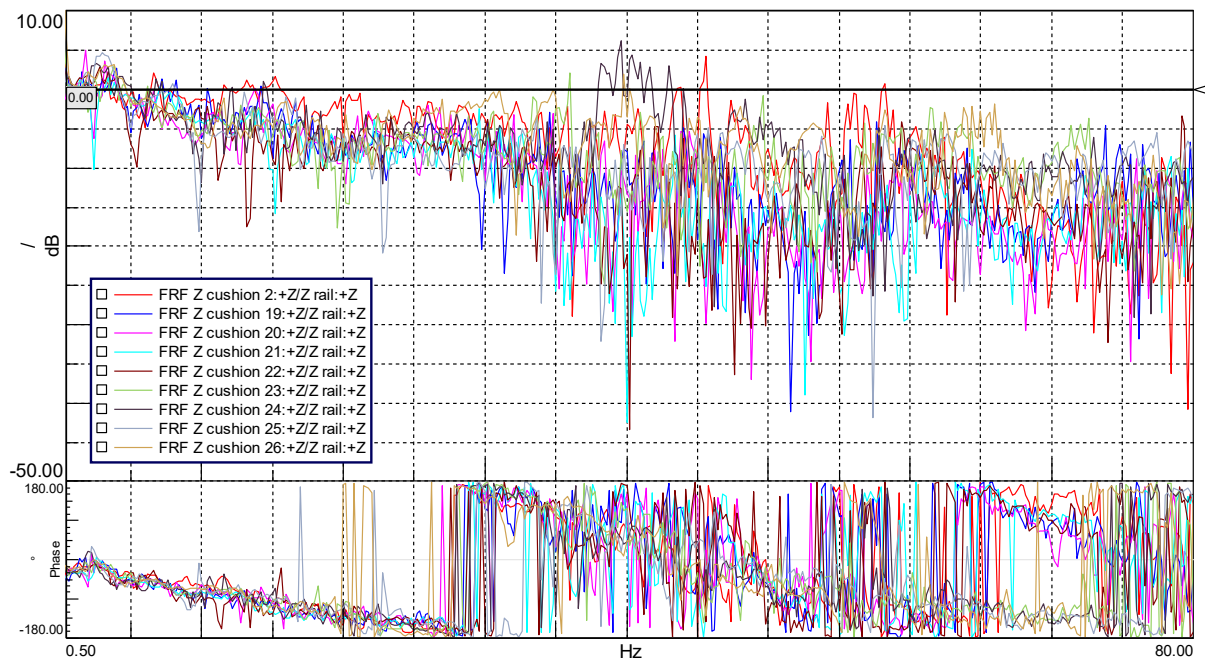
7.4.1 Vehicle A FRF trends
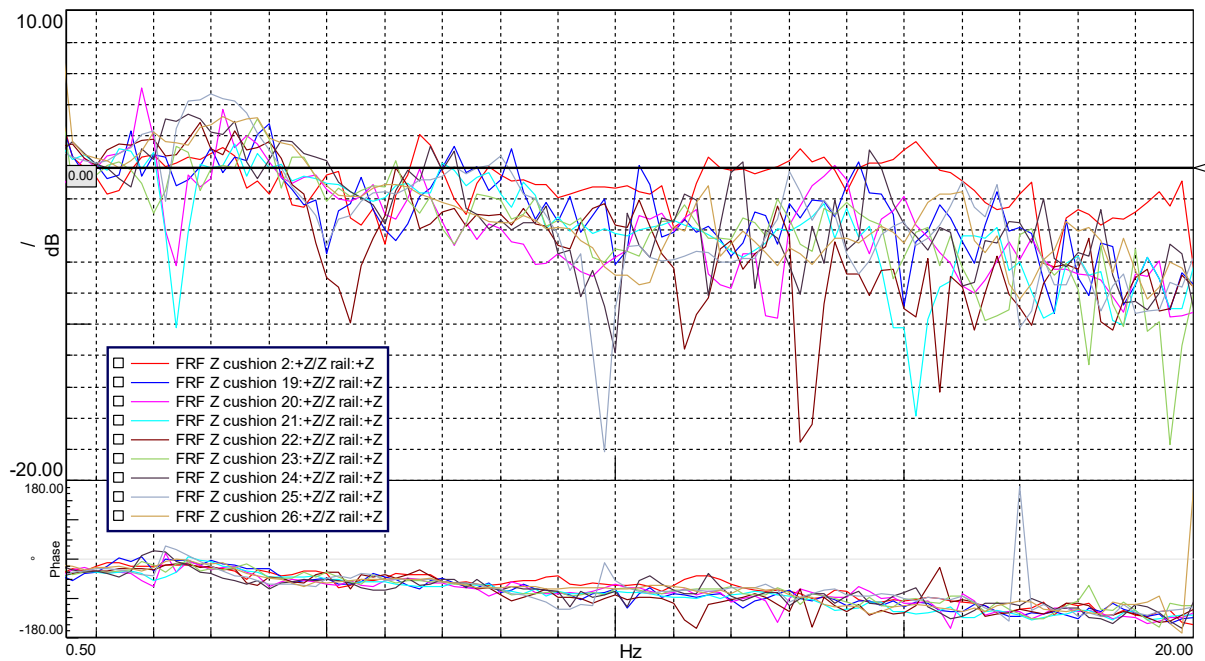

Figure 7.45: Vehicle A runs FRF$_z$ cushion curves.

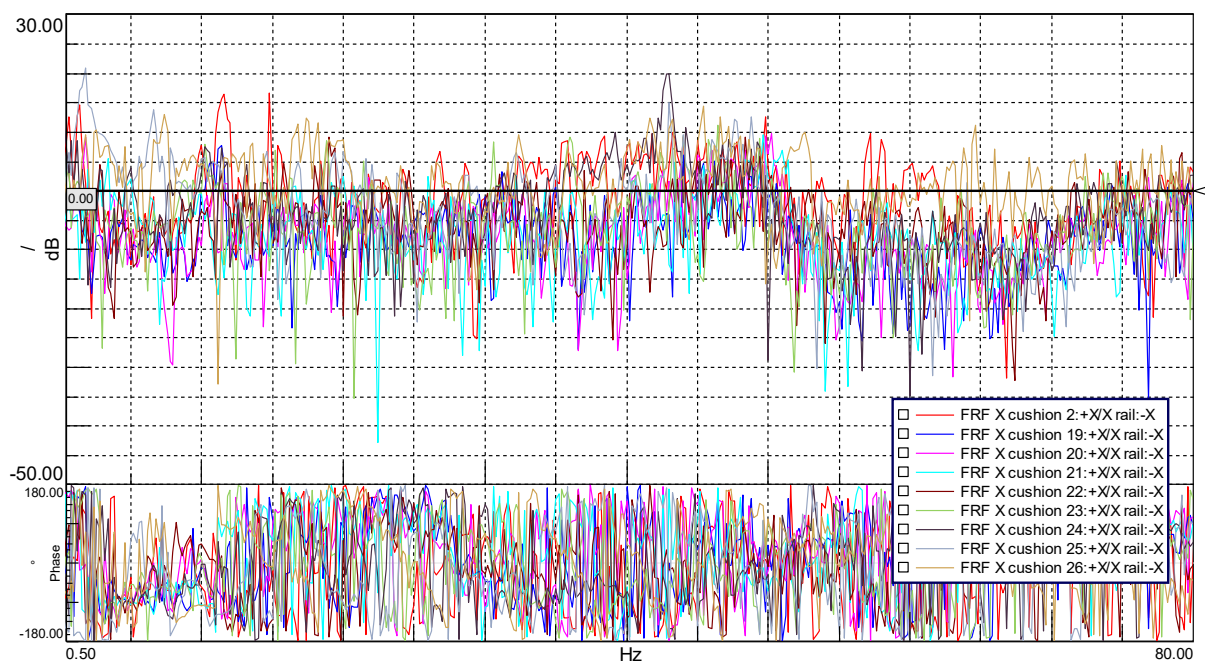**Figure 7.46**: Vehicle A runs FRF$_z$ cushion curves, detail.
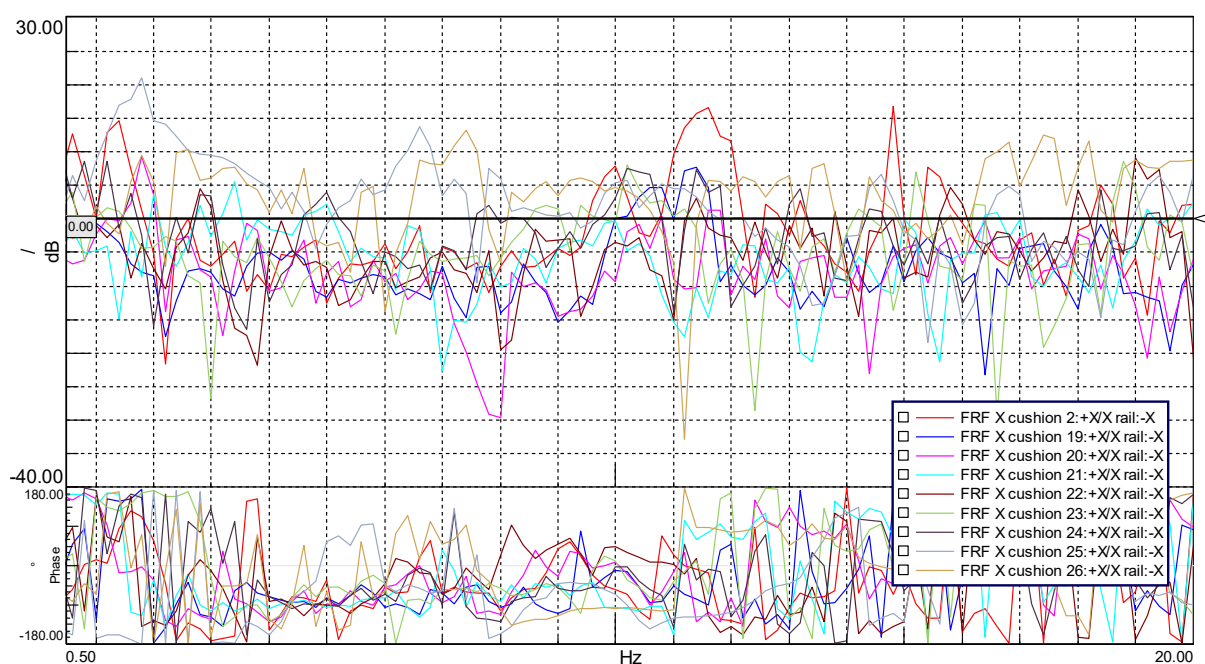
Figure 7.47: Vehicle A runs FRF$_x$ cushion curves.

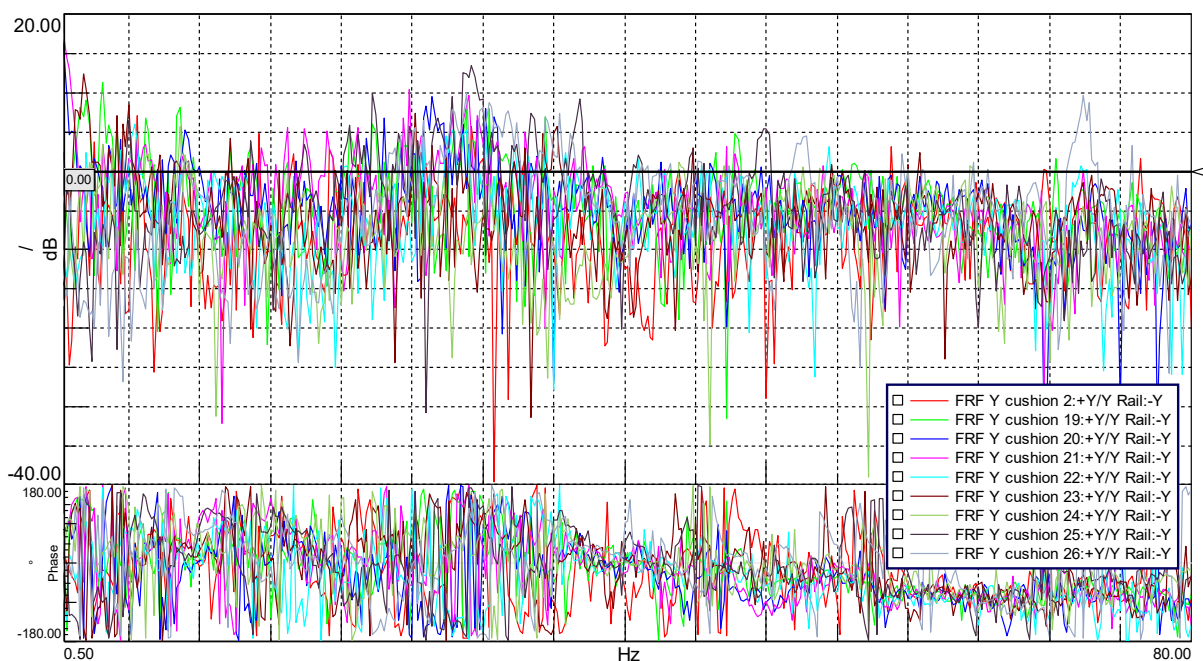**Figure 7.48**: Vehicle A runs FRF$_x$ cushion curves, detail.

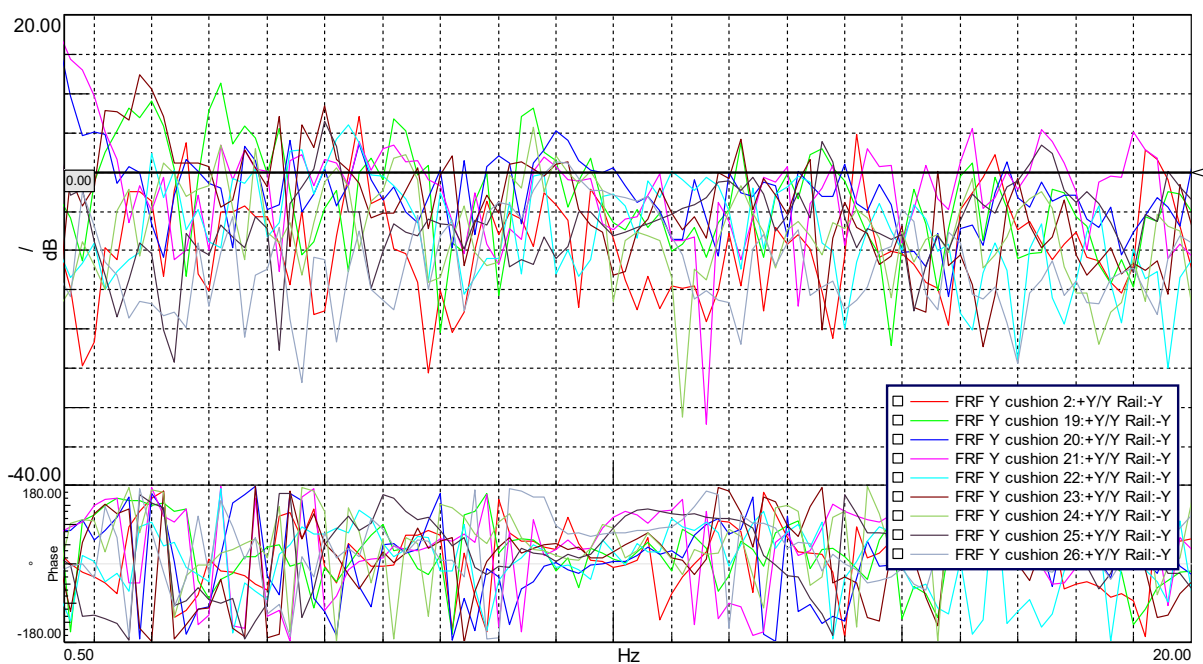**Figure 7.49**: Vehicle A runs FRF$_y$ cushion curves.

Figure 7.50: Vehicle A runs FRF$_y$ cushion curves, detail.

Having looked at these graphs, a summary of the several FRF$_Z$ characteristics in each single run is presented:

- Run 2 (wide bump): the overall value of the FRF is pretty near to the critical threshold for most part of the frequency range, presenting several points over the 0 dB line, in particular in the 0.5-16 Hz range; in addition, a 5 dB peak is located in proximity of the 46.5 Hz zone, while a not very high attenuation is provided across the mid-high frequency range.

- Run 19 (off-road): the curve of the FRF is below the critical threshold for all the frequency range above about 14.25 Hz; for higher frequencies indeed, the curve shows a trend oscillating around a level comparable to the others examined.

- Run 20 (off-road): this FRF curve is relevantly similar to the run 19 one, being both the function recorded during off-road tests, with different speed. More in detail, it is possible to observe that the curve for this Run indicates a larger amplification concerning Z transmissibility, with the maximum of 5.17 dB located at 1.80 Hz, while no amplification is observable for frequency higher than about 8.30 Hz.

- Run 21 (off-road): compared to the others, also in this case the FRF curve appears really similar to the trends observed for the other off-road tests recordings. In this case, for frequency higher than about 7 Hz, the curve stays below the critical threshold, indicating that no more amplification is present. Moreover, as all the off-road FRF curves examined before, a specific improvement in the filtering capability of the seat is recognisable from a relevant drop of the average curve level for frequency higher than 35 Hz.

- Run 22 (off-road): this FRF curve is related to another off-road test, though, this has been executed with quite high velocity on a particular oath, with really severe ground irregularities, dips, bumps, etc. regarding this test-run the better seat filtering occurs in the frequency range 35-60 Hz. Conversely, the curve is above the 0 dB line for almost all of the range comprised between 0-4.30 Hz, denoting a certain amplification for very low frequency, even without reaching the dB value of the run 20 curve.

- Run 23 (paved): this FRF curve indicates across all the range a moderate filtering capability, in particular, the specific trend stays below the critical threshold for almost all the range between 6.30-80 Hz, while for lower frequencies the line is oscillating between the amplification and attenuation zones, remaining quite close to the 0 dB line, reaching a maximum of 3.16 dB at 3.80 Hz. On the other hand, a filtering deficiency is noticeable in the abscissa position corresponding to 36 Hz, where an amplification of 2.64 dB takes place.

- Run 24 (paved): this curve concerns one of the most challenging condition encountered during the tests, the relatively high speed adopted in this bumps sequence scenario is well notified by the an FRF curve that denotes significant criticalities across the 38-43 Hz range, where several amplification peaks are observable, with a maximum of about 6.5 dB at 39.60 Hz; while for frequency higher than 50 Hz the filtering trend is comparable to the others. Furthermore, considering the low frequency, amplification crests are recognisable in correspondence of 2-3 Hz, 7 Hz and 14.5 Hz.

- Run 25 (bump sequence): the considered FRF trend dose not presents any observable amplification observable above approx. 8.20 Hz. Actually the filtering behaviour at low frequency is almost the same, in particular, two critical amplification zones are comprised between 1-2.10 Hz and 2.30-4.15 Hz, with a maximum of 4.60 dB at 3 Hz.

- Run 26 (bump sequence): this FRF curve is characterized by a trend not too different from the previous one, indeed, the ground is the same, whereas the speed difference is moderate. The general trend consists in a worse filtering at mid-high frequencies with respect to the run at lower speed; specifically, an amplification peak of 2 dB at 40 Hz is present. Conversely, regarding lower frequency range, the amplification is slightly more limited with respect to the run at lower speed, the most critical zone is located in between 1.50-4.70 Hz, the maximum of 3.40 dB is in correspondence of 3.80 Hz. As a further remark, the range between 0.5-1 Hz, where almost all the runs have an amplification zone, is particularly enhanced in this case, with a very large portion of diagram between the FRF trend and the 0 dB line in comparison with the usual behaviour.
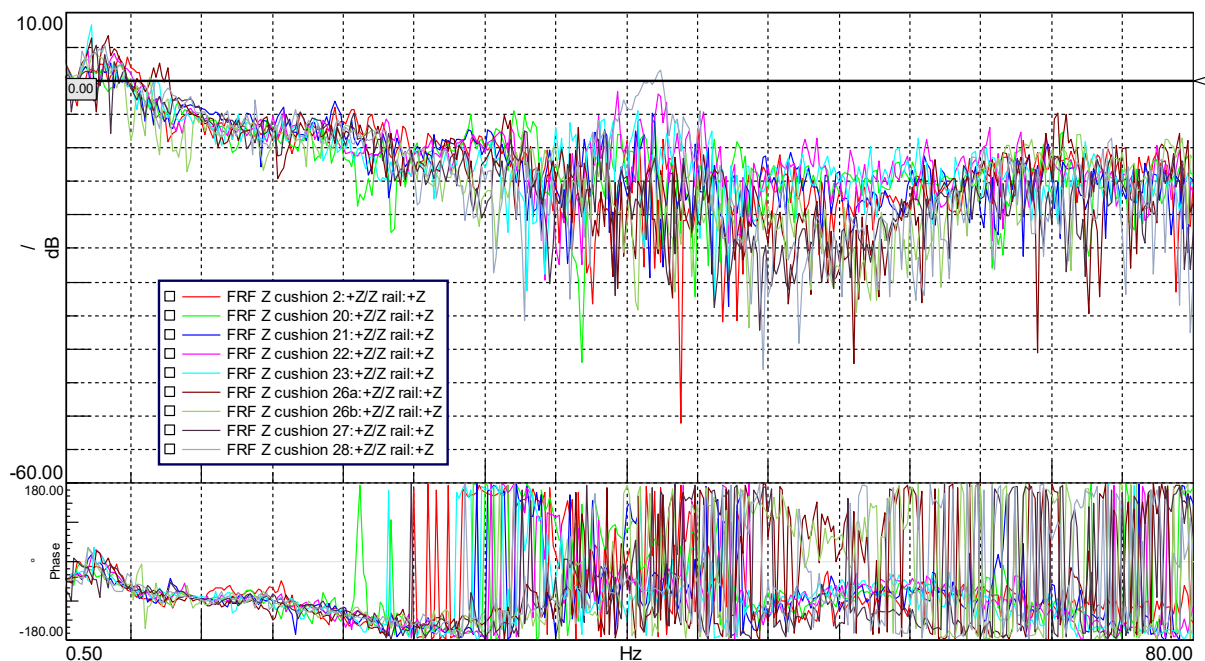
7.4.2 Vehicle B FRF trends
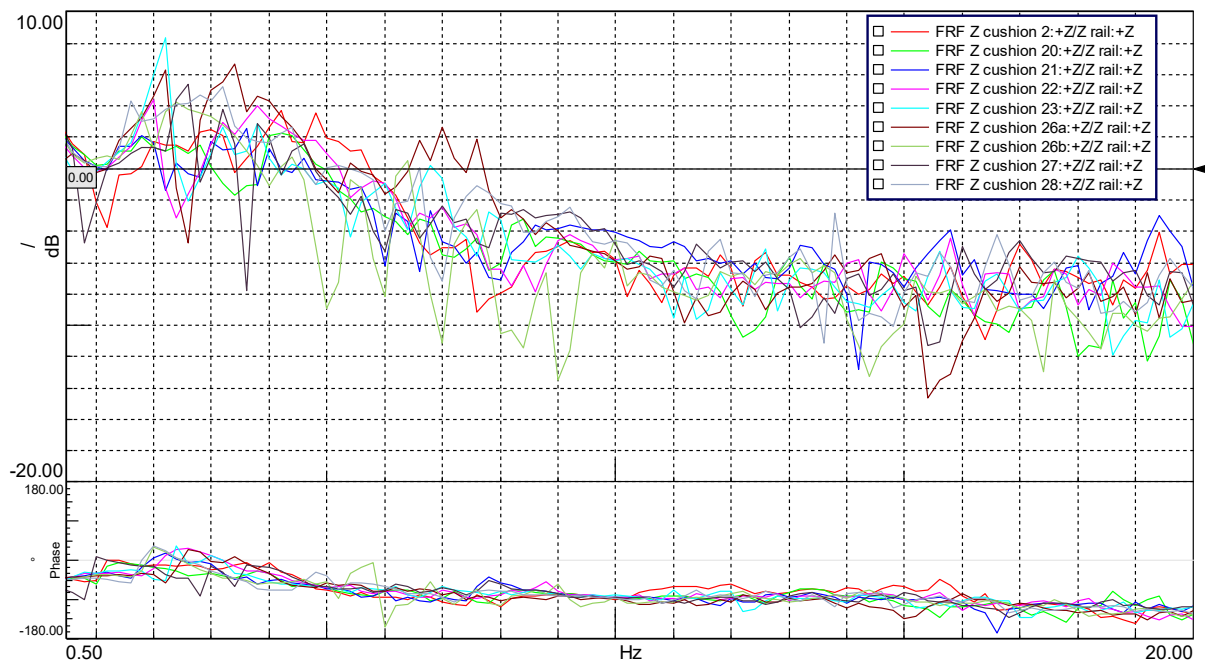

Figure 7.51: Vehicle B runs FRF$_z$ cushion curves.

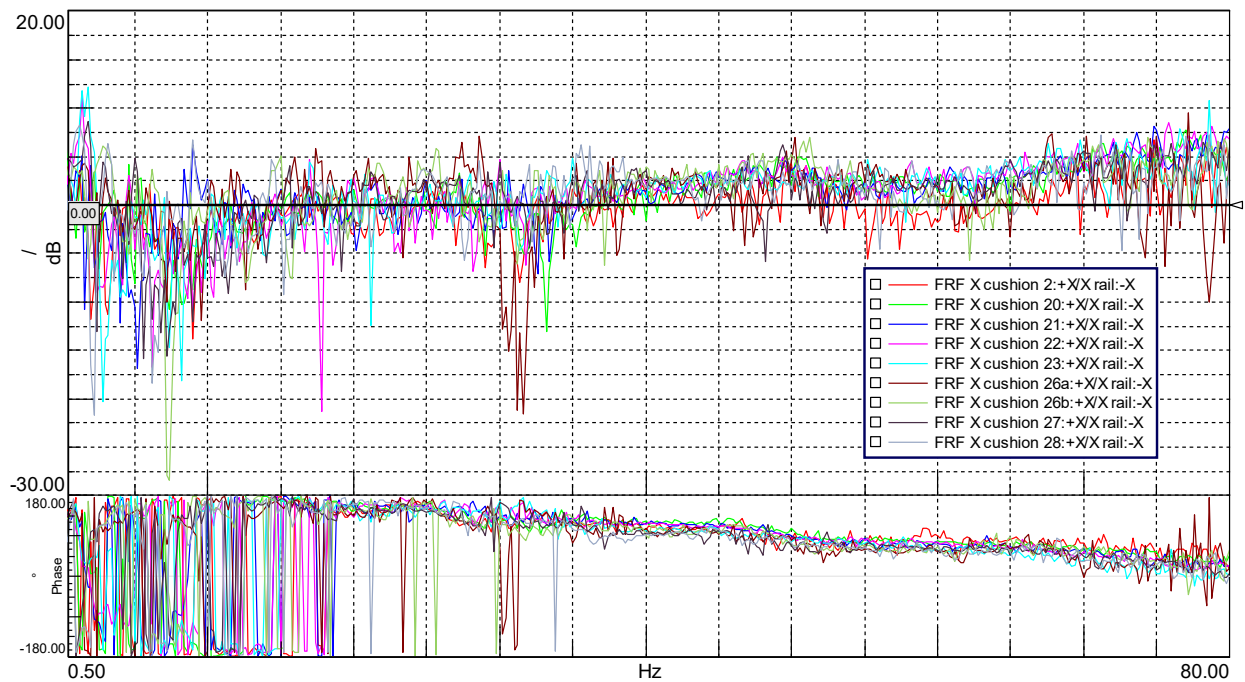**Figure 7.52**: Vehicle B runs FRF$_z$ cushion curves, detail.
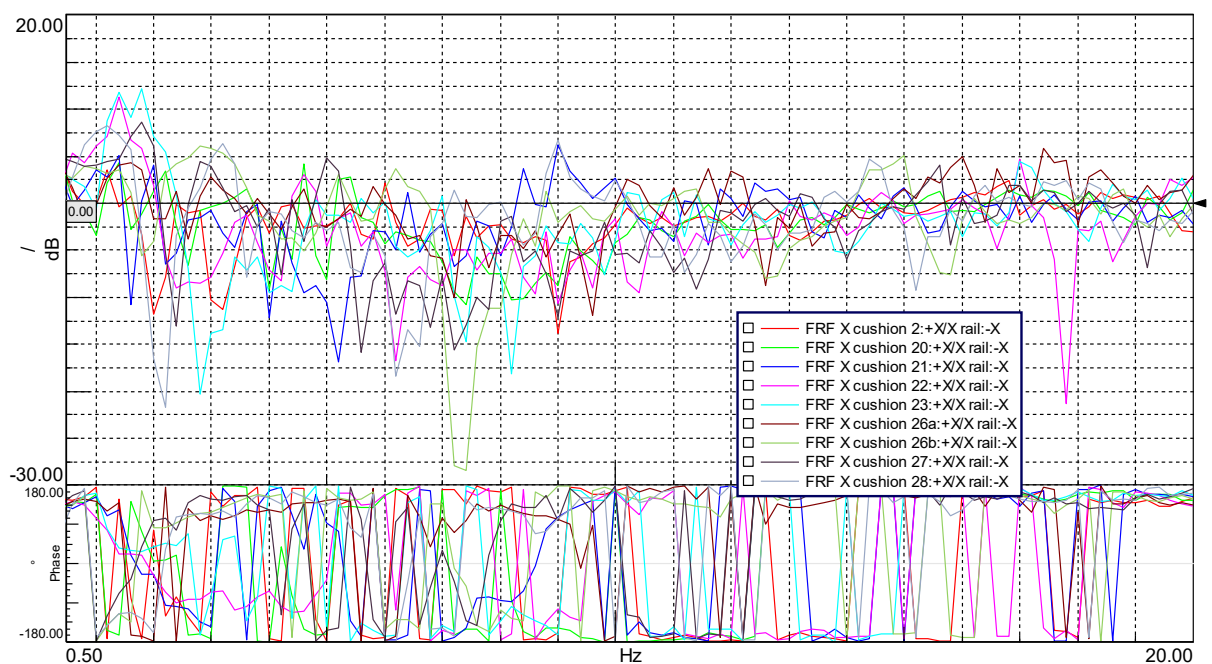
Figure 7.53: Vehicle B runs FRF$_x$ cushion curves.

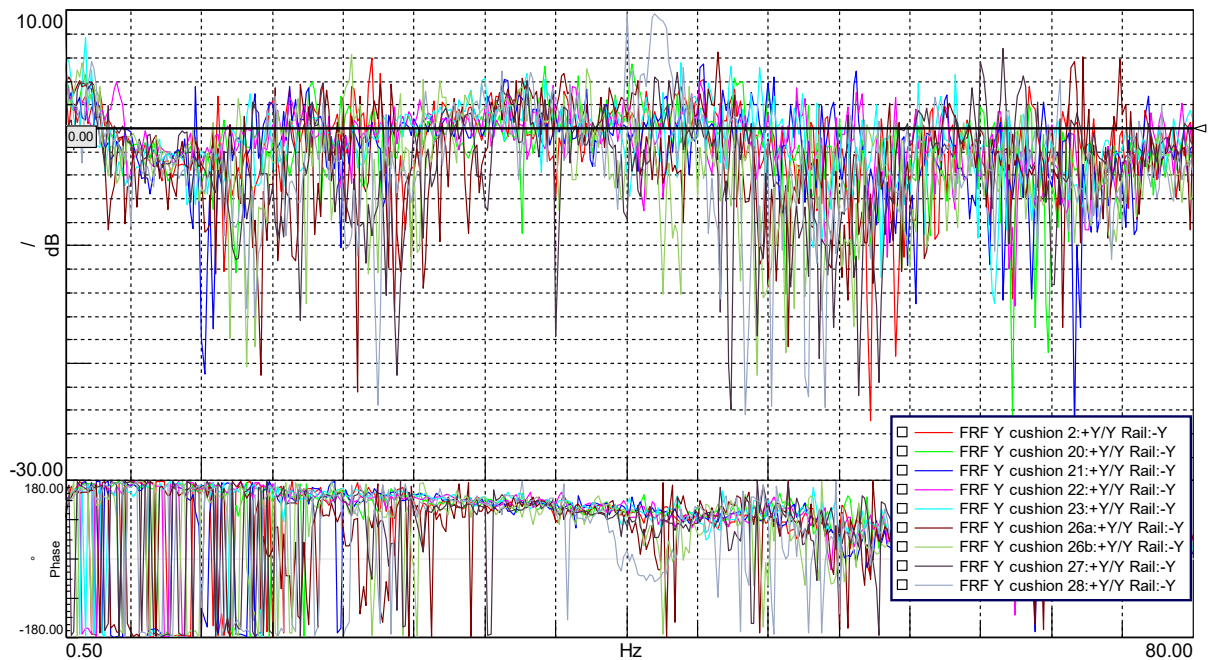**Figure 7.54**: Vehicle B runs FRF$_x$ cushion curves, detail.

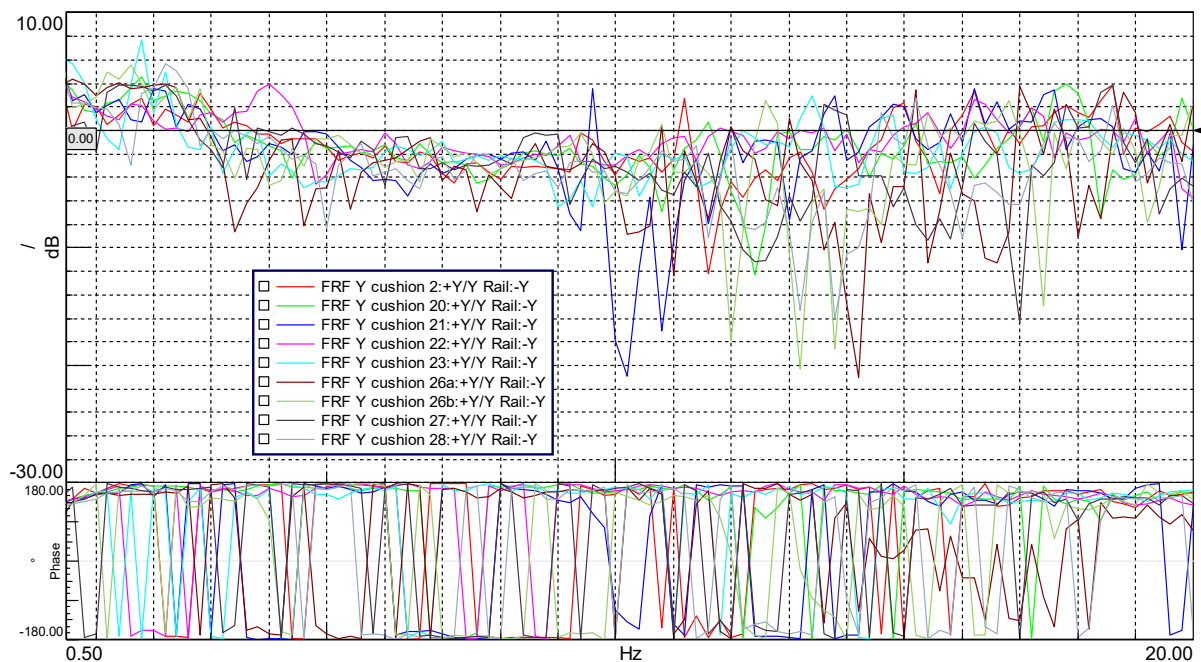**Figure 7.55**: Vehicle B runs FRF$_y$ cushion curves.

Figure 7.56: Vehicle B runs FRF$_y$ cushion curves, detail.

As in the CX-5 case, also for the Panda a brief summary of the different FRF$_Z$ characteristics for every run is included in the following:

- Run 2 (wide bump): this FRF curve shows a significant filtering property of the seat cushion across a wide range, in particularly, for frequencies above 5.75 Hz, no amplification is observable, whereas the contrary occurs between 1.70-5.75 Hz. Still, the maximum level of amplification is limited to about 3.80 dB, at 4.20 and 4.80 Hz.

- Run 20 (off-road): the trend of this FRF is comparable to the average one for most the frequency range. The most noticeable singularity is a negative filtering peak at about 36.80 Hz. At 5 Hz it is possible to observe the 0 dB crossing, whereas the largest amplification zone is comprised in the range 3.90-4.80 Hz, with a maximum of approx. 2.30 dB at 4.20 Hz. In addition, this run shows the most critical amplification behaviour between 0.5-1 Hz in comparison with all the other ones recorded on this vehicle.

- Run 21 (off-road): the general FRF tendency is pretty similar to the previous one, again being on off-road terrain. As a matter of fact, a good filtering is provided across all the mid-frequency range, as above 30 Hz the function tends to oscillate around an attenuation level of -16 dB attenuation line. Regarding lower frequencies, the border line between amplification and attenuation can be observed about 4.70 Hz; most relevant amplification intervals are located between 0.5-1Hz, 1.25-2.10 Hz, 2.85-3.75 Hz, with amplification peaks of 3.65 dB and 2.70 dB sited respectively at 0.20 Hz and 3.60 Hz.

- Run 22 (off-road): considering this FRF curve at a first glance, the most relevant difference in relation with the general tendency of the other ones is a frequency range in which the otherwise appreciable filtering capability is worsened; this is put in evidence by a shortening of the distance between the FRF line and the critical threshold, in particular at 39.40 Hz with a minimum filtering of -1.5 dB, but also at 41, 42.20-42.80, 45.4 Hz. Concerning the lower frequency range, the trend is comparable to a sort of mixed behaviour between run 21 and run 22 FRF; the 0 dB frequency is about 5.20 Hz, most noticeable amplification portions are comprised in the 1.20-2.15 Hz and 2.85-5.20 Hz, with a maximum of 4.60 dB at 2 Hz.

- Run 23 (off-road): considering this FRF curve, it is possible to assess that the filtering of the seat cushion is provided for all the mid-high frequency range; though, also in this case a certain weakening of this capability is observable within the 35-46 Hz range, even if the minimum filtering of -4.40 dB at 40.80 Hz is less critical than the corresponding minimum values of attenuation founded in the run 22 analysis. Considering lower frequencies, the FRF curve denotes a behaviour comparable to the run 22 FRF as far as amplification zones are concerned, but a more pronounced maximum peak of about 8.5 dB at 2.20 Hz is encountered in this case, representing the highest of all the tests considered, together with the largest amplification zone in the 0-0.60 Hz range is present. The critical frequency seems to be located at 4.50 Hz, but at 6.80 Hz a quick worsening of attenuation is put in evidence by the FRF curve trespassing of the 0 dB line by a poorly perceptible amount.

- Run 26a (bump sequence): this FRF curve denotes an attenuation field across all the mid-high frequency range, with local weakening of the filtering capability at 31 Hz and 70-71 Hz. For frequency higher than 7.70 Hz, no amplification phenomena are detected. In particular, most relevant intervals of amplification zones are within 1.20-2.40 Hz, 2.70-4.80 Hz and on a smaller scale 6.40-7.70 Hz.

- Run 26b (bump sequence): compared to the others, this FRF curve, as the other relative to other bumps sequences, indicates a good attenuation along almost all the frequency range. Moreover, considering also the previous run FRF, in both cases the range 55-61 Hz seems to be host the most effective attenuation capability zone. On the other hand, the only relevant amplification zones are present within 0.20 Hz and 4.50 Hz, with a maximum level of about 4.50 dB at 2.40 Hz, whereas above 6.42 Hz there is no more trespassing of the critical threshold .

- Run 27 (paved): this roughly paved road test FRF curve shows a trend comparable to the generic average tendency, with appreciable attenuation for almost all the frequency range with some amplification phenomena lower frequencies. Significant amplification zones are observable in the band 0-0.65 Hz, 1.20-2.80 Hz, 2.90-3.45 Hz, 3.75-4.15 Hz. Furthermore, the threshold frequency for the low pass filter can be defined to be 4.80 Hz.

- Run 28 (paved): the FRF of this test, performed in conditions of paved road similar to the ones of the previous run, indicates a severe filtering deficiency within the mid frequency range, especially between 40 Hz and 45 Hz, indeed, amplification up to 1.25 dB is encountered in the 42-42.55 Hz range, whereas an attenuation weakening is put in evidence by a peak at 13.80 Hz. Taking into account these exceptions, a conservative position for threshold ì frequency may be defined around 6.60 Hz, over which the general FRF trend stays always below the 0 dB line. In the low frequency range, instead, important amplification regions are observed within 1-4.60 Hz, with a maximum of approx.. 1.85 dB at 3.20 Hz.

Having at disposal a relevant number of functions for each car, the subsequent step consisted in performing an average FRF computation, to obtain a comprehensive FRF_Z mean for both the two vehicles, considering off-road and paved road runs (Figures 7.57–7.68). FRF means have been calculated also for X and Y axes for sake of completeness. though, the focus remains on comparing the FRF_Z curves.
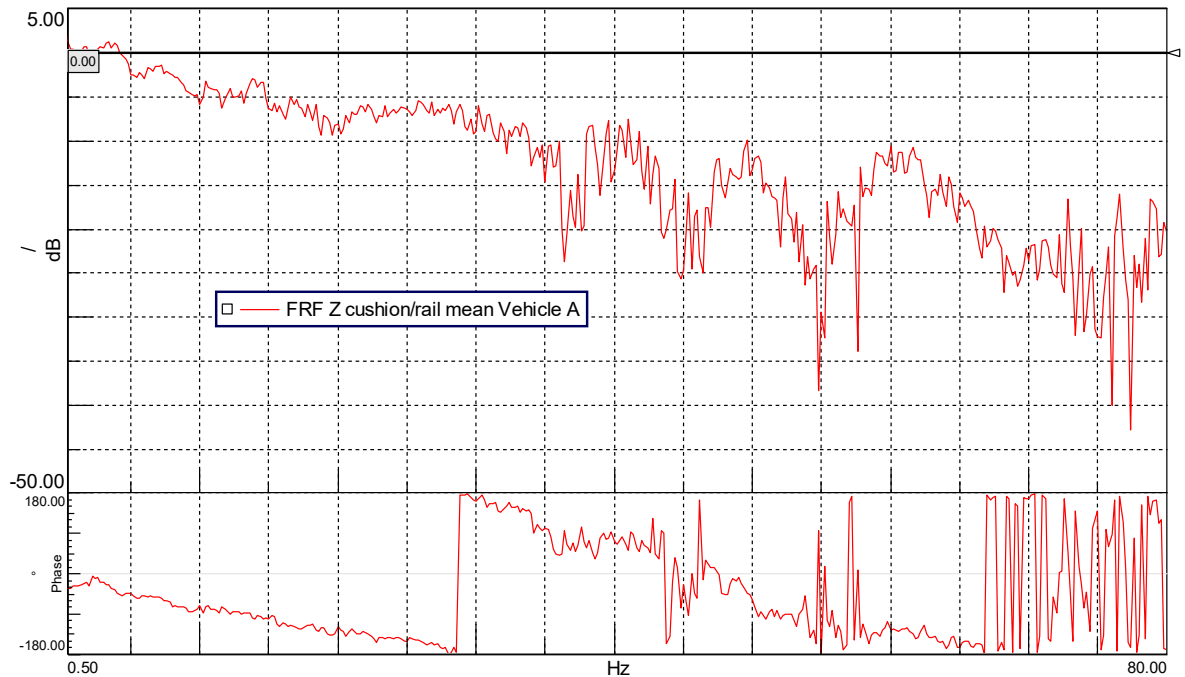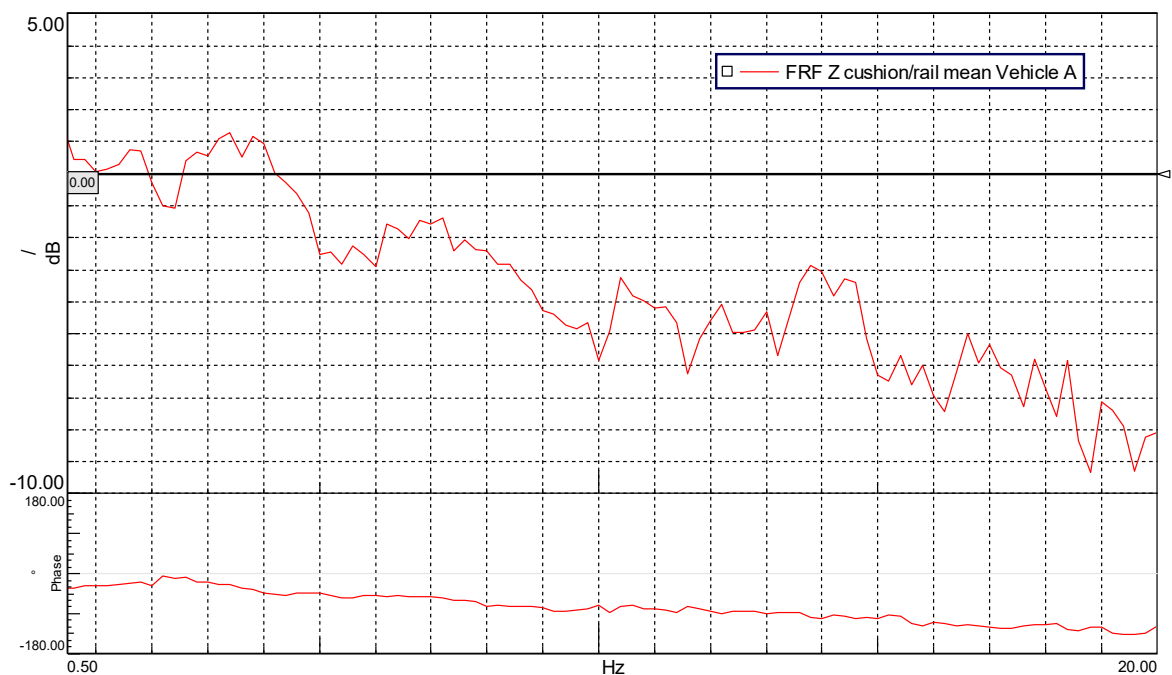

Figure 7.57: Vehicle A FRFz cushion mean curve.

Figure 7.58: Vehicle A FRFz cushion mean curve, detail.
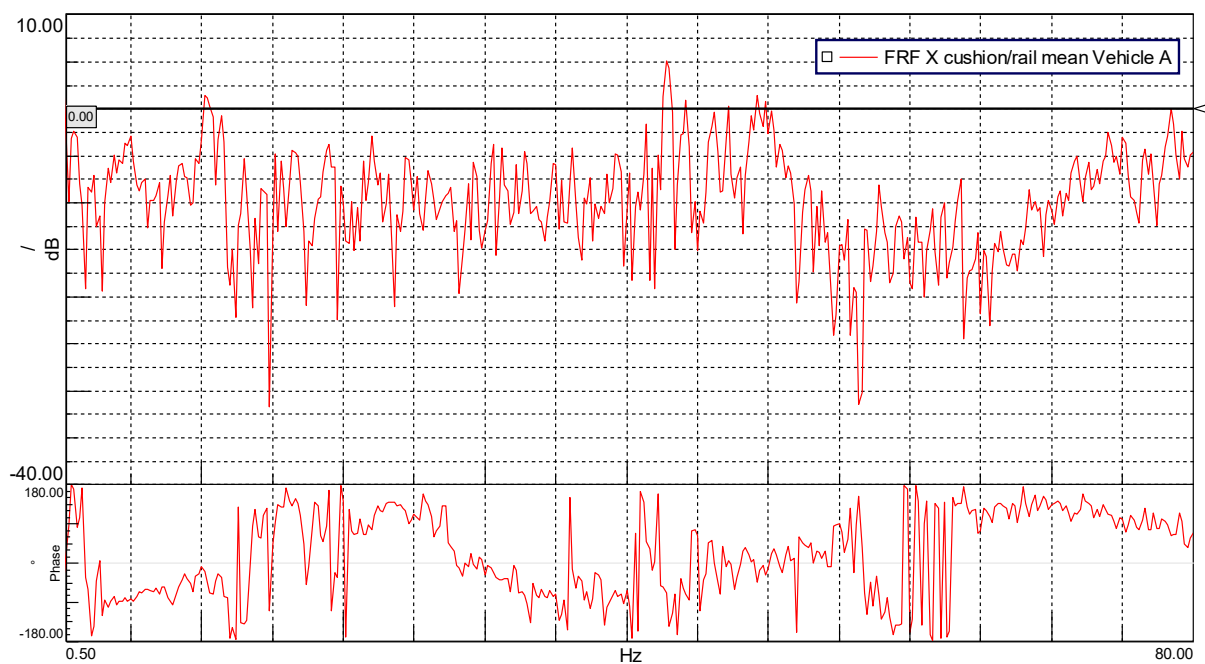
Figure 7.59: Vehicle A FRFx cushion mean curve.
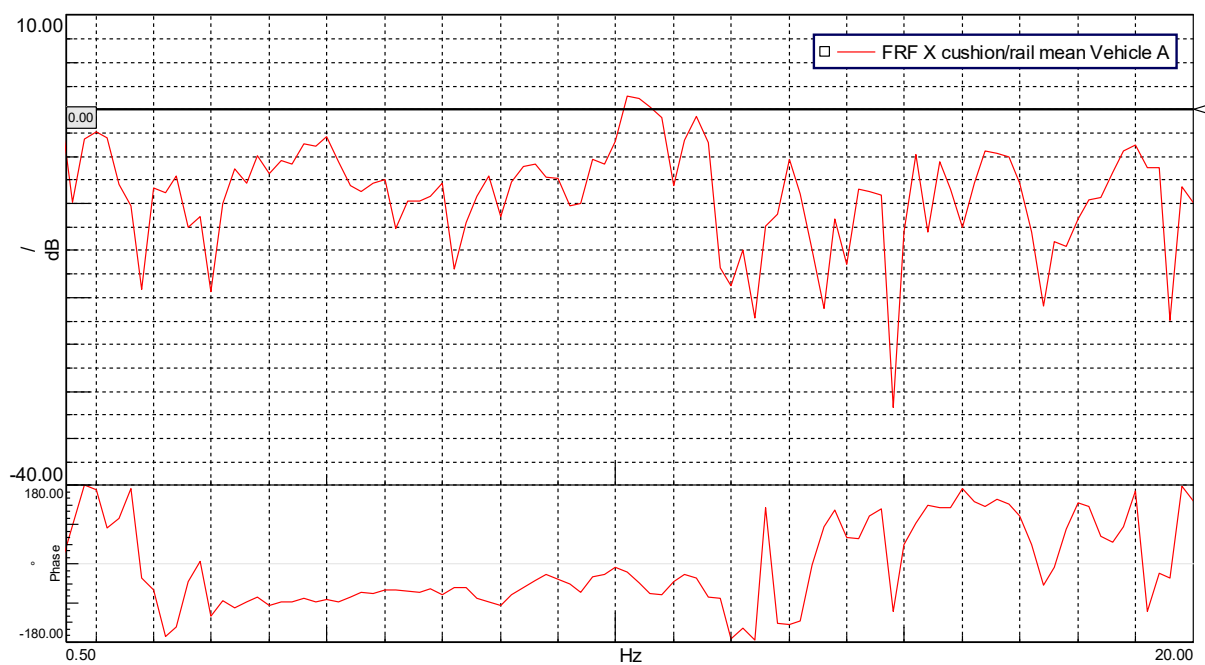
Figure 7.60: Vehicle A FRFx cushion mean curve, detail.
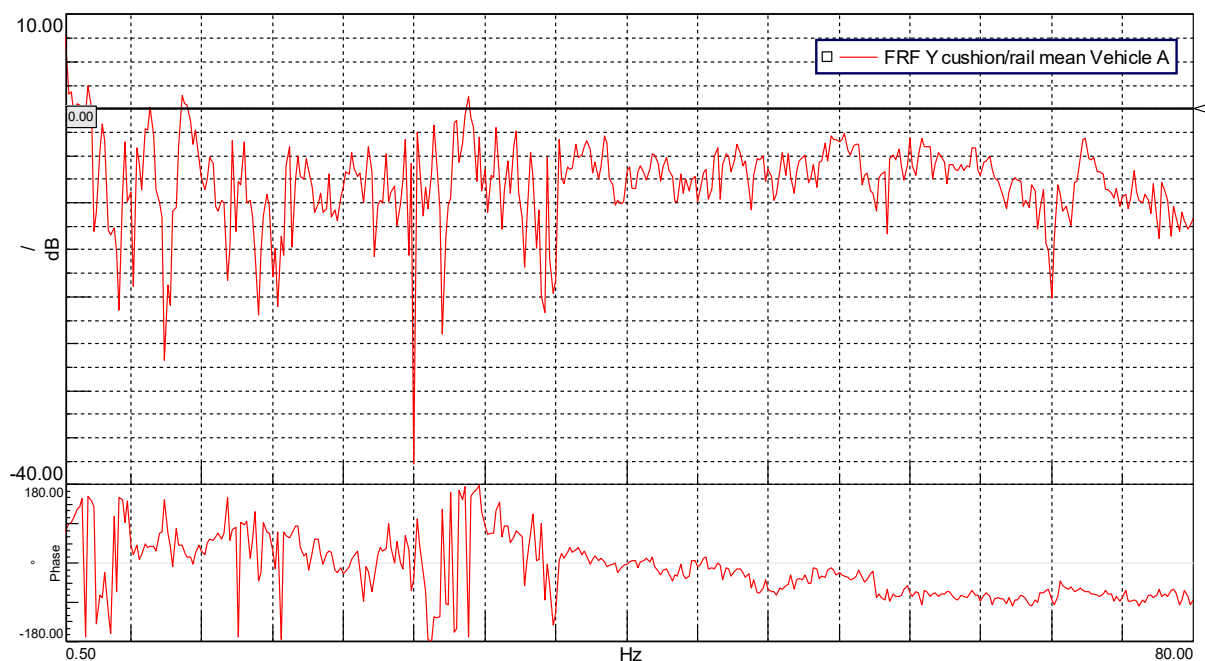
Figure 7.61: Vehicle A FRFy cushion mean curve.
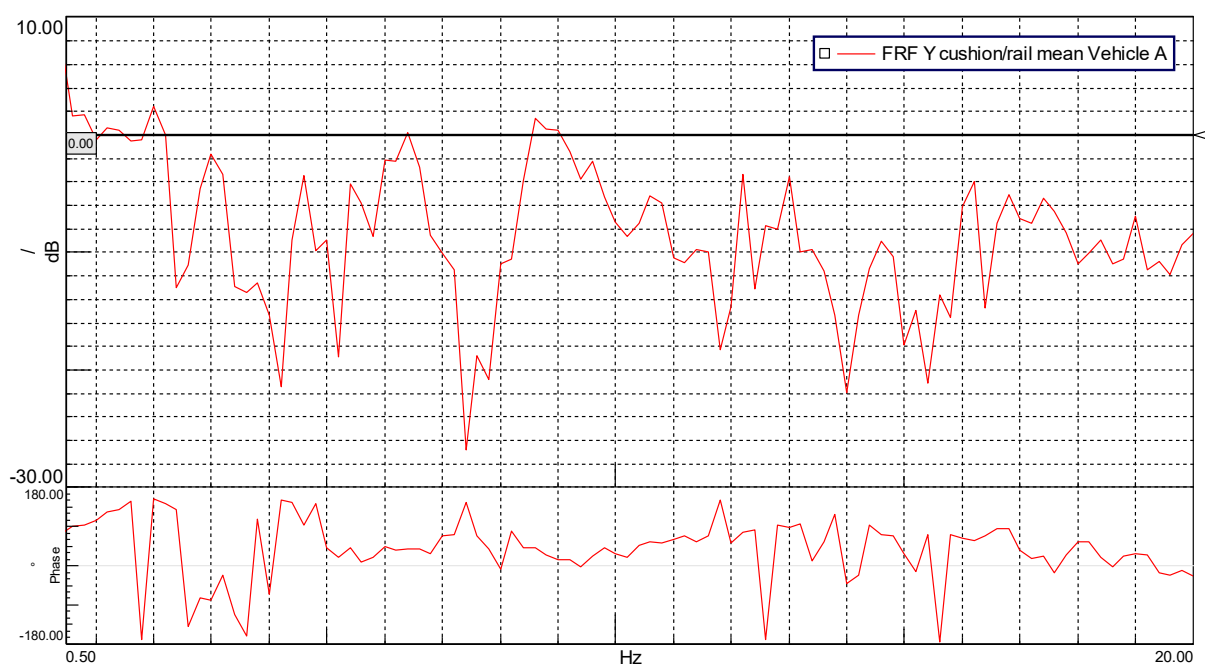
Figure 7.62: Vehicle A FRFy cushion mean curve, detail.
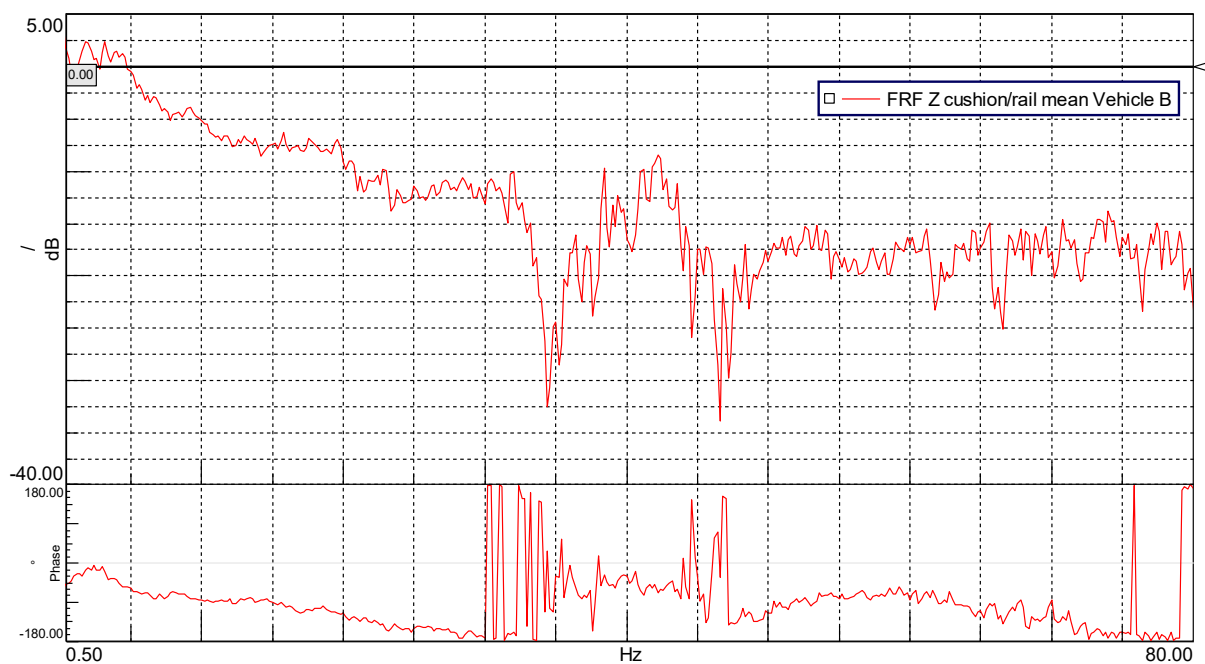
Figure 7.63: Vehicle B FRFz cushion mean curve.
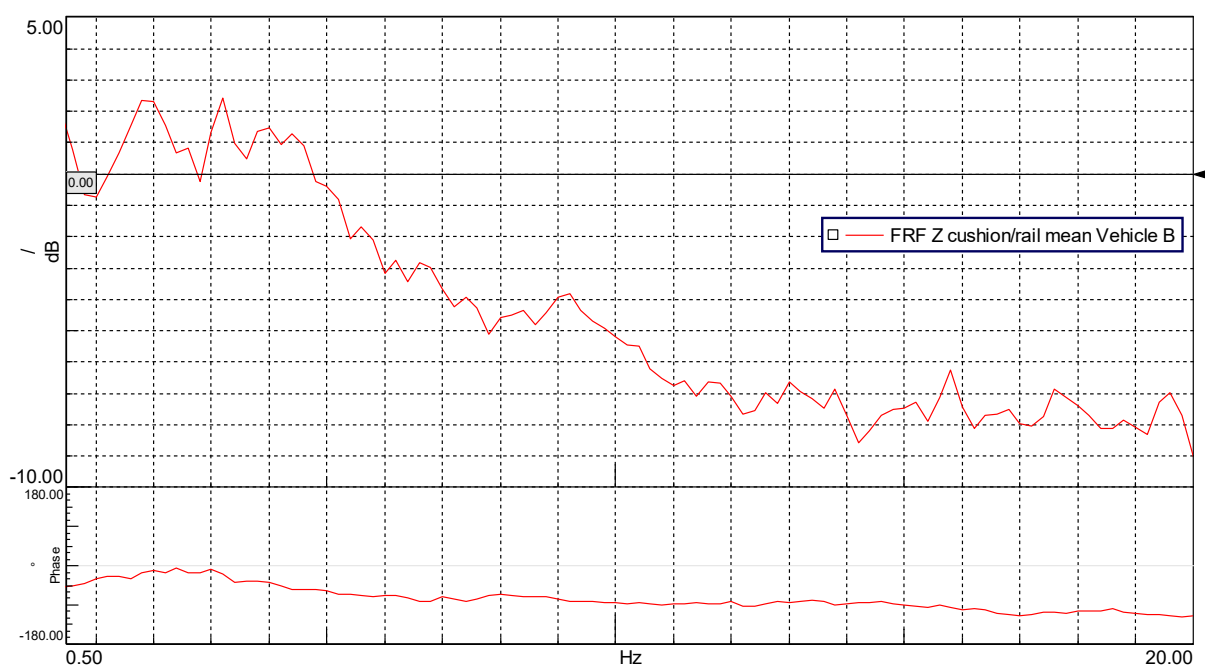
Figure 7.64: Vehicle B FRFz cushion mean curve, detail.
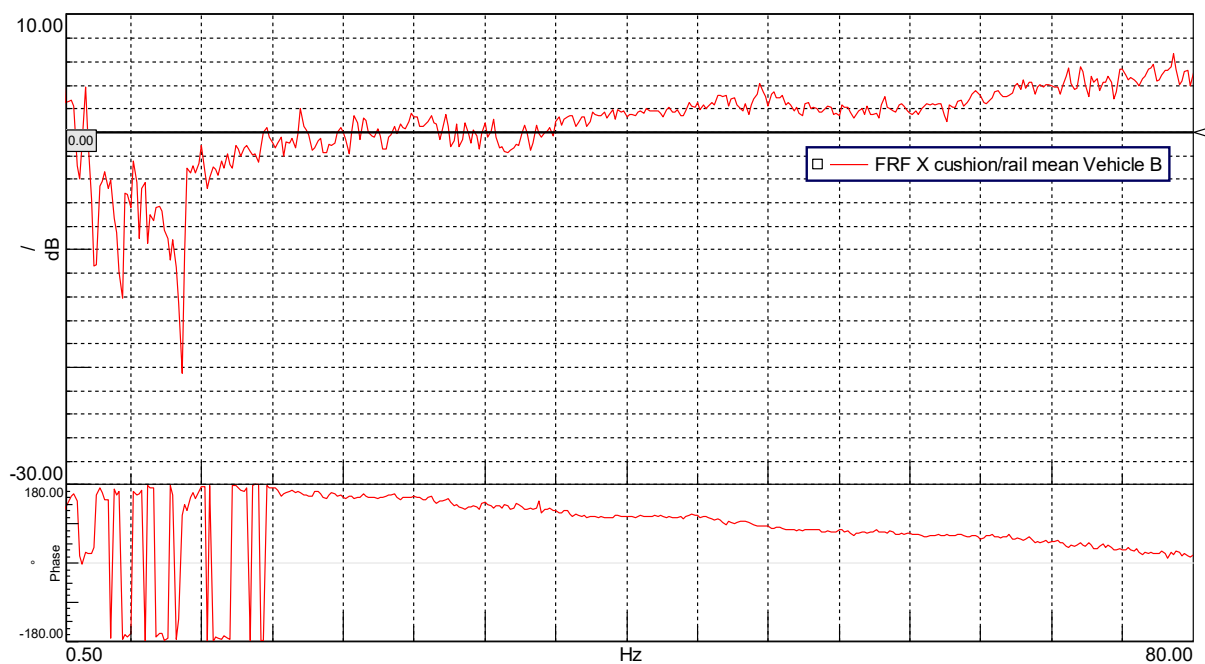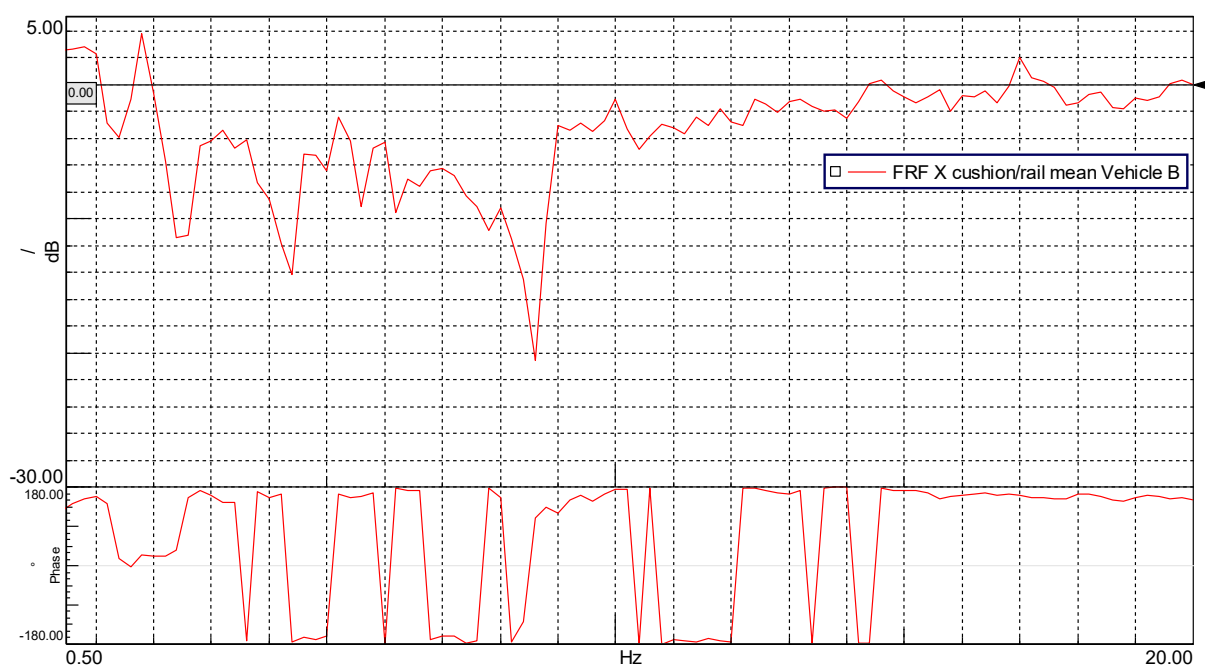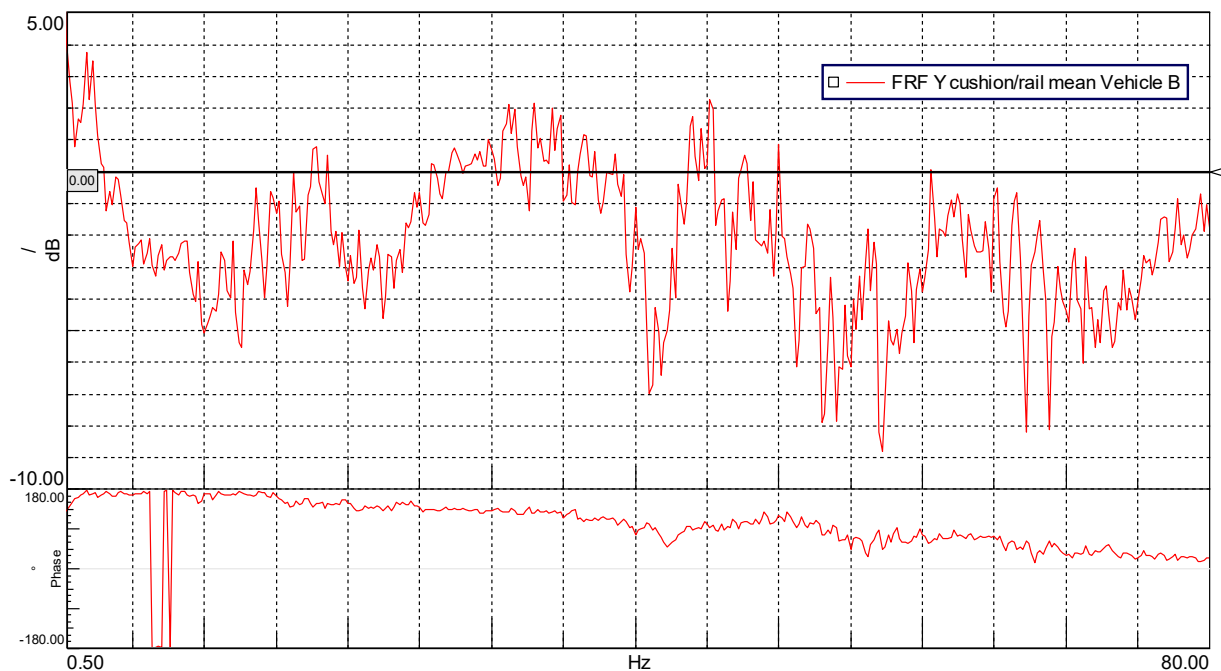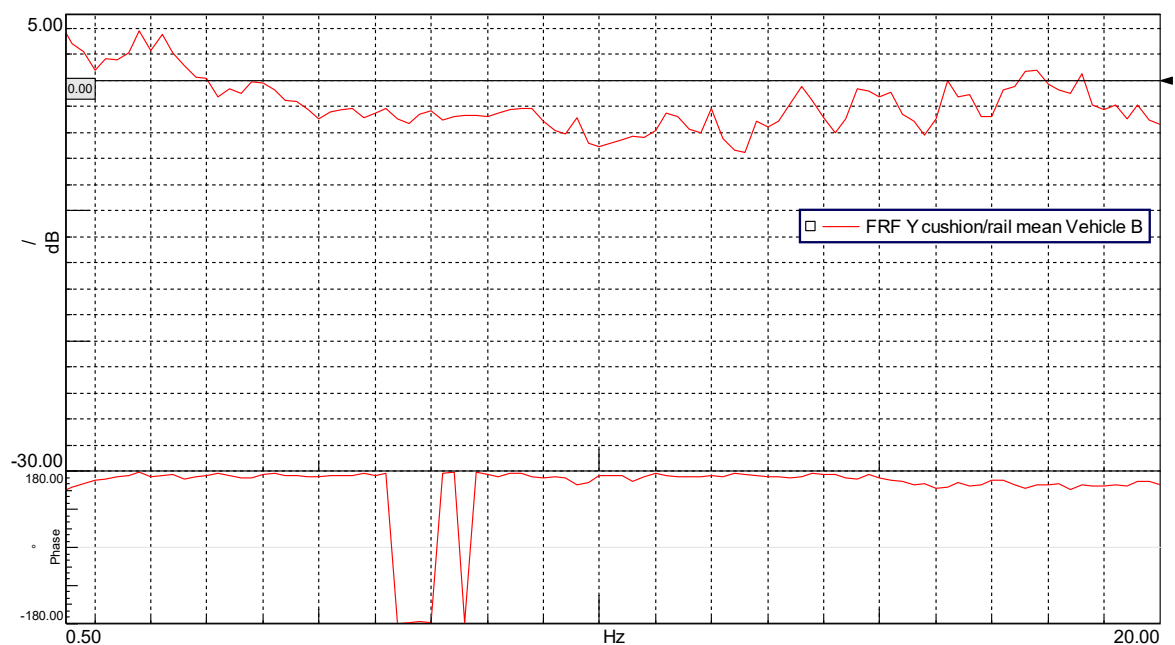
Figure 7.65: Vehicle B FRFx cushion mean curve.

Figure 7.66: Vehicle B FRFx cushion mean curve, detail.

Figure 7.67: Vehicle B FRFy cushion mean curve.

Figure 7.68: Vehicle B FRFy cushion mean curve, detail.

From the graphs and the data analyzed in this part, some general considerations on the comparison between vehicle A and vehicle B FRF_z are drawn, in order to provide a wide glance on their similarities and differences in relation to the seat transmissibility functions, focusing on the means computed with LMS Test.Lab.

Figure 7.69 depicts the comparison between the specific vehicle FRF means in the range 0.5 – 80 Hz, while Figure 7.70 illustrates in a more detailed way the functions trend across the interval 0.5 – 20 Hz.
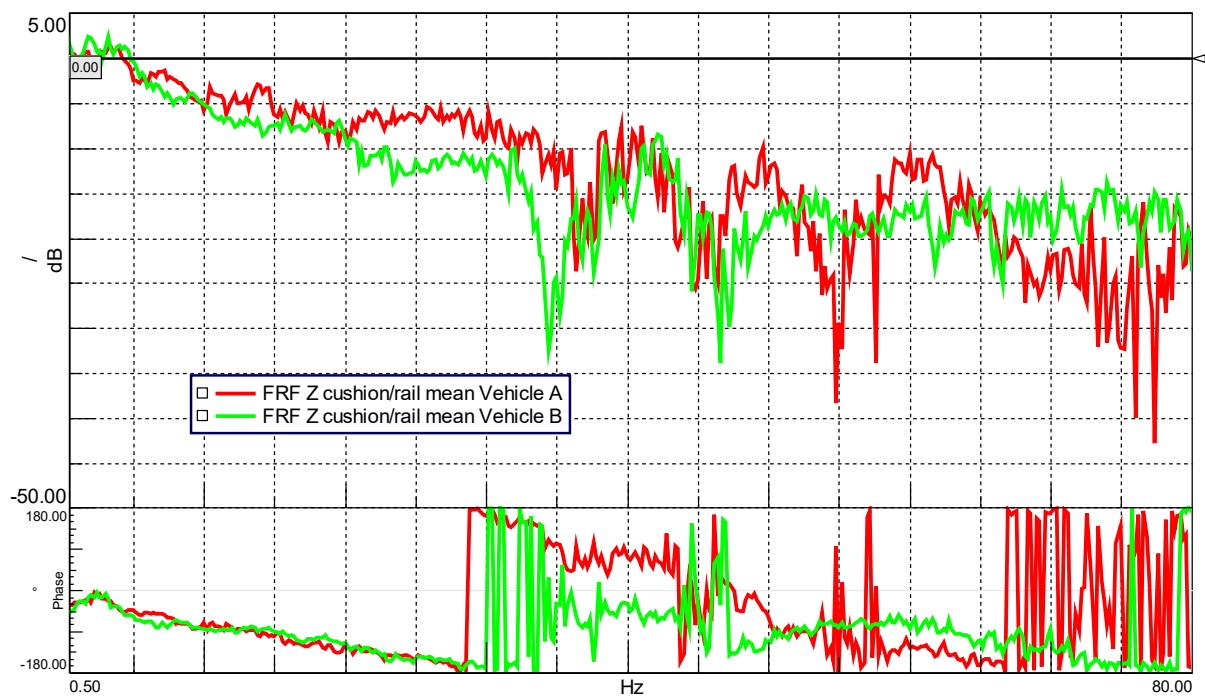

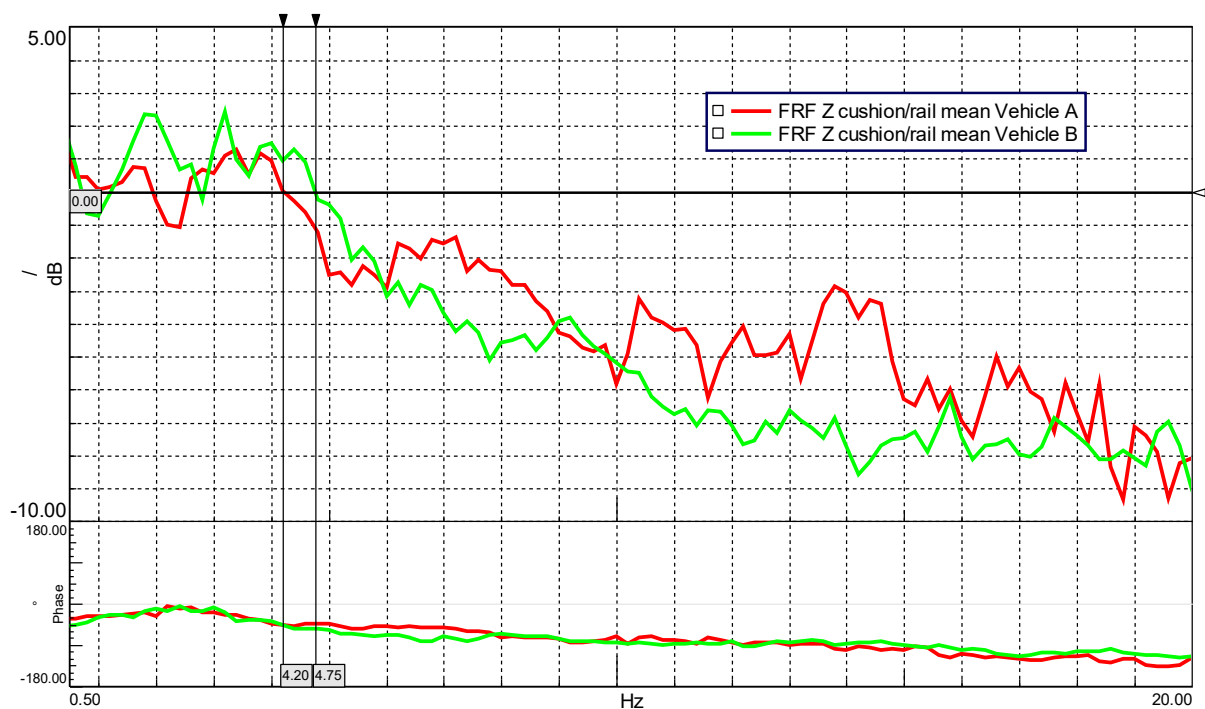**Figure 7.69**: FRF$_z$ mean trends comparison.

Figure 7.70: FRF$_z$ mean trends comparison, detail.

Comparing the mean FRF_Z of the two adopted vehicles, the first thing to be put in evidence is the divergence concerning the FRF trend as the frequency grows up.

Considering the detail view, the critical frequency for the low pass filter can be defined as 4.20 Hz for vehicle A and 4.75 Hz for vehicle B.

Above these value, the corresponding functions tend to stay below the critical threshold till the highest frequency considered, 80 Hz.

Generally, at lower frequencies, both the FRF curves denote some amplification zones, vehicle B behaviour is globally worse within 1.30-4.80 Hz, the respective maximum values are about 2.25 dB and 2.60 dB, whereas in the 0.5-1.30 Hz range the filtering/attenuation characteristics seem to better than vehicle A ones.

Concerning higher frequencies, instead, the overall tendency for the seat cushion/seat rail FRF along the Z axis appear to be better for vehicle B.

This is likely due to higher softness of its seat cushion, which, despite possibly penalizing comfort at lower frequencies, succeeds in attenuating more effectively the higher frequency excitation, even though an opposite situation is spotted above 66 Hz, up to 80 Hz, possibly indicating the vehicle A cushion seat capable of a superior isolation regarding the highest frequency field considered in the FRF analysis.

As a further remark, best attenuation peaks achieved in vehicle B case are located at about 34.5 Hz and 46.5 Hz, with relative values of -33 dB and -34 dB; while in vehicle A they are present at frequencies of 55, 76, 77.5 Hz with values of -38.5 dB -40 dB and -42.5 dB respectively.

8 Psychoacoustics analysis results

As far as the psychoacoustics parameters are concerned, the project focused on collecting the related data by exploiting the binaural headset and elaborating the graphs indicating the general trend and level of the several acoustics entities considered.

In particular, working with the Sound Diagnosis tool, the diagrams reporting the different curves for both cars have been saved, in order to make a closer comparison by plotting the level functions for selected test runs. Also in this case, specific options have been selected in the Time Data Processing worksheet to obtain the desired results.

- Channel processing data
    - Function: Spectrum;
    - Window: Hanning;

- Acquisition parameters
    - Measurement mode: Tracked;
    - Method: Time;
    - Duration: 20 s;
    - Increment: 0.5 s (sound metrics), 0.05 s (colour maps);
    - Bandwidth: 20480 Hz:
    - Resolution: 0.5 Hz;
    - Spectral lines: 40960;
    - Frame size: 2.0 s.

Most of graphs presented in the following depicts the functions trend of the considered vehicles in direct comparison, thus, the data in the upper part of the legends always refer to vehicle A, while the data in the lower part of the legend are related to the vehicle B.
The main indexed analysed include:

- Articulation Index;
- Loudness Zwicker (ISO 523B);
- Roughness;
- Sharpness (Diffuse Field);

A quick summary to recall the various runs considered for this psychoacoustics assessment is reported in Table 8.1.

Table 8.1: List of considered tests in psychoacoustics assessment.

Vehicle A	Vehicle B
PSYCHOACOUSTICS STUDY TESTS	
Run 4 urban road 40 km/h	Run 4 urban road 40 km/h
Run 5 urban road 70 km/h	Run 5 urban road 70 km/h
Run 7 run up 70-120 km/h	Run 7 run up 70-120 km/h
Run 12 extra-urban mixed tarmac 70 km/h	Run 16 extra-urban mixed tarmac 70 km/h
Run 14 run up 70-110 km/h	Run 15 run up 70-110 km/h
Run 15 up-hill road trait 80 km/h	Run 14 up-hill road trait 80 km/h
Run 16 Racconigi road course 60 km/h	Run 19 Racconigi road course 60 km/h
Run 18 run up 50-130 km/h	Run 17 run up 50-130 km/h
Run 24 paved urban road 30 km/h	Run 29 paved urban road 30 km/h

As a relevant remark, it is worth of notice that, due to the frequent disturbs produced by vocal naming of the several runs to get an ordered list for working at the start of the recording, the different pictures provided often show an abscissa axis not starting from 0 seconds, but from a subsequent time instant, in which no more vocal speech affected the sound recording performance. In addition, looking at the following graphs, particularly important is the difference between the two cars in relation to their gear-shift concept.

Furthermore, it is worth of notice that, due to equipment limitations, the several acceleration run-up tests would have been better performed and presented as function of vehicle speed instead of time, as it is; therefore, on equal time, the tests executed on vehicle A, which has at disposal a higher engine power, will probably lead to higher accelerations and thus higher speeds with respect to vehicle B ones. Because of these constraints, the comparison between the two cars is not to be considered as a scientifically accurate statement, but may serve as a purely indicative source of information on the generic psychoacoustic characteristics.

In Figures 8.1 – 8.9 articulation index function curves are illustrated.
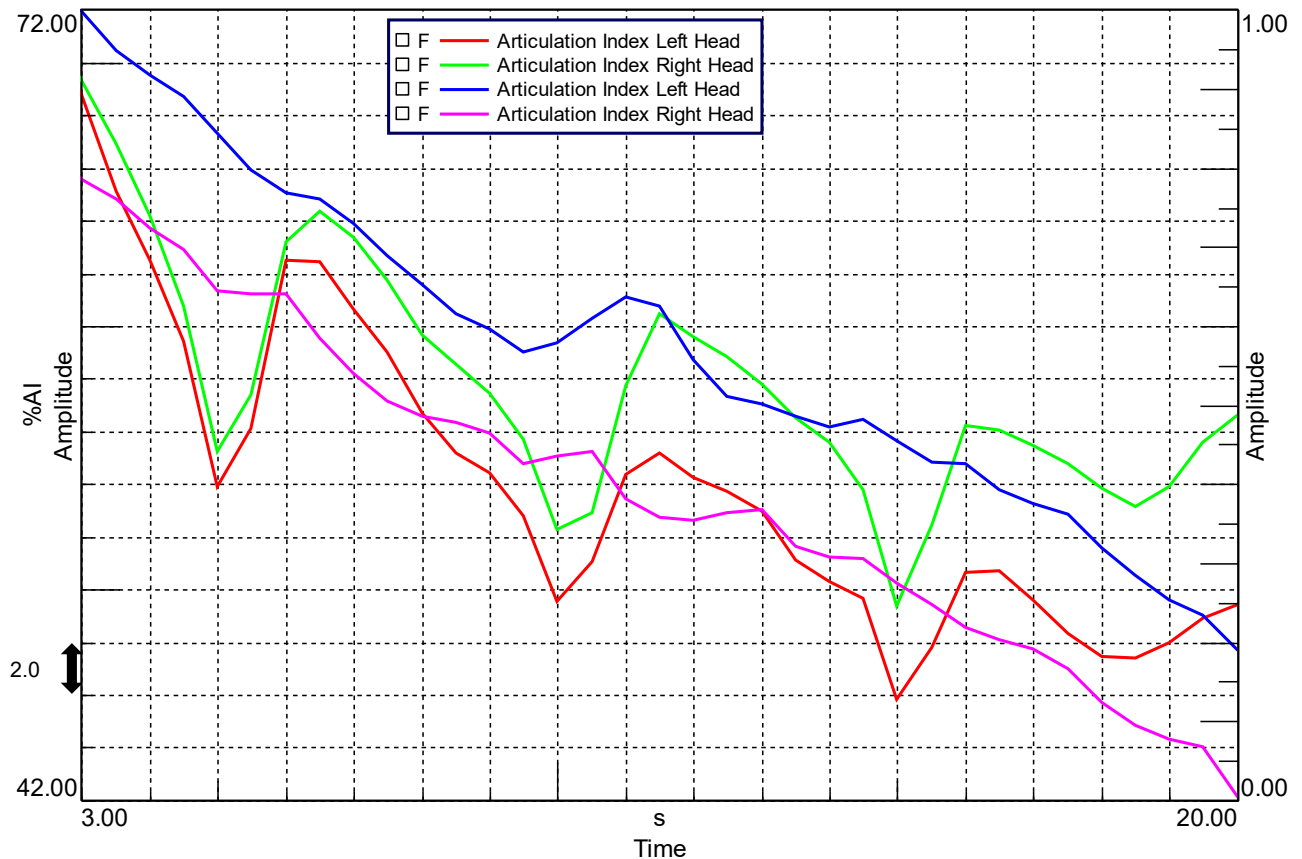
8.1 Articulation index trends

Figure 8.1: Articulation index, run 18/17, run up 50-130 km/h.

Looking at this figure, vehicle A curves have a more oscillating trend, likely due to the manual shifts mode enabled during the acceleration, with the clicks of the gear stick that contributed to the overall AI. Anyway, the two vehicles have similar behaviours in this regard, the range of AI being comprised between 72% and 42% in the vehicle B, while the vehicle A interval is smaller, between approximately 69% and 50%.

The results are in line with the prevision, as at higher speeds, the contribution of wind and rolling resistance noise due to reduced insulation and aerodynamic characteristic is far more noisy on the vehicle B with respect to the vehicle A, while the engine contribution of the former is quite limited, whereas the diesel engine of the latter has a more significant influence.
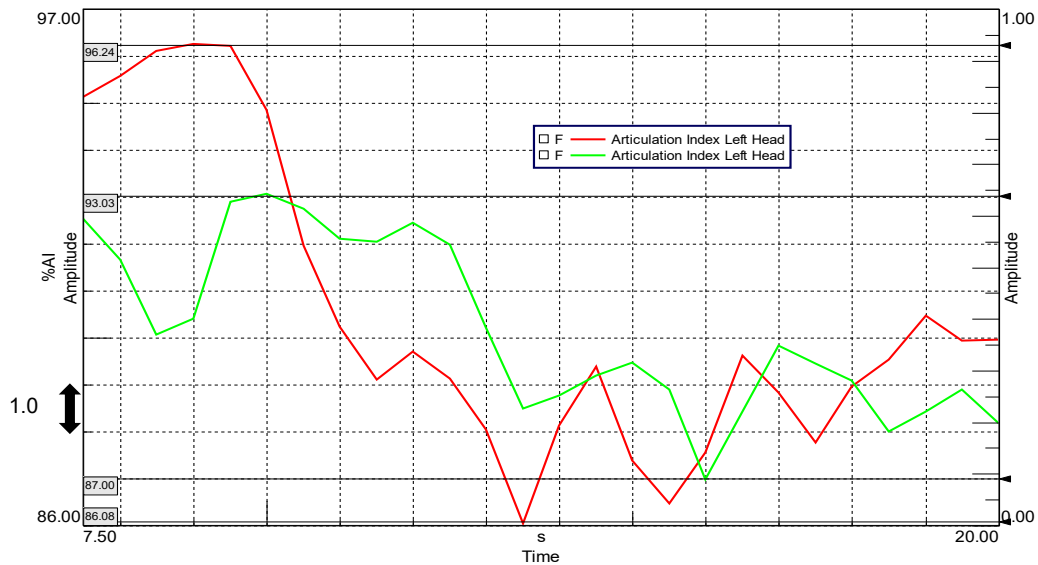
Figure 8.2: Articulation index, run 4 urban road 40 km/h.

In this graph, t vehicle A curve is more subject to deviations, as from seconds 8-10 a relatively smooth road and good environmental conditions have been spotted; subsequently, road irregularity disturbs and a defined acceleration noise, due to the traffic conditions, affected severely the articulation index trend, with a relevant drop. Still the final AI value is higher than in vehicle B, the two ranges being comprised between 96% and 86% for the former and between 93% and 87% for the latter.
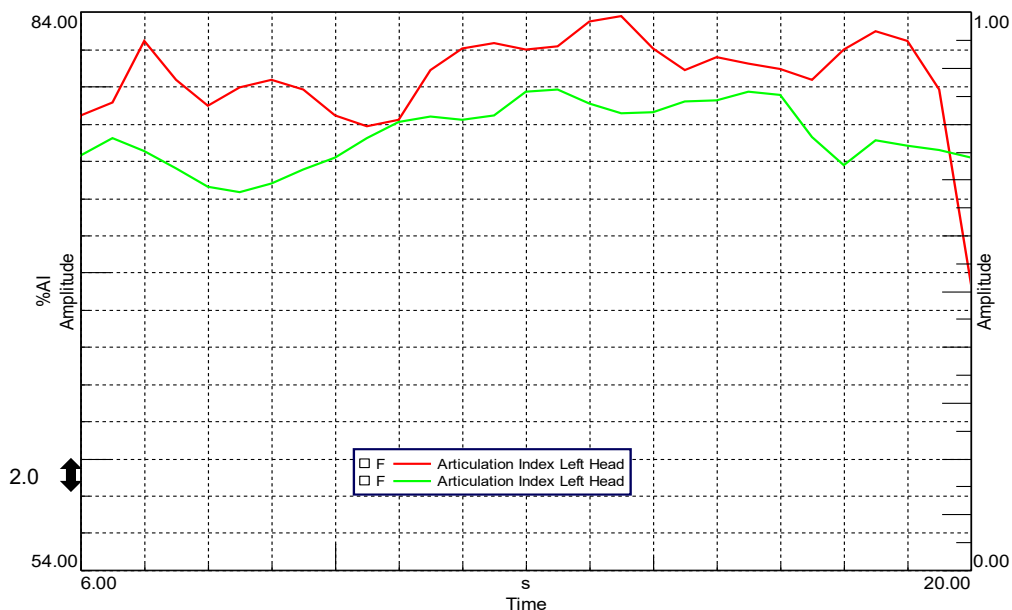
Figure 8.3: Articulation index, run 5 urban road 70 km/h.

The curves are quite similar for the two cases, vehicle A A.I. remains at a higher level for almost all the test duration, around the 80% region, even though in the final part it drops down to 69%; while in vehicle B the value is generally lower to then stabilize at about 76 %
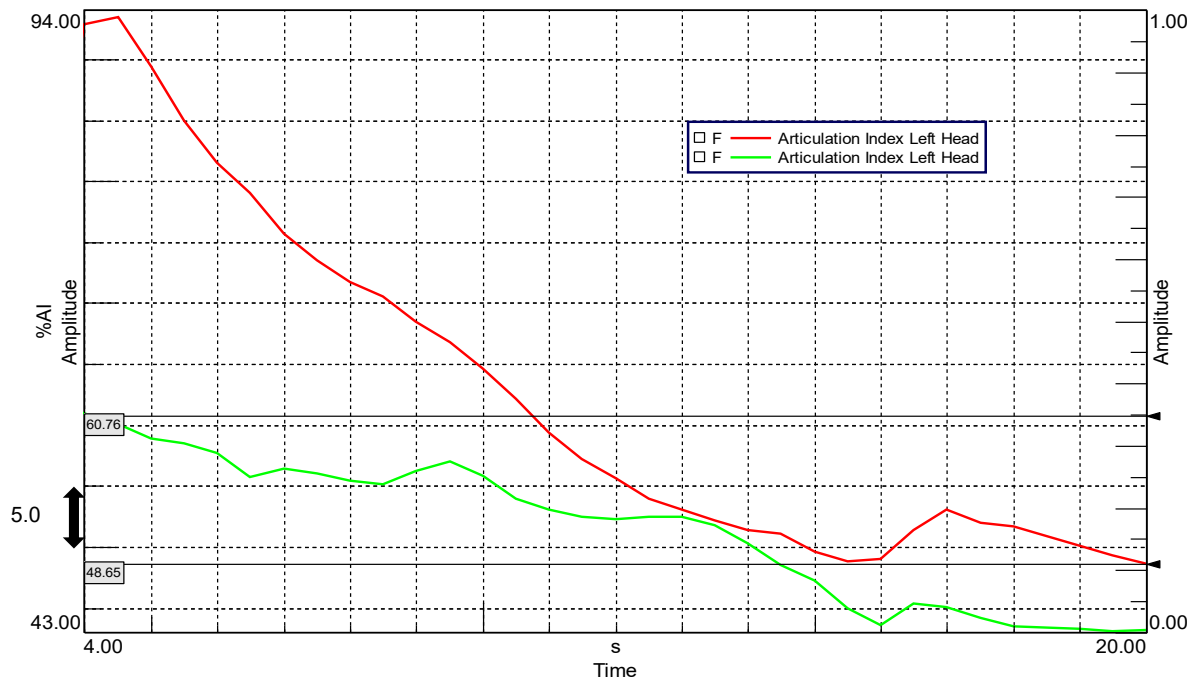
Figure 8.4: Articulation index, run 7 run up 70-120 km/h.

In the first part, the values highly differ one another, vehicle A reaching a maximum of about 93%, whereas vehicle B is more near the 60% region; then, as the acceleration grows up, the former value drops rapidly, setting at 48% in the last part, whereas the latter curve goes down smoothly, stabilizing at 43% in the last seconds.
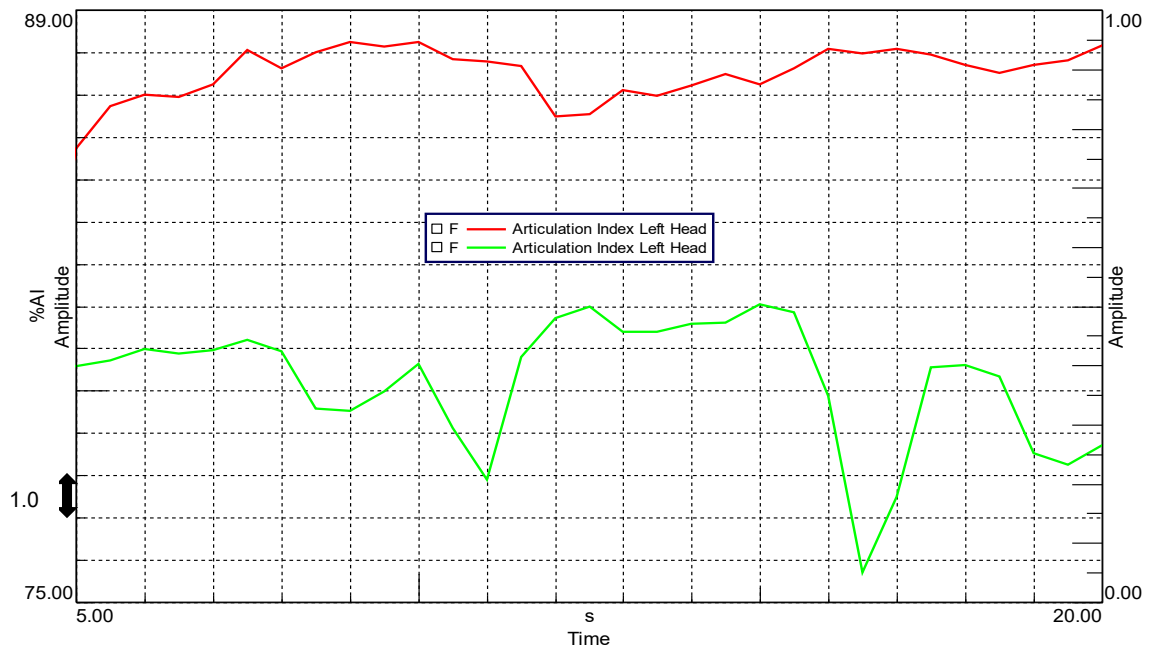

Figure 8.5: Articulation index, run 16/19 Racconigi main road course 60 km/h.

Vehicle A A.I. remains significantly higher for all the test duration, near the 87-88%, whereas vehicle B A.I. is more irregular, on a lower level ranging from 76-80%.
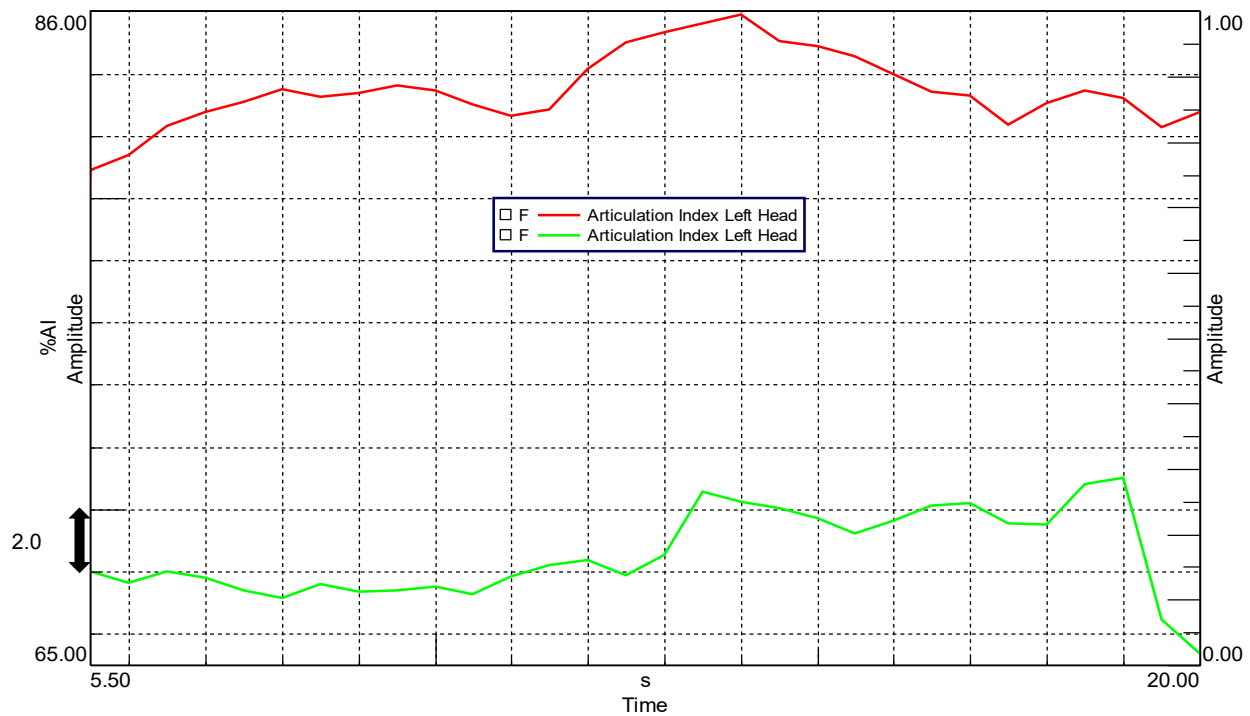
Figure 8.6: Articulation index, run 15/14 up-hill road trait 80 km/h.

Vehicle A A.I. remains significantly higher for all the test duration, near the 81-86%, whereas vehicle B A.I. is more irregular, on a lower level ranging from 66-68%.
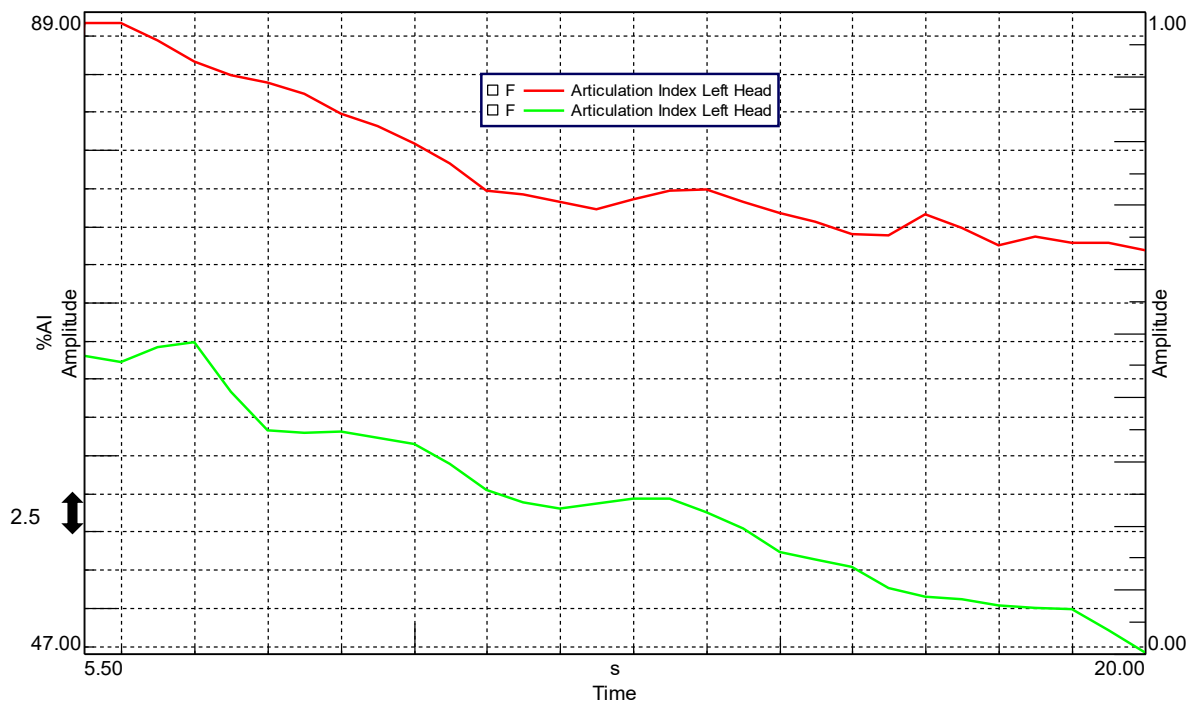

Figure 8.7: Articulation index, runs 14/15 run up 70-110 km/h.

Both the cars show a decreasing trend for the AI curves, still, vehicle A A.I. level is better, ranging from 89% to 73%, whereas vehicle B A.I. ranges from 66% to 47%
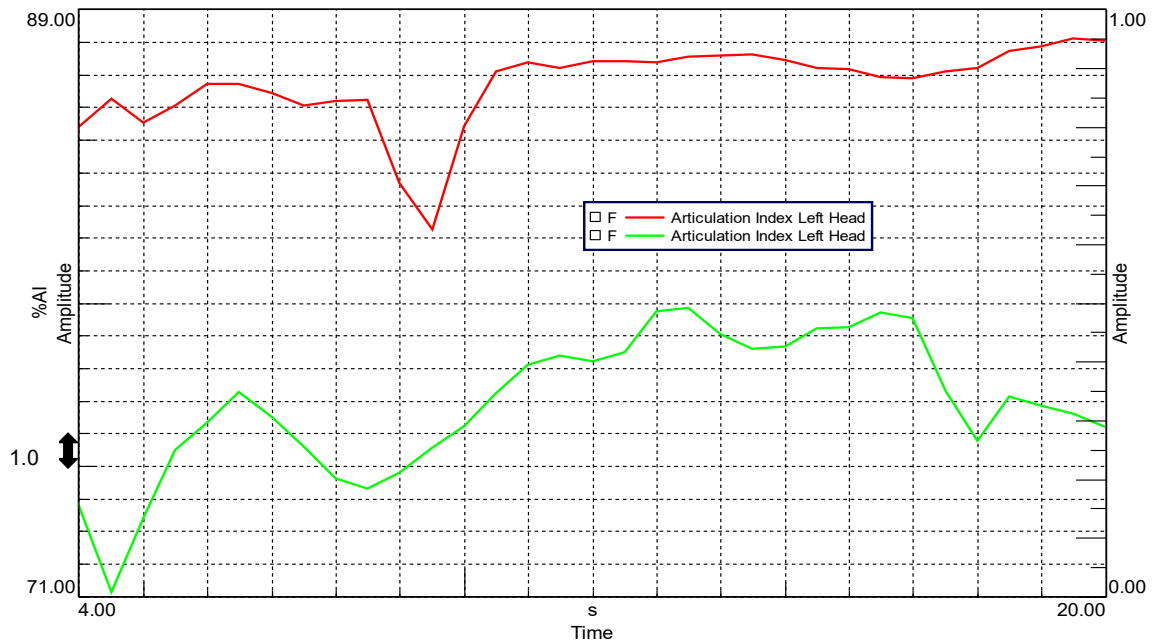
Figure 8.8: Articulation index, run 12/16 extra-urban mixed tarmac 70 km/h.

In this test, the A.I. functions shows a quite unstable trend, still slightly increasing; the vehicle A A.I. remains better also at constant speed, 85%-88%; on the other hand, vehicle B level varies between 71% and 80%
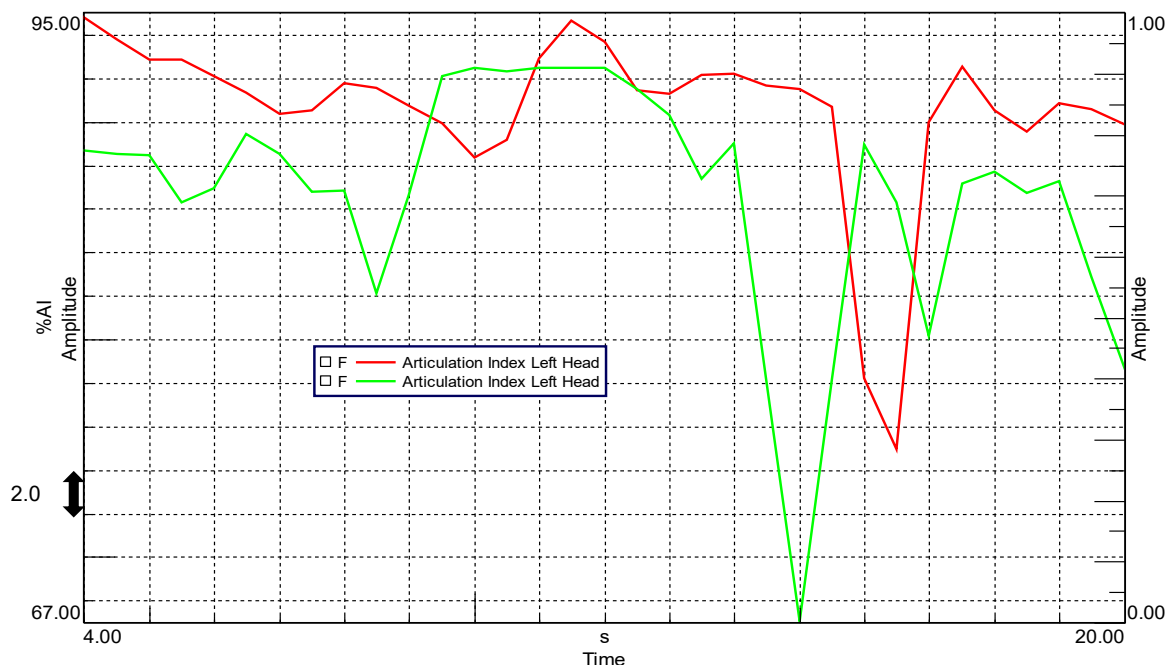

Figure 8.9: Articulation index, runs 24/29 paved urban road 30 km/h.

On paved road, both the A.I. curves shows a relevant drop in correspondence of a city centre urban bump, the value is still higher for vehicle A. The general trend is in the 80% region, but the negative peaks in the panda are more severe, down to 67% level.
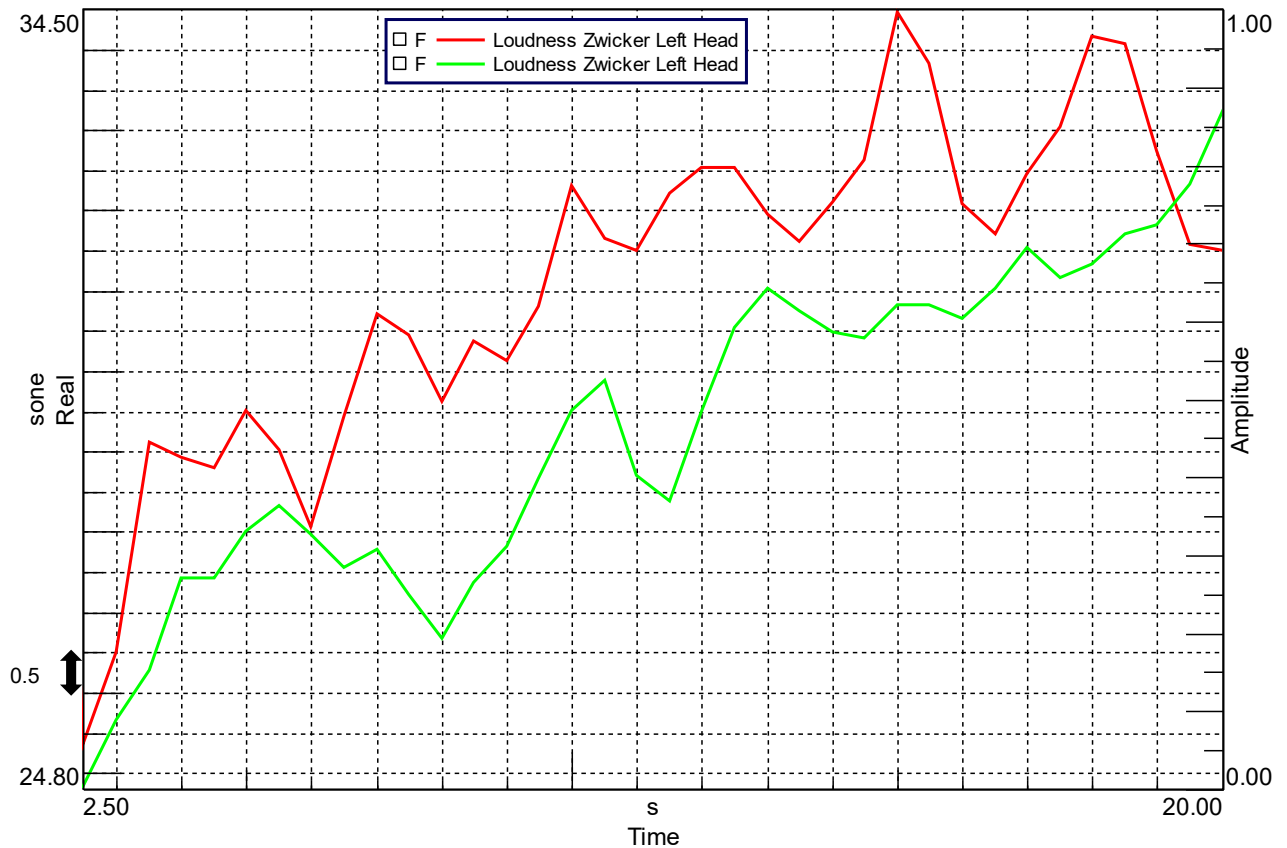
8.2 Loudness trends

Figure 8.10: Loudness Zwicker, run 18/17 run up 50-130 km/h.

Considering the Loudness, sone level for vehicle A is higher than vehicle B one; in addition, both trends show a certain increment, as it is expected in acceleration, overcoming the 30 sone value for both cases. In particular, the red function curve of vehicle A is characterized by two quite relevant peaks in the last part of the abscissa axis, where the ordinate value achieves its maximum level, denoting in this way the highest loudness condition, consisting in the maximum speed situation during the full throttle acceleration test. However, after the last high peak, the loudness level of the vehicle A seems to stabilize around 31.50 sone; whereas vehicle B green function curve ending portion show still a rising trend, towards 33 sone.
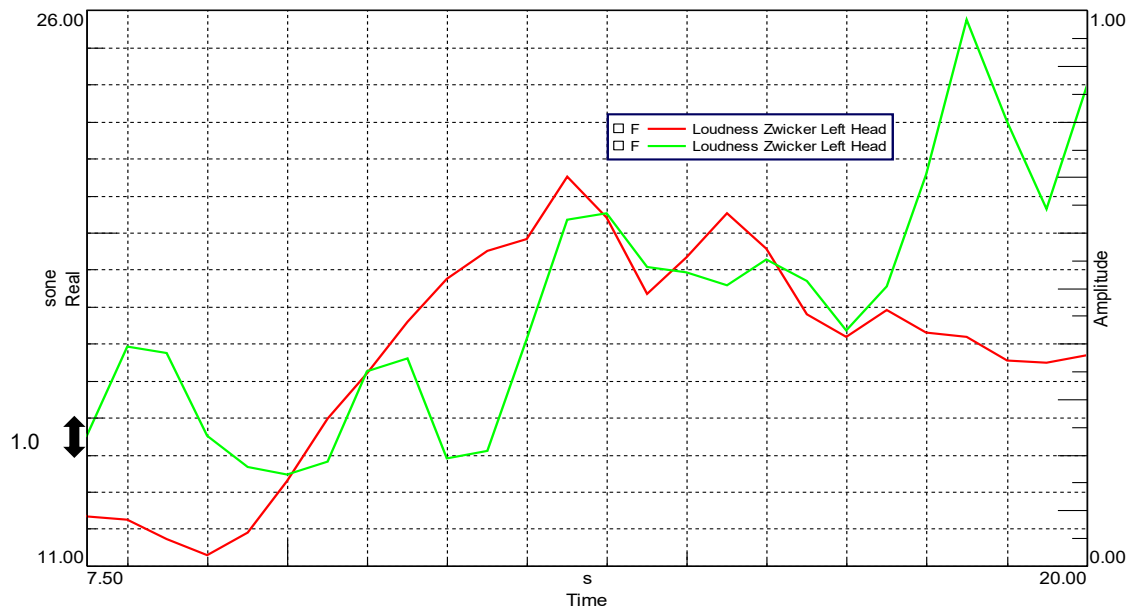
Figure 8.11: Loudness Zwicker, run 4 urban road 40 km/h.

Vehicle B function shows an oscillating behaviour, increasing its value from about 14 to 24 sone. Vehicle A function starts from a lower level, 12 sone, to achieve a maximum at half of the diagram, about 21 sone, then the value decreases, stabilizing at about 15.5 sone.
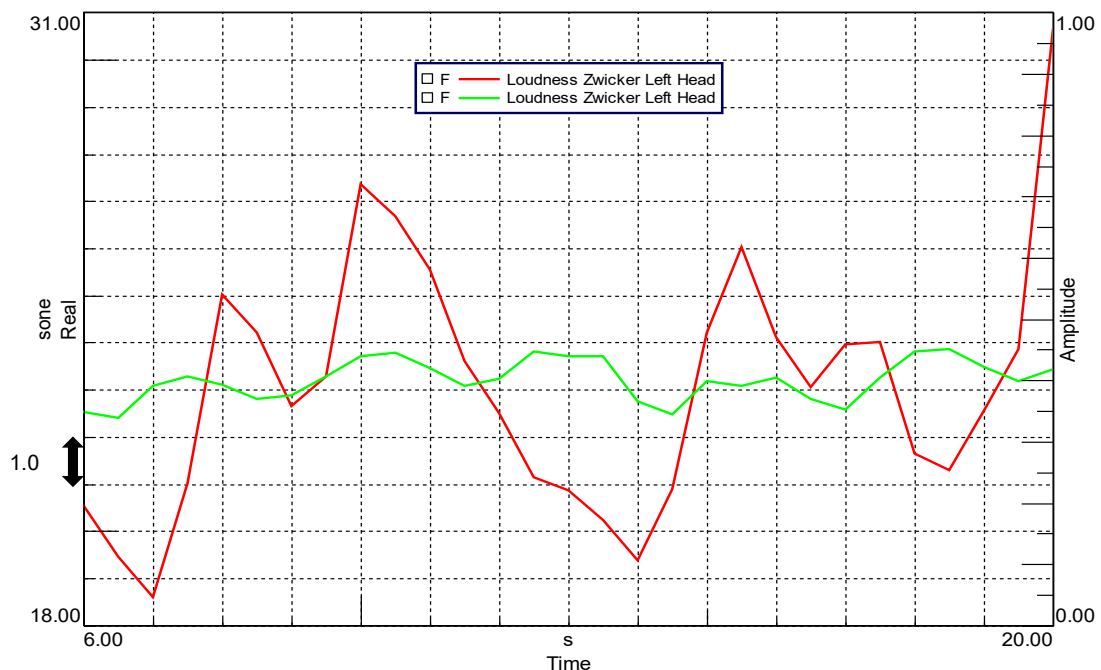

Figure 8.12: Loudness Zwicker, run 5 urban road 70 km/h.

The different road and traffic conditions during the two tests are observable in this diagram, vehicle A trend is highly irregular, with positive and negative peaks that space in the interval between 19 and 32 sone, while vehicle B trend Is more stable, near the 19 sone region.
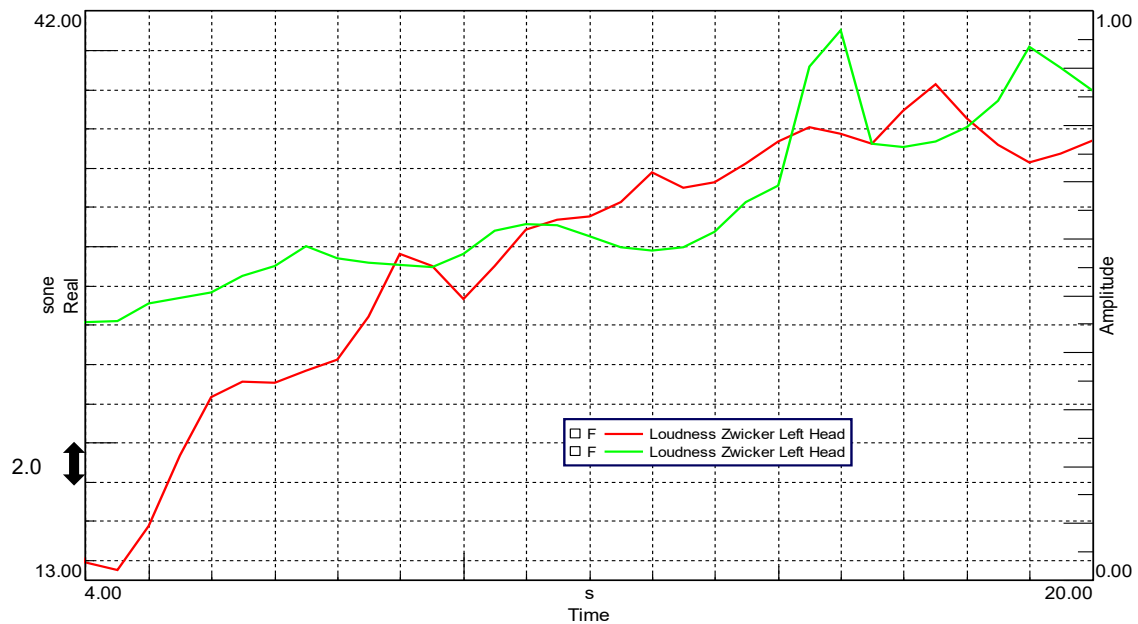
Figure 8.13: Loudness Zwicker, run 7 run up 70-120 km/h.

In this run up verification, the two increasing trends are comparable, especially in the last part. As a matter of fact, vehicle B level starts higher, 26 sone, then shows two main peaks and terminates with a value of 38 sone. Conversely vehicle A level is lower at the beginning, near 14 sone, then increase with a regressive behaviour, to finish in the proximity of 36 sone.
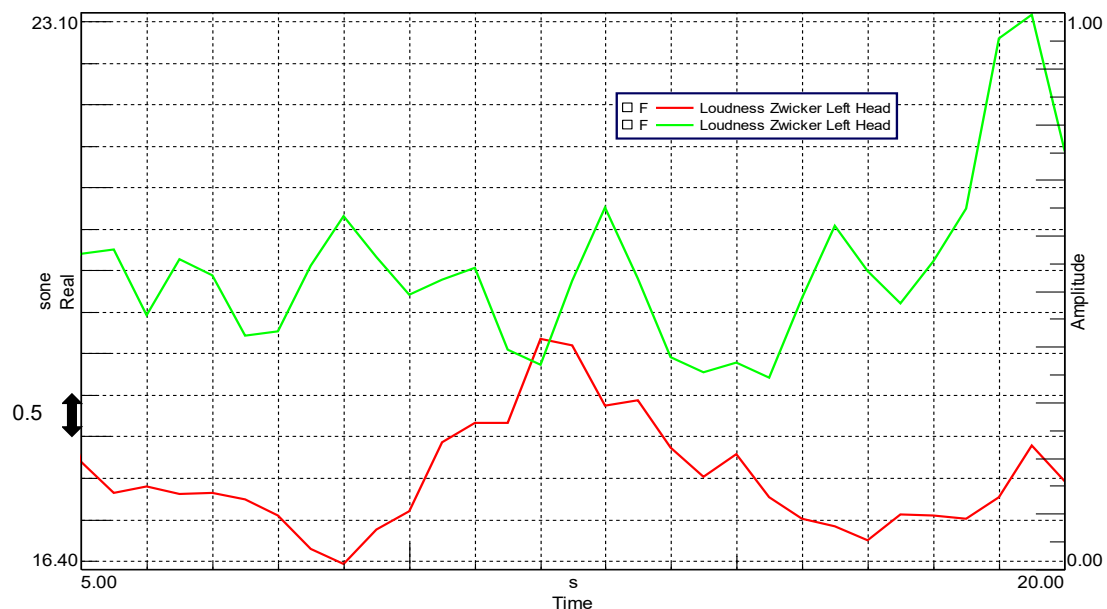

Figure 8.14: Loudness Zwicker, run 16/19 Racconigi main road course 60 km/h.

This diagram at constant speed test 60 km/h illustrates two different curves, that have in common a fairly reduced level of loudness. Vehicle A trend has a central peak, but the overall level stays lower, between 16.50 and 19 sone, whereas for vehicle B the level is generally higher, about 20 sone, with a final peak of 23 sone.
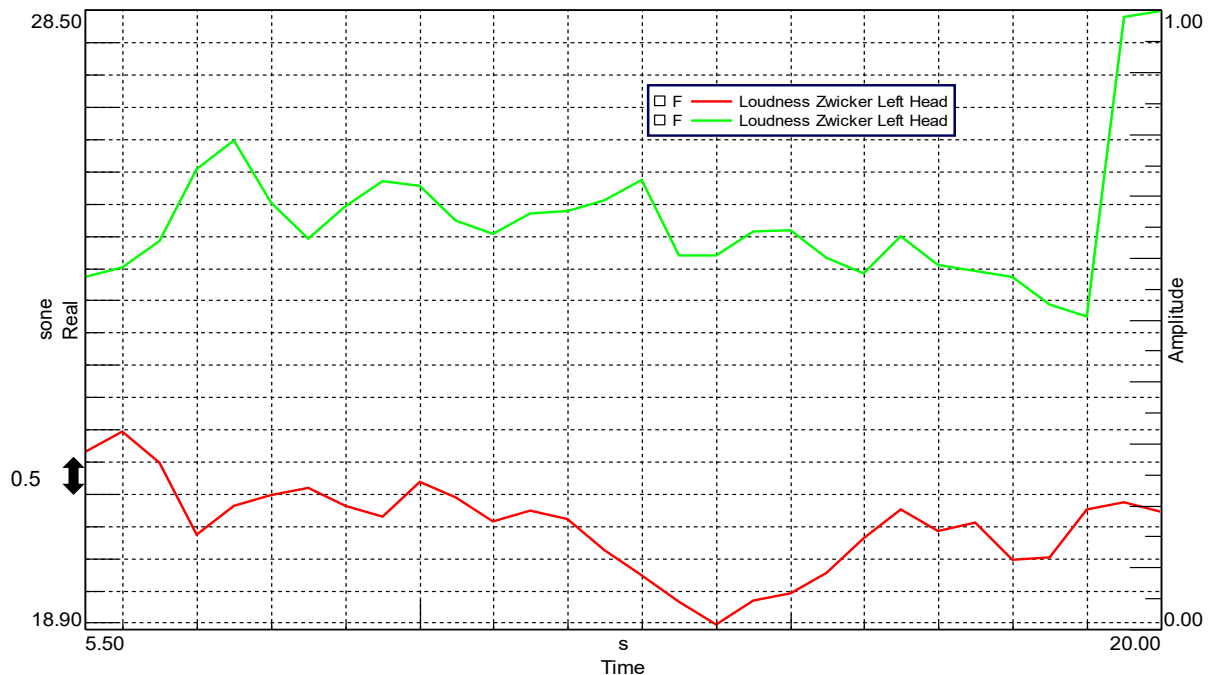
Figure 8.15: Loudness Zwicker, run 15/14 up-hill road trait 80 km/h.

Vehicle B loudness is higher, about 25 sone and gets to a final peak of 28.5 sone, while vehicle A loudness level is more stable, ranging from 19 to 22 sone.
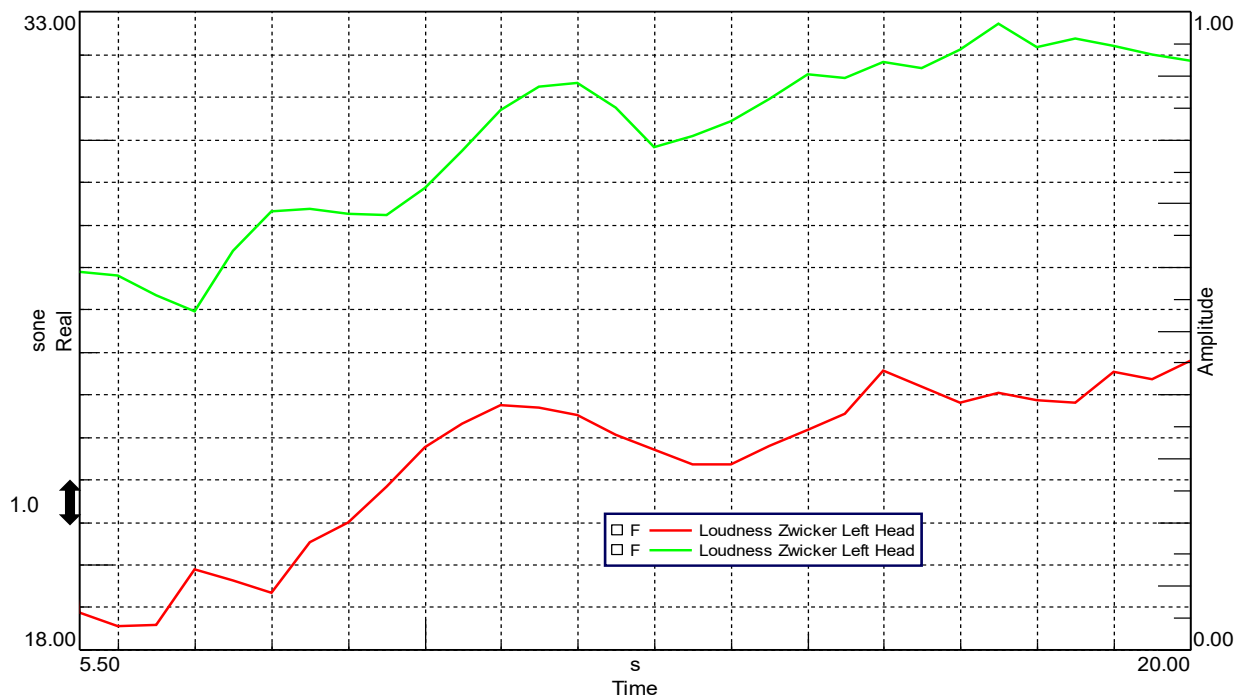

Figure 8.16: Loudness Zwicker, run 14/15 run up 70-110 km/h.

As expected, in this run up test the loudness levels are both steadily increasing; in particular, vehicle B curve values are highly in the entire field, 27-32 sone, vehicle A curve values pass from 19 to 25 sone.
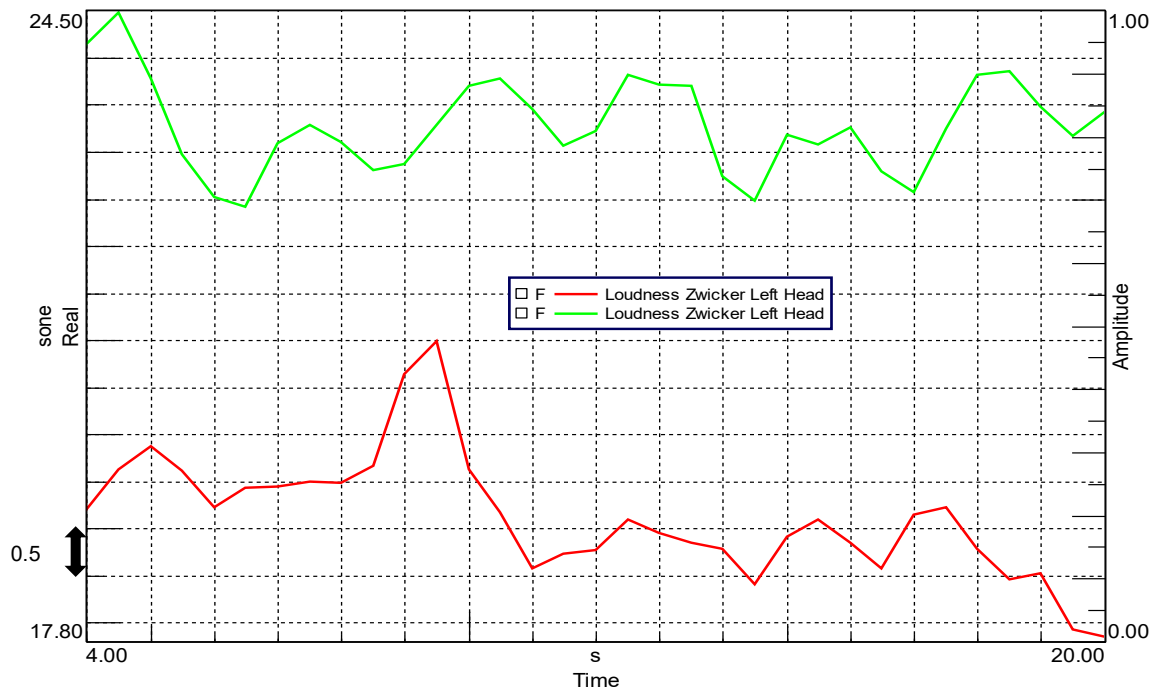
Figure 8.17: Loudness Zwicker, run 12/16 extra-urban mixed tarmac 70 km/h.

In this test at constant speed, vehicle B curve has higher values, 22.5-24.5 sone, while vehicle A trend is lower, 19.5-21 sone.
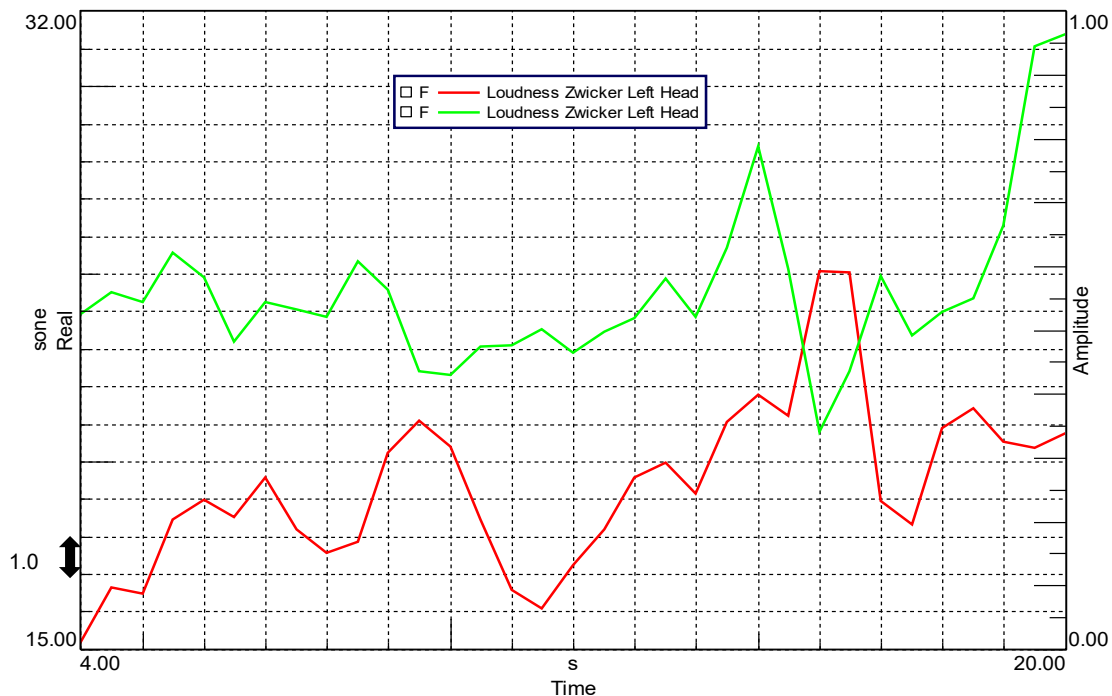

Figure 8.18: Loudness Zwicker, run 24/29 paved urban road 30 km/h.

In the paved road test, the two curves are both quite irregular, denoting a vaguely rising trend, 15-21 sone for the vehicle A, 24-31 sone for the vehicle B, whose curve is characterized by a final incremental peak.
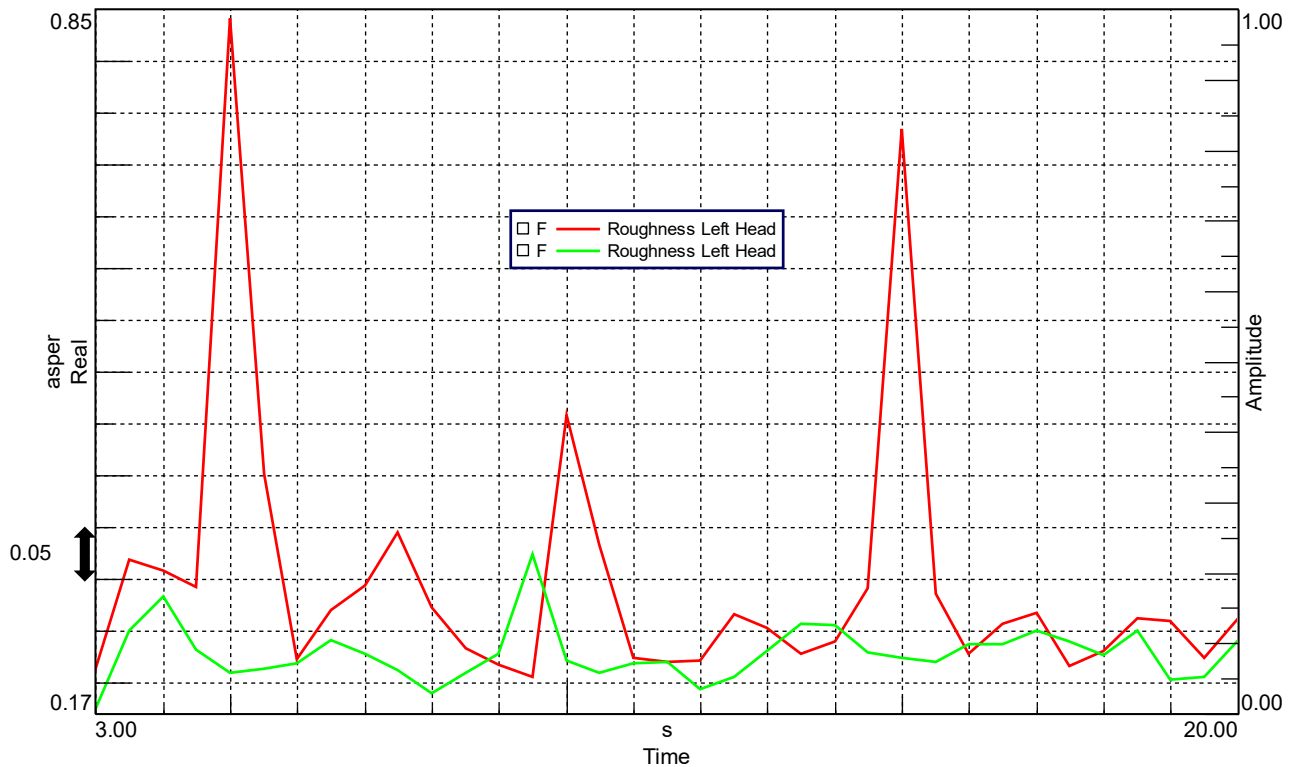
8.3 Roughness trends

Figure 8.19: Roughness, run 18/17 run up 50-130 km/h.

In this run up test, both the curves have an overall similar level for most the duration of the run, in the proximity of 0.20-0.25 asper; however, vehicle A curve shows three critical positive peaks, up to 0.85 asper, which corresponds in time to the negative peaks of the articulation index diagram for the same test. This may be likely related to the manual shift mode utilized, with the most critical peaks being in correspondence of the maximum rev instantaneous conditions of the diesel engine, just before the gear shifts. In detail, the most severe peak is the first, followed by the third, about 0.75 asper, while the less critical is the second one, approximately 0.45 asper. Conversely, vehicle B function curve features a more regular and flat tendency, with values comprised in the range 0.17-0.33 asper.
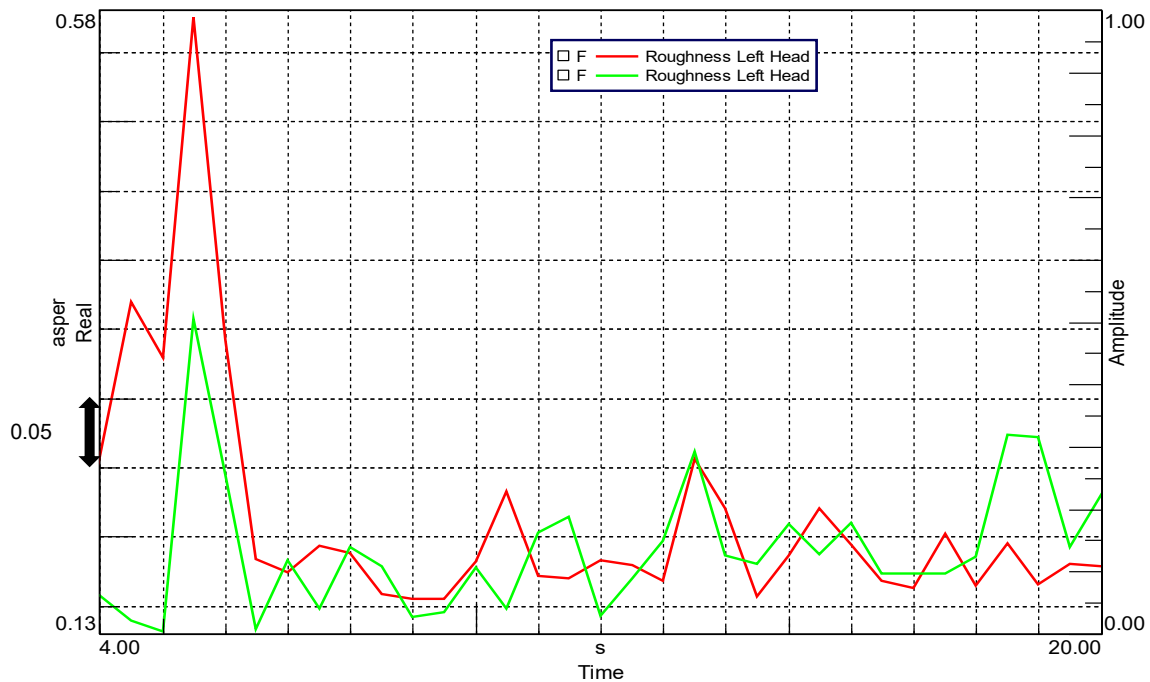
Figure 8.20: Roughness, run 4 urban road 40 km/h .

The two vehicles show a similar peak at the beginning, related to road irregularities then the trends are comparable, with some oscillations, around 0.20 asper.
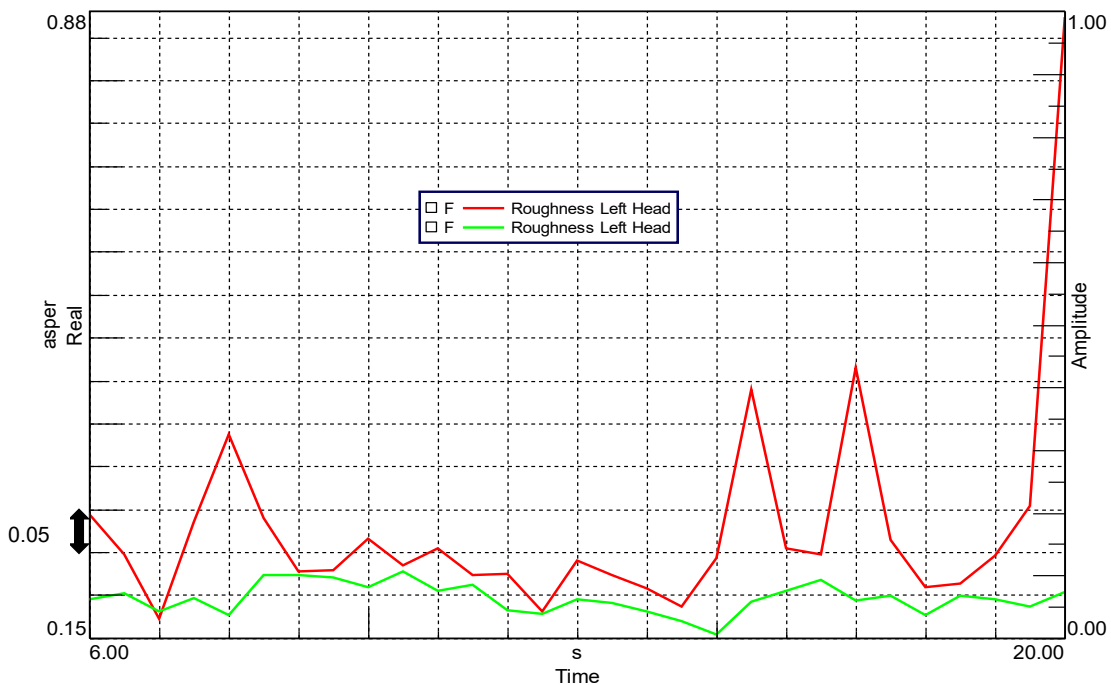

Figure 8.21: Roughness, run 5 urban road 70 km/h.

Both the trends are quite comparable, even if vehicle A curve presents more severe peaks; the general level is lower for vehicle B, near 0.2 asper, with a final peak for vehicle A, till 0.85 asper, likely due to some exceptional surrounding condition.
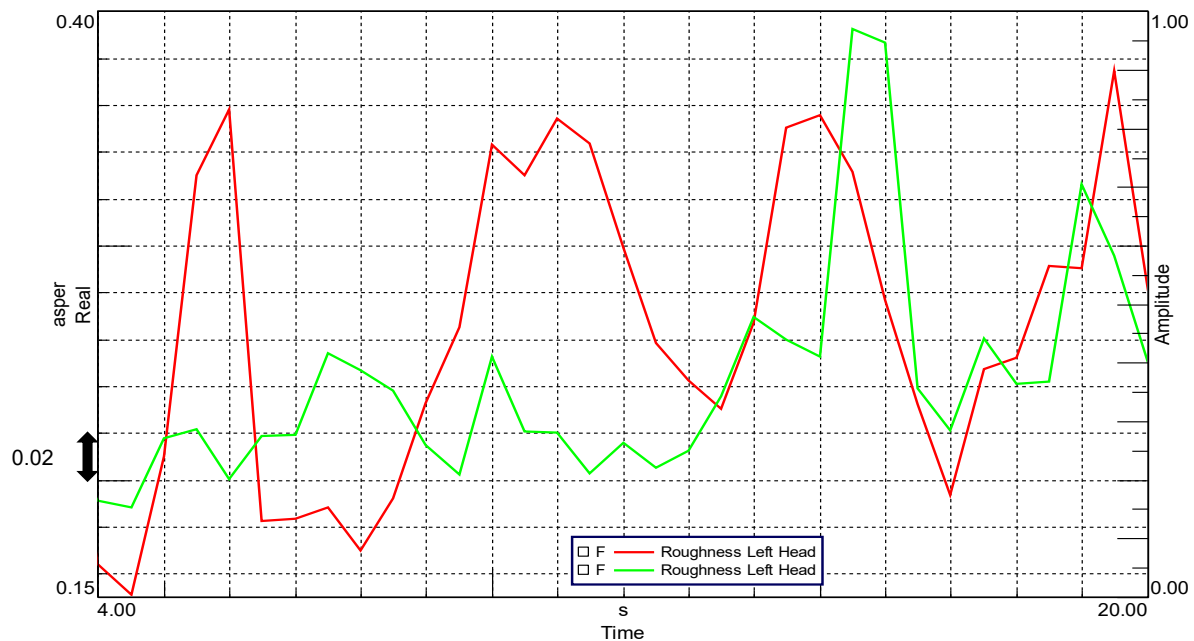
Figure 8.22: Roughness, run 7 run up 70-120 km/h.

In this test, vehicle A curve shows several peaks, of similar max value, approx. 0.36 asper, while the overall level pass from 0.16 to 0.28 asper. The vehicle B roughness curve is characterized by a more stable increment, with only one severe peak at 0.39 asper; the level pass from about 0.19 asper to 0.25 asper.
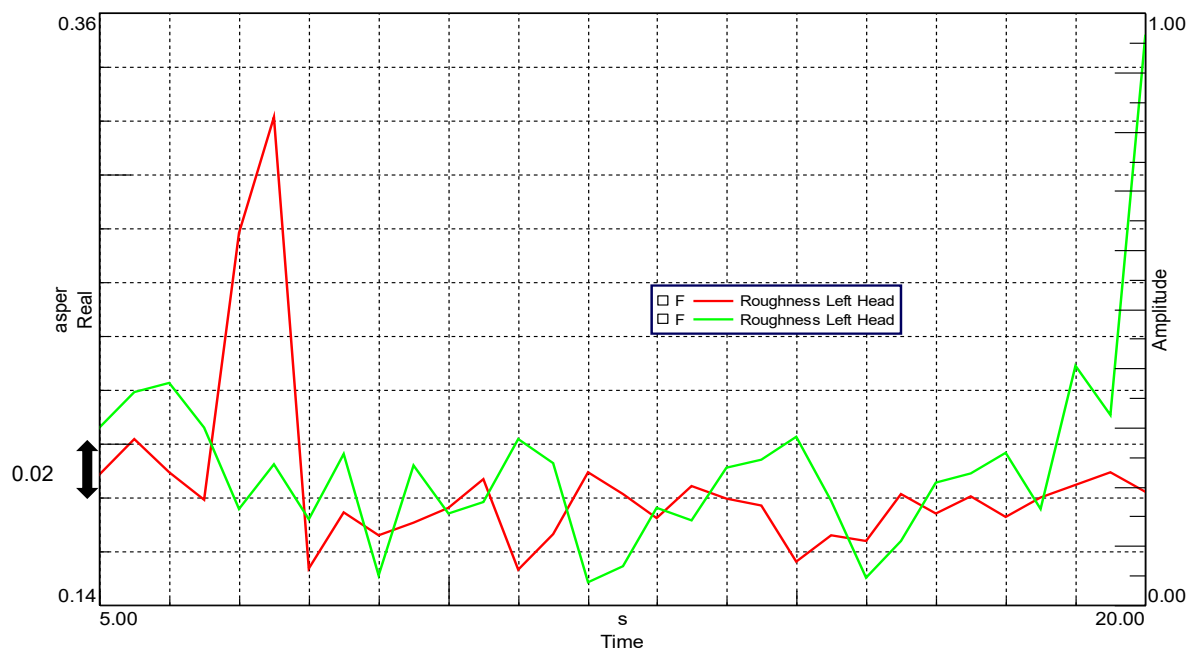

Figure 8.23: Roughness, run 16/19 Racconigi main road course 60 km/h.

The roughness level is quite similar for both the vehicles, about 0.16-0.20 asper; though, vehicle A curve has a peak in the first part with a max value of 0.32 asper, whereas vehicle B max value is at the end, achieving 0.35 asper.
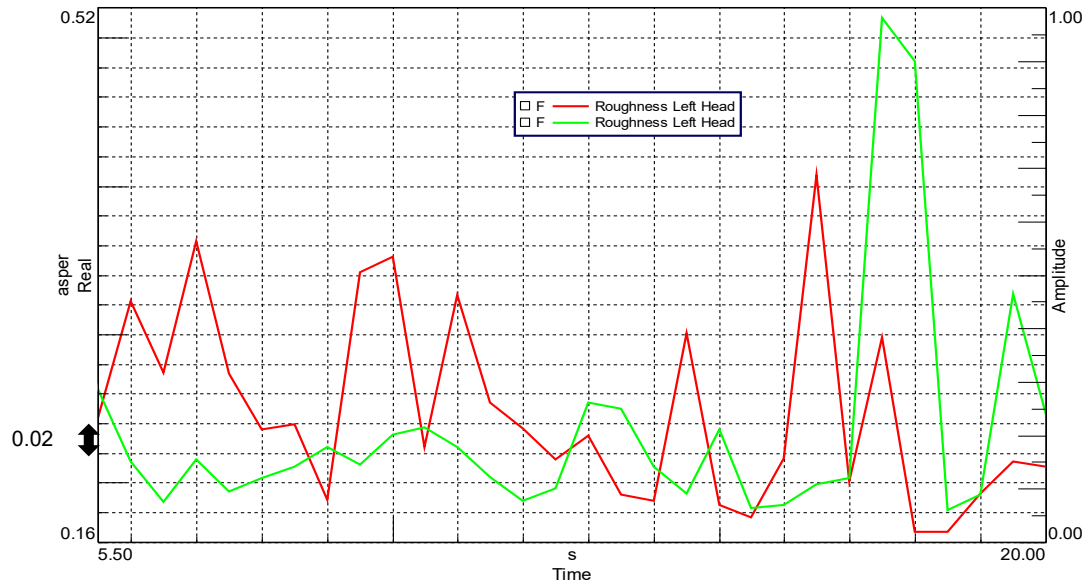
Figure 8.24: Roughness, run 15/14 up-hill road trait 80 km/h.

In the uphill test, vehicle A trend is noticeably irregular, with several peaks, whose roughness value ranges from 0.24 to 0.41 asper, to terminate in the last part at approximately 0.21 asper; conversely, the curve for vehicle B has a more plain behaviour, staying in the nearby of 0.20-0.24 asper for most the test duration, except for a very high peak towards the proof end, reaching about 0.52 asper.
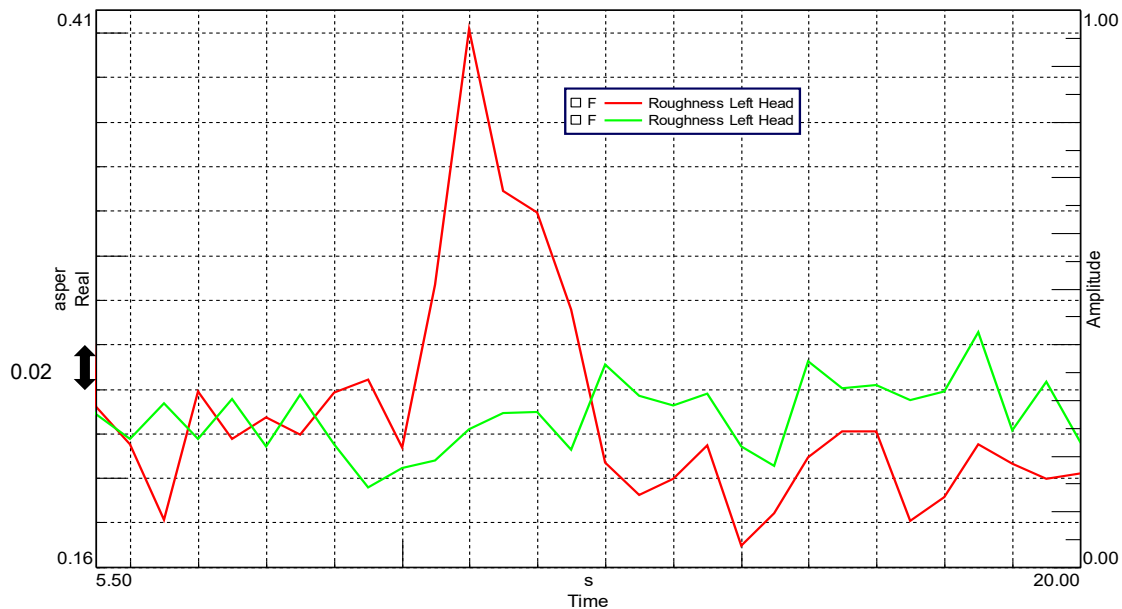
Figure 8.25: Roughness, runs 14/15 run up 70-110 km/h.

During this run up performance, the roughness level of vehicle A shows a critical peak getting till 0.41 asper, in correspondence of the starting acceleration phase, where the engine growl is clearly perceived, to then decrease again at limited levels, about 0.20 asper. Vehicle B function instead has no relevant peaks, the level oscillating between 0.20-0.26 asper with a pretty constant trend.
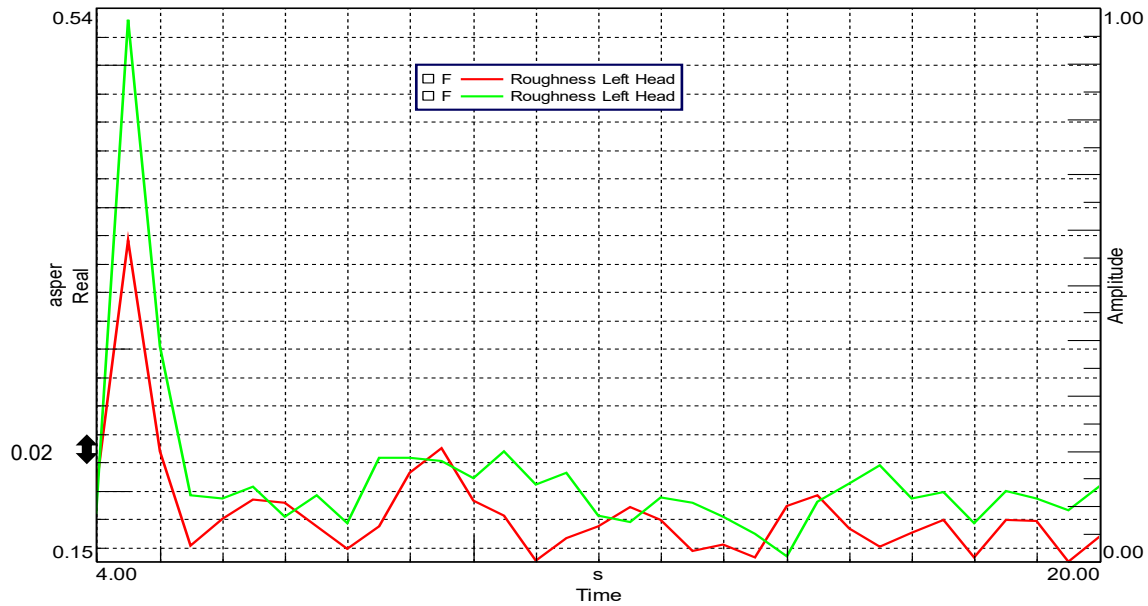
Figure 8.26: Roughness, run 12/16 extra-urban mixed tarmac 70 km/h.

In this constant speed verification, the two trends are pretty similar, the roughness level being limited for the major part to 0.15-0.23 asper; however, both curves have a massive peak at the beginning, which is higher in vehicle B case, 0.53 vs. 0.38 asper, similarly to the overall level value.
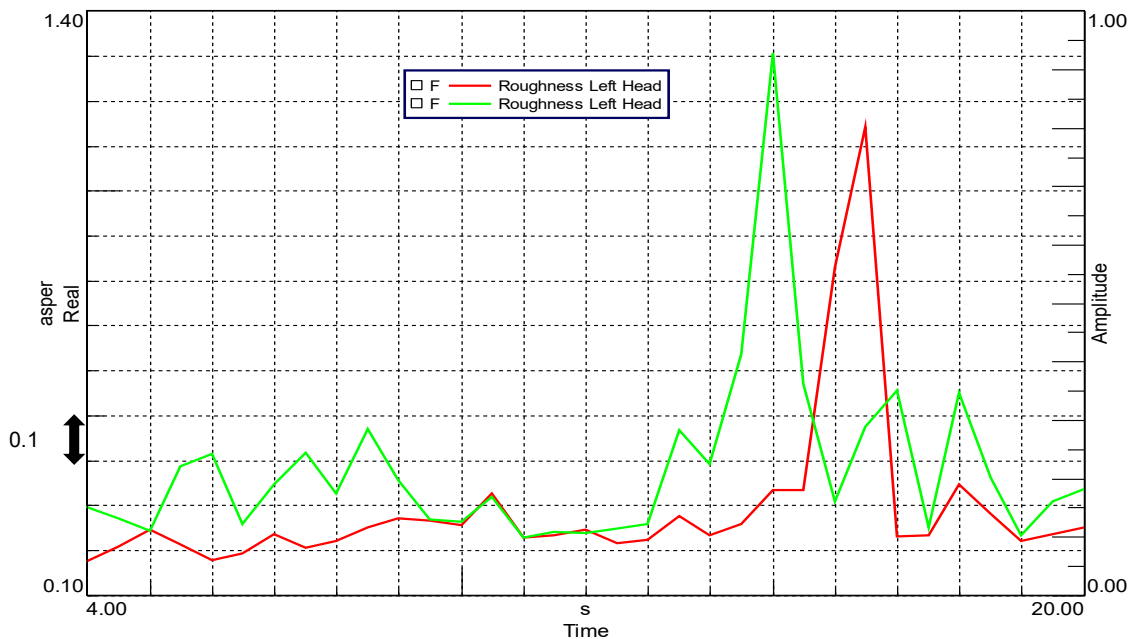
Figure 8.27: Roughness, run 24/29 paved urban road 30 km/h.

In the paved road test, the roughness value is generally higher for vehicle B with respect to vehicle A; these are comprised respectively in the interval between 0.20-0.45 and 0.15-0.25 asper for the most time. Nevertheless, both present a relevant peak, probably in correspondence of the urban paved bump, with a value which is higher in the former case (1.30 asper), lower in the latter (1.15 asper).
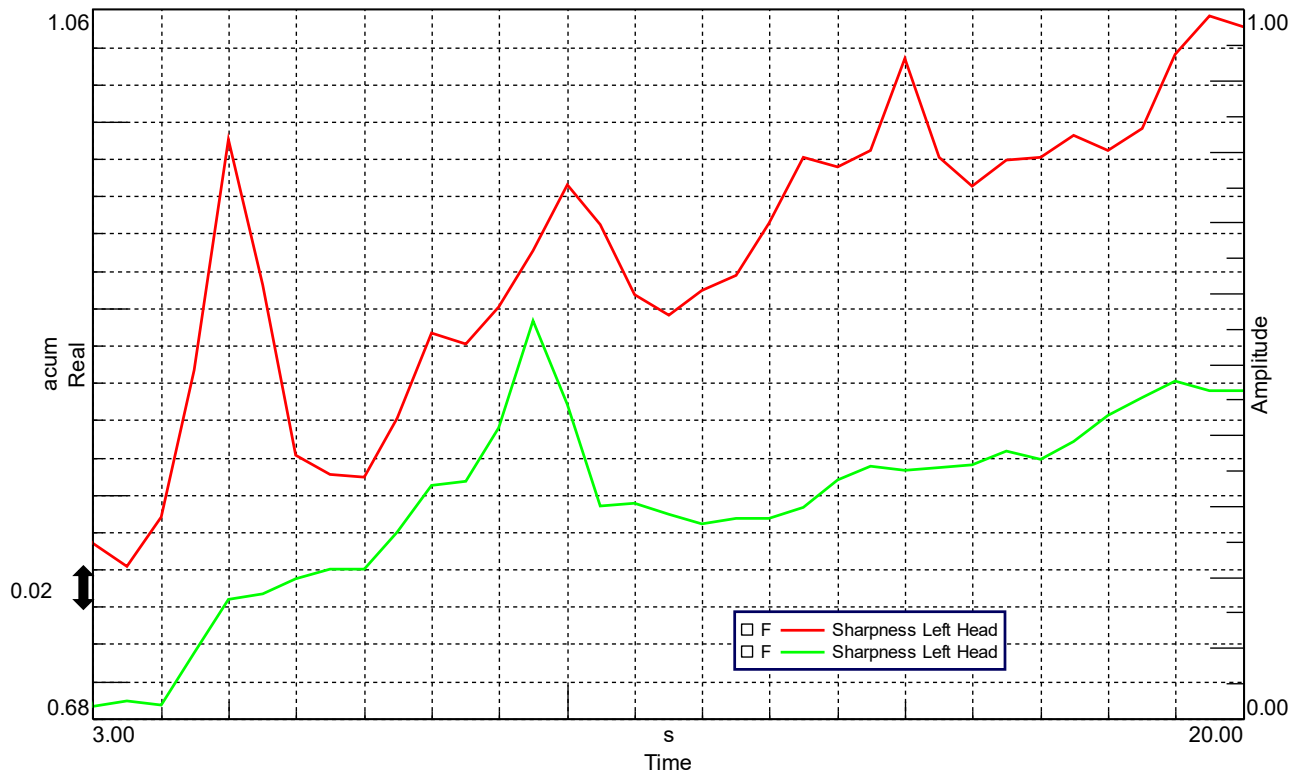
8.4 Sharpness trends

Figure 8.28: Sharpness, run 18/17 run up 50-130 km/h.

Concerning the sharpness parameter, both the vehicles feature an increasing trend, vehicle A having an higher value for all the duration and three main peaks in comparison with a single main peak in vehicle B case, representing again a typical characteristic of this test run, which occurred also in the analysis of the psychoacoustic entities considered in the previous paragraphs.

Actually, in this case the peaks severity is less critical than in the roughness study, but vehicle A values remain higher than the ones reached by vehicle B, respectively 0.98, 0.97, 1.04 acum and 0.90 acum. Conversely, the respective comprehensive levels vary respectively between 0.76-1.05 acum and 0.69-0.86 acum.
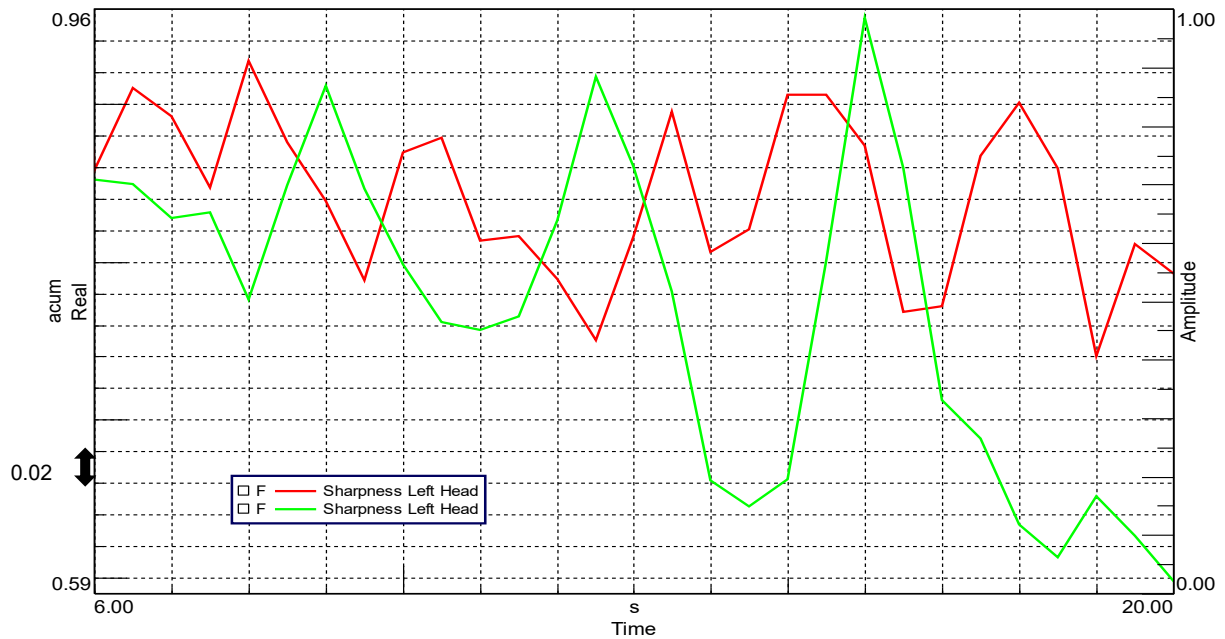
Figure 8.29: Sharpness, run 4 urban road 40 km/h.

The value of sharpness for both the vehicles in this test is highly oscillating. The general trend for vehicle A is more regular, comprised between 0.74 and 0.92 acum, while vehicle B curve has more important peaks, whose value goes from 0.60 to 0.96 acum.

Figure 8.30: Sharpness, run 5 urban road 70 km/h.

Even in this constant speed test the general trend of the sharpness curves is in the region 0.67-0.78 acum for vehicle B and between 0.68-0.80 acum for vehicle A, at the beginning the vehicle B curve has a high peak at 1.41 acum likely due to particular conditions.
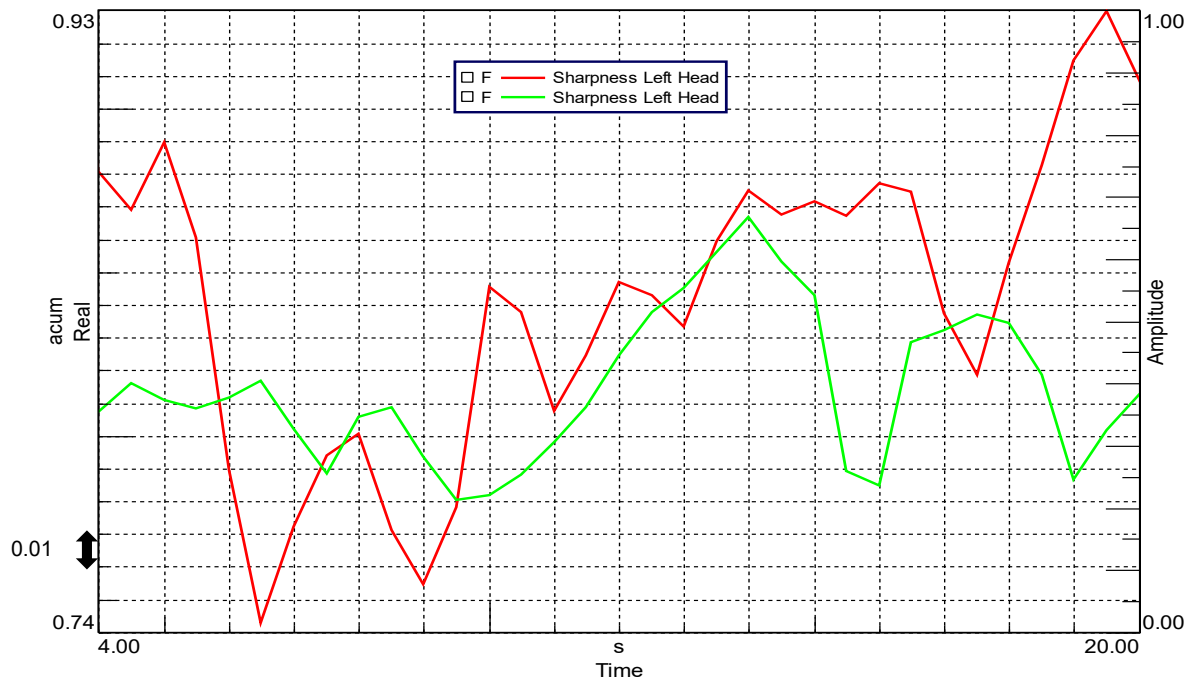
Figure 8.31: Sharpness, run 7 run up 70-120 km/h.
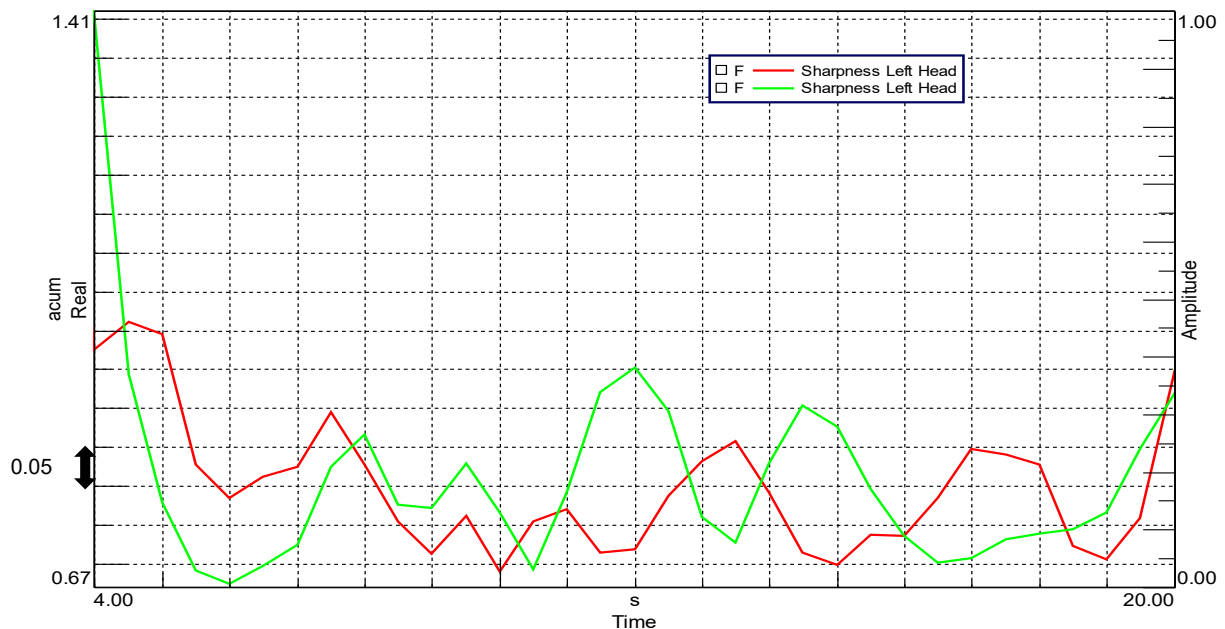
The sharpness levels in this run up test are quite oscillating, especially in vehicle A case, which gets as minimum and maximum value 0.74 and 0.93 acum, while in vehicle B this interval is limited to 0.78-0.86 acum.

Figure 8.32: Sharpness, run 16/19 Racconigi main road course 60 km/h.

In this constant speed test vehicle A sharpness level curve present two main peaks in the first seconds, then it drops to a more stable trend around 0.72 acum, whereas vehicle B level behaviour oscillates for the entire test duration, ranging from 0.68 to 0.77 acum.
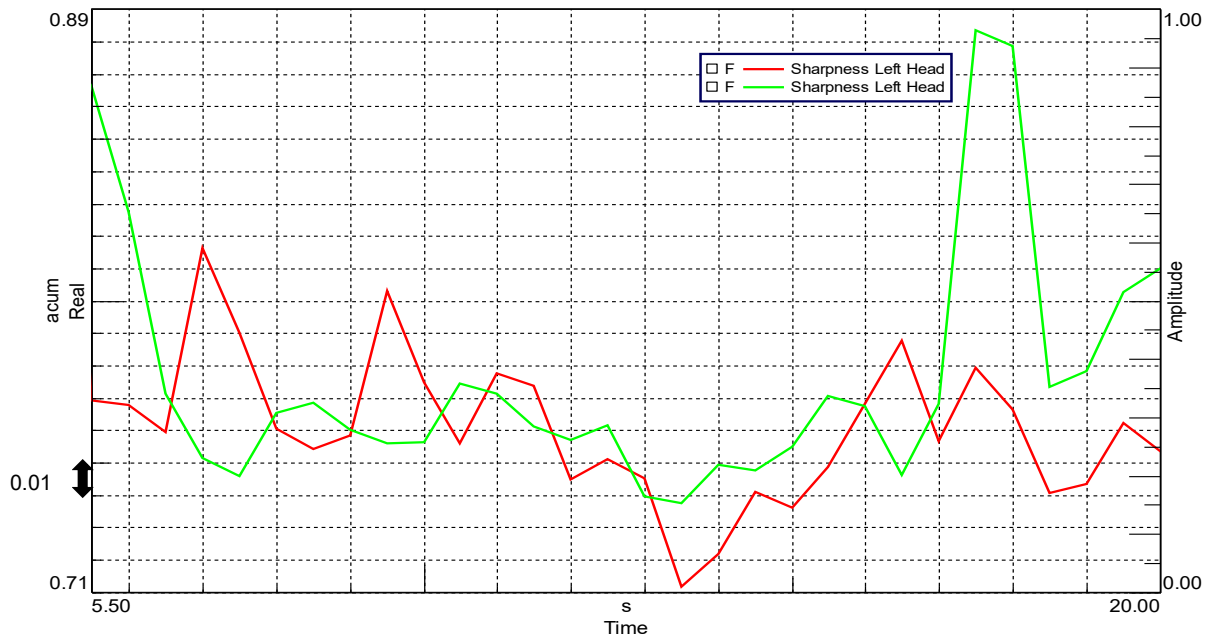
Figure 8.33: Sharpness, run 15/14 up-hill road trait 80 km/h.

In this uphill test, the sharpness parameter curve for the two vehicles is poorly comparable, vehicle B curve has a minimum at 0.74 acum and shows two main peaks up to 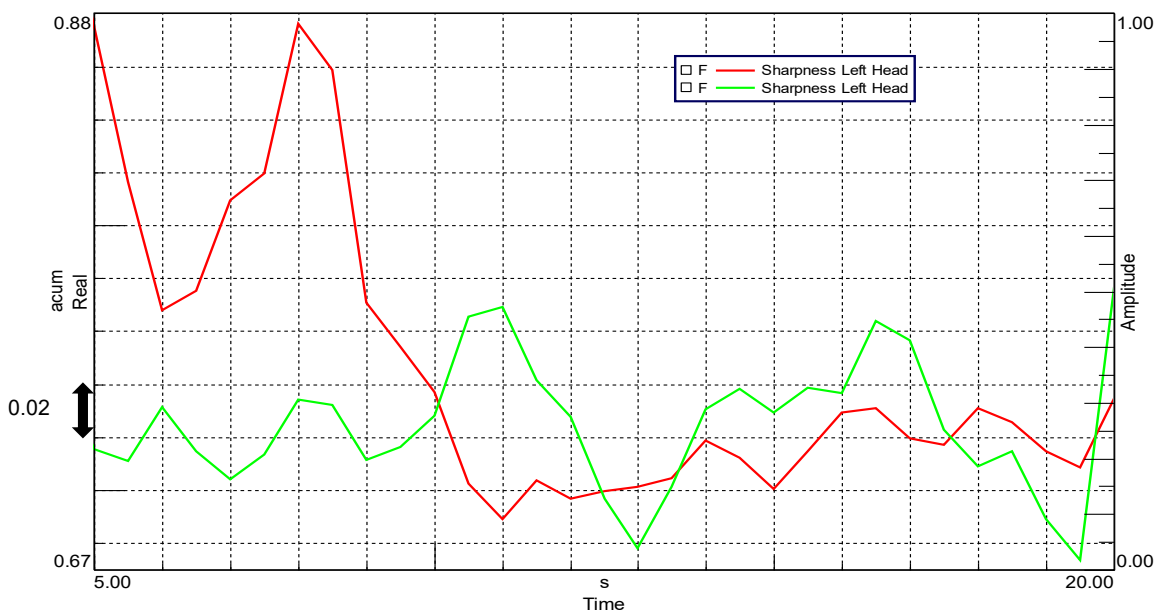0.88 acum, at the beginning and in the proximity of the termination, while vehicle A trend varies in a more limited range, between 0.71 and 0.82 acum.

Figure 8.34: Sharpness, run 14/15 run up 70-110 km/h.

Regarding vehicle B, sharpness level steadily increases along all the duration of the recording, passing from 0.73 to 0.90 acum, whereas vehicle A behaviour is more irregular, having a noticeable negative peak at second 10 and ranging from 0.71 to 0.80 acum, remaining lower than the compared level for almost all the test.
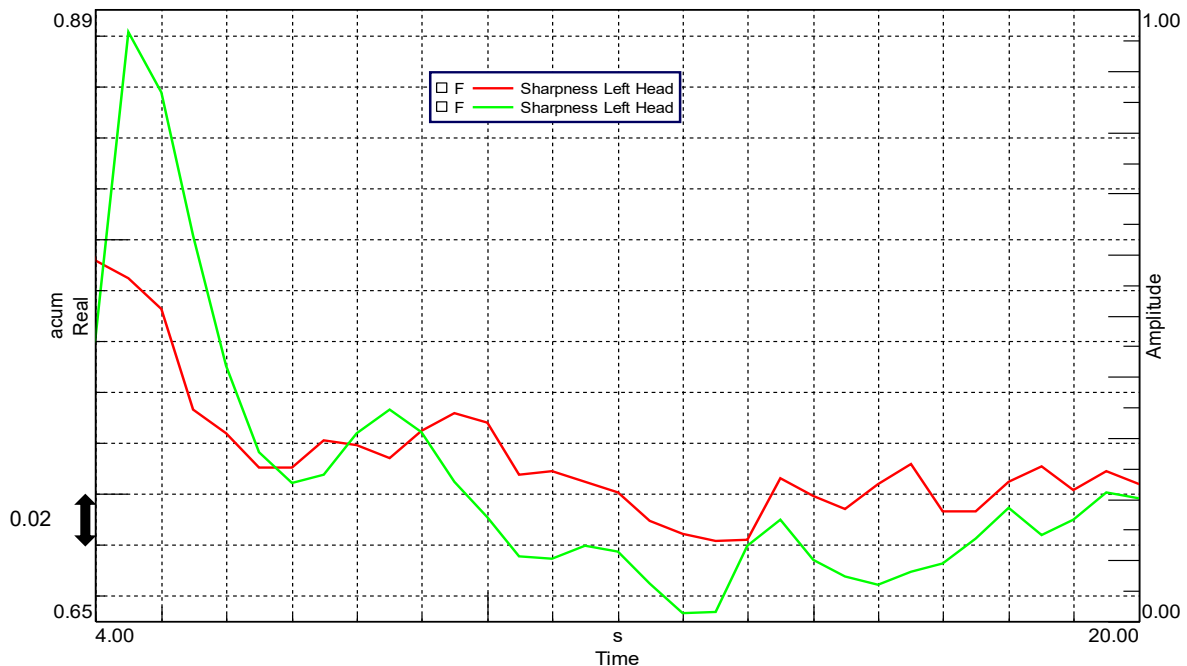
Figure 8.35: Sharpness, run 12/16 extra-urban mixed tarmac 70 km/h .

In this test the sharpness levels decrease for both the tested cars; in particular vehicle B curve has a peak till 0.88 acum at the beginning, then its trend rapidly drops to lower values about 0.66-0.70 acum, while vehicle A curve starts at approximately 0.80 acum and drops to 0.68-0.70 level value.
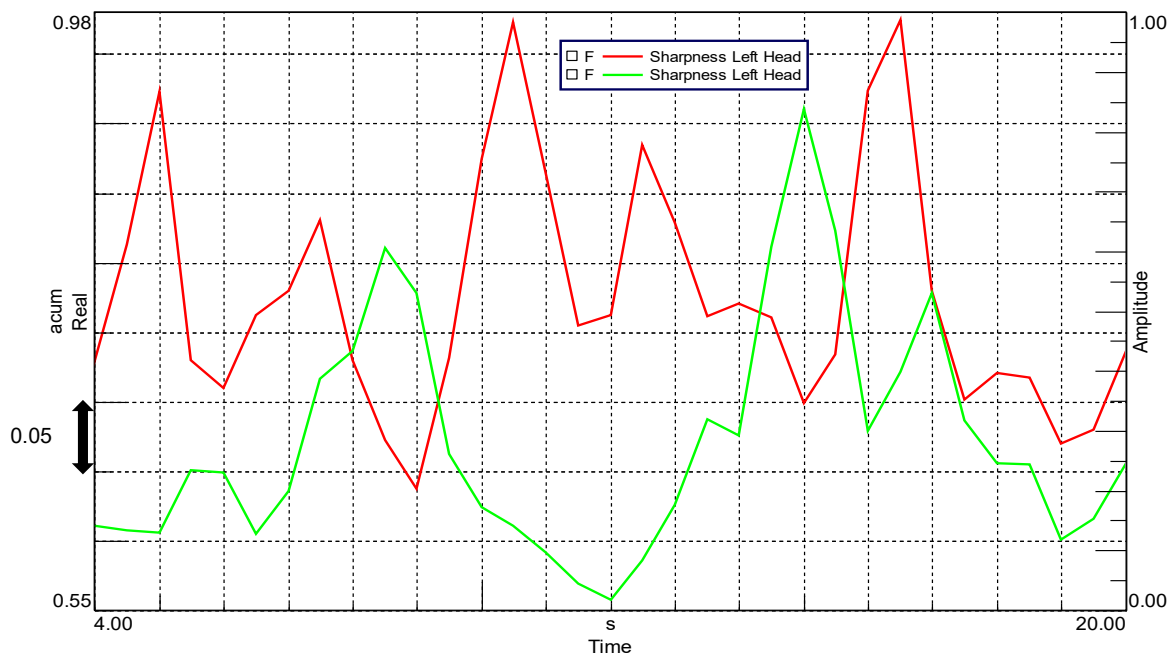
Figure 8.36: Sharpness, run 24/29 paved urban road 30 km/h.

In the paved road test, vehicle A sharpness level is considerably higher for most the time, though, both the vehicles feature severely oscillating trends with peaks, ranging from 0.65 to 0.98 in the former car and from 0.55 to 0.90 acum in vehicle B case.

At this point, considering the several parameters examined in the previous paragraphs, some subjective judgements based on the listening of the various recordings are collected in Table 8.2.

Table 8.2: Subjective assessment and characterization of the acoustic recordings.

| TEST / P.A. parameter	SUBJECTIVE JUDGEMENT	
	Vehicle A	**Vehicle B**
Run 4 urban road 40 km/h	More characterful, conspicuous	More characterless, inconspicuous
Run 5 urban road 70 km/h	Cleaner, distinct, richer	Vaguer, flatter
Run 7 run up 70-120 km/h	Sporty, more exciting, distinct	Less distinct, vague
Run 12/16 extra-urban mixed tarmac 70 km/h	Softer, more relaxed	Louder, tenser
Run 14/15 run up 70-110 km/h	Tranquil, pleasant, distinct	Harder, tenser
Run 15/14 up-hill road trait 80 km/h	Softer, relaxed	Louder, busier
Run 16/19 Racconigi main road course 60 km/h	Calm, relaxed, weaker,	Tense, stronger
Run 18/17 run up 50-130 km/h	Powerful, sporty, exciting, pleasant, distinct, deep	Strong, vaguer, inconspicuous
Run 22/23 severe off-road	Deep, calm, vague	Deep, calm, vague
Run 24/29 paved urban road 30 km/h	Busy, vague, nor loud nor soft	Busy, vague, nor loud nor soft

8.5 Audio spectrum

Having looked to the general psychoacoustics parameters for both the two vehicles, the subsequent step consists in the observation of the specific audio spectrum colour maps computed by using the proper options in the Time Data Processing section of LMS Test.Lab software. A colour map displays spectral map data in a customized intensity graph, using a rainbow colour scale to represent the signal power distribution, thus proving to be typically useful for offline analysis.

Indeed, by comparing the display results with different formats and units, it is possible to gain a complete knowledge of the signal, such as how the amplitude of the signal relates to time, speed, frequency, and order. In detail, referring to our purpose, the colour map display is used to display a series of data functions in relation to a third parameter, such as time, in this case. This parameter is plotted along the Z axis. The Y (ordinate) value of each block is represented as a colour, thus providing a two dimensional map of X against Z. In LMS Test.Lab, this data is represented by a Waterfall icon and it can be displayed in a Colour map window.

In creating the colour-map diagrams listed in the following, the orientation has been changed, as described in chapter 6, in order to have a more clear view of the evolving spectrum, the frequency range has been limited to the interval 0 – 300 Hz, to allow a distinction among the various colour shades and have a more understandable glance on the acoustic range realistically interested by the observed phenomena, as it is highly unlikely to receive audible noises and sounds with frequency higher than 500 Hz on street cars (Figure 8.38 – 8.43).

Having the same clearness leitmotiv in mind, the resulting SPL in Pascal, has been expressed as the effective dB value referred to the audibility threshold (20uPa), weighted with A filtering, therefore representing the dB(A) level, whose upper and lower thresholds have been modified depending on each test result to have the best possible picture in each situation. The choice of expressing the data as dB(A) values, thus adopting a weighted SPL, allows a good understanding of the diagrams in relation to the most relevant frequency interval detected by human hearing system.

As in the previous acoustic studies, the time interval considered for each recording corresponds to about 20 seconds. In particular, the audio-spectra analysis focuses on the recorded runs representing relevant acceleration conditions, occurring during the so-called run-up tests, utilizing the LMS binaural headset, (Table 8.3).

Table 8.3: List of considered runs in colour-map audio-spectra assessment.

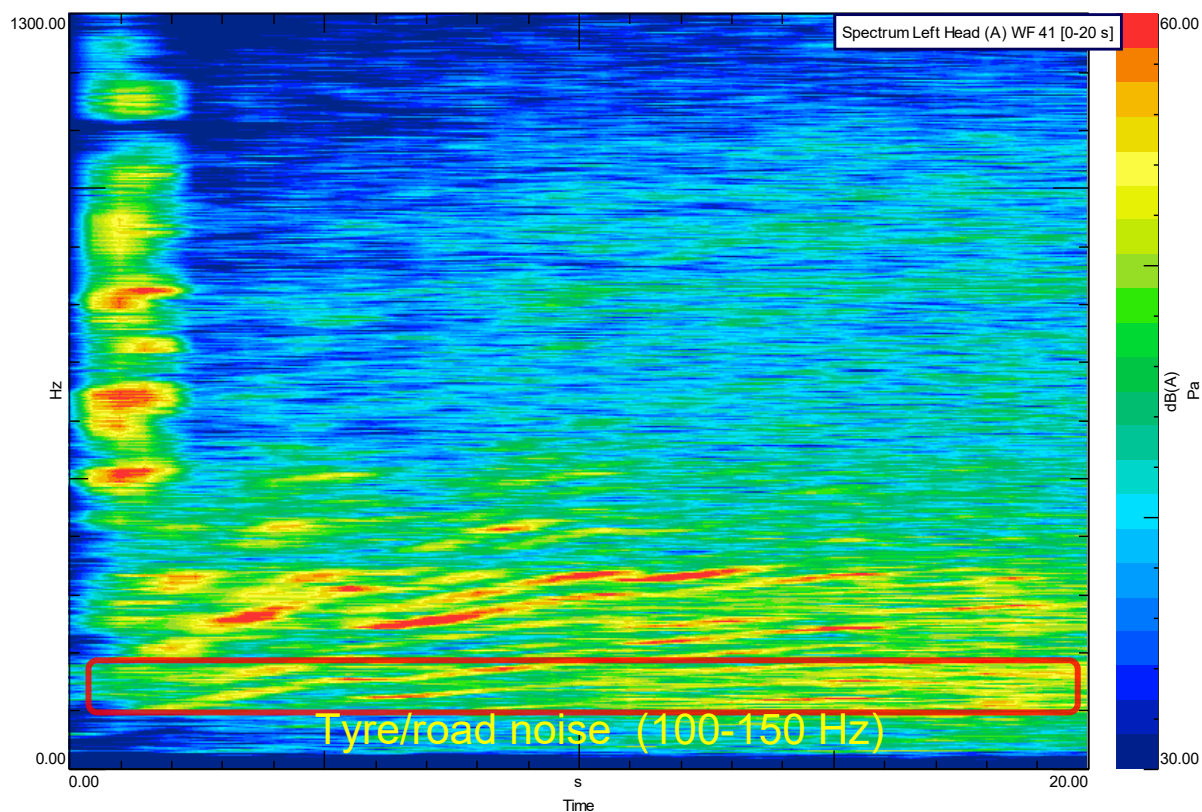| Vehicle A	Vehicle B
AUDIO-SPECTRA STUDY TESTS	
Run 7 run up 70-120 km/h	Run 7 run up 70-120 km/h
Run 12 extra-urban mixed tarmac 70 km/h	Run 16 extra-urban mixed tarmac 70 km/h
Run 14 run up 70-110 km/h	Run 15 run up 70-110 km/h
Run 18 run up 50-130 km/h	Run 17 run up 50-130 km/h

Figure 8.37: Vehicle A audio-spectrum, run 18 detail, (run up 50-130).
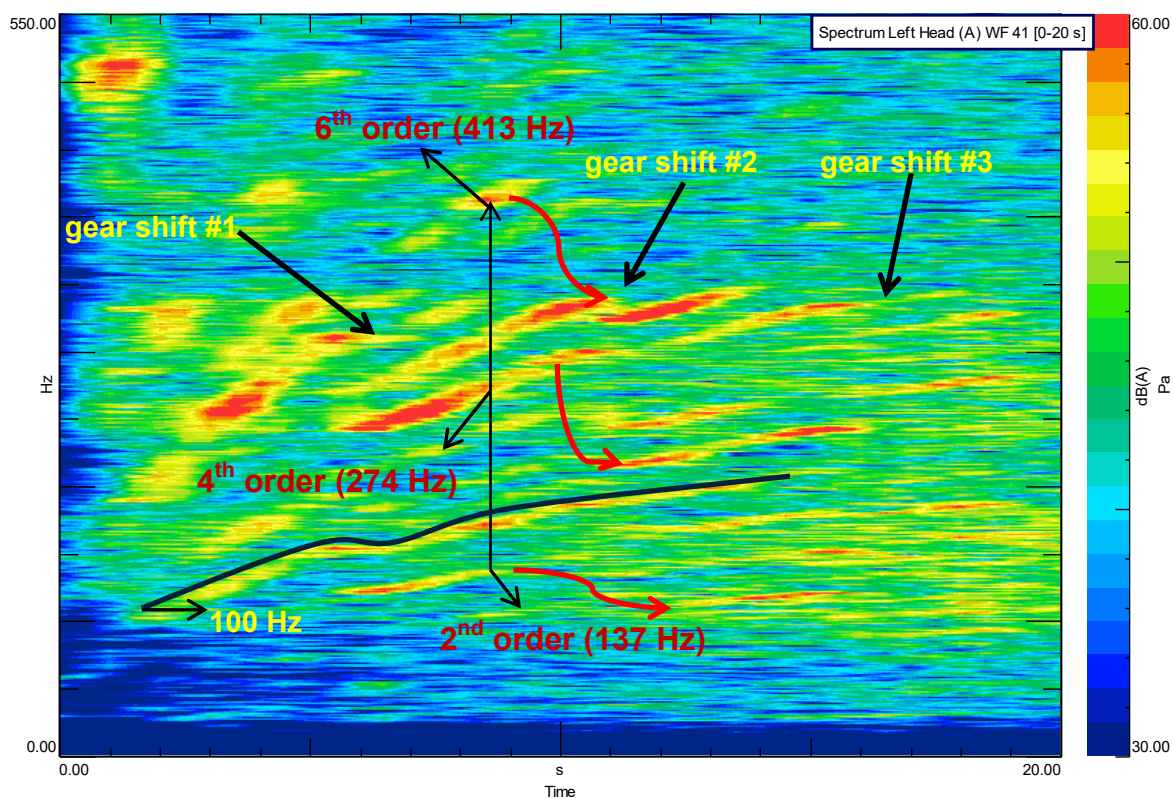

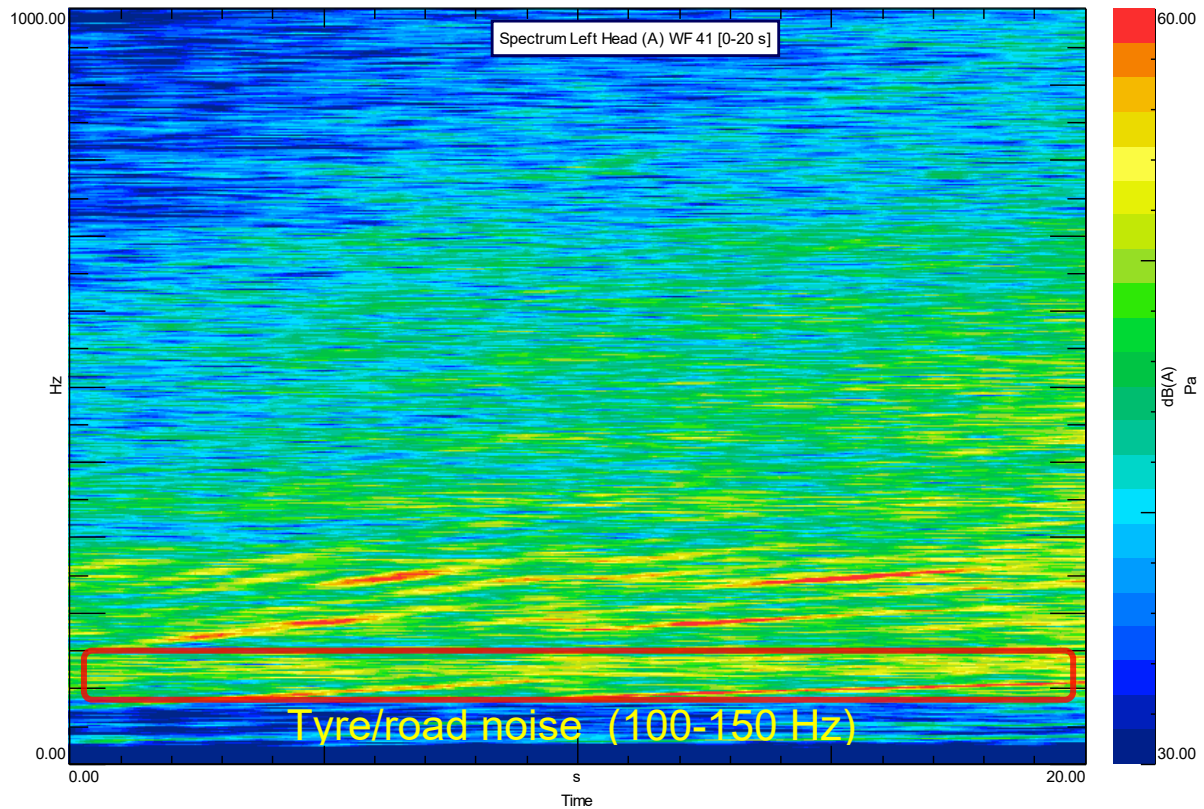**Figure 8.38**: Vehicle A audio-spectrum, run 18 detail, (run up 50-130).

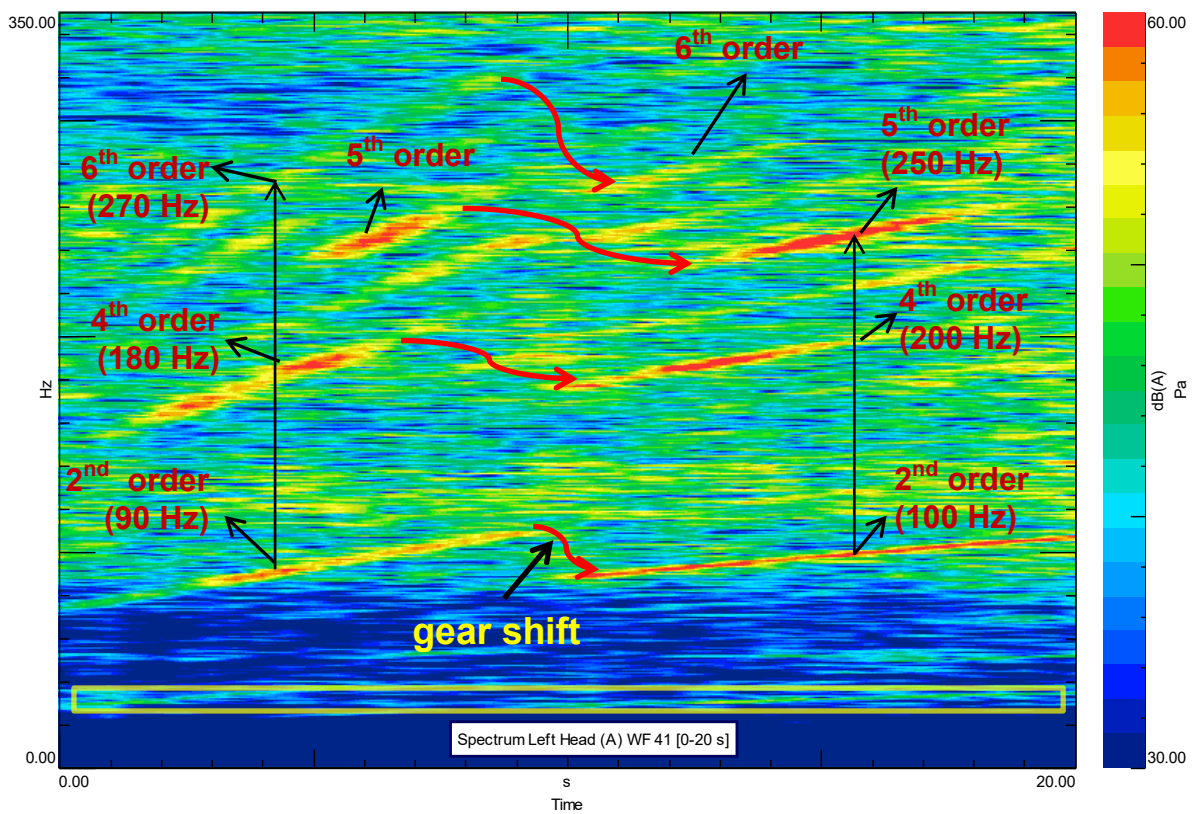**Figure 8.39**: Vehicle B audio-spectrum, run 17, (run up 50-130).

Figure 8.40: Vehicle B audio-spectrum, run 17 detail, (run up 50-130).

The pictures above show a wide-open throttle situation, in which the acoustic spectrum recording is influenced by the environmental noise and engine characteristics, however, the main harmonic orders tracks are distinguishable, as put in evidence by the black arrows, within the rising increasing trends in diagrams. Besides, being these colour-maps referred to a run-up acceleration test, the gear shifts are present too, often recognisable by a flexion or an interruption in the signals shapes, which are put in evidence by the yellow arrows added in the figures.

On the other hand, the red spline curves link the harmonic orders prosecution along the time duration of the recording.

Concerning vehicle A, three gear shifts are recognisable, whereas, regarding vehicle B, the different transmission design and ratio is evident in the length the acoustic signals, more pronounced and representing only one gear shift.

This is coherent with the fact that the small gasoline engine vehicle has only 5 gear speeds, with quite long transmission ratios, whereas the larger diesel engine vehicle has a 6 gear speeds-automatic system, with considerably shorter transmission ratios and more torque, coupled with a lower redline.

Moreover, it is possible to observe how the definition of the harmonic orders becomes more confused and less understandable in the final temporal segment of the run, likely because at the high speed reached, approximately highway speed, the wind noise and rolling resistance noise contributions becomes relevant and severely affect the engine sound component, disturbing the recording quality.

From the data emerged in the colour map it can be observed a particular spectrum characteristic during vehicle A manoeuvre execution, which is enhanced by the black spline curve, starting about the second order origin signal and continuing with a trend roughly correspondent to 15x the vehicle wheel angular speed, thus not correlated to the internal combustion engine harmonics; therefore, considering its dependency with vehicle speed, it can involve only elements downstream of the gearbox, it may be related to rolling resistance phenomenon or to the differential system/AWD system mechanism. Conversely, analysing vehicle B spectrum, a specific structural frequency of the car chassis is detected around 60 Hz. As a further remark, looking at the same acoustic spectra in a wider frequency range it is possible to observe the tyre/road noise fascia, comprised approximately between 100-150 Hz, (Figures 8.37 and 8.39)
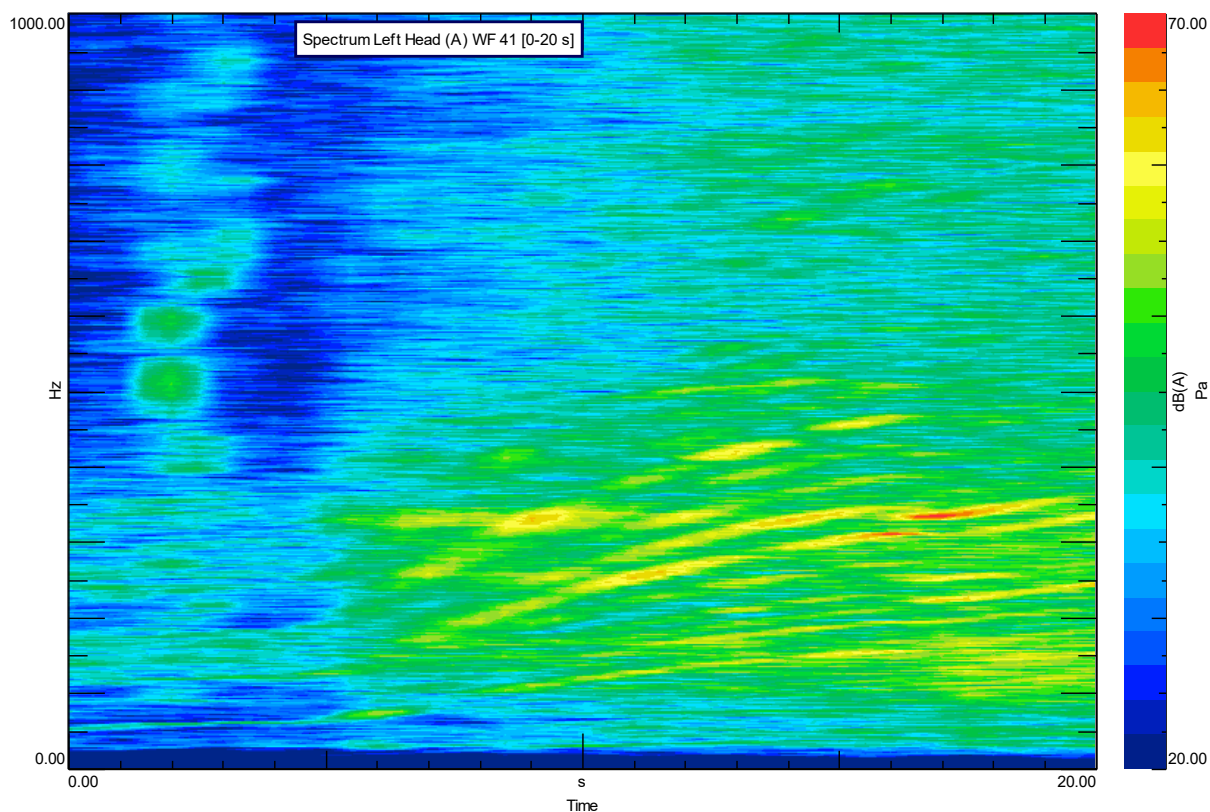
Figure 8.41: Vehicle A audio-spectrum, run 7, (run up 70-120).
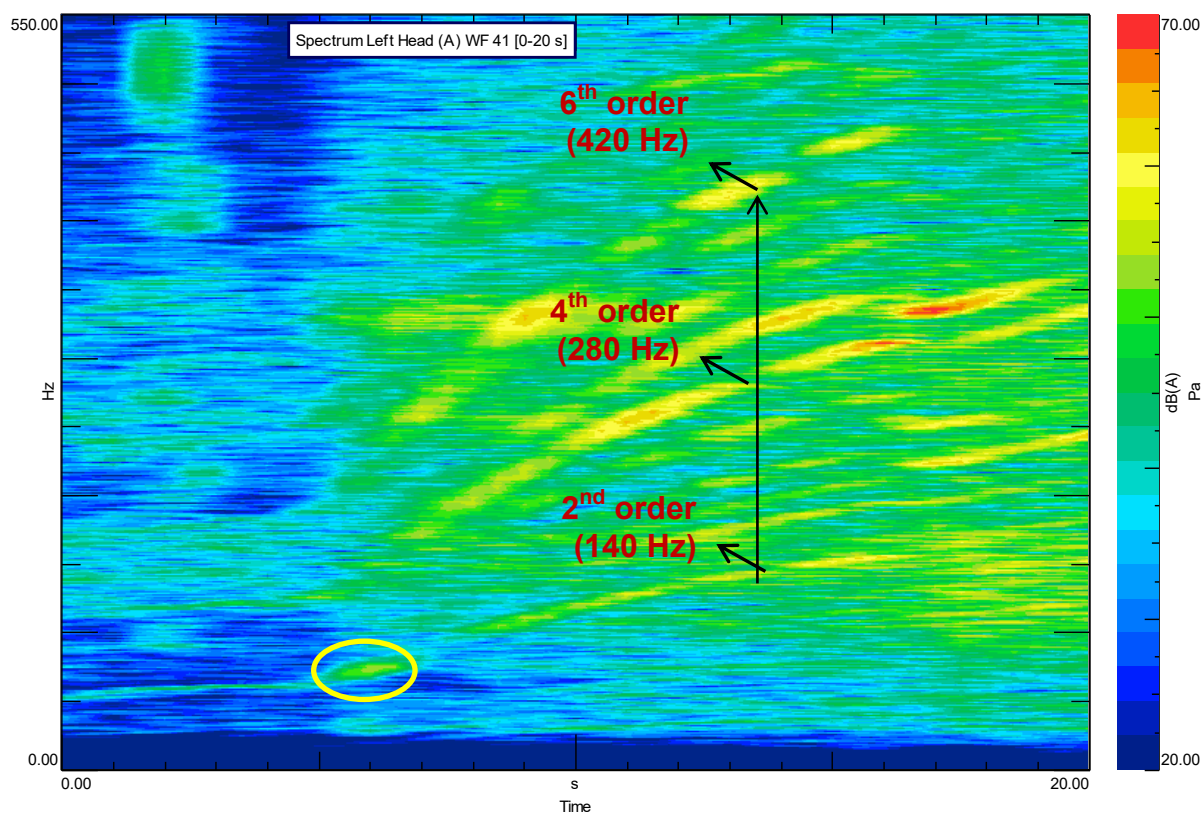

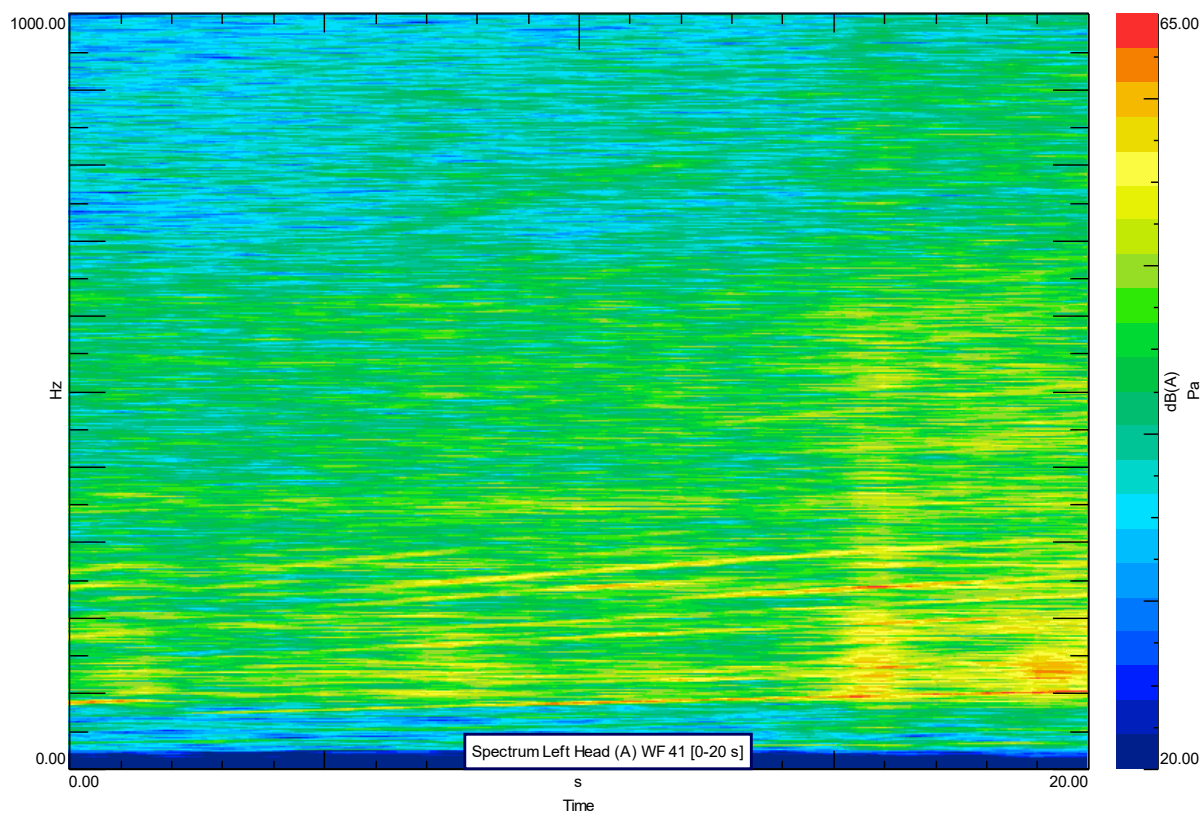**Figure 8.42**: Vehicle A audio-spectrum, run 7 detail, (run up 70-120).

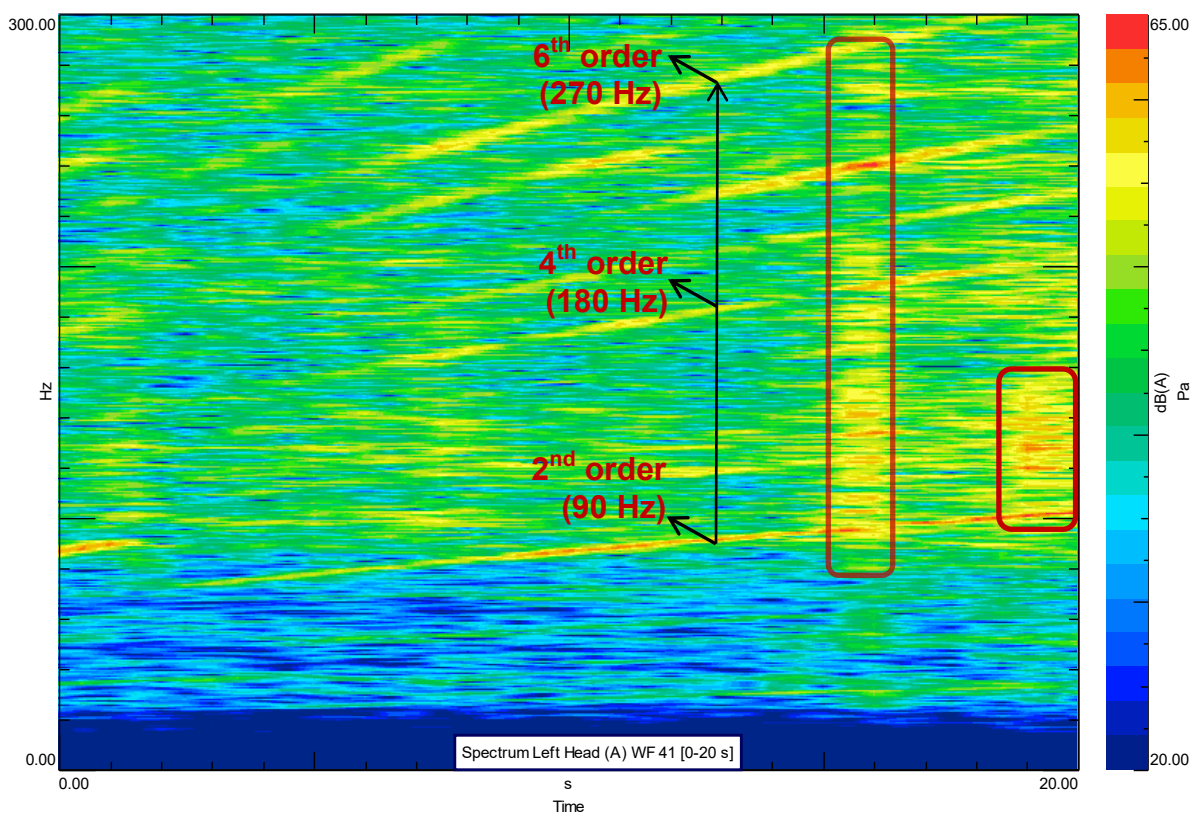**Figure 8.43**: Vehicle B audio-spectrum, run 7, (run up 70-120).

Figure 8.44: Vehicle B audio-spectrum, run 7 detail, (run up 70-120).

Looking at these figures referring to a slightly different acceleration test, with a more limited speed range, is it again observable the progressive rising of the frequency with the time, thus, increasing the speed, with the main engine orders highlighted by the black arrows. Also in this run up comparison, vehicle A sound spectrum curves seems to define a more bent line in the time progression, whereas vehicle B spectrum signals appear as more straight and regular lines.

Moreover, the dB levels enhanced by the colour scaling are not much different, even though former value can be defined differently distributed with respect to the latter one, as in the previous analysis; however, some peculiarities emerge by considering peculiar regions in the two pictures, representing particular features within the analysed spectrums.

In particular, observing Figure 8.42, vehicle A spectrum shows a globular zone towards the beginning of the test, about second 7, located in the frequency range between 68 – 76 Hz, which defines the starting point for the rising curves trend that progressively achieve frequency values in the order of 360 Hz.

Actually, this can be related to the initial downshift performed by the driver to prepare the acceleration, causing a quick increment in the engine RPM and a consequent increase in sound and noise at low frequency, typical of the Diesel engines tonality.

Conversely, taking vehicle B into account, the colour map trend is more regular and linear, with no pronounced bending of spectrum lines. Nevertheless, a singularity is put in evidence by a really outstanding characteristic zones located in the ending portion of the picture, about seconds 15-16 and 19-20; indeed, in correspondence of these time instants, the otherwise regular dB level stripes assume a peculiar shape and their colour denotes a high dB value, clearly recognisable by two little columns formed by pseudo-rhomboidal globules that extend in a frequency interval mainly comprised between 95 – 155 Hz.

These features seem to represent the acoustic contribution given by some potholes, thus attributable to road irregularities solicitation on both axles. On the whole, the overall acoustic behaviour of the two engines is quite different, as expected, not much from a purely acoustic power concern, but especially from the harmonic extension and sound orders development, where vehicle B overall noise spectrum seems to be less defined and conspicuous with respect to the mid-SUV one; also, the extension of the frequency range involved by the spectrum stripes in this case remains more limited, with no relevant acoustic regions occurrence above 300 Hz.

8.5.1 Seat rail spectrum analysis

For sake of completeness, the spectral assessment has been extended to the seat rail accelerometers, thus collecting information related to the same data, in this case focusing on the structural path for vibration and noise propagation.

With the same acquisition and processing options used for the audio-spectrum study, the colour maps for the three main axes, x, y, z have been computed, adopting as a unit measure scale the logarithmic m/s^2 (Figures 8.45 – 8.50).

Figure 8.45: Vehicle A seat rail X spectrum, run 18 (run up 50-130).

Figure 8.46: Vehicle A seat rail X spectrum, run 18 detail (run up 50-130).

Figure 8.47: Vehicle A seat rail Y spectrum, run 18 (run up 50-130).

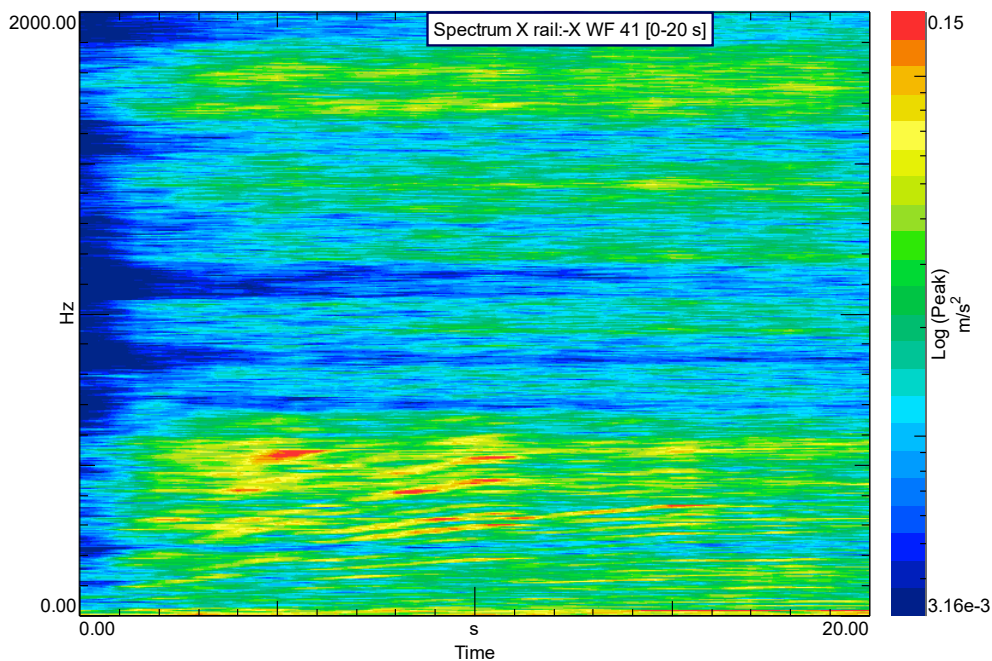**Figure 8.48**: Vehicle A seat rail Y spectrum, run 18 (run up 50-130).

Figure 8.49: Vehicle A seat rail Z spectrum, run 18 (run up 50-130).

Figure 8.50: Vehicle A seat rail Z spectrum, run 18 detail (run up 50-130).

Figure 8.51: Vehicle B seat rail X spectrum, run 17, (run up 50-130).

Figure 8.52: Vehicle B seat rail X spectrum, run 17 detail, (run up 50-130).

Figure 8.53: Vehicle B seat rail Y spectrum, run 17, (run up 50-130).

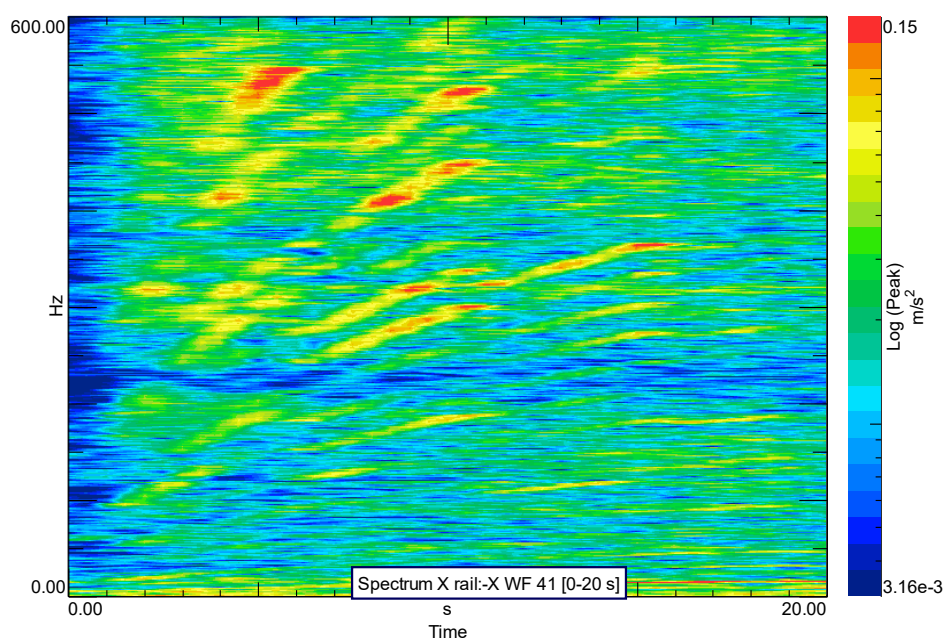**Figure 8.54**: Vehicle B seat rail Y spectrum, run 17 detail, (run up 50-130).
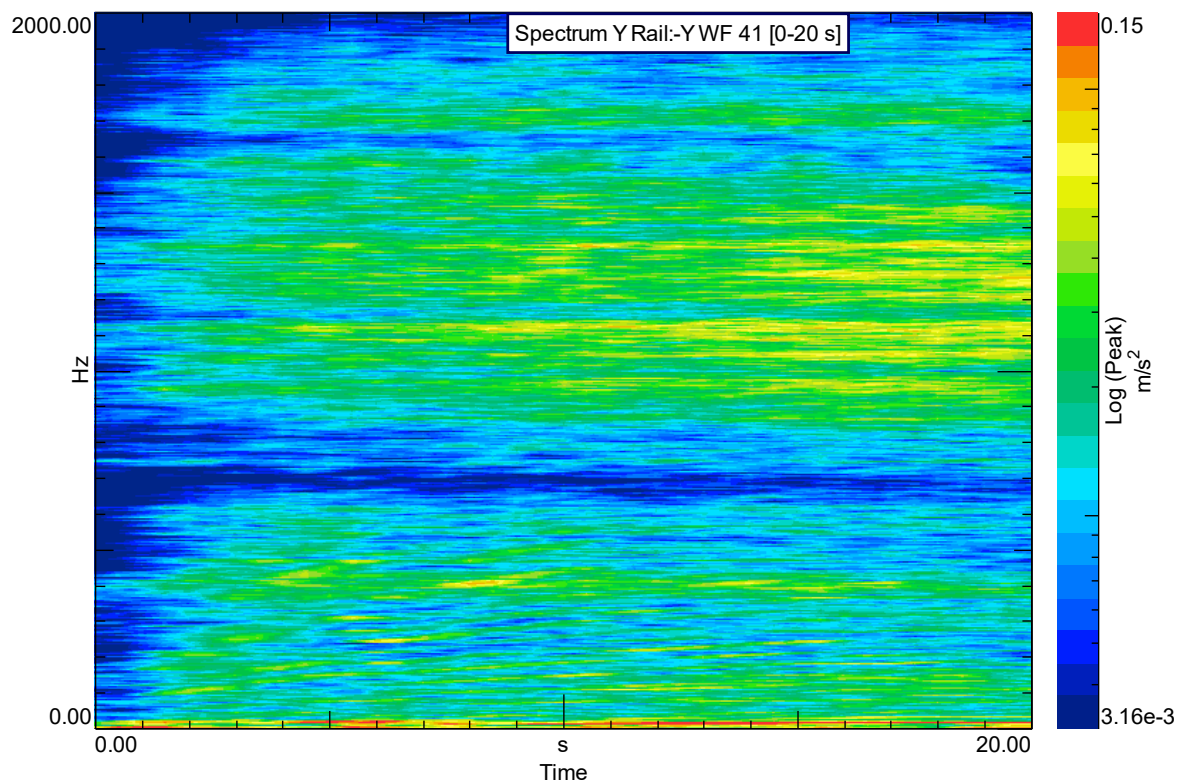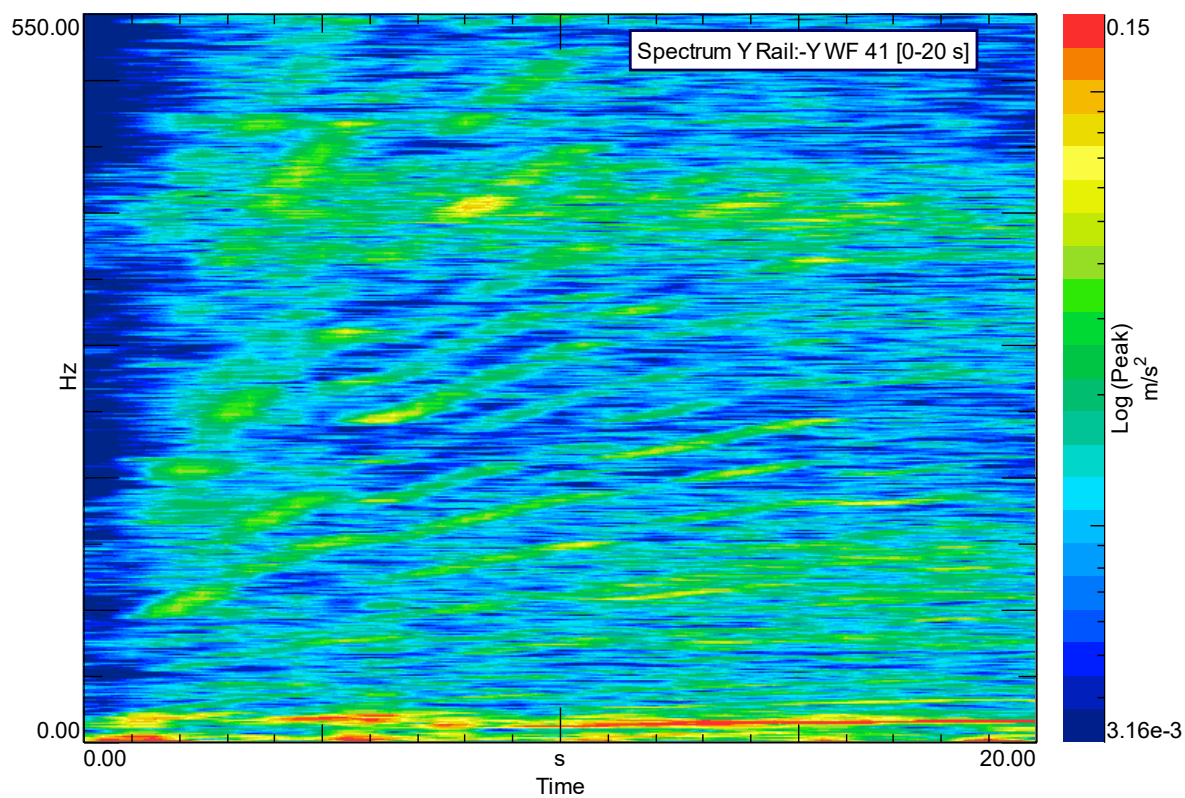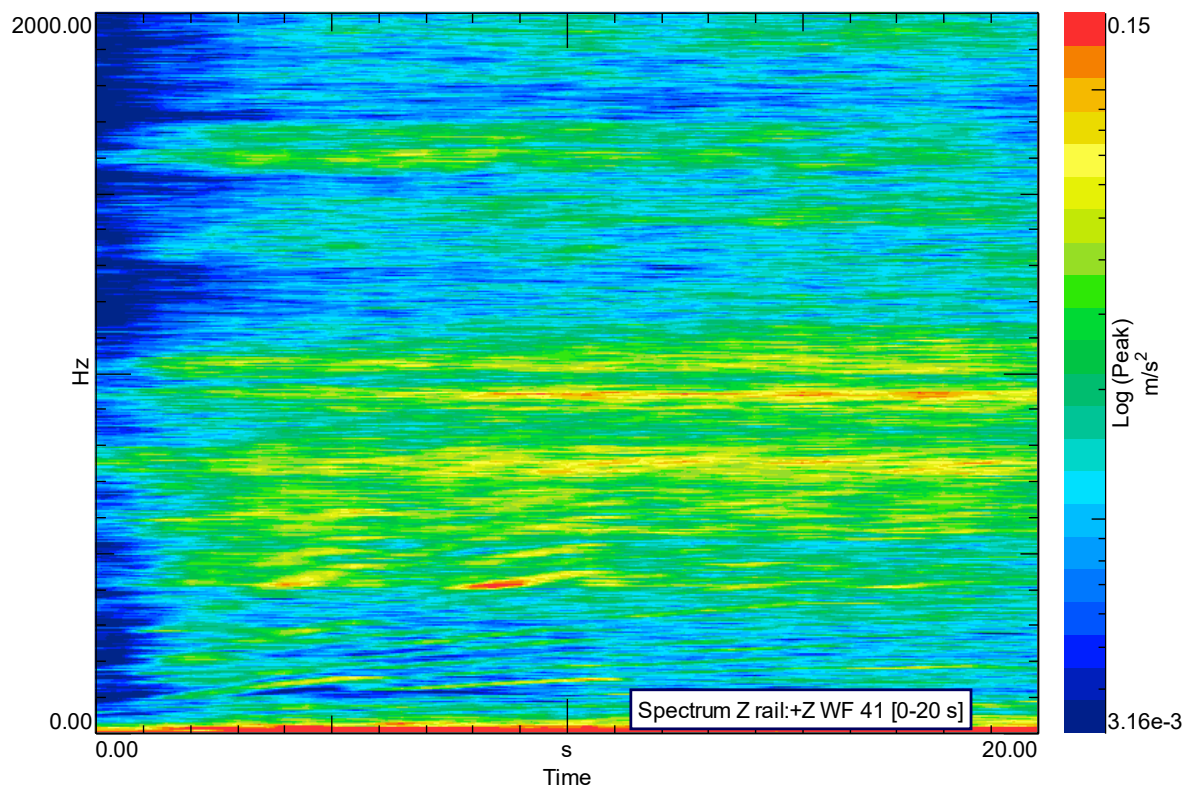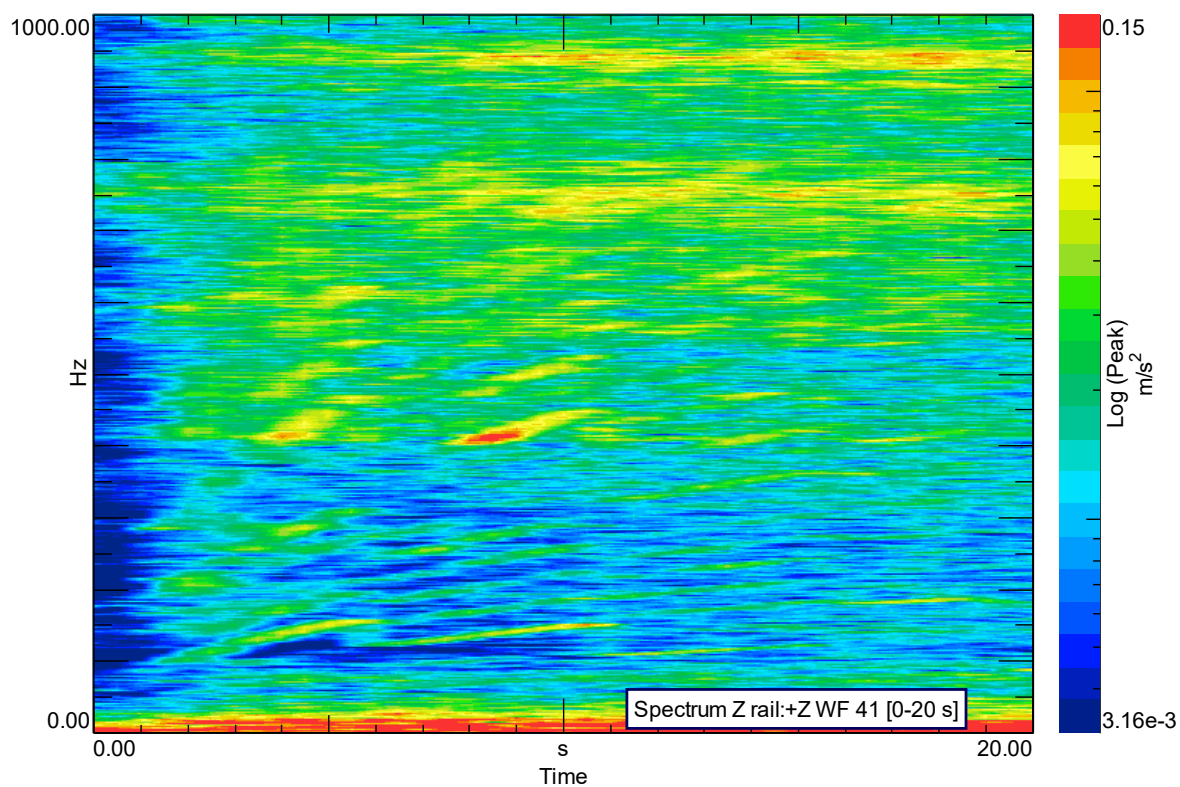
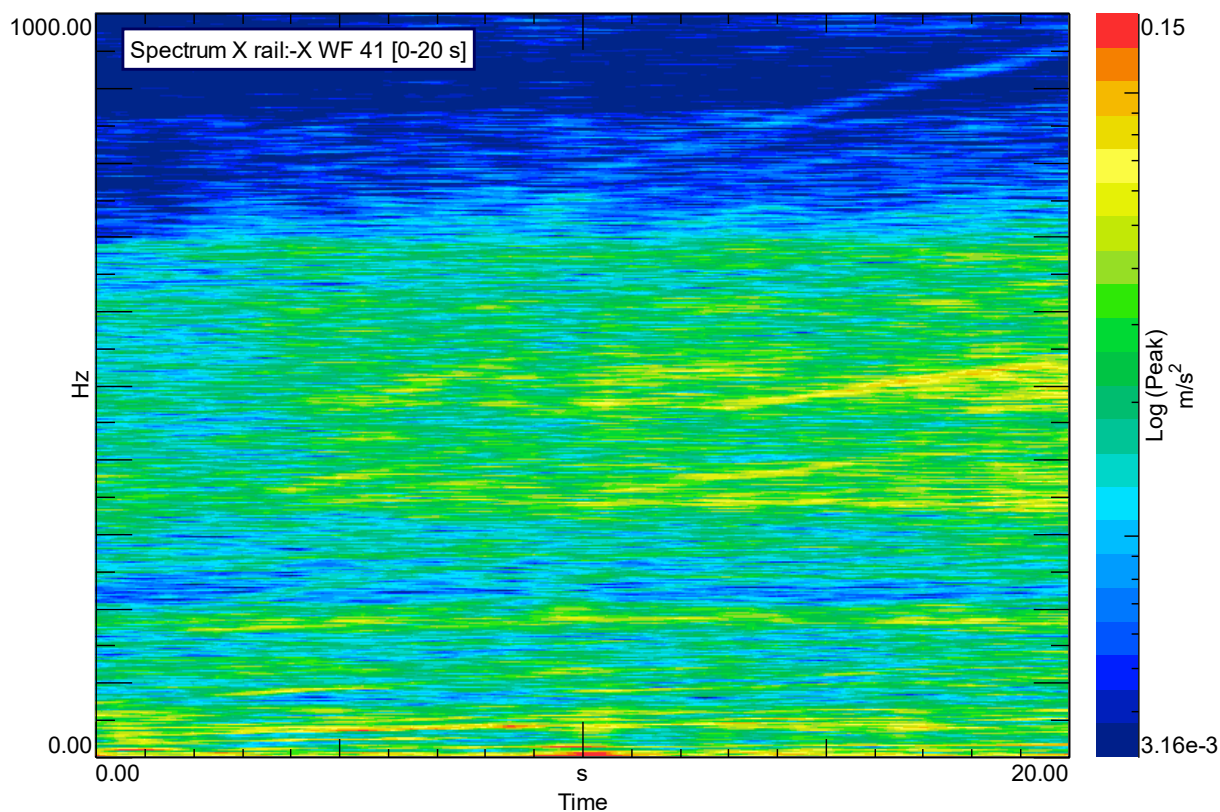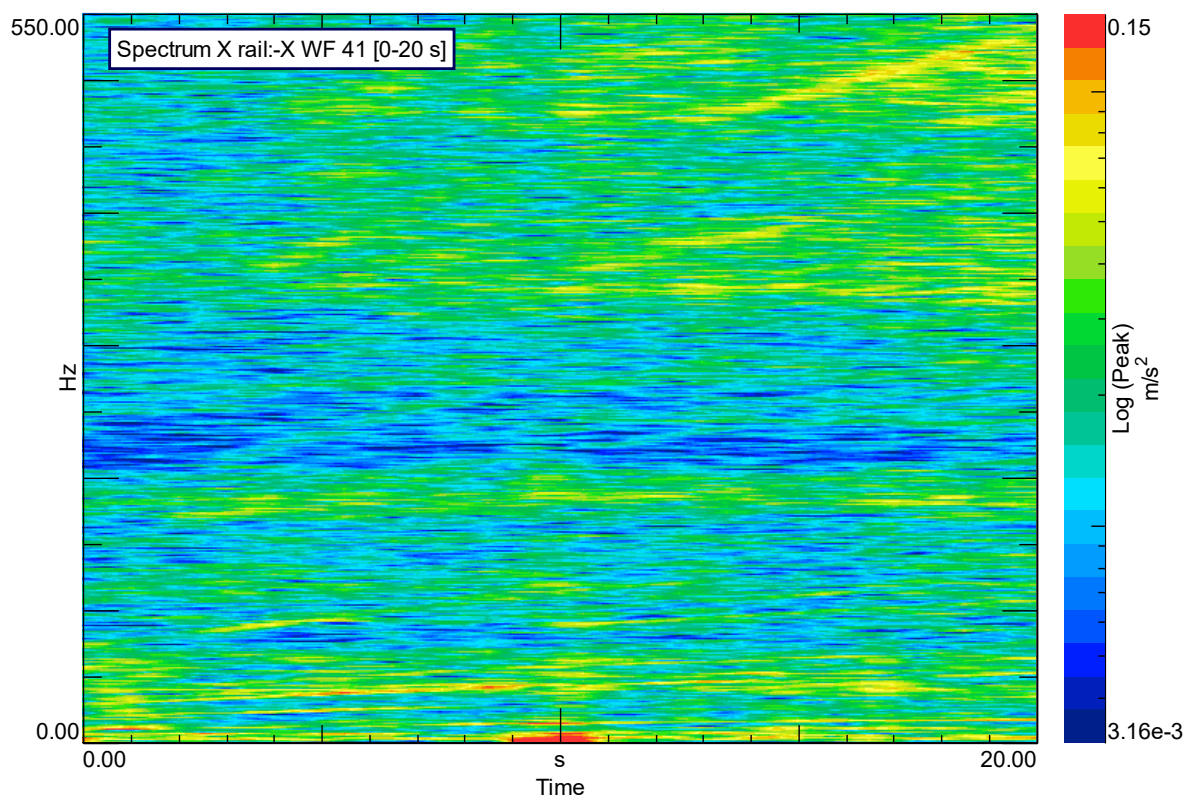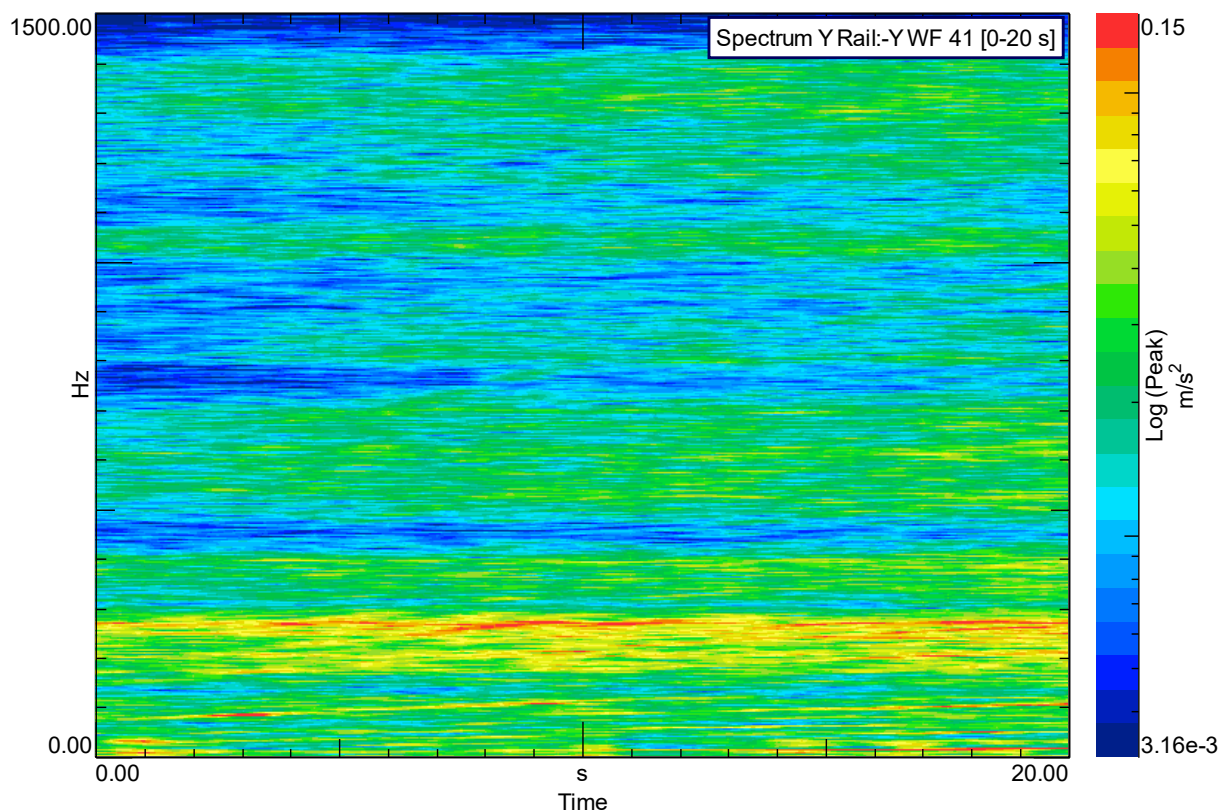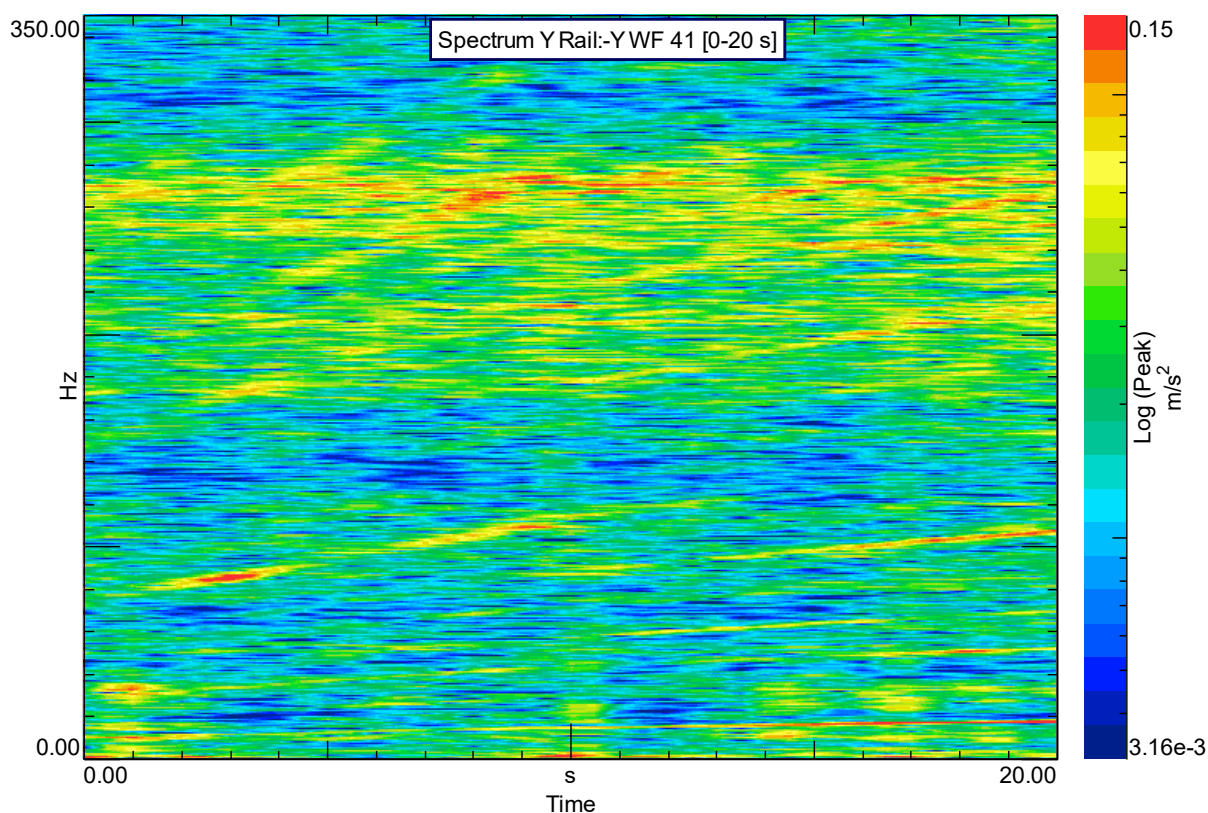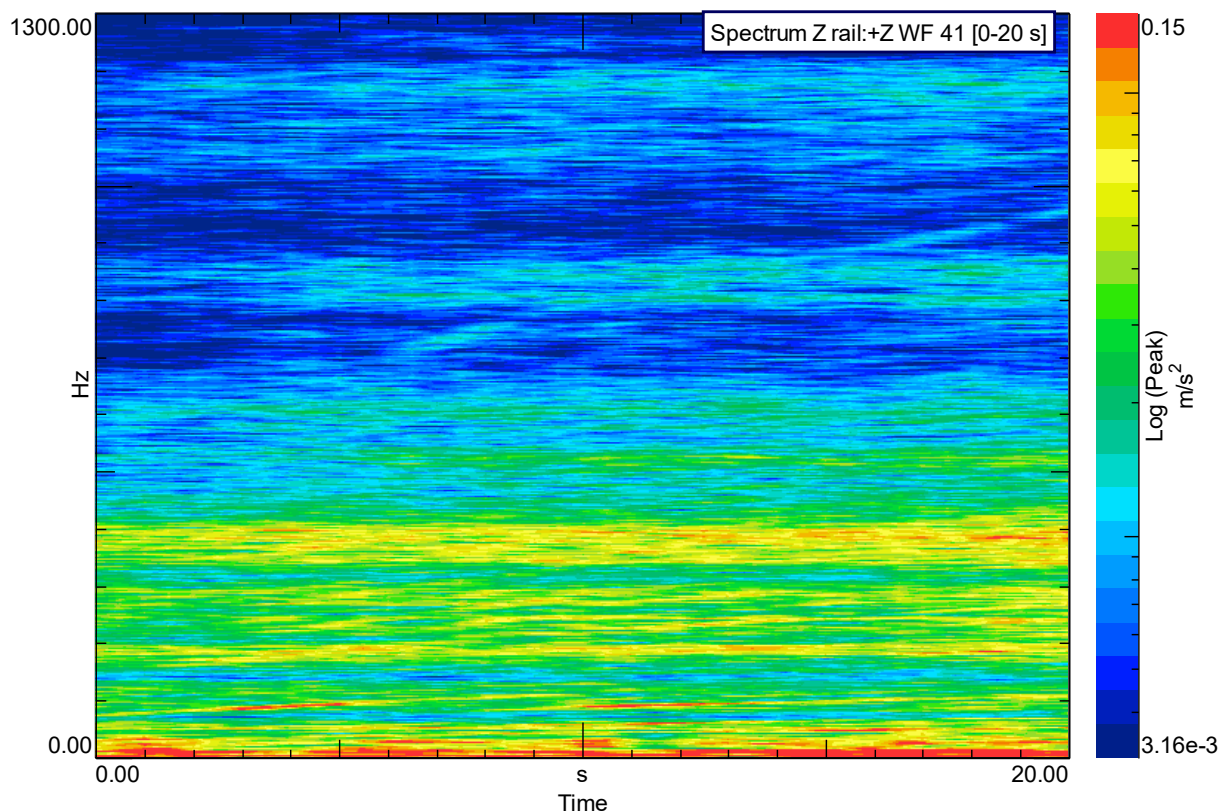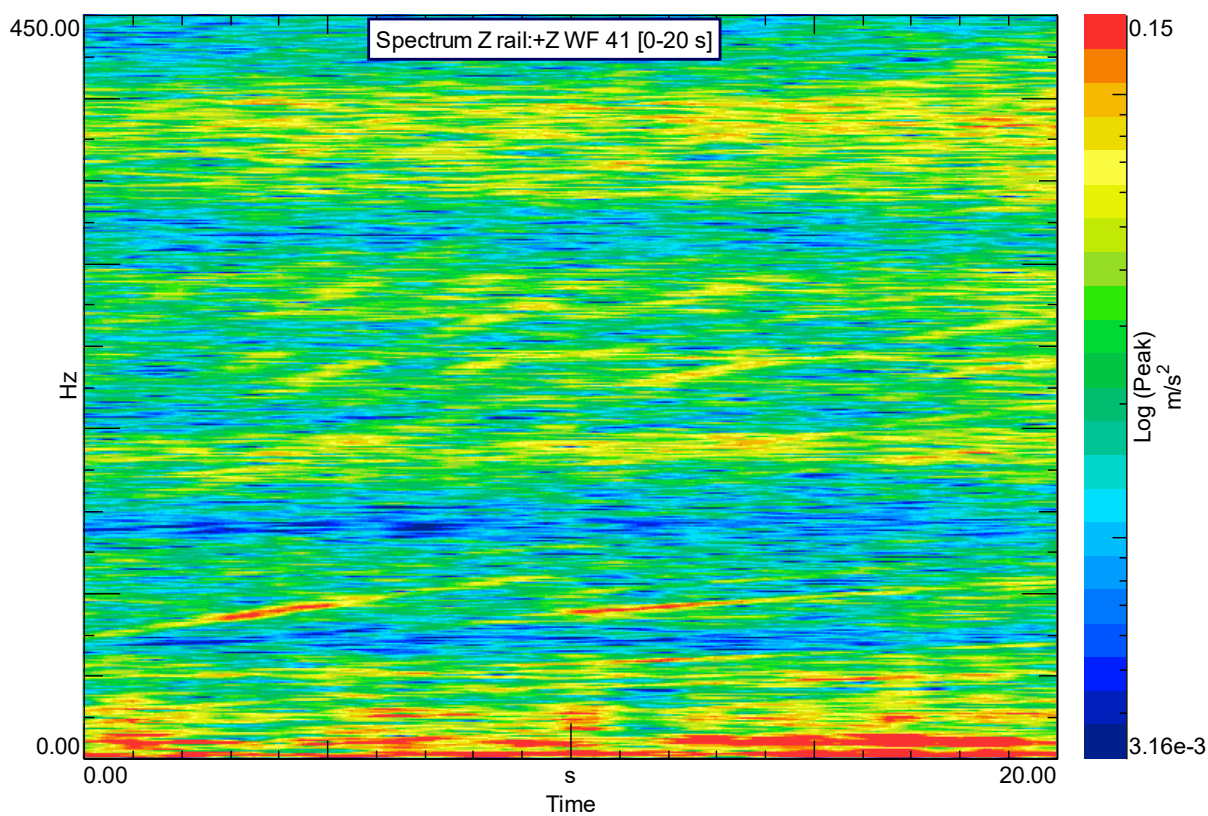**Figure 8.55**: Vehicle B seat rail Z spectrum, run 17, (run up 50-130).

Figure 8.56: Vehicle B seat rail Z spectrum, run 17 detail, (run up 50-130).

As a first remark, in relationship with the audio-spectra examined in the previous paragraph, for both the cars in exam the same harmonic orders are again recognizable within the frequency/acceleration distribution, especially concerning the Z-axis rail colour maps, even though with a different degree of understanding and legibility, depending on the minimum and maximum thresholds chosen as extreme of the logarithmic scale, respectively 3.16e-3 and 0.15 m/s^2.

Analysing the different colour maps related to vehicle A seat rail spectrum, it can be observed the overall higher peak level present studying the X and Z axes directions spectra with respect to the Y axis one, the former ones overcoming the 0.15 m/s^2 log value, respectively in the main frequency intervals 300-550 Hz and 400-420 Hz, the latter showing lower peak levels on the scale.

All the three cases indicate a relevant spectra extension till to approximately 2000 Hz; besides, the Y-spectrum is characterized by a specific frequency range in which the acceleration level is quite negligible, 600-800 Hz, whereas no evident zones of such kind are clearly present in X and Z spectrum. Concerning low-mid frequency study, X-spectrum indicates a pretty high level till 600 Hz; contrariwise, the Y-one is characterized by quite limited levels of acceleration, concentrated mainly around 380-420 Hz; instead, regarding X-spectrum, significant peak zones are localized in the intervals across 400-800 Hz and 900-1100 Hz.

On the other hand, considering higher frequencies, X-spectrum features middle-level characteristic between 1600-1800 Hz, Y-spectrum between 900-1500 Hz and Z-spectrum between 1550-1700 Hz.

As far as vehicle B seat rail spectrum, the Z axis direction spectrum put in evidence the highest acceleration level, in particular with respect to the X axis one, while the Y-spectrum is characterized by relevant peak values too, both Y and Z trespassing the 0.15 m/s^2 log value, respectively in the main frequency intervals 80-110 Hz, 250-280 Hz and 80-100 Hz. The several bandwidths are noticeably different one another, the X one is mainly comprised between 0-700 Hz, Y kind has the widest extension, till to approximately 1450 Hz, whereas Z-axis bandwidth ranges from 0 to 1200 Hz, even though no relevant acceleration level is detectable above 850 Hz.

About low-mid frequency characteristics, X-spectrum level is mostly relevant within 330-530 Hz, otherwise featuring quite limited levels of acceleration, Y peaks are concentrated especially around 170-300 Hz; concerning X-spectrum, its main high level zone is in common with the Y characteristic, though, another significant zone is located between 330-430 Hz. Conversely, talking about higher frequencies, the Y bandwidth is the only one putting in evidence a decent amount of acceleration value distribution across the 500-700 Hz range.

8.6 Conclusive considerations and future developments

This project treated a huge and deeply diversified topic, that cannot be fully exhausted in here. Departing from a general overview on the massively extended state of the Art relative to Human Vibration and Psychoacoustics, the thesis work has been developed on some specific experimental analysis to obtain results based on focused tests and conditions, involving several indexes and parameters that take into account a multitude of different factors and are managed by really complex algorithms implemented by high-level industrial software houses that requires great expenses and deep knowledge to be properly used and mastered.

As expected, the two examined vehicle provided significantly different results, these being largely affected by the different conditions peculiar of each tests, other than by the obvious differences in car design, mission and specific characteristics.

The major difficulties consists not much in the computation and definition of the many indexes established by the official regulations and normative entities, but in trying to build a relationship between these effective parameters and the typically subjective characteristics that have to be put in evidence by each of them.

In this regard, a further step related to future developments may be represented by connecting real-time subjective scorings to evaluate the single objective quantities computed, thus establishing a complete correlation between the two fields of study.

9 Acknowledgements

First of all, my gratitude goes to prof. Enrico Galvagno, supervisor of this thesis project, which followed me in this long and challenging journey, with never-ending support and help along the writing and the unforgettable testing sessions in the countryside roads and not only, testing his car without hesitation.
Without him, this work wouldn't be possible.

Special thanks to all my family, without their constant moral and economic helping all of what I am today would not exists, comprised the long path that leaded me here.

Heartfelt thanks go to all my friends too, who accompanied me along the difficulties and the joys of the life.

Last, but not list, an inexpressible thank to O.

10 References

[1] N. J. Mansfield, Human Response to Vibration, London: CRC Press, 2004.

[2] S. J. Park and M. Subramaniyam, "Evaluating Methods of Vibration Exposure and Ride Comfort in Car," *Journal of the Ergonomics Society of Korea,* vol. 32, no. 4, pp. 1-7, August 2013.

[3] International Organization for Standardization, *ISO 2631-1: Mechanical vibration and shock - Evaluation of Human Exposure to Whole Body Vibration,* Geneva, 1997.

[4] British Standards Institution, *BS 6841: Measurement and evaluation of human exposure to whole-body mechanical vibration and repeated shock,* London, 1987.

[5] M. J. Griffin, Handbook of Human Vibration, London: Academic Press, 1990.

[6] S. L. Y. N. Y. L. J. a. K. J. Park, ""Seating physical characteristics and subjective comfort: Design Considerations," *SAE Technical Paper, 980653,* 1998.

[7] International Organization for Standardization, *ISO 8727: Mechanical vibration and shock: Human exposure-biodynamic coordinate system,* Geneva, 1997.

[8] International Organization for Standardization, *ISO 8041: Standard for instruments measuring human response to vibration,* Geneva, 2005.

[9] International Organization for Standardization, *ISO 5349-1: Mechanical vibration- Guidelines for the measurement and the assessment of human response to hand transmitted vibration,* Geneva, 2001.

[10] G. Paddan and M. Griffin, "Effects of seating on exposures to whole-body vibrations in vehicles," *Journal of Sound and Vibration,* pp. 215-241, 2002.

[11] K. Parsons and M. Griffin, "Methods fr Pedicting Passenger Vibration Discomfort," *SAE Technical PAper 831029,* 1983.

[12] S. J. Park and C. Kim, "The Evaluation of Seating Comfort by the Objective Measures," *SAE Technical PAper 970595,* 1997.

[13] M. J. Griffin, "A comparison of standardized methods for predicting the hazards of whole-body vibration and repeated shocks," *Journal of Sound and Vibration,* vol. 215, no. 4, 1998.

[14] C. H. Lewis and M. J. Griffin, "A comparison of evaluation and assessments obtained using alternative standards for predicting the hazards of whole-body vibration and repeated shocks," *Journal of Sound and Vibration,* vol. 4, no. 215, 1998.

[15] X. Wang, "Vehicle Noise and Vibration Refinement," *Woodhead Publishing in mechanical engineering,* 2010.

[16] Gabriella Cerrato, Sound Answers Inc., "Automotive Sound Quality-Powertrain, Road and Wind Noise," *Sound & Vibration,* April 2009.

[17] F. Penne, "Shaping the Sound of the Next Generation BMW," in *International Conference on Noise and Vibration Engineering ISMA*, Katholieke Universiteit, Leuven, Belgium, 2004.

[18] C. Drioli and N. Orio, "Elementi di Acustica e Psicoacustica Cap.2," 1999.

[19] "The Engineering Toolbox," [Online]. Available: https://www.engineeringtoolbox.com.

[20] F. Winckel, Music, Sound and Sensation: A Modern Exposition, Courier Corporation, 2014.

[21] J. O. Smith III, Spectral Audio Signal Processing, Stanford University: W3K Publishing, 2011.

[22] ARPA Piemonte, "Introduzione alla psicoacustica e ai possibili campi di impiego nell'acustica ambientale," in *Analisi delle Migliori Pratiche e Tecnologie Disponibili nei Settori della Misurazione e Registrazione del Rumore e in quello della Psicoacustica*, 2013.

[23] H. Fletcher and W. A. Munson, "Loudness, its definition, measurement and calculation," *Journal of the Acoustic Society of America 5,* 1933.

[24] "HyperPhysics Sound Measurement," [Online]. Available: http://hyperphysics.phy-astr.gsu.edu/hbase/Sound/dbcon.html#c1.

[25] International Organization for Standardization, "ISO 131: Expression of physical and subjective

magnitudes of sound or noise in air," 1979.

[26] International Organization for Standardization, ISO 532 Acoustic method for calculating loudness level, Geneva, 1975.

[27] E. Zwicker and H. Fastl, Psychoacoustics: Facts and Models, X ed., Springer, 1990.

[28] C. V. Pavlovic, "Derivation of primary parameters and procedures for use in speech intelligibility predictions," *Journal of the Acoustical Society of America,* no. 82, 1987.

[29] L. L. Beranek, Criteriafor Noise and Vibration in Communities, Buildings and Vehicles in Noise and Vibration Control, McGraw-Hill Inc., 1988.

[30] International Organization for Standardization, ISO 10326-1 Mechanical vibration: Laboratory method for evaluating vehicle seat vibration, Geneve, 1992.

[31] G. J. Stein, R. Chmùrny and V. Rosik, "Compact Vibration Measuring System dor in-vehicle Applications," *Measurement Science Review,* vol. 11, no. 5, 2011.

[32] H. Nahvi, M. Hosseini and M. Nor, "Evaluation of Whole-Body Vibration and Ride Comfort in a Passenger Car," *International Journal of Acoustics and Vibration,* vol. 14, no. 3, 2009.

[33] N. Radic, C. Novak and H. Ule, "Experimental Evaluation of Vehicle Cabin Noise using Subjective and Objective Psychoacoustic Analysis Techniques," *Canadian Acoustics,* vol. 39, no. 4, 2011.

[34] M. A. Panza, "A review of experimental techniques for NVH analysis on a commercial vehicle," in *ATI 2015 - 70th Conference of the ATI Engineering Association*, Napoli.

[35] International Labour Office, "ILO Encyclopaedia of Occupational health and Safety," Workplace Health and Safety Information, [Online]. Available: http://www.ilocis.org/documents/chpt50e.htm.

[36] S. Patil, "On-Road Ride Comfort Test and Simulation Analysis of Passenger Cars with Emphasis on Indian Suburban and Rural Road Conditions," *SAE Technical Papers,* 2016.

[37] S. V. Ohlsson, Floor vibrations and human discomfort, Goteberg: Chalmers University of Technology, Division of Steel and Timber Structures, 1982.

[38] "Larson Davis," [Online]. Available: http://www.larsondavis.com/applications/hvm/handarmvibration.

[39] M. L. M. Duarte, M. d. B. Pereira, M. R. Misael and L. E. d. A. Freitas Filho, "Is Age More Important than Gender, Corporeal Mass Index (CMI) or Vision on Whole-Body Human Vibration Comfort Levels?," in *Conference Proceedings of the Society for Experimental Mechanics Series*, Belo Horizonte, 2006.

[40] M. Concha-Barrientos, D. Campbell-Lendrum and K. Steenland, "Occupational noise: Assessing the burden of disease from work-related hearing impairment at national and local levels," *Environmental Burden of Disease Series,* no. 9.

[41] OSHA, "Occupational Safety and Health Administration," United States Department of Labor, [Online]. Available: https://www.osha.gov.

[42] NIOSH, "Noise-induced loss of hearing," National Institute for Occupational Safety and Health, Cincinnati, OH, 1991.

[43] NIOSH, "Criteria for a recommended standard: occupational noise exposure. Revised Criteria," National Institute for Occupational Safety and Health, Cincinnati, OH, 1998.

[44] [Online]. Available: http://www.who.int/occupational_health/publications.

[45] [Online]. Available: https://www.cdc.gov/niosh/.

[46] CCOHS: Canadian Centre for Occupational Health and Safety, "OSH Answers Fact Sheets: Noise - Occupational Exposure Limits in Canada," [Online]. Available: https://www.ccohs.ca/oshanswers/phys_agents/exposure_can.html.

[47] Council of the European Union, "Noise limits for motor vehicles," Brussels, 2013.

[48] European Automobile Manufacturers Association, "Vehicle noise : Setting the right sound levels," [Online]. Available: www.acea.be.

[49] H. Fastl, "Psychoacoustics and Sound Quality," Technical-Acoustics Group, Department of Human-Machine Commmunication, Munich.